

M. J. Lucio

From MSC

STUDY OF
SELENODETIC MEASUREMENTS
FOR
EARLY APOLLO MISSION

FINAL REPORT
CONTRACT NO. NAS 9-2803
JANUARY 22, 1965

Prepared for
NATIONAL AERONAUTICS AND SPACE ADMINISTRATION
MANNED SPACECRAFT CENTER
HOUSTON 1, TEXAS

By
GEONAUTICS, INC.
1346 Connecticut Avenue, N. W.
Washington, D. C. 20036

FOREWORD

This report is submitted under the terms of contract NAS 9-2803 which was awarded to Geonautics, Incorporated on May 1, 1964. Purpose of the study is to determine selenodetic measurements and experiments to be performed during the early lunar surface Apollo missions.

The study was conducted under cognizance of the Lunar Surface Technology Branch, Advanced Spacecraft Technology Division of the Manned Spacecraft Center. Mr. James Sasser was Technical Representative of MSC and maintained close liaison with Geonautics' staff during the period of the study and provided technical data and direction. He and Mr. John Dornbach periodically reviewed program progress, and their cooperation and assistance throughout the study were most helpful. Members of Geonautics' staff primarily engaged in the study, and the areas of their contributions, are listed in the Introduction.

ABSTRACT

23697

Purpose of this study has been to investigate and recommend types of measurements and experiments during early Apollo missions to (i) refine present estimates of size and shape of the moon, (ii) establish a selenodetic datum and the beginnings of a selenodetic control network, and (iii) establish horizontal and vertical control for improved lunar mapping. To accomplish these purposes, measurements were investigated that could be obtained from lunar surface survey operations, from maximum utilization of Lunar Orbiter photography, and from observations using on-board equipment of the CSM, actually, the space sextant. Theory, equipment, operational methodology, and data reduction procedures applicable to these techniques and their objectives are set forth, along with estimated accuracies of results.

A long range view was taken in the study in that some procedures are recommended which will result in immediate benefits to selenodesy, others are recommended which will become significant only with repeated landings and more extended coverage than can be provided during the initial missions, and some are recommended because they will provide the ground work and experience for learning what can or should be done during extended missions. In all aspects of the study, full consideration was given to the astronaut's capabilities and his presence on the lunar surface or in the CSM, and only measurements are recommended which can be done better and more accurately because of his presence.

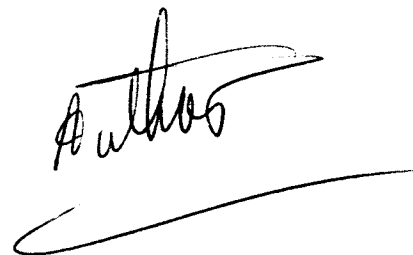


TABLE OF CONTENTS

Section	Title	Page
	FOREWORD	ii
	ABSTRACT	iii
	TABLE OF CONTENTS	iv
I.	INTRODUCTION	1
	A. Purpose and Scope	1
	B. Support of Mapping Programs	3
	C. Guides and Constraints	3
	1. Mission Constraints	3
	2. Environmental Constraints	4
	D. Direction of the Study	7
	1. Lunar Surface Measurements	7
	2. Use of On-Board Equipment	7
	3. Analysis of Orbiter Photographic Coverage	8
	4. Environmental Factors and Review of Available Equipments	8
	E. Value of Man in the Operations	9
II.	REPORT SUMMARY AND RECOMMENDATIONS	10
	A. Recommended Measurements	10
	1. Basis of Recommendations	10
	2. Lunar Surface Measurements	11
	(a) Determination of lunar celestial pole	11
	(b) Observation of astronomical position and azimuth reference at landing site	12
	(c) Photography of the CSM against the star background	12
	(d) Emplacement of a beacon to be observed from the earth	13
	(e) Gravity observations	13
	(f) Establishment of horizontal and vertical control in vicinity of the LEM	14

TABLE OF CONTENTS (CONT'D)

Section	Title	Page
	3. Use of Equipment On-Board the CSM	15
	(a) SXT photographic observations of selected landmarks	15
	(b) SXT visual observations of selected landmarks	16
B.	Coordination With Lunar Orbiter Photography	16
C.	Landmark Identification Studies	17
D.	Equipment to Be Developed	17
E.	Astronaut Training	19
F.	Data Reduction	20
G.	Summary Tables	20
	1. Study Flow Chart	22
	2. Surface Measurements and Estimated Results	23
	3. CSM Techniques for Positioning LEM and Lunar Landmarks	24
	4. Equipment for Selenodetic Operation on Lunar Surface	25
III.	PROBLEMS IN ESTABLISHING A TRUE SELENODETIC COORDINATE SYSTEM AND TRANSFORMATIONS BETWEEN COORDINATE SYSTEMS	26
A.	Introduction	26
B.	Coordinate Systems Involved in the Problem	27
C.	Elements of the Problem of Transfers Between Systems	28
	1. Link 1	29
	2. Link 2	29
	3. Link 3	29
	4. Link 4	31
	5. Link 5	33
	6. Link 6	34

TABLE OF CONTENTS (CONT'D)

Section	Title	Page
D.	Estimate of the Magnitude of the Errors of Coordinate Systems and the Ties Between Them	36
1.	Tracking Station Topocentric Coordinates	36
2.	Transfer to Geocentric Coordinates	41
3.	Transfer to Barycentric Coordinates at the Moon	42
4.	Transfer from Barycentric Coordinate System of the Spacecraft to the Morphocentric Coordinate System of Lunar Maps	49
5.	Errors of Landmark Coordinates with Respect to its Own Mapping System	51
6.	Direct Ties Between Earth and Moon	52
7.	Summary of Errors in Location Affecting the Capability of Landing a Vehicle on a Selected Site	52
E.	Remarks on the Establishment of a Selenodetic Datum, and Selenodetic Surveys	54
IV.	DETERMINATION OF THE LUNAR POLE	58
A.	Introduction	58
B.	Procedure	58
C.	Estimate of Accuracy of Pole's Coordinate Determination	59
V.	USEFULNESS OF A BEACON EMPLACED ON THE MOON, TO BE OBSERVED FROM THE EARTH	60
A.	Introduction	60
B.	Optical Methods	61
C.	Optical Beacon Types	62
1.	Mirrors	63
2.	Laser Corner Reflectors	66
3.	Bright Light Beacon	66

TABLE OF CONTENTS (CONT'D)

Section	Title	Page
	D. Radio Methods	67
	1. Directional Information	67
	2. Range Information	68
VI.	DETERMINATION OF ASTRONOMICAL POSITION AND REFERENCE AZIMUTH OF THE LANDING SITE	76
	A. Introduction	76
	B. Procedure	76
	C. Accuracy of Results to Be Expected	77
	1. Astronomical Position	77
	2. Astronomical Azimuths and Zenith Distances	78
VII.	USE OF GRAVITY OBSERVATIONS FOR SELENODETIC PURPOSES	79
	A. Introduction	79
	B. Measure of the Moon's Radius	79
	C. Sampling Size of Lunar Gravity Anomalies	82
	D. Instruments to Measure Surface Gravity	83
VIII.	USE OF HORIZONTAL AND VERTICAL CONTROL POINTS ON THE LUNAR SURFACE, AND PROCEDURES PROCEDURES FOR OBTAINING THEM	87
	A. Introduction	87
	B. Value of Local Horizontal and Vertical Control	87
	1. Mapping Control Points	88
	2. Positioning of Geophysical Equipment	91
	C. Review of Procedures and Equipment for Establishing Control Points	92
	1. Distance Measuring Devices	92
	2. Angle Measuring Equipment	93

TABLE OF CONTENTS (CONT'D)

Section	Title	Page
D.	Selected Survey Procedures	94
1.	Range and Angle Method	95
2.	Short Base Method	97
3.	Comparison of Survey Methods	105
E.	Accessory Survey Equipment	107
1.	Leveling Device	107
2.	Camera Supports	108
3.	Stadimeter	110
IX.	SUGGESTED SYSTEMS AND PROGRAMS FOR CONDUCTING SELENODETIC OPERATIONS ON THE LUNAR SURFACE	111
A.	Introduction	111
B.	System I Utilizing Cameras and Laser Ranger	111
C.	System II Utilizing Cameras and Stadia	116
D.	System II Extended to Additional Station	119
E.	Recommended Priorities	119
F.	Tentative Operational Programs	121
X.	ANALYSIS OF LUNAR ORBITER PHOTOGRAPHY	133
A.	Introduction	133
B.	Results of Error Analysis	133
XI.	USE OF OPTICAL EQUIPMENT ON BOARD THE CSM FOR SELENODETIC OPERATIONS	136
A.	Introduction	136
B.	Analysis of Concept	136
1.	Review of SXT Properties	136
2.	Characteristics of a Single Sighting of a Landmark	137

TABLE OF CONTENTS (CONT'D)

Section	Title	Page
3.	Characteristics of Multiple Sightings on a Landmark	139
4.	General Principles for Ensuring "Good Geometry"	146
5.	Concept of "Weight per Unit Solid Angle" as a Means of Planning Sighting Observations	155
6.	Observing Schemes	157
7.	Observing Scheme "A" for a Fix on a Single Landmark	159
8.	Critique of Observing Scheme "A"	167
9.	The Concept of Efficiency: Application to Observing Scheme "A"	172
10.	Observing Scheme "B": A Small Number of Fairly High-Weight Observations per Landmark	174
11.	Critique of Observing Scheme "B"	181
12.	Distant Landmarks: Observing Scheme "C"	190
13.	Summary of Observing Schemes	197
14.	Table XI-2: Observing Schemes - Summary of Characteristics	198
C.	Analysis of Equipment and Observing Schemes	202
1.	Photographic Methods for the SXT Observations	202
2.	Photographic Requirements for SXT Dual LOS Method	207
REFERENCES		211
APPENDICES		
A.	Analysis of the Accuracy of Lunar Orbital Photography for Determination of Selenodetic Positions	A1-33

TABLE OF CONTENTS (CONT'D)

B.	Determination of the Instantaneous Pole and Astronomical Latitude of the Moon by Moon- Based Fixed Cameras	B1-13
C.	Observations From the Moon of the Earth's Position Against the Background of the Stars for Selenodetic Purposes	C1-6
D.	Formulas for Reduction of Panoramic Photography to Determine Astronomical Position and Azimuth, and Selenocentric Coordinates of Survey Targets	D1-25
E.	Proposed Camera Characteristics for Surface Selenodetic Operations	E1-17
F.	Survey Targets for Use on the Lunar Surface	F1-6
G.	Comparative Evaluation of Laser and Radar for Ranging on the Moon	G1-6

SELENODETIC MEASUREMENTS FOR EARLY APOLLO MISSIONS

SECTION I INTRODUCTION

A. PURPOSE AND SCOPE

The Apollo missions constitute an important step in the conquest of space leading to the potential of visiting other planets in the solar system. In the first manned explorations of the moon, it is desired to obtain scientific data that cannot be obtained, at least to the same degree of certainty, by earth-based observations or by unmanned equipment on the surface of the moon or in orbit around it; and to accomplish measures that will pave the way for more extensive investigations in the future.

Selenodesy, the lunar counterpart of geodesy, encompasses both these aspects. In the broader sense, it is the study of the size and shape of the moon, its gravity field and hence something of its internal structure and density distribution, which are matters of great interest in determining the origin, history, and internal structure of the moon. In addition, selenodesy involves large-scale mapping of the moon, including the precise positioning of identifiable points on its surface in a well-defined coordinate system. Mapping is essential to the planning and execution of landing missions and to later more extensive exploration.

It has thus been the purpose of this study to investigate and recommend types of measurements, either on the lunar surface or from an orbiting spacecraft, with the objective of:

1. Refining present estimates of size and shape of the moon which, when combined with gravitational data, will tell something about the internal structure of the moon.

2. Establishing a selenodetic datum, and the beginnings of a selenodetic control network that may be required to support future lunar operations.
3. Establishing horizontal and vertical control for improved lunar mapping, consistent with requirements and standards of mapping techniques planned during the time of the Apollo missions and a reasonable period thereafter.

Equipment, operational methodology, and data reduction procedures for accomplishment of (1), (2), and (3) above are included in the investigations.

While the greatest possible precision is desired in selenodetic measurements, it is noted that high-order accuracies as defined for surveys on earth probably cannot be attained, at least not during the Apollo mission phase. Anticipated environmental conditions will be severe at best, and it is unlikely that the standards of work on earth, which are realized only with difficulty under optimum conditions, can be matched. Also, unless there were at least three stations in a net occupied at one time or another by instruments, there would be no closing errors in either angle or displacement, and thus no way to estimate the internal precision of a survey according to terrestrial standards. It seems doubtful that as many as three intervisible stations could be established during the Apollo missions, unless so close together as to nullify their usefulness.

Therefore, MSC requested that this study investigate and consider all even remotely reasonable methods for achieving objectives outlined above to the best possible accuracy, even if such accuracy is low, as long as it represents a worthwhile improvement over, or a contribution to selenodetic knowledge at time of the missions.

Three general categories of measurements have been investigated in detail; those obtainable from:

1. Ground survey operations.
2. Lunar Orbiter photography.
3. Space sextant sightings of selected landmarks from the CSM

B. SUPPORT OF MAPPING PROGRAMS

In reviewing the total usefulness of possible selenodetic programs, it became apparent that their greatest value will probably come from the support they give to lunar mapping programs. Various projects are under way and will continue at the Army Map Service, Aeronautical Chart and Information Center, and U. S. Geological Survey for mapping of the moon, at ever larger scales. This is being accomplished by earth-based observations, yielding maps as large as 1:500,000 scale, which over a period of many years to come will be filled in with larger scale mapping derived from photography obtained by lunar orbiting vehicles. Construction of these maps would be simplified and their utility enhanced for scientific purposes, and for navigation and planning of lunar missions, by establishment of accurate control points properly identified on the lunar surface to which photography and cartography can be fitted. In executing this study, primary attention was given to this purpose.

C. GUIDES AND CONSTRAINTS

1. Mission Constraints

The initial mission profile has been assumed to provide three excursions from the LEM by one astronaut at a time lasting 96, 154 and 132 minutes respectively, spread over a period of 15 hours and 5 minutes, this period representing the maximum span between observations. It has also been assumed that the time between separation and rendezvous maneuvers would be approximately 24 hours, during which period the third astronaut in the CSM would be able to make observations therefrom.

Present plans call for three similar Apollo missions, with subsequent missions providing longer times on the lunar surface and in orbit. We have concluded that the nature of the selenodetic work would not change appreciably from one mission to the next. We have provided, however, for measurements that would be useful under both extremes of assumptions; namely (1) that each mission would land in a different region of the moon, and repetition of the same type measurements on each mission would provide a foundation for wide-area coverage, some redundancy for increased accuracies, and a basis for time sequences where these greatly enhance the scientific value of the results (e. g., motion of the lunar celestial pole); (2) the selenodetic operation is carried out only once, at one landing site.

It was further assumed that the maximum instrument payload is 250 pounds with a bulk of 10 cubic feet, but that this payload is for all scientific purposes; so efforts were made to keep the equipment required for selenodetic purposes to a fraction of this total.

Other significant limitations on the achievable scope and accuracy of selenodetic surveys are imposed by the restricted mobility and dexterity of the astronauts, closeness of the visible horizon, shortness of any possible base for resection work, possible lack of sharply defined terrain objects as control points, and extreme difficulty of ranging to distant natural objects that will appear above and beyond the horizon. In order to determine practicable methods of accomplishing the work outlined, study was made of a broad range of such known and assumed environmental factors and constraints based on recent literature and Apollo project studies. These are summarized below:

2. Environmental Constraints

(a) Landing Site and Nearness of the Horizon. Landing will presumably be in a generally flat area, with a horizon distance of about 2.5 km from an astronaut's height of eye and about 5 km from the top of the LEM.

This limits the area of surface operations to not more than $20-80 \text{ km}^2$, except possibly for higher features whose base is beyond and below the visible (near) horizon.

(b) Space Suit Impediments. Because of these impediments, it has been considered that requirements for digital dexterity or exacting ocular work must be kept to an absolute minimum. Precise instrument pointing or circle reading and complicated manipulations have been avoided.

(c) Lunar Surface. The character of the ground, its bearing strength, and the presence or absence of loose dust, perhaps electrostatically charged, are presently unknown factors. Possible answers to these questions are covered in other studies [1, 2] and will not be repeated here. These imponderables together with space suit impediments, etc., have indicated that demands on the astronaut to move around must be kept to an absolute minimum, so selenodetic operations have been designed primarily for execution from the CSM and the LEM. Under this heading it should also be pointed out that the probable scarcity of sharply defined terrain objects which would constitute natural targets within the astronaut's range of observations has been taken into account; and that although mountains or highlands may appear at a distance beyond the horizon, they probably cannot be accurately located by operations from the neighborhood of the LEM alone.

(d) Atmosphere. The absence of atmosphere will eliminate refraction, scintillation, extinction of star light, air glow, scattered background light, and of course, weather, thus favoring photography of distant terrain, star background, etc., and completely eliminating the need to correct for or avoid refraction errors that are typical of terrestrial observations. This fact allows a much freer handling of vertical or oblique angles than is possible on the earth.

(e) Radiations. Energetic particle radiation is not considered a serious danger in view of the possibility of receiving warnings in

time to abort in the event of a strong solar flare. Survey instruments, except camera films, will not be affected adversely. Radiation-resistant films are available and light-weight shielding of cameras appears practicable. The intense solar thermal radiation will require reflectorized packaging of cameras and some thermal insulation. Cameras on ground supports will require protection from heat conduction from the ground, which may reach temperatures of 360°K during the planned operation. Temperatures of solid state devices would have to be controlled somewhat. Meteoritic impacts will constitute a negligible danger, or at least no more of a danger than to any of the other operations (including of course injury to the astronaut himself).

(f) Photometric Conditions. Lunar surface photometric conditions have been extensively examined [3, 4, 5] to determine that the terrain photography described in the study is practicable, and it appears that such photography is certainly possible, in spite of the singular properties of ground reflectance and luminescence. Moreover, experience of the Ranger photographic mission confirms that shadow effects and the varied luminance of ground slopes permit excellent results. The questions of photographic identification of natural terrain features with a low albedo contrast and color differentiation have also been considered. Application of Fedorets' photometric function studies and other analyses indicate that luminances of the terrain feature facets vary moderately but not strongly [4, 5]. There will be low contrast among sun-lit features looking in the direction away from the sun; the sun-lit horizons showing against a black sky and the shiny surfaces of survey targets (suggested below) will stand forth brilliantly.

(g) Gravity. The low value of the acceleration of lunar gravity, about 164 cm/sec^2 is presumed to favor astronaut mobility and the handling of equipment. It will also obviate some difficulties with the flexure of instruments. There appears no reason to doubt that it can readily be sensed by plumb lines or level bubbles, although the time required to reach equilibrium will be longer.

(h) Lunar Rotation. The slow lunar rotation favors the use of a fixed camera mount to take trailed star photographs, i. e., eliminates the necessity of using an equatorial mount. Other things being equal, for a given exposure, star trails will be only $1/27.5$ as long as for a terrestrial photograph (hence more point-like), and the limit of photographable faint stars will be extended $3\frac{1}{2}$ stellar magnitudes from this cause along. Photographs of a rapidly moving Orbiter or the CSM will require a shutter. The slow lunar rotation also causes the timing of astronomic camera observations to be less critical than on earth, except in the case of exposures involving orbiting spacecraft.

D. DIRECTION OF THE STUDY

Under direction of Mr. Bernard A. Claveloux, Senior Engineer, who monitored and participated in all phases, the study was broken down into four areas of investigations as follows:

1. Lunar Surface Measurements

Under the direction of H. MacDonald Harper, Geodetic Engineer, a team comprised of Thorsten L. Gunther, Geodetic Engineer, Carl I. Aslakson, USC&GS (ret.) and Floyd W. Hough, Geodesists, a broad range of measurements was investigated, including some 22 techniques and methods for achieving them. Trade-offs were made in the light of mission constraints and selenodetic value of the measurements, with the result that only six techniques and the resulting measurements were selected as comprising a workable system of substantial value.

2. Use of On-Board CSM Equipment for Selenodetic Measurements

With mathematical analysis and advice supplied by Dr. Edward R. Dyer, Jr., applied Mathematician and Astronomer, a team composed of Dr. Alan D. Morris, Physicist and James S. Reece, Mathematician, examined the possible use of the optical alignment telescope, landing radar, scanning

telescope and space sextant as means of obtaining selenodetic measurements, and considered the types of measurements that might usefully be made from the CSM. Proposals to include substantial new equipment for selenodetic data, such as stereographic cameras and long-range ranging devices, although attractive, were ruled out of consideration by the ground rules of the study. As a result, all possibilities were eliminated except use of the SXT which, with what appears to be minor modifications, offers exceedingly attractive possibilities. A complete system and operational method for the use of the SXT was derived by this group.

3. Analysis of Orbiter Photographic Coverage

This phase was handled exhaustively by Dr. Heinrich K. Eichhorn-von Wurmb, with some assistance from Dr. Dyer, in order that a thorough understanding and appreciation could be gained of the quality of lunar mapping which will be obtainable from the presently planned programs. These results were coordinated with the other study groups in order that all measurements recommended could be mutually supplemental and beneficial.

4. Environmental Factors and Review of Available Equipments

Under the direction of Elliott B. Roberts, Captain USC&GS (ret.) an investigation was made of environmental and mission constraints and their effects on selenodetic operations. Terrestrial surveying techniques and equipment that might conceivably be applicable to the lunar missions were thoroughly reviewed by this group, as were techniques and accuracies of earth-based lunar mapping programs under way at various government agencies.

In addition to the foregoing, contributions were made by Robert K. Salin, navigational systems, Edwin G. Collen, Optical-Mechanical Engineer, Henri A. Richardson, Mathematician, and George T. Bell who directed the preparations of and edited the final report. There was substantial contribution and back-up to this study from output of the Pilotage Navigation Study

(Contract No. NAS 9-3006), especially on the subjects of mission profile, astronaut duties, use of on-board equipment, and human factors elements. It also instilled an appreciation of the value of improved maps for navigation and landing purposes, and probably increased the rating of the value of SXT observations that might be made in connection with selenodetic endeavors.

Although studies proceeded along the four lines and groupings outlined above, all personnel worked closely together in order to arrive at a total interrelated selenodetic scheme which will provide immediate utility to man's exploration of the moon, and form the basis for future expansion of desirable surveys.

E. VALUE OF MAN IN THE OPERATIONS

In all studies undertaken, full consideration was given to the astronauts' capabilities and his presence on the lunar surface or in the CSM. It goes without saying that man has unique ability to recognize and identify objects in the objective world, make value judgments about what is important and what is irrelevant detail in a particular situation, and make decisions on choices between several possible courses of action. The most efficient system is one of man-plus-machine or instruments, in which the foregoing functions are assumed by the man. It is, of course, conceivable that an automated instrumental system can be devised, placed in an appropriate location, and instructed simply to collect all data of certain types, the types being made inclusive enough to avoid missing any data of importance. The result is that the system amasses great quantities of detailed data, mostly superfluous, which still must be presented to a man for evaluation, selection, and interpretation. A system whereby these functions can be exercised during the data collection process itself is greatly to be preferred. Recommendations of this study are based upon utilizing the astronauts' identification, selection and judgment capabilities, with instruments utilized to measure and record.

SECTION II

REPORT SUMMARY AND RECOMMENDATIONS

A. RECOMMENDED MEASUREMENTS

1. Basis of Recommendations

In reviewing possible measurements or experiments in order to select those that will produce the most important results per unit of time and effort, attention was directed to the following factors: (1) provision of an adequate number, selenographic distribution, and accuracy of control points over the largest possible part of the moon's surface accessible to coverage by Apollo and lunar Orbiter missions, necessary to tie the area together in some single coordinate system; (2) provision of an adequate number of control points to carry out reliable transfers between the several coordinate systems, in particular the following four systems or sets of systems: (a) the system of current lunar maps (actually several different subsystems, as derived by different research agencies); (b) a barycentric coordinate system describing the position of a circumlunar vehicle with respect to the moon's center of mass, and derived ultimately from terrestrial tracking data (actually also several subsystems, one for each of the circumlunar vehicles); (c) the system attached to a photographic survey carried out by a lunar Orbiter, which will resemble systems of type (a) or type (b) in varying degrees, depending on what controls are applied to the photogrammetric reductions; and (d) an ideal selenodetic system, with the axis of symmetry aligned with the mean axis of rotation of the moon as embedded in the physical body of the moon, with the correct value of the radius from the moon's center of mass to a datum point on the surface, and the other parameters that make up a complete selenodetic datum. (See Section III)

Parameters to describe the departures of the moon's gravitational field from spherical symmetry or, what amounts to the same thing, departures from spherical symmetry of an equipotential surface approximating the real surface, should some day be determined and added to make up a complete datum, although these steps are beyond the scope of anything that can be

accomplished during the Apollo missions, except possibly by refined treatment of the terrestrial tracking data. This is a good example of the kind of information which is required for a complete selenodetic description, but which is inaccessible to Apollo operations, and serves to exemplify the fact that in the current study we have tried to take a long-range view. This view has influenced what is included in the recommendation in the following respects: (1) None of the procedures recommended is a blind alley; that is, none of them represents work that would later have to be undone. (2) Some procedures are recommended which cannot be expected to yield important results on a single landing, but which will come into their own with repeated landings and extended coverage: astronomical position determinations and surface gravity measurements are good examples of such results. (3) Some activities and techniques are recommended, not so much because of what they are expected to accomplish during the first several Apollo landings, but because they will provide the groundwork and experience for learning exactly what can or should be done in the long run: local surveying techniques fall into this category.

Recommended measurements comprise the following:

2. Lunar Surface Measurements

(a) Determination of more exact terrestrial right ascension and declination of the lunar celestial pole, both instantaneous and as they vary with time. A knowledge of the direction of the moon's axis of rotation in celestial coordinates would lay the foundation for astronomical selenodesy (analogous to its terrestrial counterpart). It would simplify the later determination of astronomical coordinates for any point on the moon's surface (see (b) below) and make possible eventual determinations of deflections of the vertical, and the geophysical information about detailed internal mass distribution that the deflections reveal. It would make possible a determination of the wandering of the lunar pole, which would also yield geophysical information about the mass and internal rigidity of the moon. Variation with time of the lunar celestial poles would be a direct measure of the physical librations, which are a function of the generalized large-scale

mass distribution in the moon. (Obtaining a sufficiently dense time sequence of such observations for this purpose will probably be difficult, and the observation from earth of beacons emplaced on the moon may be more effective -- see (d) below.)

Coordinates for lunar navigation would incidentally be improved, but in no very significant way, since the error arising from the present uncertainty of 0.01° or so in the location of the lunar celestial pole contributes only 300 m to an error of an astronomical fix on the surface, and contributes nothing to the error of relative position of two fixes. This matter is mentioned again under (b) (iii) below.

(b) Observation of the astronomical position and a reference azimuth at the landing site. This observation would accomplish the following in whole or in part: (i) it would furnish an improved zero-point datum for a system of selenocentric latitudes and longitudes for any selenocentric system, i. e., one that is a better fit to the moon's real axis of rotation; (ii) other sites can be occupied later and tied to the first site so that intercomparison between astronomic positions and selenodetic position will give deflection of the vertical and hence information on mass distribution; and (iii) even if subsequent sites are not tied to the first site by a common selenodetic net, it would be useful to have astronomic fixes at all sites in order to establish the relative positions of any two sites with an uncertainty no greater than the combined uncertainty of the astronomic fixes at the two sites, plus the (unknown) differences of the deflection of the vertical at the sites.

(c) Photography of the CSM against the star background. This photography will complement observations made with the SXT aboard the CSM to determine the position of the landing site in the barycentric coordinates system of the CSM, and will be useful in making transfers between the barycentric system, the system of existing lunar maps, the local survey system, and the eventual selenodetic system (including the selenocentric astronomical system). If SXT observations from the CSM are unsuccessful or infeasible, observations of the CSM from the surface become essential, for

they would provide the only link between the barycentric system and the others.

(d) Emplacement of a beacon to be observed from the earth. Observation of the location of beacon from the earth and the motion of the beacon with respect to the moon's center of mass would aid in determining the physical librations of the moon better than they are known at present. In addition, coordinates of the beacon in terrestrial tracking coordinates could be used as a datum tie between terrestrial tracking coordinates (and hence barycentric CSM coordinates) and coordinates referred to a lunar surface datum.

There is some question whether the beacon should be an optical beacon (probably a mirror or corner reflector for a laser beam) or a radio beacon. The advantage of an optical beacon is that it provides a point that can be observed precisely in at least two degrees of freedom (transverse to the line of sight) -- three if ranging with a laser is possible -- and would be most useful near the center of the moon's visible hemisphere. By contrast, a radio beacon provides information only in one degree of freedom (along the line of sight), and is truly useful for librations only near the limb. On the other hand, a radio beacon can be observed any time it is above the terrestrial horizon of the tracking station, while a laser reflector requires a powerful cooperating terrestrial laser with a clear sky above it, and the geometry of the reflection of sunlight from a mirror limits its observability still further, unless one goes to a mirror size unmanageably large for the Apollo missions. Decision on the type of beacon is reserved until more is known about probable technological advances during the next several years.

(e) Gravity observations. Gravity observations will undoubtedly be made in connection with the geological and geophysical efforts, and they also will be useful in the long run for higher precision mapping, i. e., in combination with measurements of deflections of the vertical, or to predict the deflection at untied points. Even though such deflections will not be of practical selenodetic value until large area surveys are under way, measuring the

moon's acceleration of gravity at even a single point on the moon surface will be useful either (i) to obtain a value for the moon's radius independent of other methods of measurement; or (ii) to obtain a sample of the lunar gravity anomaly which (if it is very different from zero) would suggest the order of magnitude of other anomalies to be expected, and perhaps provide a guide for future surveys. (To obtain (i), (ii) must be assumed, and vice versa.)

(f) Establishment of horizontal and vertical control in the vicinity of the LEM. If the top of the LEM can be used as an observation post (and assuming there are no measurable landmark features appearing above the horizon), visibility will be limited by the curvature of the moon's surface to approximately 5 km, so that any control network will cover about 80 km^2 . If observations must be made from the ground, visibility will be about 2.5 km resulting in an average visibility of approximately 20 km^2 . In the fortunate circumstance that identifiable distant features can be observed and measured, the controlled area will be considerably larger, but the accuracy of control will deteriorate because of either too short a baseline or the difficulty of ranging to more distant landmarks. In any event, a control network consisting of directions (two angles, referred to a definite coordinate system, e. g., the stars) and ranges from the LEM to identifiable landmarks (or artificial reflectors) would be valuable to:

- (i) provide a local reference system for detailed mapping of the landing area which may be accomplished in connection with geophysical and geological exploration;
- (ii) provide accurate control for lunar Orbiter or other photography which may cover the landing area;
- (iii) provide ties between a provisional selenodetic datum, including the astronomic coordinates obtained in (b) above, and existing maps; and
- (iv) constitute a practical experiment to determine the problems and practicalities in performing selenodetic surveys during future missions.

Suggested means of supplying control with a precision of $\approx 1:5000$ include the use of a panoramic camera, and laser ranging to artificial targets. Control to an accuracy of $\approx 1:2500$ can be accomplished by establishment of a short base, or by photographic stadiametric methods.

As more landings are made and the range of exploration around the landing areas becomes greater, the coverage, accuracy and value of such networks will be increased. In fact, one of the most important consequences of the surface operations during the initial landing may be the development and refinement of selenodetic techniques in order that full advantage can be taken of later extended missions.

3. Use of Equipment On-Board CSM for Selenodetic Purposes

Analysis of results which may be achieved by lunar Orbiter photography of the type presently planned, indicates that it should provide map coverage of a number of 200 km x 200 km squares within which precisely identifiable landmark features will have a relative accuracy of ± 65 meters and which can be tied to the map system of control points with an error of ± 30 -250 meters, depending upon accuracies and numbers of control points available. To approach the high precision end of this range of uncertainty, it will be necessary to provide 100 control points (landmarks with known coordinates) having an accuracy somewhere around ± 200 meters in the desired coordinate system. The most optimistic projections of NASA-MSR, however, predict about 40-50 control points within a map square with an accuracy of ± 200 meters at the center area of the visible face of the moon, degrading to approximately ± 1000 meters toward the limb. This deficiency of control points in accuracy and distribution limits the utility of lunar Orbiter photographic missions, and the accuracy of maps resulting therefrom or from earth-based observations. It is recommended, therefore, that:

(a) SXT observations be made from the CSM of selected landmark features. As described in body of the report, a minor modification to the SXT (consisting of making the attenuating neutral filter in the fixed line of sight interchangeable to the movable line of sight), and the addition of a small removable photographic recording camera that can be fastened to the SXT at the eyepiece crook, will permit observation and recording of the positions of from ≈ 50 to ≈ 200 landmarks, depending upon the desired accuracy of the fixes, distances of the landmarks from the subsatellite

track, and the astronauts' duty schedule. (See Section XI.) The landmark positions could range from close to the subsatellite track out to ~ 600 km each side of the track, and could have an accuracy for each degree of freedom of approximately ± 15 m per single complete observation (close to the track) to several times this amount (far from the track). This is the uncertainty of the position with respect to the CSM. If the error of the CSM position with respect to the moon's center of mass is 50 m, the total resultant error of landmark location would be 50-100 m. If the CSM error is as large as 200 m, the total landmark location error would be little larger than 200 m. (see Section III.) These points would thus have an accuracy better than could be obtained by earth-based methods, and would represent a substantial contribution to the control of lunar mapping done by Orbiters or otherwise. (Terrestrial tracking of lunar surface beacons could provide slightly better accuracy, but emplacement of a commensurate number of beacons similarly distributed is not feasible.) They could also provide navigation references outside Orbiter coverage.

(b) Carrying out the same SXT measurements visually rather than photographically, if photography proves infeasible. If the SXT cannot be modified and the camera added, the same angle measurements (but a smaller number) can be made by the astronaut visually and recorded; however, resulting errors will be an order of magnitude larger, ranging from ± 150 meters for landmarks close to the subsatellite track, to perhaps 1 km for landmarks on the skyline, all with respect to a mean barycentric CSM position. The total error in barycentric coordinates would thus be approximately ± 160 meters for close landmarks, increasing to about 1 km at extreme range. Inasmuch as the horizontal coordinates of control points near the center of the moon can be established from earth-based operations (hopefully) to an accuracy of ± 200 meters, but degrading to about ± 1000 meters toward the limb, these observations would be of benefit for horizontal control in the limb areas, and vertical control near the center. This would be of some value, and the exercise would determine the utility and validity of these observations for future missions, or the validity of modifying the SXT on future missions.

B. COORDINATION WITH LUNAR ORBITER PHOTOGRAPHY

As indicated earlier, the analysis of the potential results of lunar

Orbiter photography (see Appendix A), shows that with the proper distribution of reasonably accurate control points, excellent mapping can be accomplished. The analysis also shows that, with an appreciable modification of the lunar Orbiter camera configuration, (namely the addition of a star camera back-to-back to provide precise orientation data) the accuracy can be further increased.

It is therefore recommended that additional study be given to the sequence of orbiter missions, including planned orbits, regions to be covered, and control requirements in order that the resultant photography can be fully supported by the potential SXT landmark positioning that the astronauts may be able to provide during Apollo missions. Furthermore, with close coordination between the Apollo and lunar Orbiter programs right up to the time of the Apollo launchings, detailed lists of control points in the regions to be surveyed can be selected and the particular points observed which will be of greatest value to control extension procedures involved in the lunar mapping programs.

C. LANDMARK IDENTIFICATION STUDIES

Throughout this study, the problem has continually arisen and the questions asked "What is a well-defined landmark? What will be the problems of identification of landmark features?"

None but obvious answers have become apparent during the study because of the still limited knowledge of the character of the lunar surface at the scales of interest. The problem, however, is a very real one, lying more in the realm of photo interpretation. As more large-scale lunar photography becomes available, it should be continually studied and simulation exercises undertaken in the rapid identification and selection of, and centering on, suitable features.

D. EQUIPMENT TO BE DEVELOPED

Accomplishment of measurements and experiments recommended will require development of up to ten items of equipment as shown in Chart IV

(depending upon the amount of weight that can be carried, and the amount of astronaut's time that can be utilized for selenodesy) and a minor modification to the space sextant. These developments should begin at once in order that there will be adequate time for engineering design, instrument construction and testing for reliability, durability and accuracy.

In approaching these developments, the following priorities are suggested:

1. Inasmuch as the fixing of well-defined landmark features by means of space sextant photography appears to offer the greatest benefits with the minimum expenditure of weight and astronaut's time, it is strongly urged that the space sextant modification suggested in Section XI be investigated at once so that the modification can be incorporated in the equipment. Design of the SXT recording camera would then proceed concurrently.
2. Decision should be made at an early date as to whether or not both the panoramic camera and the precision frame camera can be carried on the missions. If they can, development of both should proceed; if they cannot, the precision frame camera can be constructed in such a manner as to provide the necessary measurements.
3. Decision should be made as to whether or not the top of the LEM can be used as an observing platform and such use provided for, in order that proper camera supports can be developed.
4. For the highest accuracy of results, the laser ranger is a key item of equipment. In order to fulfill accuracy requirements, development should begin at an early date.
5. No comments are being made regarding development of the gravimeter, as that item is being provided for geophysical purposes. Other items listed in the chart can probably readily be developed.

Development efforts should include:

1. Detailed engineering design.
2. The best in rugged and precise construction.
3. Extensive tests under simulated lunar conditions to determine: reliability, durability, repeatability, handling characteristics and accuracy of reduced data.

Continuous attention should be given to the state of the art relating to these items of equipment up to the latest possible time when any modifications could be made. This is particularly true relative to design of equipment supports to be used on the lunar surface and the design of the laser ranger; however, the other items of equipment could be frozen much earlier.

E. ASTRONAUT TRAINING

All equipments and systems have been designed to require minimum effort and specialized training on the part of the astronauts. This is particularly true with regard to the lunar surface measurements. However, training and simulation exercises must be conducted in pressurized space suits in a topographic environment as comparable to the moon as possible in order for the astronauts to have a thorough understanding of the procedures involved, and to gain manual dexterity and a realistic time schedule for the operation.

With regard to SXT observations, the following is recommended:

1. The astronauts must be thoroughly trained in lunar terrain feature recognition and landmark identification. This will undoubtedly be undertaken in connection with navigational exercises, and it will have equally valuable application here.

2. A considerable amount of dexterity will be required to fix on the reference stars and the desired landmarks accurately enough to make the results useful for selenodetic purposes. Intensive exercises in a simulator should be undertaken in order to achieve the necessary proficiency.

Inasmuch as all data will be recorded either photographically, or verbally on tape, and reduced by post mission analysis, no training in this area will be required.

F. DATA REDUCTION

Reduction of photographic data contemplated in these experiments will be by well established standard techniques utilized for similar type observations on earth; and these methods are not detailed in this report. The possible exception is the utilization of a panoramic camera for astronomic observations; so formulas for this purpose have been derived and are included in Appendix D.

As a byproduct of the error analysis made to determine the potential accuracy of control points and mapping that could be derived from lunar Orbiter photography, mathematical concepts and formulas were derived which if applied would represent a refinement in precision of results as compared with current practices. This mathematical analysis is also presented in Appendix A .

G. SUMMARY CHARTS AND TABLES

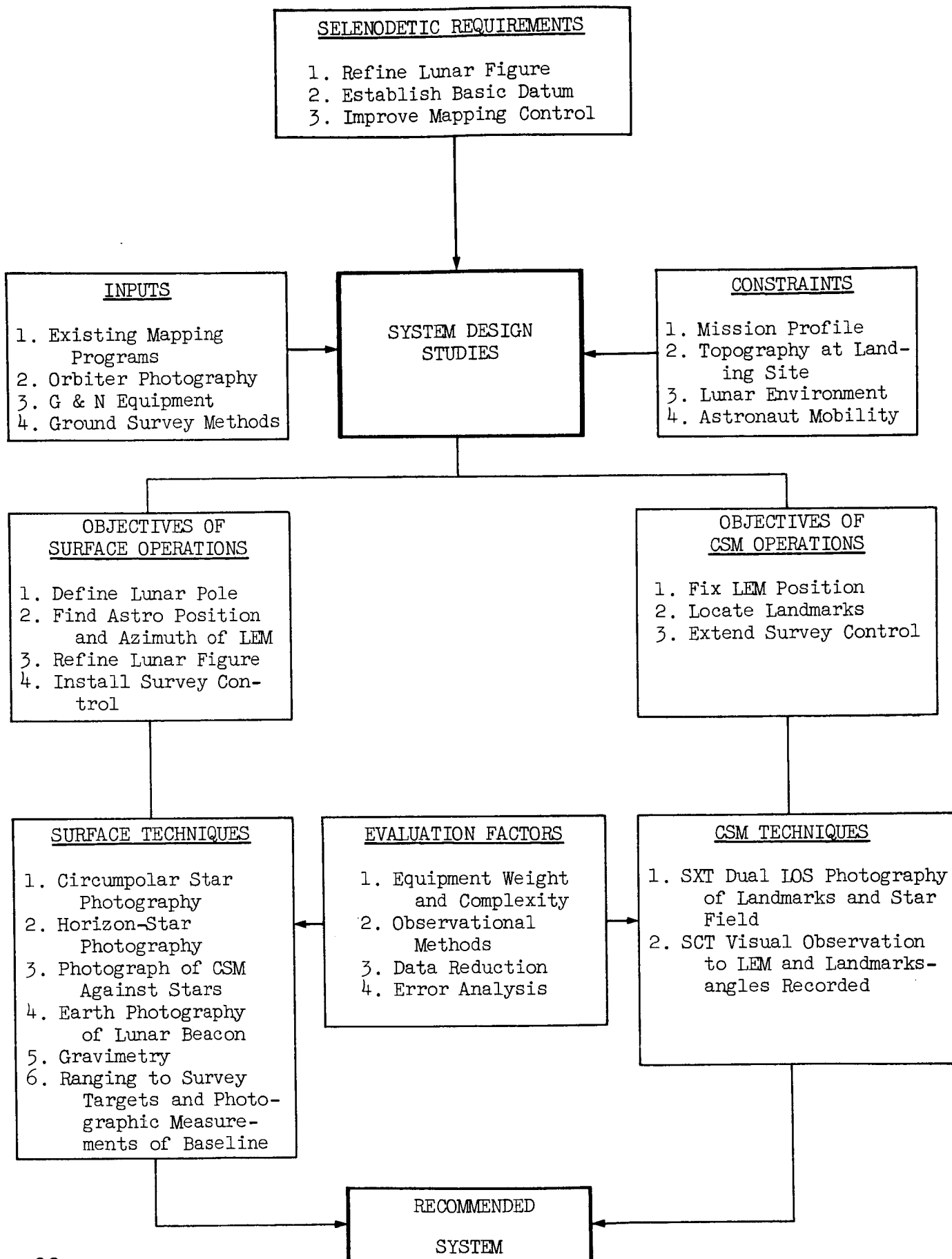
Tables which follow summarize in condensed form the course of the study and its conclusions.

Chart I is a flow chart of the study process and lists recommended techniques.

Chart II shows a tabulation of the six lunar surface techniques listed in Chart I, including objectives to be achieved, instrumentation needed and estimated accuracies of results.

Chart III summarizes the two methods of making observations from the CSM, giving procedures and expected accuracies.

Chart IV summarizes the proposed equipment recommended for lunar operation including pertinent characteristics, and size and weight.



SUMMARY CHART II

PROPOSED SURFACE MEASUREMENTS AND ESTIMATED RESULTS

OBJECTIVE	TECHNIQUE	INSTRUMENTS	ESTIMATED ACCURACY
Position of Lunar Pole	<u>Circumpolar star photography.</u> Photograph polar star field every 12 hours.	Precision frame camera	± 7 seconds
Astro Position and Azimuth Reference	<u>Horizon-star photography.</u> Obtain series of photos of horizon-star field.	Panoramic camera	Position and azimuth within ± 10 seconds
Position Relative to CSM Orbit	<u>Photography of CSM.</u> Photograph CSM against star background in different portions of its orbit.	Precision frame camera	Position within 25 m. of known CSM position
Physical Librations	<u>Optical beacon at landing site.</u> Leave optical beacon for observation from earth.	Optical beacon-mirror or corner reflector	
Acceleration of Gravity	<u>Gravimetry.</u> Gravity reading observed while in LEM.	Gravimeter	± 10 milligals
Local Horizontal and Vertical Control	1. <u>Horizon photography and laser ranging.</u> Eject survey targets (balloons). Photograph landscape and obtain distances to targets. Observe from top of LEM. 2. <u>Horizon photography from baseline.</u> Eject survey targets (balloons). Measure baseline distances by photographing LEM. Photograph landscape from ends of baseline.	1. Panoramic camera (as above). 2. Laser ranger. 3. Survey targets - ReflectORIZED mylar balloons w/launcher. 1. Panoramic camera (as above). 2. Precision frame camera (as above). 3. Surface targets (as above). 4. Stadia targets on LEM.	Control points to distance of ≈ 5 km within ± 3 meters. Control points to distance of ≈ 2.5 km within 3 meters.

SUMMARY CHART III

PROPOSED CSM TECHNIQUES FOR POSITIONING LEM AND LUNAR LANDMARKS

METHOD	PROCEDURE	COMMENTS
SXT dual line of sight photography of lunar landmark and star field	<p>Attitude of CM is changed by astronaut to bring SXT fixed LOS to desired star field. SCT in 00 mode is used as aide for selection of star field. SCT in slave mode drives SXT movable LOS to target. IMU not required. Obtain photo of landmark and superimposed star field. Record SXT angles and time of photo observations.</p> <p>IMU is fine aligned. CM attitude controlled by G and N system to drive SXT fixed LOS to desired star field. SCT is used in slave mode to drive SXT movable LOS to lunar landmark. Obtain photo of landmark and superimposed star field and record SXT angles and time of photo recording.</p>	<p>High precision ≈ 20 seconds. Requires minimum CSM electrical power and attitude control fuel.</p> <p>High precision ≈ 20 seconds. Minimizes astronaut work load.</p>
SXT visual observation to LEM and landmarks.	IMU is fine aligned. SCT used to visually sight on landmark. Time and angle recorded.	<p>Low Precision ≈ 1 mr. Depends on visual sighting capability and IMU alignment.</p>

SUMMARY CHART IV

PROPOSED EQUIPMENT FOR SELENOTETIC OPERATION ON LUNAR SURFACE

Item	Descriptive Data	Size (inches)	Volume (cu. ft.)	Weight (lbs)	Quantity Needed
Panoramic Camera	Lens: 100 mm focal length, $f/3.5$. Field of view: 25° vertical, 350° horiz. Focal plane: cylindrical Image format: 60 mm x ~610 mm (70 mm roll film) Metric accuracy: 10 arc-seconds	10 x 10 x 15	0.9	15	1
Precision Frame Camera	Lens: 150 mm focal length, $f/3$ Image format: 110 x 110 mm (125 mm roll film) Metric accuracy: 5 arc-seconds	8 x 8 x 8	0.3	5	1
Laser Ranger	Semi-conductor laser Range: 300 m - 5 km (20-30 km desirable) Range resolution: 1/5000 Power: 100 watts (average)	8 x 8 x 30	1.2	15	1
Balloon Survey Target	10-foot diameter, reflectorized mylar balloon.	2 x 2 x 4	0.01	1	5
Balloon Launcher	Cylinder for gas cartridge projector; base plate and elevation angle indicator.	10 x 10 x 20	1.2	15	1
Gravimeter	Pendulum or miniaturized Worden.	4 x 4 x 12	0.1	1	1
Stadia Targets (Top of LEM)	Two 50 mm circular targets on calibrated invar wire w/bracket for top of LEM.	2 x 2 x 30	0.1	1	2
Camera Support (Lunar Surface)	Tripod support with leveling head and centering rod.	5 x 5 x 30	0.4	5	2 or 3
Camera Support (Top of LEM)	Bracket, w/azimuth circle and leveling head.	2 x 10 x 10	0.1	2	1
Optical Reflector	Collapsible mirror or corner reflector	6 x 12 x 12	0.5	1	1

SECTION III

PROBLEMS INVOLVED IN ESTABLISHING A TRUE SELENODETIC COORDINATE SYSTEM AND TRANSFORMATIONS BETWEEN COORDINATE SYSTEMS

A. INTRODUCTION

Before proceeding with discussions of means of implementing selenodetic measurements during the Apollo missions, it would seem useful to define the essence of selenodesy itself and to highlight the problems which selenodesy is endeavoring to solve.

For purposes of this discussion, selenodesy will be defined as "the science of measuring the size and shape of the moon and determining positions and distances thereon". This implies the establishment of a lunar coordinate system suited to accomplish this purpose with appropriate accuracy. Inasmuch as one of the objectives of such an endeavor is to permit the picking of landing sites on the lunar surface and accurate navigation to these landing sites, suitably accurate transformations must also be possible from the lunar coordinate system to earth-based coordinate systems, in which tracking data are accumulated and guidance and navigation maneuvers defined and oriented, and vice versa.

Perhaps the best way to sketch the problem of interrelationships of the various coordinate systems involved is to consider the guidance requirement of the Apollo spacecraft system and its LEM. It has been specified that the guidance and control systems of the Apollo vehicles, using position and velocity data originally obtained from terrestrial tracking stations, but later referred to other coordinate systems and thus making use of transformations between the coordinate systems, should be capable of bringing the LEM to a safe landing on a preselected site on the moon's surface, with a c. e. p. of no more than 0.5 nautical miles (900 meters approximately). This requires that the "position error" of the spacecraft be no greater than 1500 feet (450 m approx.). The expression "position error" is set in quotation marks here to indicate its ambiguity, namely, "position error with

respect to what coordinate system?" To resolve this ambiguity we must consider a series of coordinate systems, errors in each, and errors in transformations between them. (There are, of course, errors in the guidance and navigation equipment and its operation which are not our concern in this analysis.)

B. COORDINATE SYSTEMS INVOLVED IN THE PROBLEM

For the sake of clarity, it is advisable to set forth a few explicit definitions, elementary and commonplace though they may be, as we shall be dealing with a number of coordinate systems, some of which closely resemble each other and invite confusion.

In what follows, the distinction between a spherical (polar) coordinate system and its associated righthanded rectangular (Cartesian) coordinate system will be disregarded: they will be treated as two interchangeable representations of the same system. If the z-axis (x_3 -axis in vector notation) of the Cartesian system is the axis of symmetry of the polar system, and the xy-plane (x_1x_2 -plane) of the Cartesian system is the "equatorial" plane of the polar system, then the rectangular coordinates (x, y, z) are related to the polar coordinates (r, θ , ϕ) by the equations:

$$\begin{aligned} x &= r \cos\phi \cos\theta \\ y &= r \cos\phi \sin\theta \\ z &= r \sin\phi \end{aligned} \qquad \begin{aligned} r &= (x^2 + y^2 + z^2)^{1/2} \\ \theta &= \arctan(y/x) \\ \phi &= \arcsin(z/(x^2 + y^2 + z^2)^{1/2}) \end{aligned}$$

From these equations it is obvious that we have adopted the astronomical-geophysical convention of measuring the second angle ϕ from the "equatorial" plane (xy-plane), positive "northward" or "upward" (toward positive z) and negative "southward" or "downward" (toward negative z), rather than the usual mathematical convention of measuring the second angle ("polar angle") from the positive z-axis. Thus, in our case, ϕ ranges from $-\pi/2$ to $+\pi/2$, rather than from 0 to π . Furthermore, the equations show that $\theta = 0$ in the xz-plane, and increases in a counterclockwise direction if viewed from the positive z side of the xy-plane.

It will sometimes be convenient to treat (x, y, z) or (x_1, x_2, x_3) as a vector and denote it by \bar{x} ; also to rotate \bar{x} by an angle α around one of the axes x_i and to denote the corresponding rotation matrix by $R_i(\alpha)$. The error, sometimes used as equivalent to standard deviation, of a quantity q will be denoted E_q in this section. The error analysis in this section is not intended to be sophisticated or exhaustive; it is only intended to show clearly their nature and some of the effects they produce.

We shall be dealing with the following coordinate systems, which will be defined and examined:

- Type I: terrestrial topocentric systems, with the terrestrial tracking station at the origin.
- Type II: geocentric systems, with the earth's center of mass or attraction at the origin.
- Type III: selenocentric systems, some with the moon's center of mass or attraction at the origin (Type IIIa), others with the moon's center of figure at the origin (Type IIIb).

(The fact that these systems are not identical is one source of difficulty to be examined. It is also one source of confusion.)

- Type IV: lunar topocentric systems with the LEM, or nearby defined point on the moon's surface, as the origin.

C. ELEMENTS OF THE PROBLEM OF TRANSFERS BETWEEN SYSTEMS

There now follows an outline of the elements of this problem, which will also serve as an outline of what remains to be done. Take the problem in its most stringent form: a requirement to direct a vehicle to a point on the moon's surface, selected from a photograph of the lunar terrain, with a c. e. p. of 900 m. The elements involved in carrying out this requirement form a sort of chain, which is outlined below.

1. Link 1. At the outset, the Apollo vehicle is tracked from a DSIF station on the earth; and the observed quantities are the position and velocity vector of the vehicle with respect to that station in topocentric coordinates, probably altazimuth (Type I). These observations are affected by uncertainties due to the performance of the equipment and the uncorrected effects of the environment, such as propagation errors. Symbolize these errors by E_1 (the symbol is not intended to be an algebraic quantity or quantities).
2. Link 2. Next, the position and velocity vectors of the vehicle are represented in geocentric Cartesian coordinates with origin at the supposed center of attraction or mass at the center of the earth (Type II). (Unless the mass of a body is distributed very unsymmetrically, the center of attraction, the center of mass, and the center of figure can all be taken to be identical.) To make the transfer from topocentric coordinates (I) to geocentric coordinates (II), the radius vector of the tracking station and its velocity due to the earth's rotation are used. The transfer is thus affected by the uncertainty in these quantities, due to an imperfect knowledge of (i) the location of the station with respect to a particular geodetic net, and of (ii) the goodness of fit of the geodetic datum to the real earth, i. e., its "ties" to a hypothetically perfect world system; or (iii) in some cases, errors of direct ties between the station and coordinate system II, carried out by analyzing "station errors" in tracking data. Item (ii), of course, includes any uncertainty in the earth's radius. Call the collective effect of all these uncertainties E_2 .
3. Link 3. At a later stage, the Apollo vehicle (CSM and LEM still fastened together) is injected into a circumlunar orbit. After a certain amount of tracking data is accumulated, a circumlunar orbit and ephemeris can be computed, with positions and velocities still in geocentric coordinates (system II). The orbit would be greatly simplified by a transformation of coordinates to a new origin, namely its own attracting focus in the moon, which is,

of course, the center of mass of the moon. The Keplerian elements of an unperturbed orbit a (semimajor-axis), e (eccentricity), and T (time of pericentric passage) or its equivalent M_0 (mean anomaly at epoch) are invariants in the geometric-transformation sense of the word; and the angular elements i , ω , and Ω are invariant to within an arbitrary constant, depending on the orientation in space of the reference plane and direction, i. e., the orientation (Euler) angles of the selenocentric coordinate system. In the original solution carried out in geocentric coordinates (II), the coordinates of the attracting focus inside the moon, which we shall take to be identical to its center of mass or barycenter, can in principle be treated as unknowns, and solved for. To treat the geocentric coordinates of the moon's barycenter of attraction as completely unknown would lead, however, as we shall see, to enormous and unnecessary complications; furthermore, this procedure would amount to discarding the already quite accurate information we have on the motion of the moon's barycenter around the earth accumulated over centuries of observation. Therefore, a solution in which the geocentric coordinates of the moon's barycenter are treated as approximately known, and small differential corrections to those coordinates are treated as unknown, is definitely to be preferred. Either way, the solution will lead to a set of geocentric coordinates of the moon's barycenter, which will serve as the origin for the new system of selenocentric coordinates. We shall call such a system a "barycentric system", (Type IIIa) understanding that it refers to the center of mass of the moon. ("Selenobarycentric" might be a more precise expression, but seems too cumbersome.) The "improved" geocentric coordinates of the moon's barycenter (which are time-dependent) provide the tie to make the transfer between geocentric and the new barycentric systems.

The foregoing solution seems to involve no further original sources of error than E_1 and E_2 ; but the solution for the differential corrections to the geocentric coordinates of the moon's barycenter

will have errors that are functions of errors of types E_1 and E_2 , and of the variables. Furthermore, it seems likely that the solution for the coordinates of the moon's barycenter may be affected by systematic errors due to the peculiar distribution of the circumlunar tracking data. For instance, the fact that the Apollo vehicle cannot be tracked behind the moon might be expected to permit errors analogous to errors of closure to arise. Such errors would tend to smooth out during the course of a lunation as the gap in the tracking data moves around the orbit, but the Apollo vehicle will be tracked for at most two or three revolutions before the LEM is released for descent. Also, tracking by range data and range-rate data (with directional data having lower weight) leads to solutions analogous to the solution of double-star orbits from spectroscopically determined Doppler shifts: in these solutions the semimajor-axis a , and the inclination of the orbit to the plane of the sky I occur only in the product $a \cdot \sin I$, and hence cannot be separated. Also the position angle of the line of nodes (intersection of orbital plane with the "plane of the sky", perpendicular to the line of sight) is completely indeterminate. In our case, however, these effects may not be especially severe. This whole subject will be treated in greater detail below.

4. Link 4. The next step involves a transfer from the set of (lunar) barycentric coordinates just described, i. e., those in which the circumlunar orbit or ephemeris of the Apollo vehicle are expressed (Type IIIa), to a quite different set of selenocentric coordinates corresponding to some lunar map; for instance, the ACIC, AMS, or similar systems (Type IIIb). Map systems of this type are typically the result of an over-all least-squares adjustment of the three-dimensional positions of lunar landmarks obtained from (two-dimensional) measurements of the coordinates of the landmark with respect to the apparent limb (or apparent center of the lunar disk) at different librations, the librations providing enough of an equivalent parallactic effect to make a three-dimensional stereoscopic solution. Most recent measurements of the two-dimensional positions of lunar landmarks x' , y' on the plane of the sky have been carried out almost

entirely on photographs, but the reduction of these measurements typically makes use of the earlier heliometer measurements of a number of well determined points as reference points. [6]

The original measurements x'_m , y'_m may correspond to an arbitrary origin and orientation of the photographic plate (just as in the case of photographic reductions of astrometric star positions), or they may be positions relative to some landmarks taken as reference points. In the case of the heliometer work, the measurements consisted of position angle of the heliometer displacement axis (i. e., a line seen against the sky passing through the landmark and the center of the apparent disk) and the arc distance of the landmark from the limb. The measurements are reduced in such a way that the origin of the reduced x' , y' system is supposed to be the "mean libration point"; that is, the point on the surface of the moon in the center of the visible hemisphere whose excursions from the center of the apparent disk, due to the moon's librations, average to zero in the long run. The crater Mösting A, a fairly sharply defined feature near the mean libration point, is used for a primary tie between mapping systems.

Finally, the three-dimensional coordinates of landmarks are fitted to an origin at the center of a sphere which best fits the apparent figure of the moon, with (what we shall call) the x-axis passing through the mean libration point and the z-axis parallel to the moon's (supposed) axis of rotation. Since the measurements are commonly given in fractions of a lunar radius, the scale of the whole system in meters or kilometers is given by the assumed value of the radius of the best-fitting sphere. Such a selenocentric system, with its origin at the center of figure of the moon, might be called "morphocentric" or "selenomorphocentric", in contradistinction to "barycentric" for a center-of-mass system.

There appears to be a discrepancy between the positions of the center of mass and center of figure of the moon, which is almost

without question due to the way a sphere has been fitted to the mean figure. The discrepancy is in the sense that the center of figure is displaced 0.3" to 0.6" (arc-seconds) toward the lunar south pole from the center of mass, corresponding to a linear displacement of 500 - 1100 m. (There might also be a component of displacement in the direction of the moon's x body-axis, but data are too meager to hazard a guess as to the amount.) Chester Watts, author of the atlas, The Marginal Zone of the Moon, (Astronom. Papers AE & NA, Vol. 17, USNO) stated in a private communication that he is satisfied that the discrepancy can be completely explained as follows (somewhat simplified): Near the south pole of the moon, there is a series of mountain ranges parallel to the limb and to each other, so that librations in latitude causes each of these ranges to rise or set behind the one in front of it, in such a way that the ranges maintain an unusually high skyline at the limb, and never allow a view of the lower lunar terrain between the parallel ranges. In order to explain the magnitude of the discrepancy in a simple way, these mountain ranges need only be about 500 to 1100 m higher, i. e., farther from the moon's center of mass, than the average level of the terrain near the south pole. The situation is actually somewhat more complicated than described here; it is discussed by Watts, loc. cit., p. 950-951.

At this juncture, it is not particularly important to pin down in a definitive way the numerical value of the discrepancy or offset of the center of figure from the center of mass, but simply to make allowance for the possibility that one exists when setting up the equations expressing the transformation from barycentric to morphocentric coordinates, and vice versa.

As noted below, we shall call mapping system errors E_3 .

5. Link 5. At this point we take note of the fact that the transformation between barycentric system IIIa to morphocentric system IIIb contains dynamic elements. The instantaneous orientation in space of

of the physical body of the moon, and therefore any coordinate system attached to it, depends on the moon's physical libration, in latitude and longitude, which are functions of the time. Ephemerides of the physical librations are given in the national almanacs, e.g., the American Ephemeris and Nautical Almanac, U.S. Government Printing Office; they are on pp. 314-321 in the issue for 1965. Their amplitude is small ($< 0.04^\circ$), and their uncertainty, i.e., the uncertainty of the direction of the moon's axis of rotation in space, as calculated by the formulas used in the almanacs, is of the order of $\pm 0.01^\circ$ (possibly $\pm 0.02^\circ$ in some cases). This corresponds to ± 300 m, or somewhat more, on the moon's surface.

It is also possible that the body of the moon shifts with respect to the axis of rotation in a way analogous to the wandering of the terrestrial poles. The dynamic stability of the moon's motions require, however, that such a wandering of the lunar poles be small and, in any case, the data are inadequate to detect any such motion. The data are barely adequate to evaluate the physical librations, as exemplified by the numerical information in the last paragraph.

Errors arising from the transfer from the barycentric coordinates of the circumlunar trajectory to the morphocentric coordinates of a mapping system we shall label type E_3 , including those arising from the imperfect knowledge of the direction of the moon's axis of rotation.

6. Link 6. Finally, there are the uncertainties of location of a particular lunar landmark or set of landmarks with respect to its own origin, tied to the craterlet ["]Mosting A. These uncertainties, both present and prospective for 1969, are shown in Table III-1. We see that they range from 220 m for prospective horizontal components near the center of the visible hemisphere to 1300 m for present horizontal components near the limb. The placement of

TABLE III-1

ESTIMATED UNCERTAINTIES IN SELENOGRAPHIC MAP
COORDINATES ESTABLISHED FROM EARTH-BASED PHOTOGRAPHY

(Values in Meters)

<u>Longitude</u>	<u>AMS</u>		<u>Existing</u>		<u>AFCL</u>		<u>MSC</u>	
	H	V	H	V	H	V	H	V
0°	240	830	300	800	250	1350	240	830
30°	660	1000	620	800	720	1180	660	1000
60°	1320	780	830	1000	1190	700	1320	780
<u>Projected</u>								
0°	225	660	250	680	170	900	275	660
30°	475	800	300	590	480	780	475	800
60°	930	570	760	400	790	460	1120	570

The coordinates to which these uncertainties refer belong to a system of map coordinates based on the figures of the moon, i.e., the best fitting circles or sphere, and the center thereof. They, therefore, do not include displacement of center of mass from center of figure which may be as large as 500-1000 meters. These values were compiled by the NASA Manned Spacecraft Center.

a particular landing site (selected from a photograph of the moon's surface) in such a system of map coordinates involves an error of the same general type as that involved in deriving the coordinates of any arbitrary point on the moon's surface. These errors, which we shall label type E_4 , are a compound of (i) the collective systematic error of the particular set of reference landmarks chosen as a reference for the arbitrary point (since this error is the collective effect of the accidental errors of the individual reference points, it may be made comparatively small, simply by using a large enough number of reference points), and (ii) the accidental errors of measurement of the arbitrary point. In the case of a landing site, the contribution of (ii) is likely to be greater than average, because the area will presumably be smooth, without many usable reference points in the immediate vicinity, and hence more difficult than average to define with respect to local coordinates tied to the nearest reference points. The influence of (i) may also be larger than average, if reference landmarks in the neighborhood are scarce.

D. ESTIMATE OF THE MAGNITUDE OF THE ERRORS OF COORDINATE SYSTEMS AND THE TIES BETWEEN THEM

1. Tracking Station Topocentric Coordinates (I): Errors of Type E_1

Here we adopt the estimate given by Bissett-Berman (Capabilities of MSFN for Apollo Guidance and Navigation, Final Report on Contract NASw-688, Amend. 1, 2 March 1964, hereinafter referred to as BB) for Radar A and "lunar rendezvous" situations, based on information obtained from JPL and the Goddard Space Flight Center (p. 4-3 of the report). These instrumental errors are:

RMS error in range r_t , $E_r = 15$ meters

RMS error in range rate \dot{r}_t , $E_{\dot{r}} = 0.03$ meters/sec

RMS error in altitude angle α_t or azimuth β (actually

$\beta_t \cos \alpha_t$), $E\alpha = E\beta \cos \alpha = 8 \times 10^{-4}$ radian

Data sampling rate: 1 sample/min.

The subscript t refers to the "topocentric tracking" coordinate system. These estimates apply for a single tracking station.

The total error E_r also contains a contribution from the uncorrected part of the propagation error. Near 2000 Mc/s, propagation effects amount to possibly 4 to 40 meters, depending on the total electron content per cm^2 cross section along the beam path. The total number per cm^2 depends primarily on the state of the ionosphere and the altitude angle α of the beam. The interplanetary medium contributes very little. To the extent that the state of the ionosphere can be predicted from its correlation with time of day, time of year, geographic location, and level of solar activity, the corrections can be calculated; in any case they can be computed after the fact if data on ionospheric electron density distribution are available. In this way the uncorrected part of the ionospheric propagation error can probably be reduced to 10% of the error -- negligible in comparison to other errors. (See also Bissett-Berman, Appendix K.)

Similarly the total errors, E_α and $\cos\alpha E_\beta$, contain contributions from what might be called ionospheric refraction errors. The latter is affected by horizontal refraction, which is usually smaller than the vertical. The contribution E_α of vertical refraction at 1000 Mc/s is of the order of 15×10^{-6} radians ($< 15^\circ$ from the zenith) to 100×10^{-6} radians ($< 15^\circ$ from the horizon). These are average daytime figures; nighttime refraction is even smaller, and it is smaller at higher frequencies (e.g., the planned frequency near 2000 Mc/s). (See e.g., Handbook of Geophysics, Rev. Ed. USAF/GRD, MacMillan 1960, Chap. 15.) These errors are all smaller than the instrumental angular pointing error; but these effects are systematic at a particular station and should therefore be removed by corrections.

The angular error in pointing at a single station is, of course, too large to contribute any weight to determining position at lunar distances, in that it leads to a transverse error E_p of $8 \times 10^{-4} \times 384,400$ km, or about 300 km at the distance of the moon. (Here p represents a linear coordinate perpendicular to r , or perpendicular to the line of sight.) But it is

nowhere suggested that one will have to rely on radar measurements from a single station to track a circumlunar vehicle with precision.

Let us consider two stations working in concert at the ends of a baseline of length b , but not like the two components of an interferometer, which would require simultaneous intercomparison of the phase of the incoming signal at the two stations. Each station has a range error $E_r = 15$ m. The transverse error along a line parallel to the baseline joining the stations is $E_p = r \cdot E_\psi$, where E_ψ is the error in the angle ψ at either station, subtended by the other station and the vehicle. In other words $\psi = \arccos(\bar{r} \cdot \bar{b}/rb)$, where barred symbols are vectors and unbarred symbols are scalars. (Now p stands for a transverse coordinate containing the component parallel to the baseline.) E_ψ is approximately $(\sqrt{2}/b \sin \psi) E_r$ in which the following approximations have been used:

$$r_1 \approx r_2 = r, \quad \psi_1 \approx \psi_2 = \psi \lesssim \pi/2$$

The error E_b contributes so little to E_p that it makes no difference whether b is perfectly known or not. If we assume that b is a little larger than the radius of the earth for two well-spaced tracking stations, say, 7700 km so that $r \approx 50 b$, then $E_p = 1060$ m.

Strictly speaking, our estimate was based on the situation where the baseline connecting the two tracking stations is approximately perpendicular to the direction to the moon. The full expression for E_p in oblique cases becomes rather complicated, but the approximate expression $(\sqrt{2}/b \sin \psi) r \cdot E_\psi$ can still be used.

The uncertainty E_q in the position of the spacecraft in the transverse direction, perpendicular to the baseline connecting the two tracking stations, will be as large as the transverse error for a single station, unless some constraints are added that make q a function of p and r , for example, a gravitationally controlled trajectory. But in this section we are considering the uncertainties from the standpoint of pure tracking. This discussion shows that it would be desirable to have three tracking stations, arranged

in the largest possible equilateral triangle projected against the "plane of the sky" (plane perpendicular to the line of sight) as seen from the moon. Ideally, they would be distributed in such a way over the surface of the earth that, as the earth rotates, and as a station that is the vertex of a large triangle is rotated to within a few degrees of the earth's east limb (as seen from the moon), another has risen on the west limb. Such an arrangement would be achieved by two rows of tracking stations, one along a zone in middle north latitudes and the other along the corresponding zone of south latitude, spaced say, $1/5$ the circumference of the latitude circle apart ($\approx 72^\circ$ of longitude); but those in the northern row could be offset half a space (about 30° - 40° in our example) east or west with respect to the members of the southern row.

This particular example would thus lead to ten stations altogether. It is, of course, absurd to try to fit such a distribution exactly; even fairly large departures from it do not make much difference. (See also BB, Appendix I and Table 2.3.) The necessity for having pairs of stations spaced sufficiently far apart in latitude in order to reduce the uncertainty of the spacecraft position perpendicular to its own orbital plane (assuming a low-inclination orbit as planned in the Apollo program) is better treated in the section below, in the context of determining the circumlunar orbital plane of the spacecraft.

Clock errors and their effects have already been thoroughly treated elsewhere (BB, Appendices F and J); it is sufficient to note here only the following facts:

- (i) Clock errors will appear in the solutions as errors in the range r , and thus contribute to total E_r ;
- (ii) Clock rate errors will appear as errors in the range rate \dot{r} or in the difference in range $r_{i+1} - r_i$ corresponding to a single observation in which either the number of cycles passing per fixed time interval is counted, or the length of the time interval required for a fixed number of cycles is measured.

- (iii) Where the clock error is identical at two stations working in concert, no error is introduced into the determination of direction; but if the clock error is different, the resulting error affecting only one of the ranges will lead to an error in direction.

Let us consider the effect on the measured direction to a spacecraft, produced by an error in the direction in space of the baseline connecting the two tracking stations. Such an error, E_d , has the effect of being directly reflected in the direction from either of the stations to the spacecraft, as determined by the two stations acting in concert. The location of Station 2 with respect to Station 1 was denoted above by the vector \bar{b} . Let us say that the observed relative location is $b_{obs} = \bar{b}_{true}$ plus a vector displacement error $\bar{E}b$. (The component of the error $\bar{E}b$ aligned with \bar{b} corresponds to the scalar error E_b in the discussion above.) The component of $\bar{E}b$ perpendicular to \bar{b} , which we may designate $\bar{E}b'$, leads to an error in the direction of \bar{b} equal to E_b'/b in amount, and lying in the plane defined by \bar{b} and $\bar{E}b$. If the direction to the spacecraft forms an angle χ with this plane, then the magnitude of the transverse error at the spacecraft due to this cause will be $r \cdot \cos \chi E_b'/b$. If $b = 7700$ km (as before) and $E_b' = 77$ m, then $E_b'/b = 10^{-5}$, and $r \cos \chi E_b'/b = 3.8 \cos \chi$ km. This example, better than any other, brings out the importance of having accurate geodetic ties between tracking stations if they are going to be used in concert to determine accurate direction, without the help of dynamic constraints or input of other data. The best existing estimates of the relative position of two well-determined tracking stations some distance apart (e.g., some of the SAO Baker-Nunn stations), is of the order of ± 25 m; only part of this uncertainty lies in the earth-spacecraft line (or earth-moon line) -- statistically about 50% -- so that even under the best present circumstances $E_b' = 15$, and E_p from this cause is still 400-500 m. (Izsak, JGR 69, 2621, June 1964) claims a smaller figure for station coordinate uncertainties, but since his results differ from similar results based on the same kind of data treated somewhat differently, e.g., Kaula, JGR 68, 473, 1963, these claims should be discounted somewhat.)

2. Transfer to Geocentric Coordinates (II): Errors of Type E_2

If the topocentric vector from the tracking station to the spacecraft is \bar{r} , and if the vector expressing the location of the tracking station relative to the center of mass of the earth is \bar{s}_g with an error $E\bar{s}_g$ (in the sense, true value plus the error = observed value), then the geocentric vector to the spacecraft is $\bar{r}_g = \bar{r}_t + \bar{s}_g$ or $\bar{r}_{g,obs} = \bar{r}_t + \bar{s}_{g,obs} = \bar{r}_t + \bar{s}_{g,true} + E\bar{s}_g = \bar{r}_{g,true} + E\bar{s}_g$. That is to say, the errors of geocentric position of the tracking station are reflected directly in parallel components of error in the spacecraft position. These are of the order of ± 25 m for well determined stations, but can be as large as several hundred meters at stations on isolated islands, etc., not yet tied to any geodetic datum. Errors of stations with respect to nets surrounding them can be made almost arbitrarily small, especially if geodetic stations in the net are not very far away. The errors of the ties connecting individual geodetic datums to other datums or to a world datum vary from about 15 m to 100 m. These are therefore estimates of the displacement errors of the spacecraft position in geocentric coordinates (in addition to tracking errors already discussed).

The direct effect of errors is not particularly serious, especially since there is every prospect that during the next several years, the geocentric coordinates of tracking stations will be refined, either by direct surface surveys or by analysis of the behavior of "station errors" in satellite tracking data. The latter has already been done for some stations, e. g., the SAO work with residuals in the photographic positions from Baker-Nunn plates, already cited, or the work at the Applied Physics Laboratory and the Naval Weapons Laboratory with Doppler techniques. Similar work tying stations to each other, rather than to the earth's center of mass, has also been carried out.

As we have seen in the last section, however, the indirect effect of station location errors, relative either to each other or to the center of mass of the earth, can be quite damaging.

Errors in the velocity of the tracking station relative to the geocenter, which affect Doppler velocities referred to the same center, are on the whole too small to worry about. The error in the tracking station motion, due to an error in distance from the axis of rotation (the radius of rotation) is 7.28×10^{-5} m/sec per meter error in the radius. At low latitudes, where the radius is predominantly vertical, for stations connected to datums by surveys, the error in the radius of rotation is compounded of the error in elevation above sea level, and the error in geoid height, typically 1 or 2 m and 20 m respectively. At high latitudes, where the radius of rotation is more nearly horizontal, and horizontal station errors may reach 100 m for poorly tied stations, the error in the velocity of the station would still be less than 1 cm/sec.

3. Transfer to Barycentric Coordinates at the Moon (III)

If one attempts to analyze in all generality the errors involved in the transfer from geocentric coordinates (II) to a new origin at the center of mass of the moon (IIIa) the situation becomes immensely complicated. As stated above in subsection C, Link 3, it is possible in principle to leave all the parameters of the moon's geocentric orbit as unknowns, but the number required to describe the complicated motions of the moon with sufficient exactness (< 100 m, in order not to degrade the results that can be obtained from the spacecraft tracking data) would run into the thousands or tens of thousands, would require years of tracking data, and would thus be hopelessly impracticable for the present. In fact the only really feasible and effective way is to adopt a reasonably well fitting reference orbit defined by a set of parameters, then use the tracking data to correct the parameters by differential corrections. In a computation in which linear equations are set up with the differential corrections to assumed values of the parameters as unknowns, it does not make any difference how the assumed values are computed, provided that the differential corrections are small enough that the linear approximation is valid.

From the practical standpoint, the following appears to be the best procedure:

- (i) Find simple expressions that will represent the moon's geocentric orbit with tolerable faithfulness over a period of time equal to the duration of the Apollo mission. These expressions might be the osculating orbit or a mean orbit, possibly for an epoch half-way in time between the beginning and the end of the significant part of the mission. The period of interest would probably be bounded by the spacecraft's entry into and departure from the "lunar sphere of influence", where the moon's gravitational field predominates. Assuming that this phase lasts about 3 days, one might need to add periodic terms with periods up to about 10 times this length -- in fact any periodic term whose phase amplitude exceeds, say, 100 m in a d-day time interval.
- (ii) Of these simple expressions, choose the one with the least number of disposable parameters to which assumed values can be assigned that will represent the moon's position "satisfactorily", as defined in (iii) below.
- (iii) Set up linear equations in which differential corrections to the parameters in (ii) are unknown quantities; "satisfactory" in (ii) means that the assumed values of the parameters are close enough to the corresponding true values that the linear approximation for the behavior of the differential corrections is valid (see BB, Appendix B). It goes without saying that these equations will also contain all the other unknowns of interest, particularly the parameters of the spacecraft orbit around the moon's center of mass.
- (iv) The present state of knowledge of the moon's orbit, built up over centuries of observation, is sufficiently precise, that probably most of the discrepancy between the predicted ephemeris of the moon's center of mass (that calculated from the assumed parameters) will differ from the observed ephemeris (that

derived from the center of attraction fitted to the spacecraft tracking data) chiefly in the magnitude of the geocentric radius vector of the moon. Differences in the mean longitude at epoch may also be significant. Differences in observed and computed radius vector may well be of the order of 1-4 km.

(a) Possible difficulties in determining the semimajor axis a , and the inclination i , of the spacecraft orbit around the moon's barycenter. As noted before, there are certain resemblances between (i) the problem of finding the elements of the spacecraft's barycentric orbit around the moon from Doppler data and (ii) the problem of determining the orbit of a spectroscopic binary star from Doppler-shifted spectrograms. (For a detailed treatment, see H. C. Plummer, An Introductory Treatise on Dynamical Astronomy, Cambridge U. Press 1918, Dover Reprint, 1960, Chap. XI.) The problem for the spacecraft is somewhat simplified in that the mass of the secondary body (the spacecraft) is negligible in comparison to the mass of the primary body (the moon), and the mass of the primary is approximately known. The radial velocity V of the spacecraft can be given by

$$V = V_m + K(\cos u + e \cos \omega')$$

in which

V_m is the radial velocity of the center of mass of the system (i. e., the moon),

u is the angle in the orbital plane of the spacecraft from the "receding node" (point where the orbit pierces, in the direction away from the observer, the plane perpendicular to the line of sight through the moon's barycenter) to the spacecraft, measured in the direction of orbital motion.

ω' is the angle in the orbital plane from the "receding node" to perilune, also measured in the direction of orbital motion.

e is the eccentricity, and

K is the velocity $(GM_m/a(1-e^2))^{1/2} \sin I$, in which G is the universal constant of gravitation, M_m the mass of the moon, a the semimajor axis of the spacecraft orbit, and I the inclination of the orbital plane to the plane of the sky (plane defined under the definition of u above).

It should be noted in passing that the foregoing expression is exact only for an orbit viewed from infinity, where the lines of sight from the earth to all parts of the orbit are parallel. The moon is close enough that all the measured radial velocities will not be identical with what would have been observed from infinity, but will differ by factors ranging from 1.000 000 to 0.999 988 (i.e., $\cos(4.9 \text{ mrad})$ for an 80-nautical-mile-high orbit). Preparing the Doppler data for this treatment is certainly possible, but we are not concerned with that here: the main purpose of this section is to point up certain ambiguities in a simple way.

The parameters e , ω' , and K can be derived from what amounts to a Fourier-series fit of the radial velocity data plotted as a function of the time, using only the lowest-order terms with period P and P/2. (The higher-frequency terms will be found to be redundant, unless the orbit is not elliptical.) P is the period of the orbit, which can be obtained with reasonable precision from timing a single circuit of the spacecraft around the moon (e.g., from eclipse to eclipse, with due regard for the orbital motion of the moon around the earth during the lapse of approximately 2 hours. Making use of the relations:

$2 \times \text{areal velocity} = 2 \pi ab/P = 2 \pi a^2(1-e^2)^{1/2}/P$ (a geometric relation),
 orbital angular momentum per unit mass $= (GM_m a(1-e^2))^{1/2}$ (a dynamic relation), and the mean angular motion $n = 2 \pi /P$,
 we have

$$a \sin I = (K/n) (1-e^2)^{1/2}.$$

The parameters a and $\sin I$ cannot be separated by this means alone. Without a, it is not possible to get a good estimate of the quantity GM_m for the primary from the expression $n^2 a^3 = GM_m$.

There are several possible ways out of this difficulty, at least in principal.

First, one can use the present value of the earth/moon mass-ratio, 80.32, thought to be good to about 1:4000. With this estimate of the uncertainty, the uncertainty in a from $n^2 a^3 = GM_m$ is about 250 m. Then, with this value of a , one could get $\sin I$ from $\sin I = (K/na)(1-e^2)^{1/2}$. The relative uncertainty in a is $250/1900 \times 10^3$ or 1.3×10^{-4} , corresponding to 13 in the 5th decimal place of $\sin I$. Since the orbit is seen nearly edge-on from the earth, so that I is within a few degrees of 90° , this is not a very sensitive way to determine I . Right at 90° , the uncertainty corresponds to 0.13 millirad. This in turn corresponds to an uncertainty perpendicular to the orbital plane that ranges up to $a \cdot EI$ at 90° from the nodes. This amounts to 250 meters perpendicular to the orbital plane, as well as in the plane. (Although a is also implicit in K , that fact has no effect on the estimate of the error in $\sin I$, because K is determined from the tracking data as if it were completely independent of a .)

The second possibility is that the directional data from the tracking is good enough, or can be made good enough, to keep the out-of-plane uncertainty satisfactorily small. This is the reason that pairs of tracking stations in the same general region in longitude should have some separation in latitude (see Subsection 1 above; also BB, Appendix I). Notwithstanding this precaution, this method could easily be defeated by errors affecting the direction of the baseline between two stations. This error is a bias error of unknown magnitude as far as a particular pair of stations is concerned, and one can only hope that the bias in observations by any pair of stations, insofar as the observations affect the determination of $\sin I$, can be separated from the mass of observations from all (pairs or triplets of) stations sufficiently well to be treated as an unknown, and solved for. A bias in $\sin I$ or I would lead to a bias in the direction in space of the orbital plane with respect to the moon's equator, that is, in the standard Keplerian elements i and Ω .

In solving for the circumlunar orbit, it will often be convenient as it is in similar cases first to find the plane of the orbit, i. e., the Eulerian angles defining the position of the orbital plane with respect to the reference plane, in this case the earth's equatorial plane; then, having found the orbital plane, to rotate (and, in the case of circumlunar orbits, translate) the terrestrial equatorial coordinate system (Type II) to a new barycentric lunar coordinate system in which the principal plane is the plane of the circumlunar orbit, not the moon's equatorial plane. This coordinate system is, of course, another subspecies of Type IIIa. This transformation makes it possible to reduce the problem of solving the equations of motion for the circumlunar orbit to a problem in only two dimensions. It also assumes that the Eulerian angles, which we may label ξ , η , and ζ , are known or that they can be determined with some certainty from the tracking data. Otherwise, the final out-of-the-orbital-plane error of the spacecraft position may look as if it were zero; but it only looks that way because the problem has been reduced to a two-dimensional one, so that out-of-plane errors vanish by definition. The real out-of-plane-error is still there, but disguised in the errors of the Eulerian angles ξ , η , and ζ , as determined from the tracking data. (Actually, only two of the three Eulerian angles are required to define the orientation of one plane with respect to another.)

A third possibility for separating a and I exists, although it requires tracking over at least a quarter of a lunation, and preferably longer. It must, therefore, be done with missions other than Apollo, e. g., perhaps with Lunar Orbiters which last a good deal longer than Apollo. As the moon moves around the earth in its orbit, the inclination to the plane of the sky of a circumlunar orbiter will, during the course of a sidereal month, oscillate between I_{\min} and $\pi - I_{\min}$. Remember that I is an angle in the range $90^\circ \pm$ inclination of the moon's equator to the earth's equator \pm inclination of the orbiter's orbital plane to the moon's equator. For an orbit inclined 0° to the lunar equator, the range in I is the same as the range of libration in latitude for that lunation. This means that the quantity $a \sin I$ will oscillate during the course of the lunation, so that the time corresponding to

$\sin I = 90^\circ$ can be identified, and a separated from $\sin I$. With a clearly separated, I_{\min} can be clearly separated, and also the corresponding time, so that a solution for i and Ω now becomes possible. For orbits during time intervals near $\sin I = 1.000\ 000$, a can presumably be calculated with fairly high precision on account of the accumulation of data and the separability of some of the unknowns, like biases in the original tracking data and departures of the moon from its assumed orbit. In the light of the calculations reported in BB, p. 5-15, one might expect $Ea \ll 50$ m after a quarter of a month. It is assumed that during this interval, the orbital plane of the spacecraft does not precess or change inclination, or that the motion of that plane in space can be calculated with sufficient precision from known perturbations by the earth and sun.

It has already been mentioned that the position angle of the line of nodes of the orbital plane with the plane of the sky is indeterminate, if only range and range rate are known. One single observation of position removes this indeterminacy.

One other potential source of serious difficulty should be noted, namely the fact that the earth-based tracking data cannot cover the nearly one-half a revolution during which the vehicle is eclipsed by the moon. Orbits based on data all concentrated in approximately one-half of a circuit are notoriously susceptible to biases from the effects of selection. Examples are almost too numerous to cite, and it is not difficult to invent possibilities in the present instance leading to errors of the order of 1 km or more. There does not seem to be any certain way to avoid this situation except by tracking circumlunar vehicles for periods of at least half a sidereal month in order to observe the whole trajectory. Even longer periods would be better, i. e., a whole sidereal month, in order to be sure of separating any effects arising from other periodic effects in this selection. As in the case of separating a and $\sin I$ already discussed, such an observing program will be limited to vehicles other than Apollo, since Apollo will not be in circumlunar orbit long enough to accomplish it.

This subject is a very complicated one; there is no intention here of doing more than sounding a word of caution. In sum, errors in the barycentric ephemeris positions of a moon-orbiting spacecraft calculated from a barycentric orbit based on terrestrial tracking data, may very well be much larger than the ideal of 20-100 m, which may be reached with unbiased tracking data accumulated over some tens of revolutions, or data from which the effects of bias have been removed. In fact it appears that the errors can be as large as several km if biases, e.g., those produced by pairs of tracking stations tracking only the near side of the orbit, cannot be eliminated.

4. Transfer from Barycentric Coordinate System of the Spacecraft (Type IIIa) to the Morphocentric Coordinate System of Lunar Maps (Type IIIb): Errors of Type E_3 .

The coordinate system of lunar maps, taken as a whole, suffers from fuzzy definition; in fact, about the only way it can be defined from a working operational standpoint is in terms of the collective numerical values given to the coordinates of the lunar features. Thus, it might be possible to say that the "true" origin and the "true" rectangular axes can be defined as that point and those three mutually orthogonal lines intersecting at the point that cause the sum of the weighted residuals for all the landmarks, $x_{\text{map}} - x_{\text{true}}$, $y_{\text{map}} - y_{\text{true}}$, $z_{\text{map}} - z_{\text{true}}$ to vanish, or alternatively causes the r.m.s. of these residuals to be a minimum. But we do not have in our possession the quantities x_{true} , y_{true} , z_{true} for all the landmarks, or even one of them. If we wish, we could say arbitrarily that the coordinates of one of the landmarks are "true values" by definition, thus making that landmark a reference landmark for all the others and therefore part of a datum. The craterlet Mosting A has this status in those systems in which the coordinates of other landmarks are essentially relative coordinates with respect to Mosting A.

Of course in a strict sense we shall never have the "true values" of the landmark coordinates in any mapping system, for they will

always be subject to some error; but when improved values become available (i. e., those with a smaller standard deviation with respect to some coordinate system, not necessarily that of one of the map systems), it will be possible to use these instead of the true values to form the residuals in question. In making a least-squares fit for a lunar mapping coordinate system, if the "true" values come from some coordinate system other than the mapping system which is being improved, it would of course be necessary to put into the equations of condition, terms for the unknown parameters of the rotation and translation matrices needed to transform from the other system to the map system.

Meanwhile, about all that is possible is to tie landmarks whose coordinates are given in a lunar mapping system IIIb, to the system IIIa: The tie can be performed either (i) by observing the landmarks from the CSM, or (ii) by observing the CSM from the ground at a location that is known with respect to at least some mapped landmarks.

The first possibility can be carried out by determining the direction of a landmark from the CSM with multiple sightings with the SXT, using the stars as reference points. The potentialities of this method are explored in considerable detail in Section XI of this report. The first possibility can also be carried out by overlapping photographs taken on the Lunar Orbiter, as described in Section X.

The second possibility, consisting of photographing the CSM from the landing site against the background of stars, is discussed in Section IX. Sightings from a single point on the ground, however, will only determine the coordinates of that point with respect to the CSM coordinate system IIIa; in general, it requires three points to make a complete datum tie. If the relative scale of the two systems can be ignored, then one point and two directions are sufficient. Problems connected with supplying this kind of information are the subject matter of Section VIII, in which possible ways of carrying out local ground surveys are explored. As will appear, the scope of such surveys around a single landing site is limited.

From the CSM orbit, only those landmarks will be accessible to observation that lie within a zone bounded by two small circles of the lunar surface, one on each side of the subsatellite track, parallel to it, and some 600 km ground-arc distance from it. In addition, only those landmarks that lie in the sunlit hemisphere, and possibly a few in bright earthshine, can actually be sighted on. Obviously then, a coordinate tie based on connections in range and direction between landmarks and CSM positions will be a tie between the CSM coordinate system IIIa and a sample of map system IIIb; not of the entire map, but the map system as represented imperfectly by a selection of landmarks accessible to observation. The origin and axes of the mapping system as obtained from the mean of the positions of the measured landmarks can be expected to differ from the origin and axes as defined by the mean of all the landmarks. For example, in an equatorial zone of accessibility, let us take 400 m as a typical value of the error in the z-coordinate of the landmarks in a direction parallel to the axis of rotation. As we shall see later, the estimated standard deviation of landmark fixes with the SXT relative to the CSM positions will range from possibly as low as 11 m to as high as 70 m; we take 30 m to be a typical value. This is small in comparison with the landmark position error, and will be ignored in this illustration. If 100 mapped landmarks are fixed with the SXT, the error of the z-component of these landmarks, which serves as a zero-point for this sample of the mapping coordinate system, can be expected to be about $400/100^{1/2}$ m, or about 40 m.

5. Errors of Landmark Coordinates with Respect to their Own Mapping System: Type E_4

Table III-1 above shows both the current and projected estimates of the standard deviation of landmark coordinates in several existing mapping systems. A landing site selected on a photograph can be located with respect to neighboring landmarks with something like the same precision. With respect to the map system IIIb as a whole, one might expect somewhat greater precision, if the site can be tied on the photograph to a number of neighboring landmarks; but this expectation is actually unfounded unless the landing site is seen with

greater resolution than the average landmark. In other words, the landing site itself has a certain fuzziness, due to the low resolution available in earth-based photographs, and this fuzziness is certainly as great as it is for any other landmark; in fact, it will probably be greater, because the landing sites are generally smooth and relatively featureless.

6. Direct Ties Between Earth and Moon

The placement of beacons on the moon of course provides the means of making direct ties between systems I and II directly to IIIb, bypassing the steps II-IIIa and IIIa-IIIb altogether. This subject is discussed in Section V, to the extent that is appropriate to the Apollo mission. For radio transponder beacons, the direct tie errors are similar to those for the ties between II and IIIa described above. The capabilities of lasers are developing so rapidly that it would be meaningless to try to predict what their capabilities will be four or five years hence; but they have the potential of providing the best means of making direct ties between the earth and the moon.

7. Summary of Errors in Location Affecting the Capability of Landing a Vehicle on a Selected Site

Although interplay of the errors in the chain from topocentric tracking coordinate errors (Type E_1) to landmark location errors in a lunar map (Type E_4), is extremely complex, and their magnitude varies at each step over a considerable range that depends on the geometry of the circumstances, etc., we shall attempt to summarize on the basis of average to optimistic expectations, and see what conclusions we may reach.

Assumptions:

- I: 1000 m per sample, 1 sample per min, $1000 t^{-1/2}$ m in t mins of observation. (Type E_1)
- II: Direct effect, 50 m; indirect effect on transverse position biased for each pair of stations, but approximately random from pair to pair, 500-2000 m per pair. (Type E_2)

IIIa: (1) No bias, hours to days of tracking, a and $\sin I$ separable:
20-50 m (based on BB estimates).

(2) No bias, shorter duration tracking, a and $\sin I$ not separable,
based on range and range rate alone: 250 m.

(3) Bias, from selection or indirect errors from II, regardless of
duration of tracking up to 1-2 weeks: 1-4 km.

Note: Elsewhere in this report, we have adopted for the uncertainty of
position of the CSM in selenocentric orbit, the assumed value, 100 m.

IIIa-IIIb: SXT sighting errors: 10 to 70 m/landmark. (Type E_3)

IIIb: (1) As represented by 10 landmarks well distributed, present con-
ditions: 150 m. (Type E_4)

(2) As represented by 10 landmarks, projected conditions: 100 m
100 landmarks, projected conditions: 30 m.

Location error of landing site with respect to IIIb, today: 500 m.

Location error of site, lunar Orbiter photographs: 80 m.

The overall accumulated effect may be estimated as follows:

From I - no separate contribution, because effect is already included
in IIIa.

	Optimistic	Average
II - Direct effect only:	20	50
Indirect effects not applicable if range and range rate are used, except in IIIa below.		
IIIa	20-50	250
IIIa - IIIb	10	30
IIIb	30	150
Site Location Error	80	500
Root Sum Square	100 m.	590 m.

On this basis, there appears to be reason to hope that information will be
adequate to guide a vehicle to a chosen landing site, provided ties have already
been carried out between Systems IIIa and IIIb, either by lunar Orbiter photo-
graphs or SXT measurements.

E. REMARKS ON THE ESTABLISHMENT OF A SELENODETIC DATUM, AND SELENODETIC SURVEYS

The establishment of a full selenodetic datum, in a sense analogous to the geodetic datums, requires:

1. A system of astronomical coordinates, based on the moon's axis of rotation, hence a means of establishing the position of the lunar celestial poles referred to the stars (see Section IV), and a means of determining selenocentric astronomical coordinates (see Section VI). When combined with (2) below, the deviation of the vertical is obtained. The deviation of the vertical and gravity anomalies (see Section VII) are related through Stokes theorem, and thus there is value in measuring one to obtain the other, if both cannot be done.
2. A system of selenodetic coordinates. Classically, these would be spherical or spheroidal coordinates on a standard reference sphere of specified radius or spheroid with specified semiaxes that best fits the lunar surface, either the average of the lowest regions, or simply the average of all regions. The classical system would require for its definition: (i) a datum point, with assigned selenodetic latitude, longitude, and height above or below the reference sphere or spheroid; and (ii) an azimuth from the datum point to another point of known location. (See Sections VIII, IX, Appendices C and E.) The selenodetic coordinates of any chosen point would now be calculated from the datum point, the arc length between the datum point and the chosen point measured along the reference sphere or spheroid, and the azimuth of that arc. The coordinates of the datum point and all the other points with it would then be adjusted so that the average difference between astronomical and selenodetic position of all points on the moon's surface would vanish. (For details of classical geodesy, see any standard textbook, e. g., G. Bomford, Geodesy, 2d Ed., Clarendon Press, 1962.)

Although any system needs at least one datum point, a scale, and definition of its orientation, it is debatable whether it is necessary to follow these classical procedures slavishly when setting up a selenodetic coordinate system. The classical system is at least partly the result of historical development, influenced strongly by features of the terrestrial environment which do not apply

on the moon, namely the presence of an atmosphere that refracts light rays. The chief effect of the earth's atmosphere is, of course, to bend light rays in the vertical plane of the ray. Although this effect is fairly predictable for lines of sight inclined by more than 10° or 15° from the horizontal, it is quite unpredictable for nearly horizontal rays, easily introducing errors of several minutes of arc. Most lines of sight in surveying are of course nearly horizontal, and hence severely affected. (Refraction can also occur in the horizontal plane, i. e., a bending of the light ray in the horizontal direction, in regions where the atmospheric density has horizontal gradients. These arise principally from the local differences in the temperature of the air produced by different kinds of surface -- water, bare rock or earth, wooded areas, snowfields, etc.)

In the earliest surveying which can be called geodetic -- in Holland and France in the 17th Century -- triangulation was carried out in three dimensions; that is, the actual angle between two stations A and B subtended at C was measured at C in the plane of the triangle ABC, not in the horizontal plane. In flat country and with small triangles, this makes little difference; but in terrain where the differences in elevation of A, B, and C become great enough, the vertical component of the measured angles is affected by atmospheric refraction. This troublesome phenomenon led to the practice of separating the surveying into two parts: (i) triangulation based on horizontal angles, using the longest lines of sight possible; and (ii) leveling, in which differences in elevation above an arbitrary reference surface are determined by running short lines of sight unlikely to be greatly affected by refraction. Both (i) and (ii) required the adoption of a reference surface: in (i) the surface is needed to project the angles and distances on, and in (ii) it is needed to refer elevations to. Terrestrial oceans afford a ready-made basis for setting up reference spheroids, which are imaginary surfaces that best fit the true sea level surface, either on a regional basis or a world-wide basis.

However, the moon has neither an atmosphere to cause refraction, nor seas and oceans to use as a reference for elevations. Certain simplifications would result, if the positions of points on the moon are simply expressed in

three-dimensional coordinates in the first place, and there seems to be no reason not to do so. These coordinates may be either rectangular or spherical. Computations, e. g., distances and directions between points, are usually easier to carry out in rectangular coordinates. On the other hand, spherical coordinates are more useful in navigation on or over the surface, because of their ready interconnection with celestial coordinates. A sphere of constant r can be adopted as a reference surface for local elevations, but the sphere would be only a convenience, and not an essential part of the system, as are the reference spheroids in terrestrial geodesy.

Spherical coordinates also bear a strong resemblance to classical geodetic coordinates, which might give a feeling of familiarity and comfort. Geodetic coordinates are oblate-ellipsoidal. This arises from the fact that to a second approximation the earth is an oblate spheroid. The oblateness of the moon is so small and uncertain that there is no advantage in adopting spheroidal coordinates; and the same can be said for the ellipticity of the moon's equator.

All that is really required is to locate points on the moon's surface with respect to each other in a three-dimensional coordinate system, and to relate the system to the directions in space. For the sake of both convenience and elegance, the origin of the ideal selenodetic coordinate system should be at the center of mass of the moon, and its principal axis aligned with the axis of rotation of the moon, i. e., it should be Type IIIa. The barycentric orbital coordinate system of a particular orbiter could then in general be made to coincide with the ideal system by small rotations around a common center. Generally, no very significant change in scale would be required if the scale of the ideal system is built up in the first place from orbits based on tracking data, and if landmarks are tied to these orbits; in the case of a particular orbit, the relative change in scale will be the small quantity Ea/a , about $1:10^5$ for well determined orbits and possibly $1:10^4$ for orbits tracked only 3 days. Map coordinate systems can be made to coincide with the ideal selenodetic system by (1) rotations, expected to be of the order of 0.01° to 0.02° , the present estimated uncertainty in the position of the lunar poles; (2) a translation of possibly several hundred

meters, to bring the center of figure to the center of mass; and (3) a change in scale, of possibly as large as 1:2000, the present estimated uncertainty in the radius of the sphere that "best fits" the lunar surface.

The question of establishing a definitive scale for an ideal selenodetic system still remains largely open. It is to be hoped that the scale established by the semi-major axis of orbital coordinate systems from tracking data will agree reasonably well with the scale established on the surface by the baseline of the local survey or by the proposed surface ranging techniques. During the early Apollo surveys there will undoubtedly be discrepancies between the two systems of scale which will need to be reconciled, using standard statistical techniques which take the errors of both systems into account.

The methods described in this report show how an approach to establishing an ideal selenodetic system can be made or at least begun on the Apollo mission, although the precision associated with these first steps is not up to first-order geodetic standards.

SECTION IV

DETERMINATION OF THE LUNAR POLE

A. INTRODUCTION

Knowledge of the direction of the moon's axis of rotation in celestial coordinates would provide the basis for selenodetic astronomy that could be performed in the same manner as geodetic astronomy on earth, in that it would simplify determination of astronomical coordinates for any point on the moon's surface. Once a selenodetic datum and network is established, the differences in the selenodetic coordinates of a point on the moon's surface and the astronomical coordinates of the same point is a measure of the deflection of the vertical at that point. Knowledge of these deflections would permit correction of astronomical azimuths in carrying forward selenodetic networks, as well as being the basis for deriving geophysical information about the internal mass distribution of the moon.

In addition, knowledge of the direction of the moon's axis of rotation would permit determination of the astronomical position at the landing site. This would furnish an improved zero-point datum for a system of selenocentric latitudes and longitudes in a selenocentric system which would better fit the moon's real axis of rotation (see Section VI). It would make possible a determination of the wanderings of the lunar pole, which would also yield geophysical information about the distribution of mass and internal rigidity of the moon.

Observations from the earth of beacons emplaced on the moon, however, may be more effective than photographic observations from the lunar surface, at least until the latter have been repeated a number of times, well distributed over the complete lunar rotation.

B. PROCEDURE

Location of the pole would be derived from photography obtained from the precision frame camera as outlined in Section IX. The procedure is

simple and will not be repeated here except to point out that it will be necessary to take at least two sets of celestial pole photographs spread apart in time as far as mission schedules and constraints will permit. This is believed to be approximately 12 hours, which will be adequate. It is essential, however, that the relative positions of the camera with respect to the moon be the same for all exposures. This can be accomplished either by not allowing the camera to be moved or touched during the entire period, or by making provisions to rectify the various exposures with respect to each other. The latter procedure will probably be the most practicable approach. A portion of the lunar landscape, which will appear on the lower edge of the plates, could be used as an extended series of fiducial marks and serve this purpose adequately, as long as it is clear which image of the horizon goes with what star exposure.

The camera must point in the direction of the lunar celestial pole, which is sufficiently well known for this purpose. In order to yield not only the exact location of the lunar pole, but also the selenographic latitude of the observing station, the camera must be carefully leveled and its scale well known; so that the actual latitudes (i. e., the angular distance of the pole from the horizon), can be computed from the measurements on the plate. The balloon target provided in Section IX would serve this purpose.

C. ESTIMATION OF THE ACCURACY OF THE POLE'S COORDINATE DETERMINATION

Appendix B reviews in detail the theory and mathematical equations which lead to derivation of the lunar pole from the precision frame camera photography and presents a brief error analysis of the results, as well as indicating means of a rigorous error approach. For purposes of this study, however, the abbreviated error analysis is sufficient. This shows that if the two extreme exposures are approximately 12 hours apart, and a camera of 150 mm focal length is utilized, as provided by the precision frame camera, the pole can be determined within a standard error of 7 seconds, which over a period of several missions would surely be improved.

SECTION V

USEFULNESS OF A BEACON EMPLACED ON THE MOON, TO BE OBSERVED FROM THE EARTH

A. INTRODUCTION

The subject of emplacing a beacon on the surface of the moon has been considered by scientists during the last six or eight years as a means of furnishing a fiducial mark on the moon, the motions of which could be followed over the course of time in order to determine the physical librations of the moon better than they are presently known. Today, the coefficients of the equations for the physical librations are known with uncertainties of the order of 0.01° to 0.02° . Investigators interested in determining the physical librations more accurately have been concerned almost entirely with information that can be derived from the librations regarding the three principal moments of inertia of the moon. In turn, some information about the distribution of mass in the moon can be obtained from these moments: degree of central concentration of mass; irregular distribution of mass, indicating departures from isostasy, etc. For these purposes it is not necessary to know the absolute location (i. e., selenocentric coordinates) of the beacon or fiducial mark; it is only necessary to know how the mark moves relative to its own mean position as a function of time.

The use of beacons has also been considered for the purpose of determining the distance to the moon, and its orbital motions, but present consensus holds that these data can be obtained about as well without a beacon. Radar determination of the lunar distance (NRL, etc.) have borne out this surmise, although the standard error of the radar results is of the order of ± 1 km. Some of this uncertainty is due to the uncertainty in the radius of the moon (1738 Km), and some to an uncertainty in the velocity of light of about $1:10^6$.

There is obviously some merit, however, in marking an identifiable reference point on the moon's surface for selenodetic purposes, coordinates of which could be accurately determined by observations from the earth, to be used as a datum tie, so to speak, between (i) selenocentric coordinates

determined from the earth (such as the coordinates used to describe the ephemeris of a lunar orbiter or the Apollo CSM), and (ii) coordinates referred to a lunar datum, however provisional. The question is, how well can this be done with a beacon or reflector?

Both optical and radio beacons have been considered. An optical beacon could be observed for angular motions produced by transverse displacements; it should be placed near the center of the visible hemisphere where librations in longitude or latitude produce the largest transverse displacements for both these degrees of freedom. The optical beacon would be placed near the limb only to maximize the effect of librations in position angle. Radio beacons for measurements of range or changes in range, should be placed near the limb -- near the moon's equator for librations in longitude, and near a pole for librations in latitude. Libration in position angle cannot be determined from range measurements. Thus, other things being equal, it would take twice as many radio beacons to do less than an optical beacon can do. Furthermore, they would need to be emplaced in regions near the limb where Apollo missions do not intend to land.

B. OPTICAL METHODS

If the beacon were observable as a point with standard astrometric techniques -- i. e., if it looked like a star bright enough to photograph with a telescope designed for astrometric work, it could be positioned in celestial coordinates relative to the field of comparison stars with a precision of something better than $1''/f$, where f = focal length in meters. This would give two components of a single position, which by itself would not constitute selenodetic information. To yield selenodetic information, one of two further steps is required.

First alternative: If such observations were repeated over a sufficient period (of the order of one year) and the observations were representative of the range of librations, then the variable or librational part of the coordinates of the point could be separated from its average position with respect to the center of the visible disk of the moon. Several observations per night, for 100 nights, would give a precision of the relative angular

coordinates (right ascension and declination) of the beacon with respect to the center of the visible disk of better than $0.1/f$ -- a great deal better if the observations are well distributed and the variables well separated. This corresponds to a precision (in transverse coordinates) on the moon's surface of $190/f$ meters or better, which might be worthwhile if lunar maps do not improve a great deal between now and 1969. To accomplish this result it would be necessary to work out a fairly systematic cooperative observing program with the operators of astrometric telescopes. Whether it would be worth investing in additional astrometric telescopes to achieve this somewhat marginal result would depend on the value of the geophysical results to be obtained from the librations: that is, the question should be judged on geophysical grounds rather than selenodetic, since a selenodetic result can be obtained from the second alternative, described below.

Second alternative: The selenodetic, selenocentric, or astronomical coordinates of the beacon should be determined by operations conducted on the moon's surface. The selenodetic coordinates would be largely arbitrary in any early survey. The selenocentric coordinates could be determined by observations of the orbiting CSM from the beacon site, or by observations of the beacon (presumably near the LEM) from the CSM, by methods outlined in Section XI in this study. The astronomical coordinates could be determined from the local zenith and lunar celestial pole, also as outlined in Section VI. An element of arbitrariness, namely the selection of a zero-point for exact lunar longitudes, enters into these results. In order to eliminate ambiguities or uncertainties caused by librations, it would be necessary to make the terrestrial observations of the beacon either at some time for which the CSM orbit is well known (if selenocentric coordinates are being sought), or during the time that astronomical observations are being made by the LEM crew (if astronomical coordinates are being sought).

C. OPTICAL BEACON TYPES

Optical beacons must be objects that can be readily seen or photographed from the earth. The following have been considered: mirrors to reflect sunlight, corner reflectors for laser beams, and bright lights.

1. Mirrors

A mirror can be spherical, plane, or a faceted sphere. A specular spherical mirror would have a highlight of reflected sunlight, the brightness of which depends on the size (radius) of the sphere. The 40-m (130-foot) Echo balloon is an example of a spherical mirror, more or less specular. It appears about as bright as a star of the 0th magnitude at a distance of 1000 km, and would look like a star of about 13th magnitude at 385,000 km. The limiting useful magnitude for telescopes used with Moon Cameras [7] is about 11th, with a 10-20 sec exposure. Therefore, an Echo-type balloon would have to be increased in area by a factor of approximately 6, or in diameter by a factor of 2.5, in order to be useful; that is, the diameter would have to be about 100 m. For balloons, weight is approximately proportional to area: this implies a weight of about 500 kg (0.5 ton) which is, of course, prohibitive for the Apollo mission. Smaller balloons could be used if larger telescopes were used with Moon Cameras to observe them. If 30 kg is assumed to be the heaviest balloon beacon that could be taken on an Apollo mission (although this is actually much too large to be practicable), the weight and hence area would be diminished by a factor of 16, and the brightness of the highlight reflection in proportion, i. e., 3 stellar magnitudes. This would require a telescope of $4 \times 30 = 120$ cm aperture. The only telescope with this large an aperture, possessing at the same time a large enough field with astrometric properties, is the new USNO telescope at the Flagstaff station. In other words, this is a remote possibility.

Consider the case of the plane mirror. The mean apparent diameter of the sun is about $30'$, or $1800''$ of arc, so the (conical) solid angle subtended by its disk is approximately $2.55 \times 10^6 \text{ arc-sec}^2$. The apparent magnitude of the sun is about -26.4. Assume that a point-like reflection of stellar magnitude 9.0 would be readily observable; this would be fainter than the sun by a factor of 1.5×10^{14} . Thus, a small patch of the sun's surface (or mirror reflecting 100% of the incident light) that subtends a solid angle $(1.5 \times 10^{14})^{-1}$ times as large as the solid angle subtended by the sun would look like a 9th magnitude star. The size of this small

solid angle would be $(2.55 \times 10^8 \text{ arc-sec}^2) / 1.5 \times 10^{14}$, or $(1.3 \times 10^{-4} \text{ arc-sec})^2$, or $(0.65 \times 10^{-9} \text{ rad})^2$, which would be the equivalent of a mirror on the moon 25 cm x 25 cm square. Such a mirror could easily be carried on an Apollo mission. When the mirror is in sunlight (about half the time), and if the sunlight strikes the upper reflecting surface (rather than the underside), the mirror would reflect a conical beam about $1/2^\circ$ in diameter into space (i. e., the angular diameter of the sun). This cone would have a diameter of about 3500 km at the earth, slightly larger than the moon. The cone would be swept around the moon's axis of rotation at twice the rotation rate of the moon. For the present problem, we are interested in the rate of rotation of the cone with respect to the sun, not inertial coordinates. This rate is slightly variable, not so much because the moon rotates (in inertial coordinates) at a very slightly variable rate (= "physical libration in longitude"), which it does, but because the phase angle of the moon with respect to the sun increases at a slightly variable rate as a result of the moon's orbital motion around the earth (and also, to a lesser degree, because both the earth's orbit around the sun and the moon's orbit around the earth are slowly varying ellipses). The average rate of rotation of the moon with respect to the sun is 0.213 rad/day. The rate of rotation of the cone of visibility of the reflection with respect to the sun is twice as great, but from the standpoint of an observer on the earth about half of this double rate is undone by the moon's revolution around the earth. Therefore, the visibility cone sweeps past the earth at $0.213 \text{ rad/day} = 0.0089 \text{ rad/hr} = 3400 \text{ km/hr}$. (These are all average values.) Thus, if the angle of the mirror were correctly set to begin with, the reflection could be observed for about an hour at observing stations along the center line of the path swept out across the surface of the earth by the 3500-km diameter visibility cone. The time is increased by the earth's rotation, which carries the observer in the same general direction as the cone. It is decreased for observers off the center line.

The geometry of the visibility cone, its intersection with the earth's surface, and its behavior with time (motion, nearly periodic pattern, etc.) is similar to those of eclipses of the sun (partial and total), or of occultations. In eclipses of the sun, the diameter of the penumbra is about twice

the diameter of the visibility cone, and its speed across the earth's surface about half as great. The relative shift of the moon in celestial latitude from one eclipse to the next in the same cycle is about one-half that between analogous members of a series of visibility cone sweeps. The net effect is to reduce the frequency of visibility sweeps to about one-half the frequency of partial and total eclipses of the sun, which is of the order of three per year from somewhere on the earth's surface. From any one place, the frequency is much lower. Allowing for the effects of bad weather, it would thus take several years, even with a number of observing stations, to build up a useful sequence of observations. This might be acceptable, however, and the payload weight is greatly to be preferred over a large balloon-type spherical reflector.

A faceted spherical surface is really no more than a compromise between a true sphere and a plane mirror, and constitutes an effort to try to avoid some of the disadvantages of each. For example, a polyhedron made up of 1-ft² (25 cm x 25 cm) faces, each forming a dihedral angle of approximately 1/4° with each of its nearest neighbors, would reflect a set of almost overlapping 1/2° cones into space, each of which looks like a 9th magnitude star from the earth, and only one of which would generally be visible at a given moment, and at most 2 or 3 if the cones overlap. The number of such faces, and hence the size of the polyhedral surface, would depend on the percentage of the time it seems desirable to be able to observe the reflection. There is probably little sense in trying to guarantee that a reflection would always be observable, anywhere on earth. To do so would involve blanketing a strip, as seen from the moon, $\pm 8^\circ$ each side of the moon's equatorial plane (somewhat larger than the moon's total optical plus physical libration in latitude) and 360° in selenocentric longitude. This would require a faceted spherical surface zonal segment, bounded by two latitude circles at about $\pm 4^\circ$ and by two meridians 90° apart. Since each facet is tilted 1/4° with respect to its neighbors and is about 1/4 meter in diameter, the general curvature of the sphere to which the facets should conform is about 1°/meter. The entire array would thus be an arch, 8-10 meters wide, and 90-100 meters along the 90° of the arch. This may be feasible

some day, but is entirely too cumbersome and big to pack on an early Apollo expedition.

On the other hand, this type of analysis makes it possible to estimate how large a polyhedral surface would be required, once it is decided what kind of observational coverage is desired, i. e., what fraction of the maximum possible time, and over what geographical distribution. (The latter will be largely uncontrolled, and will be a function of the time coverage.)

2. Laser Corner Reflectors

A more desirable approach (might be to place) a corner reflector that would reflect a laser beam from the earth. Although mirrors have the advantage of being observable by existing telescopes, developments in lasers are such that by the time of the Apollo missions or shortly thereafter, a laser of reasonable power requirements could get a good return from such a reflector. In addition, the laser could provide range which would strengthen the solutions. During the meeting held at NASA Headquarters on December 4, 1964, on the subject of "Applications of Lasers to Lunar Surface Science and Technology", Hunt and Iliff of Air Force Cambridge Research Laboratories reported considerable success and progress utilizing reflectors as small as 10 cm in aperture over considerable distances. It appears that a collapsable reflector which would expand to not more than 3 feet in aperture size, and would give a much larger cone of observation than any practicable size of mirror array, would be effective and most desirable. Further information relative to type and size can be obtained through AFCRL.

3. Bright Light Beacon

The power required to make a light bright enough to be observed by batteries, a system of solar cells, or nuclear power supply, would make such a system much too heavy to take on an early Apollo mission. A study of any other means of planting a suitable bright-light beacon on the moon is of course outside the scope of this report.

D. RADIO METHODS

In the following, it is assumed that the beacon is a transponder, rather than a continuously radiating source. This provides two advantages not so easily obtained from continuous sources: (1) precise frequency control is dependent only on phase-lock circuits, not on long-term stability control; (2) ambiguities in phase can easily be eliminated.

1. Directional Information

The directional information that present-day radio beacons and special antennas can supply is, of course, vastly inferior to even rather crude optical information. It is conceivable, however, that more precise directional information could be obtained by interferometric techniques, using a long baseline (comparable to the earth's radius in length) and a frequency not overly susceptible to refractive effects in the ionosphere or the circumterrestrial plasma. Even so, it is doubtful whether the technique would be competitive with optical techniques.

If a frequency in the cm-wave region be chosen (say, S-band) and a baseline of the order of 1000's of km be used, the theoretically attainable directional accuracy would be of the order of one to several arc-seconds. A minimum of three stations would be required, in order to obtain the direction to the beacon in two degrees of freedom, stations A & B on an approximate east-west line, and station C approximately north (or south) of station A (or B). The stations must be tied with communications links good enough to allow the measurement of the phase difference of a signal from the beacon as it arrives at the two stations. The stations must be tied geodetically with an accuracy better than $1:2 \cdot 10^5$; otherwise the directional information would be degraded. Furthermore, even if these technical difficulties were surmounted, the refractive effects of the troposphere, ionosphere, and circumterrestrial medium might still be greater than several arc-seconds. Finally, even if both the technical and environmental difficulties were overcome, the result would still be no better than rather crude optical results, and so the method does not seem to be worth

the trouble, at least for the present purposes. (Precision all-weather tracking of a space probe is another matter; here interferometric tracking of the type outlined above might make considerable sense.)

It has also been suggested that a beacon, or better yet, several beacons, could be emplaced on the moon as part of a navigational system. The signal from the beacon would be radiated directly to a tracking station on the earth, and also to a transponder on a lunar-orbiting spacecraft, which would in turn relay a second signal to the same terrestrial tracking station. The phase difference between the direct signal and transponder-repeated signal, converted into a difference in length between the direct line station-to-beacon and the broken line station-to-spacecraft-to-beacon, would place the spacecraft very accurately on an ellipsoid, with the tracking station at one focus and the beacon at the other focus. A description of how such data might be used to obtain positional information lies beyond the scope of this study, except to say three things: (1) a judicious placement of several such beacons can give completely self-contained positional information; (2) the use of even one such beacon, in conjunction with ordinary Doppler tracking data for the Apollo or Orbiter, would under some circumstances considerably strengthen positional information about the Orbiter; (3) the same set-up can be used in reverse, to locate the beacon on the surface of an ellipsoid with the station at one focus and the spacecraft at the other; this would be useful for tying the beacon to the geocentric position of the spacecraft, assumed in this instance to be known from the tracking data. It is only case (3) that might be interesting in the present context.

2. Range Information

Radio beacons come into their own for the determination of distances. The main points to be borne in mind in the uses suggested below are: how to provide stability in the reaction time of the transponder, and a long lifetime in a remote beacon unattended for periods of the order of a year. (But see M.S. Hunt, "A Prototype Lunar Transponder", JGR 69, 2399, June 1, 1964, which describes a simple transponder that appears to meet all require-

ments implied in this discussion. It weighs 1.8 kg without batteries, can withstand a 3000-g shock, and is built to last for a year or more.)

(a) Case I: Near the center of the moon's visible face. A beacon in this region would be useful chiefly for determining the distance to the moon more accurately than is known today. This would depend, however, on being able to calibrate the scale to better than 1:400,000, which is roughly the present relative uncertainty. The following assumptions can be made:

1. Present-day radar transponders, like the SECOR system used by the Army Engineers on satellites for geodetic purposes, or the NASA S-band range and range-rate system on the IMP satellite (which will also be used on the geodetic satellite GEOS) give ranges with an internal consistency of instrumental performance corresponding to ± 15 meters or better, and range-rates to a few cm/sec by two-way Doppler techniques. The constant bias due to an uncertainty in the reaction time of the transponder circuit is of the order of 10 m. Scale errors could probably be calibrated to $1:5 \cdot 10^5$. It is further assumed that transponders can be designed to operate over translunar distances with this same kind of capability.
2. Corrections for propagation errors introduced by the ionosphere and the circumterrestrial medium can be calculated with an uncertainty no worse than 1-2 meters. The chief source of the uncertainty would be a lack of knowledge of the total electron content along the ray-path. Even if it were ignored altogether, at 5000Mc/s the error could hardly exceed ± 10 m.
3. The uncertainty in the value of the velocity of light, now $1:10^6$ or somewhat worse, will be improved. Whether it is or not, is of no great moment, however, because the present radar-based distance to the moon and geocentric (or topocentric) distances to circum-lunar orbiters based on tracking data will all be affected by the same error. This statement is also true for item (2) above.

As noted before, a beacon near the center of the moon's visible hemisphere will not be much use for determining librations because librations do not appreciably affect the distance to points in this region.

(b) Case II: Near the limb, at low latitude. A beacon in this position would be useful for determining the distance to the moon, as in Case I above; but in addition, librations in longitude (both optical and physical) would have a maximum effect in varying the station-to-beacon range about a mean value. The present uncertainty in the orientation of the moon on its axis, and hence in its libration, is of the order of 0.01° corresponding to a linear displacement of a point on the surface of about 300 meters. With the same assumptions made under Case I, the values of the librations and their pattern with time could be better determined. Actually, the conditions laid down under the assumptions in Case I can now be relaxed somewhat, because for librations we are concerned not so much with absolute distance (range) measurements, but with variations in range. One can assume that the velocity of light does not vary, and so can disregard assumption (3). The propagation delay time is a function of the total electron content along the path, which does vary. The variation is to some extent determinate (perhaps to a factor 2) from measurements of electron density in the ionosphere and interplanetary space. The corrections calculated on the basis of measured electron densities will thus vary; they would usually be only of the order of 1-2 m, and their range of variation is of the same order of magnitude. The errors of these calculations, which are roughly proportional to the corrections themselves, also vary, but their absolute range of variation is very small indeed -- of the order of a few centimeters.

Placement of a radio beacon on the limb of the moon would be comparatively more difficult than placement at the landing site, which is assumed to be within a few 10's of degrees of longitude of the center of the visible hemisphere. It should again be noted, however, that for librations the absolute position of the beacon on the moon's surface is of no great importance; the important thing is to be able to measure the variations in the station-to-beacon range with acceptable accuracy; therefore, for landing the beacon on the surface, a c. e. p. of 100-200 km is quite acceptable. It seems possible

to eject the beacon in a hard-landing-proof package, from either the LEM or the CSM, so as to land near the limb. Once landed, however, its east-west position needs to be known to about 3-6 km, or its longitude needs to be known to 0.1° to 0.2° . If the range to the beacon is D , the radius of the moon is R , the longitude of the beacon measured from the mean limb toward the observer is ℓ , and the (semi-)amplitude of the libration in longitude is L , then the extreme difference in range due to librations in longitude is given by the expression, $\Delta D = R \left[\sin(\ell + L) - \sin(\ell - L) \right] = 2 R \cos \ell \sin L$. The uncertainty in ΔD due to an uncertainty in longitude $d\ell$ is given by $\mathcal{E}_\ell(\Delta D) = (dD/d\ell) \cdot d\ell = -2R \sin L \sin \ell d\ell$. With $R = 1738$ km, $L = 6.5^\circ$ (a rough mean value), $\sin L = 0.11$, and $\sin \ell > 0.11$ (so that the beacon will never be turned completely over the horizon) but smaller than, say, 0.20, then $\mathcal{E}_\ell(\Delta D)$ would lie in the range $31 \cdot d\ell$ to $57 \cdot d\ell$ km, depending on the value of ℓ . Since the present value of ΔD is known with an uncertainty \mathcal{E} of 300 m, to effect a worthwhile improvement one should shoot for, say, 100 m. This leads to $d\ell = 1/300$ rad if $\sin \ell = 0.11$, and $d\ell = 1/600$ rad if $\sin \ell = 0.20$. These values of $d\ell$ correspond to uncertainties in the east-west position of the beacon of 6 km and 3 km respectively. There seems to be no practical reason why this accuracy cannot be achieved.

(c) Case III. Near the north or south pole of the moon. Similar arguments can be given concerning the placing of a beacon near a lunar pole in order to determine the libration in latitude more exactly than it is known today. These arguments therefore need not be repeated in detail. The placement can be done only from a circumlunar polar orbit, however.

(d) Discussion. Several comments should be made concerning the evaluation of librations in Cases II and III:

1. The total true libration in both latitude and longitude is, as noted before, a combination of optical and physical librations (see any issue of the American Ephemeris or the Explanatory Supplement to the Astronomical Ephemeris and the American Ephemeris and Nautical Almanac, H. M. Stationery Office, 1961, for greater

detail). Nearly the entire amount is accounted for by the optical libration, which ranges up to about 8° in longitude and nearly 7° in latitude. (In addition to the true optical libration, there is an apparent (parallactic) libration due to the offset of the observer from the line connecting the centers of the earth and moon, the maximum amplitude of which is about 1° , and which depends on the location of the observer and varies in phase with the hour angle of the moon. We shall leave this out of further account, because its magnitude can be calculated to $1:10^5$ and its effects removed from the observations.)

2. The optical librations are of no particular physical interest; it is the physical librations that supply information on the mass distribution in the moon's body. The physical librations are small quantities in comparison with the optical librations. (For a simplified mathematical treatment of the main features of librations, see Fundamentals of Celestial Mechanics, J. M. A. Danby, MacMillan Co., 1962: chap. 14.) The principal term, with by far the greatest amplitude, in the expression for the physical libration in longitude has a period of a year and an amplitude of about 0.02° ; the principal term in latitude has a period of nearly 6 years and an amplitude of about 0.04° . Both librations have many harmonics of small amplitude. One term of great interest, because it gives rather direct information about the ellipticity of the moon's equatorial section ("frozen tidal bulge") which is the subject of much dispute, is the free oscillation term in longitude, caused by the torque exerted by the earth on the moon as it swings east and west of its mean position with the period of the optical libration. This term is small and ill-determined at present. The optical librations have the same periodic terms in general as does the moon's geocentric motion, with a principal term of one anomalistic month (perigee-to-perigee).

Solutions for the amplitudes of all periodic terms of both kinds of libration can be obtained in principle using only observational

data on the selenographic latitude and longitude of the center of the disk, and the position angle of the moon's axis of rotation (or any equivalent of these quantities). In practice, however, it would be difficult to obtain correct values of the amplitudes of the physical librations from the motions of a single point because they are small differences of much larger quantities, (total libration) minus (optical libration), and because some of the harmonics of the optical librations are comparable to the entire physical libration in amplitude and period. Therefore, the best way to obtain the amplitude of the physical librations from a single point seems to be as follows: first, calculate the optical librations, which can be done from the known orbital motions of the moon, under the assumption that the moon rotates uniformly in rate and direction of axis with respect to inertial space; and second, subtract this quantity from the observed libration. This would give the departure from uniform rotation, which is of course the physical libration. The variations in the motions of the moon are known with uncertainties of about $\pm 0.2''$ in angle (from occultations, Moon Camera observations, etc.) and about 100 meters in distance. This latter figure is obtained from the uncertainty in the mean distance \underline{a} which is known to about 1 km, multiplied by twice the eccentricity $\underline{e} = 0.05$... the quantity $2ae$ being the difference between apogee and perigee distances. The eccentricity \underline{e} is known to a large enough number of significant figures that it introduces no significant additional uncertainty into the product $2ae$.

3. The angular uncertainty $\pm 0.15''$ corresponds to an uncertainty of position on the surface of the moon of about 1.3 meters, so can be effectively ignored, in comparison with the ± 100 meters or so arising from the uncertainty in the distance to the moon. It is now necessary to make assumptions about the behavior of the errors in the transponder ranging system. Let us assume that they are of the following three kinds and size: (1) an accidental error of ± 15 m in range and ± 0.1 m/sec in range rate; (2) a constant instrumental bias error (irreducible residual of cali-

bration errors) of ± 10 m; (3) a scale error of $2:10^6$, most of which is constant and contributed by the uncertainty in the value of the velocity of light, but a small part of which is variable and due to the peculiarities of the timing circuit. There is in addition, the propagation error from the intervening plasma of ± 2 m. The range in variation of the measured distance to a point on the moon would thus be subject to a total variance of $(15)^2 + (1)^2 + (4.1 \cdot 10^7 \times 2 \cdot 10^{-6})^2 + (2)^2 \text{ meters}^2 = (84 \text{ meters})^2$. Since the uncertainty in the calculated effect of the optical librations and variation in the distance to the moon has been assumed to be ± 100 m, the resulting uncertainty in the physical librations calculated from the difference, (measured total libration) minus (calculated optical libration), would be $(100^2 + 84^2)^{1/2}$, or ± 130 m. This displacement subtends $15''$ or about 0.004° at the moon's center.

The estimate, 0.004° , is to be compared with the present uncertainty of about 0.01° . (We were looking for an improvement from ± 300 m to ± 100 m to make the effort worth considering.) The improvement in our knowledge of the amplitude of the physical librations would be better than the factor 2.5 indicates, however. To begin with, the $\pm 0.004^\circ$ is a more or less "instantaneous" value; but one would expect to accumulate a large number of data over many lunations, so that the accidental effects would tend to be smoothed to a much lower value. Then, instead of using a standard value of the distance to the moon to calculate the effects of the optical librations, one could use the measured distances themselves. The principal sources of error would now be the scale factor error in the measured distance. We have treated this error as if it were accidental, when it is really systematic, but unknown. Its effect on each of the two terms of the difference, total measured libration minus calculated optical libration, would be the same, and would cancel out in the difference. What this amounts to is using the raw range data as a function of the time to solve for the following unknowns: (1) the

entire set of parameters for the physical libration, but (2) only the mean distance to the moon for the parameters of the optical libration. This is not the same thing as treating both librations as entirely unknown, which was already counterindicated in subsection (2) above.

4. The difficulties involved in sorting out the variation in range due to the physical librations and that due to the eccentricity of the moon's orbit can be largely avoided by placing beacons at opposite limbs -- east-west for librations in longitude, and north-south for latitude. (Three beacons, roughly 120° apart in position angle, would be sufficient to determine both librations very well.) The reason is obvious: The gross effect of the eccentricity of the moon's orbit on the range to all points on the moon's surface is the same, i. e., the sum of many periodic terms, but all in phase. The effect of librations on any point on the moon's surface is the sum of a different set of periodic terms, but the phase is opposite for points on opposite limbs. The two effects can now be separated. Then the effect of optical librations can be rather exactly calculated (within the limits of the scale factor error which affects everything alike) and removed; and the remaining residuals used to solve for the physical librations.

SECTION VI
DETERMINATION OF ASTRONOMICAL POSITION
AND REFERENCE AZIMUTH OF THE LANDING SITE

A. INTRODUCTION

As stated earlier in this report, observation of the astronomic position and a reference azimuth at the landing site will accomplish the following in whole or in part:

- (i) it would furnish an improved zero-point datum for a system of selenocentric latitudes and longitudes for any selenocentric system, i. e., one that is a better fit to the moon's real axis of rotation;
- (ii) other sites can be occupied later and tied to the first site so that intercomparison between astronomic positions and selenodetic positions would give deflections of the vertical; and
- (iii) even if subsequent sites are not tied to the first site by a common selenodetic net, it would be useful to have astronomical fixes at all sites in order to establish the relative positions of any two sites with an uncertainty no greater than the combined observational uncertainty of the astronomic fixes of the two sites, plus the (unknown) differences of the deflection of the vertical at the sites. It must be borne in mind that the $1/6$ lunar gravity compared to the force of gravity on the earth could well mean deflections several times those found on earth, assuming similar non-homogeneity of the moon.

B. PROCEDURE

Determination of astronomical position and azimuth reference is proposed to be accomplished by reducing the films from the panoramic camera as described in Section IX, and will not be repeated here. It should be

mentioned, however, that some experimentation on earth with the panoramic camera system, including reading and reduction of the films, should be undertaken in order to determine the number of panoramic pairs necessary to yield the varying degrees of statistical accuracy of astronomic positions. This would be the deciding factor in determining the number of panoramic photographs to be taken. For the purpose of this report, it is assumed that two sets of paired photographs will be taken.

C. ACCURACY OF RESULTS TO BE EXPECTED

Summarized in the paragraphs which follow is a preliminary error analysis of results which could be expected from this photography. Appendix D provides a derivation of formulas that may be used in actual practice in reducing the paired panoramic photographs.

1. Astronomical Position

The estimated error for astronomical latitude and longitude may be given by $\frac{\sqrt{2} 10''}{\sqrt{nN}}$ where n is the number of stars (images on the plate), since each star contributes one degree of freedom to the system of equations, and $10''$ is assumed to be the error in the vertical scaling of the plate. With 4 photographs and 50 stars per photograph, the error is $1''$.

A realistic position uncertainty, however, must take into account the standard error associated with the lunar pole. By taking 12-hour time lapse photographs of the polar star field on a single mission with a 150 mm lens of 2 or 3 inch aperture, this error will amount to $(1000/150) \approx 7''$ (see Section IV). This is the controlling error. The total error of astronomical position will initially be $7''$ or about 60 m as measured in the lunar surface. As additional pole determinations are made on subsequent missions the position of the pole will become refined and the error will be reduced. Eventually, it should be possible to calculate the position of the lunar pole with the same degree of accuracy as is possible for the earth's pole now. At any stage of this improvement in knowledge of the instantaneous position of the moon's pole, the astronomical position of the camera can be revised.

2. Astronomical Azimuths and Zenith Distances

If astronomical azimuth and zenith distances can be scaled to $10''$ in a single photograph, the azimuths and zenith distances to the same object in N photographs would be in error due to plate scaling errors by $10''/\sqrt{N}$. To this must be added the transverse error of the pole or $7''$, so the total errors in azimuth and in zenith distance will be $(\frac{100}{\sqrt{N}} + 50)^{1/2} \approx 10''$. For laying out a local triangulation network, estimates of angular measurement uncertainty between two objects is $\frac{10''\sqrt{2}}{N}$ or $10''$, since the pole error will cause a systematic error in the orientation of the whole net and will not affect angular relationships between stations of the net.

SECTION VII

USE OF GRAVITY OBSERVATIONS FOR SELENODETIC PURPOSES

A. INTRODUCTION

When ground surveys of extensive parts of the moon's surface eventually become possible, it will be desirable to make gravity surveys to (1) measure anomalies in the moon's gravitational field to obtain data pertinent to the internal mass distribution, and hence the physical structure of the moon; and (2) obtain data useful for the reduction of high-precision mapping, i. e., deflections of the vertical, "selenoid" heights, etc.

But the immediate question is, is there any value in measuring g_m , the moon's acceleration of gravity at some one point on the moon's surface? There are two possible applications of such a measurement, which need not wait for a wider-area survey to become useful:

1. To obtain a value for the moon's radius R_m , independent of other methods of measurement; or
2. To obtain a single sample of a lunar gravitational anomaly, which (if it is very different from zero) would suggest the order of magnitude of other anomalies to be expected, and perhaps provide a guide for future surveys.

It should be stressed that one cannot carry out both 1 and 2 from the same data. The difference between 1 and 2 is simply this: in 1 the measured value of g_m is assumed to be a representative value, unaffected by anomalies and R_m treated as unknown; in 2, R_m is treated as known and value of g_m computed from it, with which the measured g_m is compared.

B. MEASURE OF MOON'S RADIUS

Let us assume that the error of the CSM's position from terrestrial Doppler tracking data is ± 100 m with respect to the moon's center of mass (the location of which with respect to surface features is, however, not precisely known.

As described in detail in Section XI below, the direction of the LEM, sitting on the moon's surface, can be observed from the CSM with respect to stars, using the SXT, with an angular precision of approximately 20" per observation. A minimum of three such observations with CSM-to-LEM lines of sight crossing at large angles ($60^\circ - 120^\circ$) would give a three-dimensional fix with respect to the CSM orbital positions with precisions of about $1:10^4$. If the minimum slant range CSM-to-LEM for these observations is 200 km, the error ellipsoid of the LEM position with respect to the CSM orbit would be about ± 20 m., but can be made smaller by repeated observations, or observations at closer range, or both. Thus, the error of the LEM position with respect to the moon's center of mass would still be about ± 100 m. in each dimension, with these assumptions.

The acceleration of gravity at the moon's surface g_m is given by two components: the gravitational component, $g'_m = GM_m/R_m^2$ toward the center of mass, where M_m and R_m are respectively the mass and radius of the moon, and the centrifugal component, $g''_m = \omega_m^2 R_m \cos \phi$ perpendicular to and away from the axis of rotation, where ω_m is the sidereal rate of rotation of the moon in radians/sec. (The moon is taken to be a sphere, which it is, within all existing errors of measurement.) G is the universal constant of gravitation, 6.670×10^{-8} cm/sec² per g/cm², and ϕ is the selenographic latitude. Since $g''_m = 10^{-5} g'_m$, we may neglect g''_m in this illustration.

From the foregoing, one then has $R_m = (GM_m/g_m)^{1/2}$, which can be used to evaluate R_m independently of other measurements of R_m , given a numerical value of GM_m and measurements of g_m . The product GM_e , where G_e is the mass of the earth, is known to about $1:4 \times 10^5$, although the relative errors of G and M_e taken separately are considerably larger. That is because the product GM can be obtained very precisely from the orbits of satellites revolving around a body with mass M , but in the equations of celestial mechanics the quantity M never occurs except in the product GM .

The product GM_m can be obtained either from the orbits of satellites revolving around the moon (potentially a very accurate and powerful method, but not yet achieved), or from GM_e multiplied by the mass ratio M_m/M_e . This ratio, 80.32^{-1} , is known to about one in the last significant figure, or

1.8×10^3 . Since this error is much larger than the relative error in GM_e , it can be taken to be the relative error of GM_m . The relative error of $(GM_m)^{1/2}$ would then be 1:16,000.

Gravity meters designed for terrestrial use measure relative values of g (referred to some standard location and conditions) with great precision. With careful calibration and with short time durations, uncertainties due to the drift of the meter are minimized, and errors can be kept well below 1 milligal ($1 \text{ gal} = 1 \text{ cm sec}^{-2}$). The acceleration of gravity on the moon is approximately 164 gals (about 1/6 the terrestrial value), so that instruments designed to work on the moon must be calibrated in some way not yet tested. It may be possible to lay the meter nearly horizontal in order that it would react only to a component of the earth's field. Assuming that calibrations performed in this way would be good to only ± 10 milligals, then the relative error of a measurement of lunar g_m would be 1:16,800, and for $(g_m)^{1/2}$ it would be 1:33,000. (These questions are treated in greater detail in subsection D below.)

The uncertainty in R_m due to an uncertainty of 1:8,000 in GM_m then is

$$\epsilon_{R_m} = \partial R_m / \partial (GM_m) \cdot \epsilon_{GM_m} = 1/2 R_g \epsilon_{GM_m} = 106 \text{ m.}$$

The error in R_m due to an error in g of 10 mgals is

$$\epsilon_{R_m} = \partial R_m / \partial g \cdot \epsilon_g = -GM_m / 2R_g^2 \epsilon_g = -51 \text{ m.}$$

The total uncertainty in R_m would thus be about 120 m, quite comparable to the error associated with the value of R_m derived from the CSM orbit and LEM sightings. This means that if one assumes that the moon is free of appreciable gravity anomalies, values of R_m obtained from surface gravity measurements could have intrinsically about as much weight as those obtained by CSM tracking and LEM sightings.

The precision of the value R_m derived from surface gravity measurements would be improved if the value of GM_m could be improved. There is little likelihood that observations of the moon or its motion made from the

earth during the next five years will greatly improve the existing value, but accurate tracking of circumlunar satellites could very well do so.

The precision of measurement of lunar surface g_m can be improved by using a pendulum, if the visit to the lunar surface is long enough, although there would not be much point in it until the accuracy with which GM_m is known can be improved. Pendulums have the virtue of giving absolute, rather than relative values of g , although they are not as sensitive to small variations in g , and require several hours to yield accurate results. In subsection D, it is implied that g_m can be measured to about ± 5 mgal without too much difficulty. Then the relative error in g_m is 1:33,600, and for $(g_m)^{1/2}$, it is 1:67,000.

C. SAMPLING SIZE OF LUNAR GRAVITY ANOMALIES

In this case, one would assume the value of R_m obtained from sources other than gravity measurements (e.g., CSM tracking and LEM sightings) as a reference value. A "gravity anomaly" is the difference between the observed value of the surface gravity at a particular location, and the value of surface gravity computed for that same location according to some model. The only model available, from the viewpoint of 1965, without any evidence for departures of moon's gravitational field from spherical symmetry - at least, no real evidence for departures larger than the uncertainties themselves - is a spherical, homogeneous moon, with g_m given by $g_m = GM_m / R_m^2$. The small term due to the moon's rotation can be neglected, as before. Thus,

$$g = g_{\text{obs}} - GM_m / R_m^2$$

With the same assumptions as before regarding errors, the error of the first term in the difference is ± 10 milligals, and the error of the second term ± 28 milligals; so the error of the anomaly is ± 30 milligals. This figure would be reduced by an improved accuracy for GM_m . Even so, this precision seems to be sensitive enough to detect anomalies of a moderate size, if they exist. Anomalies of 50 mgals or less would arouse no great interest and would prove nothing, if obtained at only one location on the moon's surface, but an anomaly of, say, 100 mgals or greater would arouse great interest.

D. INSTRUMENTS TO MEASURE SURFACE GRAVITY

Gravity meters used in geodetic surveys or in geophysical investigations measure the acceleration of gravity g relative to g_0 at some standard station. The best instruments can be read to 0.01 mgal, but are accurate to only 0.1 - 0.2 mgal. These figures correspond to a resolving power of about 10^{-8} and an accuracy of about 10^{-7} .

The classical method for the determination of the absolute value of g is the measurement of the period of a pendulum swinging in a high vacuum to reduce air resistance. The typical pendulum is about 0.25 meter in length, with a complete swing, back and forth, occurring about once each second. The absolute determination of the acceleration requires a very accurate knowledge of the effective length of the pendulum, which changes with temperature, and the effects of air resistance, pivot friction, magnetic forces, and pendulum support flexure. To determine the period with the necessary refinement requires accurate timing of a great number of swings. An error in the period of 0.5 μ -sec leads to an error in g of 0.1 mgal. A determination normally requires some six hours of swinging if the total counted number of swings is timed to 0.01 sec. Necessary accessories are a vacuum chamber (on earth), an optical-electric system for counting the swings, an accurate timepiece, and an interferometer for measuring the flexure of the pendulum support.

The possibility of swinging a small bob hung from the LEM at the end of an invar wire filament, say, 4 meters long, nevertheless is an attractive one, as the device is so simple and a hard vacuum already exists on the moon. Friction arising from the flexure of the filament and the LEM frame would probably be negligibly small for small amplitudes of swing, and the relatively long period of such a pendulum in the low lunar gravity field (about 10 sec) might simplify the task of counting the swings. If the effective length of such a pendulum were known to 4 microns (that is, $1:10^6$), the error in the derived value of g would be 0.16 mgal; if the error in length were 0.4 mm, the error g would be 16 mgal. Invar has a coefficient of relative expansion ranging from 0.7×10^{-6} down to negative values; let us take 0.4×10^{-6} as a typical value. The tempera-

ture of the wire could therefore be in error by quite a large amount and still not vitiate the result completely. For example, if the temperature were in error by 100°C , the length of the wire would be in error by $0.4 \times 10^{-6} \times 400 \text{ cm} \times 100$, or 0.16 mm, and the measured gravity would be in error by 6 mgals. Even if the temperature of the filament were not measured, the temperature of a similar wire immersed in the same bath of ambient radiation could be measured with a simple thermocouple weighing at most a few grams. If sufficient pains are taken to expose the two wires to the same amount of sky, i. e., arrange them so the LEM body blanks out the same solid angle of sky and terrain, the temperature match could be made quite close; but we have seen that extreme pains are unnecessary. It should even be possible to calculate the wire temperature closely enough from the approximately known radiation field to which it is exposed. The length of the wire as a function of the tension exerted by the bob could be calibrated in a terrestrial laboratory before and after the mission. If the bob were allowed to swing for 10,000 sec (about 3 hrs.), i. e., complete 1000 swings, and the total time were measured with an accuracy of 0.01 sec, the resulting error in measured g from this cause would be 0.3 mgal. The method looks entirely feasible if a simple device can be constructed to count the number of swings automatically, and to record the times of the first and last swings with reference to the time signal available in the LEM. Possibly the shadow of the bob could be caused to fall on a photocell (twice per oscillation) and the pulses resulting from the interruption in the photon current used to operate a counting circuit, the whole thing miniaturized to weigh a few ounces.

An alternative terrestrial system is based on the timing of a body in free fall. The measurements of time and fall distance, however, must be exquisitely fine, which confines this method for the foreseeable future to the laboratory. Even there, it is surrounded by great difficulties and has not been found very satisfactory.

There are several possible systems for the measurement of differences in g between a reference point and a new point in the field. Exotic applications of accelerometers have been considered but no satisfactory method has been derived. Somewhat more success has been achieved with the

measurement of the frequency of vibration of a filament supporting a known mass. The results have been inferior, however, and the complexity of the attendant apparatus makes this method impracticable for field use. Static methods, wherein the elongation of a fiber under the load of a small mass, or the flexure of an elastic support, are found to be most convenient and useful, and most portable gravity meters are based on this principle. They are extremely sensitive to small differences in g between one place and another, even as small as 0.01 mgal. No such instruments have operating ranges admitting of absolute measures, nor of relative measures between places having wide differences of g . They must be adjusted, therefore, rather closely to the expected g value, and calibrated at a place of known g before moving to a new point.

Most gravity meters are extremely sensitive to ambient temperature and are either provided with means for temperature control, thereby requiring accessory heating equipment and power supply, or are temperature compensated. The Lacoste-Romberg gravity meter, one of the two meters best known in America has a temperature-controlled housing which weighs about 15 pounds and probably cannot readily be miniaturized much below that figure. The other widely known meter, the Worden gravity meter, is temperature-compensated, requiring no external power source. It is lighter than the Lacoste-Romberg meter, and the weight can probably be further reduced to the order of a pound or so. The Worden meter is characterized by a considerably higher drift rate than the temperature-controlled Lacoste-Romberg; however with careful use it is capable of equalling its performance. Apart from the wire-bob pendulum discussed above, the Worden meter is apparently the only gravity instrument suitable for lunar use. The problem of miniaturizing should be minor. Since the meter must be calibrated at a point of known g not greatly different from that of the place of intended use (for the moon this is about 160 gals) special means to calibrate it must be developed. No gravity field of that magnitude can be simulated on earth that lasts long enough or that is accurate enough to permit a normal calibration process. Substitute methods might, however, be devised, e. g. by inclining the instrument, or by interchanging masses of correct weights.

A development to solve the problems of miniaturization and calibration could be initiated; sooner or later it will certainly be useful for survey missions, if not used on the first missions. The makers of the Worden gravity meter have indicated that the cost would probably be in the range \$100,000 to \$200,000, depending upon the accuracy desired. They have emphasized the difficulty of calibration and have expressed doubt that a Worden type meter could be calibrated with existing methods more closely than 5 milligals or so. Therefore an accuracy of 10 milligals may be presumed to be within reach.

SECTION VIII

USE OF HORIZONTAL AND VERTICAL CONTROL POINTS ON THE LUNAR SURFACE, AND PROCEDURES FOR OBTAINING THEM

A. INTRODUCTION

Although extensive surveys cannot be carried out on the lunar surface during the early Apollo missions, it should be possible to establish a limited number of local horizontal and vertical control points (surface features or artificial targets) in vicinity of the landing sites. However, since the astronauts will not travel more than 1,000 ft. from the LEM, the size of the survey area will be restricted to a short range of visibility. Assuming the landing site will be in a relatively flat area, the maximum distance to the visible horizon will only be ≈ 2.5 km when the astronaut is standing on the lunar surface, or ≈ 5 km if he is able to observe the landscape from the top of LEM. The allowable survey region defined by the local horizon would thus be confined to an area of ≈ 20 -80 sq. km. At some of the proposed Apollo landing areas, surface features as far away as 20-30 km may be visible from the landing site; however, it is doubtful that these features could be adequately positioned with surveying equipment that can be carried in the LEM.

B. VALUE OF LOCAL HORIZONTAL AND VERTICAL CONTROL

Considering that surveys will be restricted to a small area around each landing site, their value will be discussed as related to two functions for which a network of local horizontal and vertical control points might be useful:

1. To provide mapping control for use in reduction and orientation of orbital photographs to a coordinate system oriented to the axis of the moon.
2. To aid in obtaining the precise location of geological features or geophysical apparatus which may be used during the lunar landings.

1. Mapping Control Points.

It is planned that mapping photography with a ground resolution of 8 meters will be obtained from Lunar Orbiters at 50 km heights above the moon's surface using a 3-inch focal length camera with $\approx 45^\circ$ field of view (area coverage of $\approx 36 \text{ km}^2$ on the lunar surface). [8] The photography will have 55% forward overlap to provide stereo coverage along the orbital path and sufficient sidelap from successive orbital tracks to provide continuous coverage over areas approximately $200 \times 200 \text{ km}$.

This photography will probably be reduced by conventional photogrammetric methods relying on analytical triangulation for adjustment of large blocks of photographs. For reduction purposes the reference points in the existing AMS or ACIC lunar control networks, or the known positions of the exposure stations (as determined from DSIF tracking), will be used for control.

In adjustment of block triangulation (which in the Orbiter case may include 10 or more photographic strips and ≈ 100 frames), control data could be weighted according to their estimated or known accuracies. Assuming that orbital mapping photography is of good metric quality, resulting positional accuracies of lunar features obtained from phototriangulation would depend mainly on the amount of control available, its distribution within the photographed area, and the errors of the control itself. (See Appendix A for error analysis of orbital photography.)

In view of the capabilities of photogrammetric aerotriangulation [9, 10] and results of the analysis made in Appendix A, orbital photography should be capable of providing positions of well-defined features on the lunar surface to an accuracy of 100-250 meters within a self-consistent coordinate system defined by either the orbital tracking data or reference points of the AMS (or ACIC) control networks. A positioning capability of this order of accuracy seems adequate for initial lunar operations and can be obtained without the need of control points established directly on the lunar surface.

It should be kept in mind, however, that to a very large extent measurements that can be attempted during the early Apollo landings, especially the first one, are to be considered experimental in nature, and to be the basis for deriving improved techniques, methods and equipments to be used on future missions. As the astronaut's mobility around a landing site and his range are increased, with the ultimate possibility of widely varying travel over the surface of the moon and the connecting together of landing areas, the value of establishing and extending on the surface horizontal and vertical control networks correspondingly increases. It is therefore considered important to devise a workable surface system of obtaining horizontal and vertical control, even though on the first mission the area covered will be small and its selenodetic value per se perhaps marginal.

It should also be pointed out that in the event lunar orbital photography is not successful, or that the LEM lands in an area not covered by the photography, and that SXT observations are not provided for or are unsuccessful, the value of the local horizontal and vertical control coupled with astronomic observations which will also be undertaken, becomes greater. In addition, the further utility of these observations should be considered in the light of the benefits outlined below:

- i. It would be desirable to have positions of lunar features referenced in a coordinate system oriented to the axis of the moon rather than in a barycentric coordinate system (based on orbital tracking data) or one defined by earth-based photography (AMS or ACIC system), making it necessary to adjust the map coordinate reference to a lunar astronomic reference system. This could be accomplished by establishing a number of well-distributed reference control points (with astronomic orientation) on the lunar surface. A single position as obtained from an isolated landing, however, would not be sufficient. At least three widely separated control points in the mapped region would be needed, which could be obtained only during the series of Apollo landings.

- ii. If a number of well-defined horizontal and vertical control points are available in the vicinity of the Apollo landing sites and identifiable in orbital photography, it may be possible to use these reference points, after a number of lunar landings have been made, to reduce orbital photographs independently of the existing control points in the AMS or ACIC control networks. For example, suppose that a local network of well-distributed, horizontal and vertical control points (say 4-6) are established at each landing site and that orbital mapping photographs cover the area between 2 or more landing sites. Under such conditions it may be possible to utilize each local horizontal and vertical control network as photogrammetric control for aerotriangulation operations. For this purpose, the lunar ground points could serve as independent selenodetic control to obtain scale and orientation of perhaps one or two photographic strips which, in turn, could be used to adjust a block of photo strips covering a large area of the moon's surface. The accuracy of the aerotriangulation would depend on the distribution and number of available local control networks. Since the latter would be limited by the number of actual lunar landings, careful planning and design of the aerotriangulation operations would be necessary to obtain accurate mapping results independent of the existing AMS or ACIC lunar control networks.

Although the surface control points from one landing site to the next will not be selenodetically tied together, this should not prevent aerotriangulation or bridging operations, as each local control network could be treated as independent control to provide scale and orientation for a number of widely separated photo exposures. Procedures for using independent control for aerotriangulation have been investigated extensively in recent years. One procedure, known as the Cross-Bases Method, has been found to be ideally suited for geodetically unexplored regions (such as the moon), as it is independent of deflections of the vertical. [11] In this method, the bridging of a photographic strip is accomplished using local base lengths, azimuths and vertical heights at the ends of a photo strip, without relying on geodetically connected control points over the length of the strip. The method

requires only a minimum of control; e. g., a baseline (normal to the photographic flight strip) at each end of a strip, the astronomic azimuths of these baselines, and three well-distributed vertical reference points at each end of the photo strip.

It appears that photogrammetric control of the type needed for the Cross-Bases Method could be obtained at each landing site if local surveys of the type outlined in Section D below are accomplished. These ground control requirements should not be difficult to meet; for example, a local horizontal and vertical control network accurate to 1:2500 and about 30 arc-seconds should be adequate.

On the basis of the above considerations, it appears that it would be advantageous to survey mapping control directly on the lunar surface for selenodetic operations, particularly if it is desirable to have features referenced in a coordinate system oriented to the mean axis of rotation of the moon. It is possible also that these control points could, after a number of lunar landings, provide an independent check on existing maps referenced to the AMS or ACIC control networks.

2. Positioning of Geophysical Equipment.

Local surveys of low-order accuracy will be needed in the vicinity of the Apollo landing sites to support geophysical observations that will be undertaken. One of the main purposes of these surveys would be to determine relative positions of geophysical devices that may be placed around the landing site, as well as significant geological features, and to determine their positional relationships to nearby lunar features. The needs of the geologist and geophysicist can best be met by a large-scale topographic map of the area, which could be obtained by surface photography if it is not obtainable from high-resolution orbital photographs prior to the landing. Control requirements for geophysical mapping, however, are not at all stringent, since directions (bearings) to features need to be accurate only to about $1/2^\circ$, relative horizontal distances between features to within about 1:500, and

vertical angles to within 1° - 2° [12]. Survey procedures outlined in paragraph D below would easily satisfy these needs.

C. REVIEW OF PROCEDURES AND EQUIPMENT FOR ESTABLISHING CONTROL POINTS

Applications of a wide variety of surveying methods and devices for establishing control points on the lunar surface for the above purposes were considered, taking into account operational constraints of the Apollo mission and the lunar environment. Brief comments regarding the major categories are presented in the following paragraphs.

1. Distance Measuring Devices.

(a) Taping. The simple procedure of taping a thousand feet on one, two, or three sides of the LEM to establish short baselines for use in positioning distant survey targets would be attractive, if it were not wholly impracticable. If the effort were possible in the time allowed, results obtainable would be of low accuracy and, since unverifiable, of even lower reliability.

Accuracy of a taped line is most affected by blunders, which would be unusually hard to avoid in the strange and difficult environment. Other sources of taped error are variations in temperature, tension, sag, level, alignment, and in the precise definition of the measuring end points. Each of these contributes to degradation of results.

(b) Electronic distance measuring equipment. Conventional instruments of the Geodimeter and Tellurometer types require a placed and directed reflector or transponder, which excludes them for measurements beyond the walking range of the astronaut. In addition, current models are too heavy and bulky and require more power than can be expected for this operation. Without further elaboration it is believed that other and better techniques will be available.

Radar and laser devices capable of ranging to passive targets at a five kilometer range or more are encouraging for lunar operations and, therefore, detailed consideration was given to their application. A comparison of radar and laser ranging techniques was made and results indicated that laser ranging would be more promising for survey operations (see Appendix G).

(c) Indirect distance measuring devices. These include subtense and stadia instruments, range finders, and mounted stereoscopic cameras. Insofar as they require short portable precise fixed bases they are not accurate for the longer ranges desired; and the instruments are generally heavy, bulky, inconvenient and time-consuming to operate especially for a single operator. The short-base procedure described in Paragraph D2 below is a development of stadia methods which, as modified, is considered a more practicable technique for the mission.

2. Angle Measuring Equipment.

(a) Theodolites. It is not likely that a precise theodolite, the basic tool of geodetic engineers, would be practicable for the initial missions. The time and effort required for accurate direction measurement are far out of proportion to results that may be expected from a short mission at a single location. It would be necessary to adapt the fine pointing and adjusting screws to the pressure-gloves the operator must wear. Precise sighting through the helmet faceplate would be difficult and making the readings would not be much easier. Descriptions of terrain targets would be ambiguous, and each pointing is an independent operation, which would severely limit the information than can be obtained in a short time.

Use of a conventional photo-theodolite would have most of the drawbacks mentioned for any theodolite. Its need, for example, for precise pointing and angle reading is a serious disadvantage. The concept of making angle measurements photographically, however, is well established, and implementation of this approach is described below.

(b) Photography. This is the most logical approach for obtaining angular relationships of lunar surface features or survey targets. A large number of positions of prominent features can be had from photographic intersections with a minimum of field operations; time here saved is a huge asset. The absence of any lunar atmosphere and, therefore, of any vertical refractions, insures that vertical angles taken from the terrestrial photographs are true; this means that reliable relative elevations are available on intersected terrain features. (Vertical angles taken in the earth's atmosphere are subject to considerable errors due to uncertain vertical refraction.)

The normal recording of angle readings would be highly objectionable under conditions where there is but one astronaut surveyor on the lunar surface; terrestrial photography obviates this angle recording and provides a permanent and true record of field data.

D. SELECTED SURVEY PROCEDURES

From the above considerations it appears that the most promising surveying techniques would involve either photogrammetric procedures coupled with an electronic ranging device, or exclusively photogrammetric methods. In the former method, distance measurements could be made by laser ranging to remote passive targets, and angular data to these targets could be obtained photogrammetrically; all measurements being obtained from a single station which, ideally, would be the top of LEM. For the latter method, a short baseline could be obtained photogrammetrically using the dimensions of the LEM and combined with horizon photographs taken from nearby stations to intersect distant targets. For further discussions, these methods will be designated as the "range and angle method" and the "short base method."

Possible application of these surveying techniques for determining a local network of control points in the vicinity of the Apollo landing areas is outlined in the following paragraphs, and a detailed program for use of each method in conjunction with selenodetic measurements is presented in Section IX. In outlining these methods, it is assumed that the camera equipment

(panoramic and precision frame cameras) recommended in Appendix E and survey targets (reflectorized balloons) proposed in Appendix F will be utilized.

1. Range and Angle Method.

In this method which would provide a local control net only, it is proposed that an observation station on top of the LEM be used to obtain range and angle measurements, as this location would provide the maximum range of visibility to the local horizon. Range measurements would be obtained using a laser ranger and directions (both horizontal and vertical angles) would be obtained photographically using the panoramic camera recommended in Appendix .

Since survey targets must be detectable in orbital photographs as well as being visible from the LEM, it is proposed that 10-foot diameter reflectorized mylar balloons be used. (See Appendix F for details.) These balloons would provide specular reflections of the sunlight and be detectable as point sources in both the orbital and surface photographs. They would also serve as passive reflectors for the laser ranger.

In establishing a local control network, the survey targets should be placed as far away from the LEM as the range of visibility will allow and be evenly distributed around the LEM; thus, a means of ejecting the targets (balloons) to their desired location is required. For this purpose, it is proposed that a small launcher utilizing compressed gas cartridges (or possibly other means) be used to eject the balloon targets. The balloons could be packaged in a small container weighing less than one pound and would be self-inflating after ejection. Launching of the balloons to distances of ≈ 5 km by a small self-contained ejection system seems feasible in the low gravity field of the moon.

In applying the range and angle method, balloon targets (4-6) would be launched in cardinal directions to distances of ≈ 5 km. Panoramic photographs of the horizon are then taken from a leveled support on the top of the LEM. These pictures will include the balloon targets, the landscape from

about seventy meters from the LEM to the horizon, and a belt of stars above the horizon. The camera position is also used by the laser ranger to obtain distances to each remote balloon target and, if possible, to a number of prominent terrain features. Each range reading is referenced to the others for identification purposes by rough azimuth readings using a simple pelorus or horizontal circle attached to the laser or instrument support. Readings of laser distances and azimuths could be made orally and recorded directly on the astronaut's voice tape.

Characteristics for the laser ranging device are discussed in Appendix G, together with some of the design problems that should be considered. Ideally, the laser should be capable of ranging to distances up to 20-25 km with an accuracy of at least 1:2500 for distances up to 5 km and about 1:5000 for maximum distances. It should not weigh over 10-15 pounds including its power source.

In operation the laser would be attached to a support on top of the LEM and sighted on a selected target by using simple sights or, if necessary, a specially designed telescope. Range measurements could be read visually from a digital display and recorded orally by the astronaut on the voice tape.

Detailed characteristics of the panoramic camera are presented in Appendix E which considers camera specifications for the various selenodetic experiments. As proposed, the panoramic camera would have a potential metric accuracy of 10 arc-seconds. It would provide 350° (or possibly 360°) coverage of the horizon, having a 30° field of view in the vertical direction to provide 25° coverage of the star field above the horizon and 5° coverage below to contain the terrain. The camera employs a horizontal fixed objective lens of ≈ 100 mm focal length with a folded mirror system which rotates about the vertical axis to provide an optical scan of the horizon. (See diagram in Appendix E.) The optical system uses a cylindrical focal plane which provides azimuthal angles directly and vertical angles as a function of the camera focal length. The camera uses 70 mm roll film, and provides an image format of 60 mm x ≈ 610 mm.

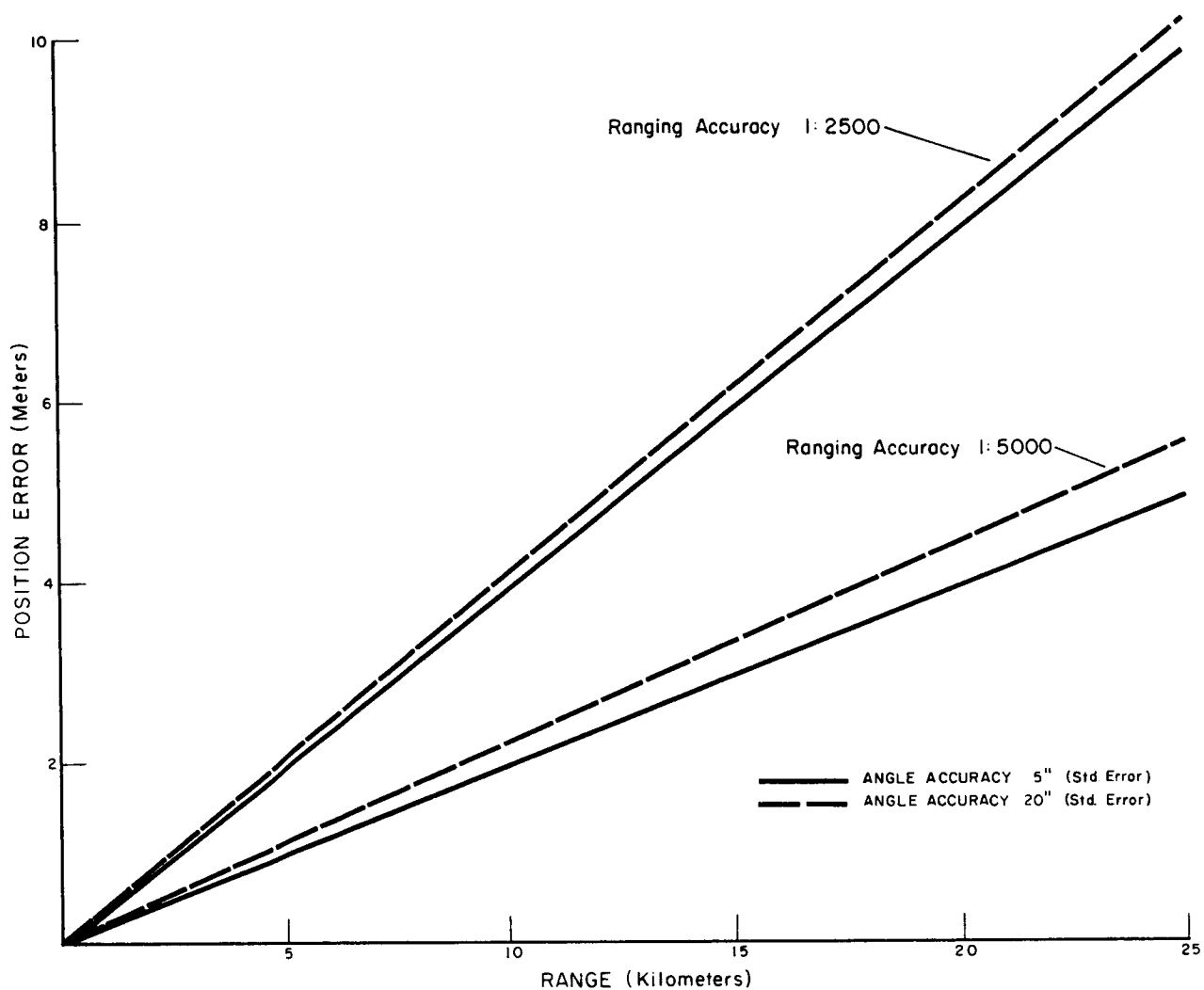
In use, the camera would be mounted on a support platform on top of the LEM and would be approximately leveled by the astronaut. Precision level vials would be provided internally and recorded on each photographic exposure, thereby eliminating the need to have the camera precisely leveled to the local vertical at the time of exposure.

Figure VIII-1 indicates the positioning error that can be expected for given accuracies in range and angle measurements. Since directions to distant targets can be precisely determined from photography, position accuracy depends primarily on the precision of range measurements. Considering that it would be desirable to position survey targets within an accuracy of 2-3 meters over distances of ~ 5 km, a ranging capability of 1:2500 would be satisfactory. For distance beyond the 5 km range (for possible positioning of well-defined lunar features which may project above the local horizon) a ranging accuracy of 1:5000 would be desirable.

2. Short Base Method.

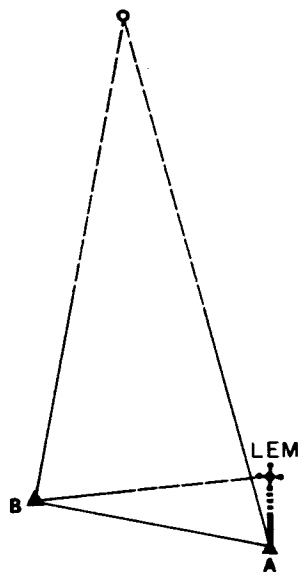
In this method, which could provide local control of lower accuracy than 1 above, but would permit mapping of terrain features, the positions of the proposed survey target balloons would be established solely by photographic procedures, using one of the survey schemes shown in Figure VIII-2. A short baseline is established indirectly between the LEM and station A by photogrammetric resection using the known dimensions of the LEM (or special targets placed thereon). For this purpose, 4 to 6 well-defined target points with known relative spatial orientation must be placed on the LEM, and these must be identifiable in photographs obtained at station A. The known relations of the target points would be utilized in post analysis for the space resection of the camera position at station A to obtain the distance between the LEM and the camera station. This baseline would then be combined with panoramic horizon photographs obtained from station A and one or two nearby stations (either Schemes 1 or 2) to obtain directions for the intersection of distance targets (either artificial balloon or well-defined surface features).

The use of a precision frame camera is recommended for the photo-

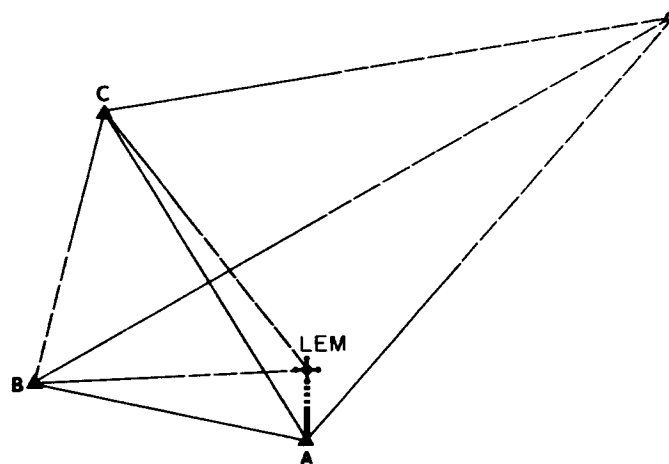


POSITION ERRORS AS FUNCTION OF RANGE
AND ANGLE MEASUREMENTS

FIGURE VIII - 1



SCHEME 1



SCHEME 2

Distance from LEM to camera station A is determined by photo space resection using known dimensions on LEM

▲ - Camera Station
○ - Intersection Station

POSSIBLE SURVEY SCHEMES FOR
POSITIONING SURVEY TARGETS
BY PHOTOGRAPHIC METHODS

FIGURE VIII - 2

grammetric determination of the distance between the LEM and Station A. Characteristics of this camera are detailed in Appendix E, which also discusses its other applications for selenodetic experiments. As proposed, the precession frame camera has a potential metric accuracy of 5 arc-seconds. It would have an f/3 lens with a focal length of 150 mm, a field of view of 40° , and an image format of ≈ 110 mm square. Since roll film is to be used, a focal plane reseau is proposed for the camera to control the effects of film shrinkage and possible distortions that occur when film is not held correctly in the focal plane.

The accuracy in determining the distance between the LEM and station A will depend primarily on the geometric distributions of the target points on the LEM and the accuracy with which they can be positioned relative to each other. They should be spaced as far apart as possible so that the distance to station A can be as long as possible while maintaining reasonable geometry of the reference points in the photographs. As a minimum requirement, the targets should have a relative positional accuracy commensurate with the measuring accuracy of the photographs. Assuming that the latter is 5-10 μ and that the precision frame camera (f=150 mm) is used at station A at a distance of ≈ 30 meters from the LEM, the targets would need to have a relative positional accuracy of 1-2 mm. This amounts to an accuracy of about 1:5000 over a distance of 18 meters which is about the maximum separation that the targets would have if attached directly to the LEM. It is reasonable to assume that preselected points or special fiducial marks on the LEM will be known within this requirement.

In addition to target markings placed directly on the LEM surface, it would be desirable to utilize specially calibrated stadia targets which could be extended from the top of LEM as indicated in Figure VIII-3. These targets would provide photogrammetric control in case there is deformation of the LEM skin or if the other target points are not identifiable in the photographs. The suggested stadia targets consist of 2 four-meter long invar wires suspended from short supports attached at the top of the LEM. Two spherical targets of about 50 mm diameter are attached to the ends of each

POSSIBLE ARRANGEMENT OF STADIA
TARGETS ON THE LEM FOR PHOTO
SURVEY OPERATIONS

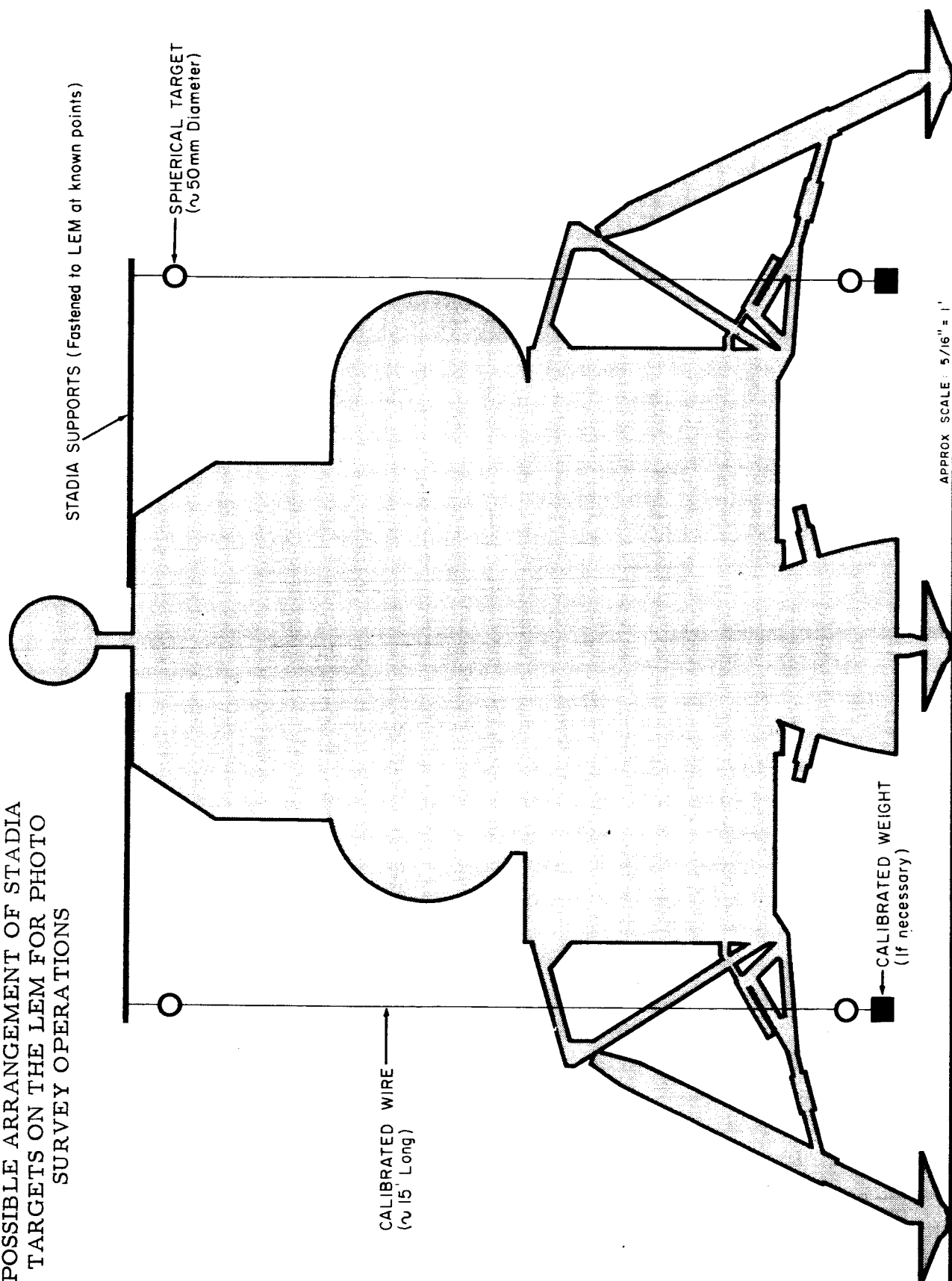
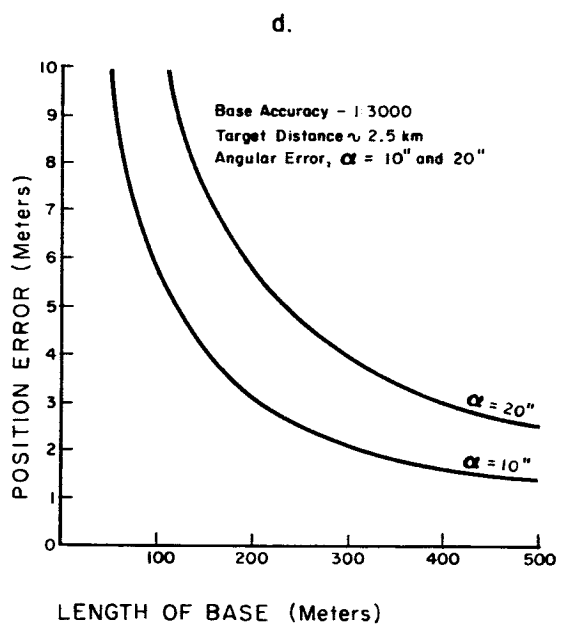
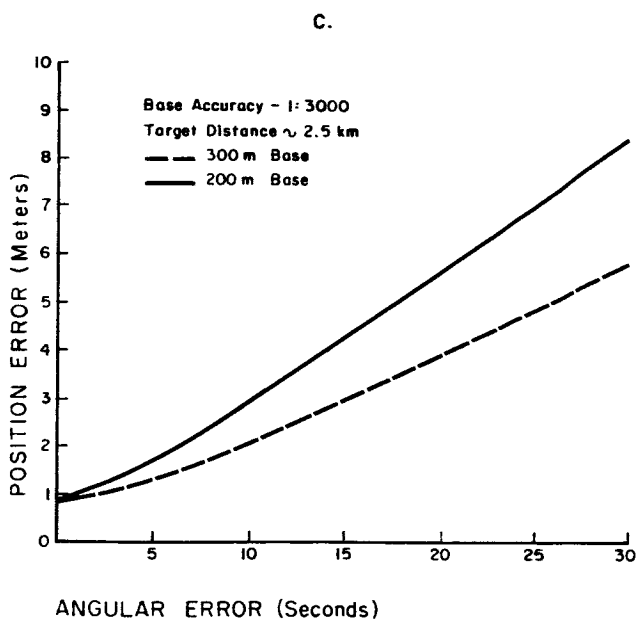
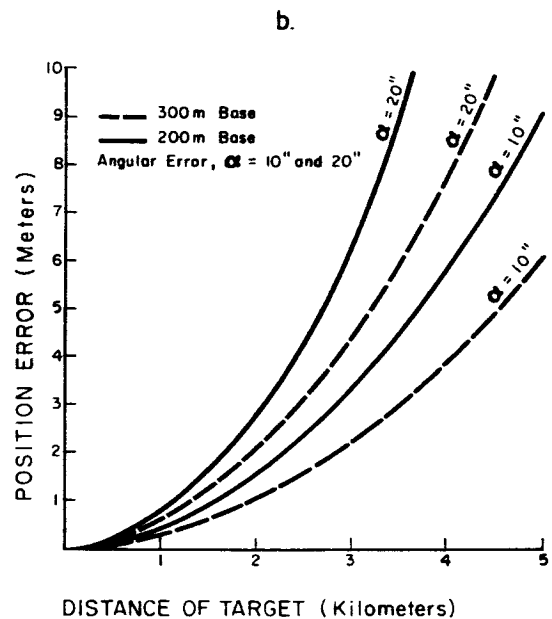
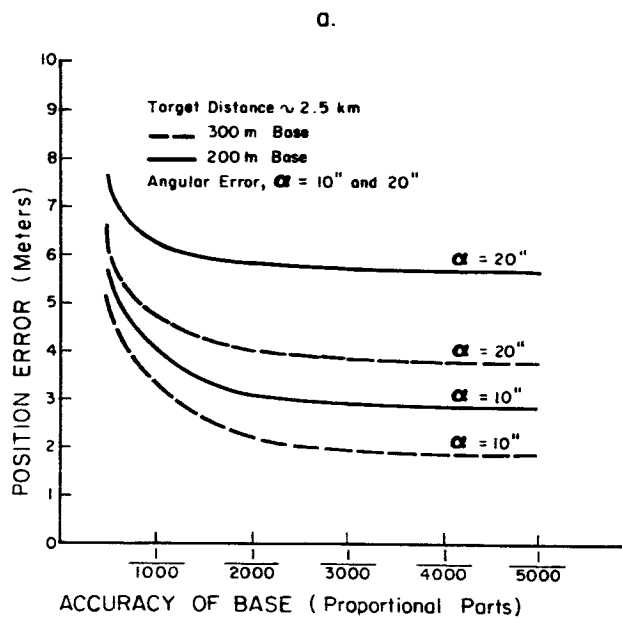


FIGURE VIII - 3

wire. The bottom target could be partially filled with liquid to dampen its oscillation or, if necessary, a liquid filled plumb bob could be used. Alternate positions for attachment of the wire support to the LEM could be provided so that the targets could be visible from any selected location for station A. The positional relationship of both stadia targets for each location of their support brackets could be precisely determined under laboratory conditions.

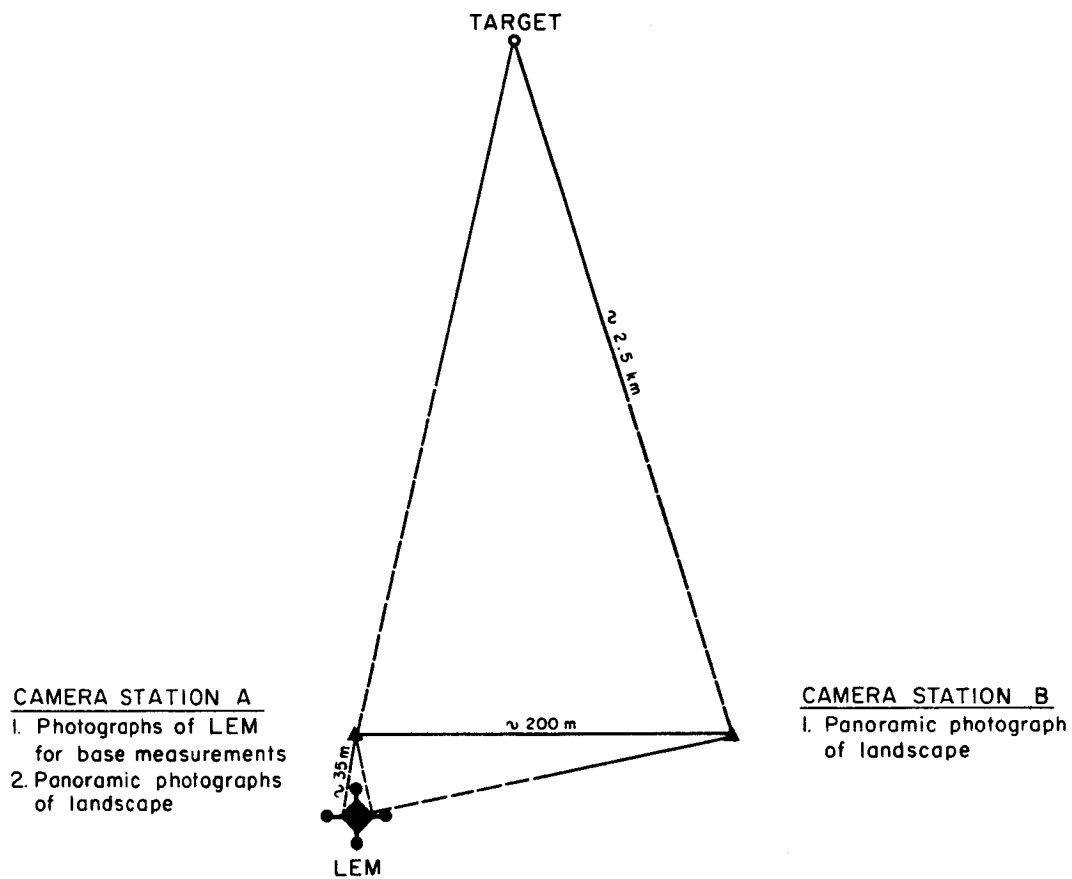
The accuracy of the short base method depends mainly on the number of camera stations used, the geometry of the triangulation, the accuracy of the measured base and the accuracy of angular observations from the camera stations. The graphs in Figure VIII-4 illustrate the effects of these parameters in positioning distant targets for the minimum survey conditions (Scheme 1 in Figure VIII-2) when targets are normal to the base. As shown in Figure VIII-4a, a target position on the visible horizon at a distance of ≈ 2.5 km can be positioned within 2-3 meters when a baseline length of 200-300 meters with an accuracy of $\approx 1:3000$ is used (with angle observations from the camera stations within 10 arc-seconds). Increasing the accuracy of the base beyond 1:3000 would offer no significant improvement in positional accuracy. Figures VIII-4b through 4d show that position errors vary nearly as the square of the target distance and almost directly as the error in angle measurements.

Through experimenting with various combinations of measurements using the graphs presented in Figure VIII-4, it becomes apparent that the most efficient way of arriving photogrammetrically at an accuracy of 3 meters at 2.5 kilometers for the minimum survey conditions, is by the configuration shown in Figure VIII-5. There is, however, considerable leeway in this configuration, enabling the astronaut to select the location of the two camera stations with a crude stadia device, if necessary, without substantially affecting the result. Although the geometric conditions for photogrammetric determination of the distance between the LEM and station A have been relaxed in the configuration in Figure VIII-5 (i. e., the vertex angle at the camera station as defined by the spread of the target points on the LEM is only $\approx 10^\circ$), the accuracy of determination of the base distance using the



EFFECTS OF BASE AND ANGULAR ERRORS
 ON POSITIONING ACCURACY
 WITH SHORT BASE METHOD

FIGURE VIII - 4



SURVEY CONFIGURATION FOR
PHOTOGRAMMETRIC EXPANSION OF SHORT BASE
TO POSITION DISTANT TARGETS

FIGURE VIII - 5

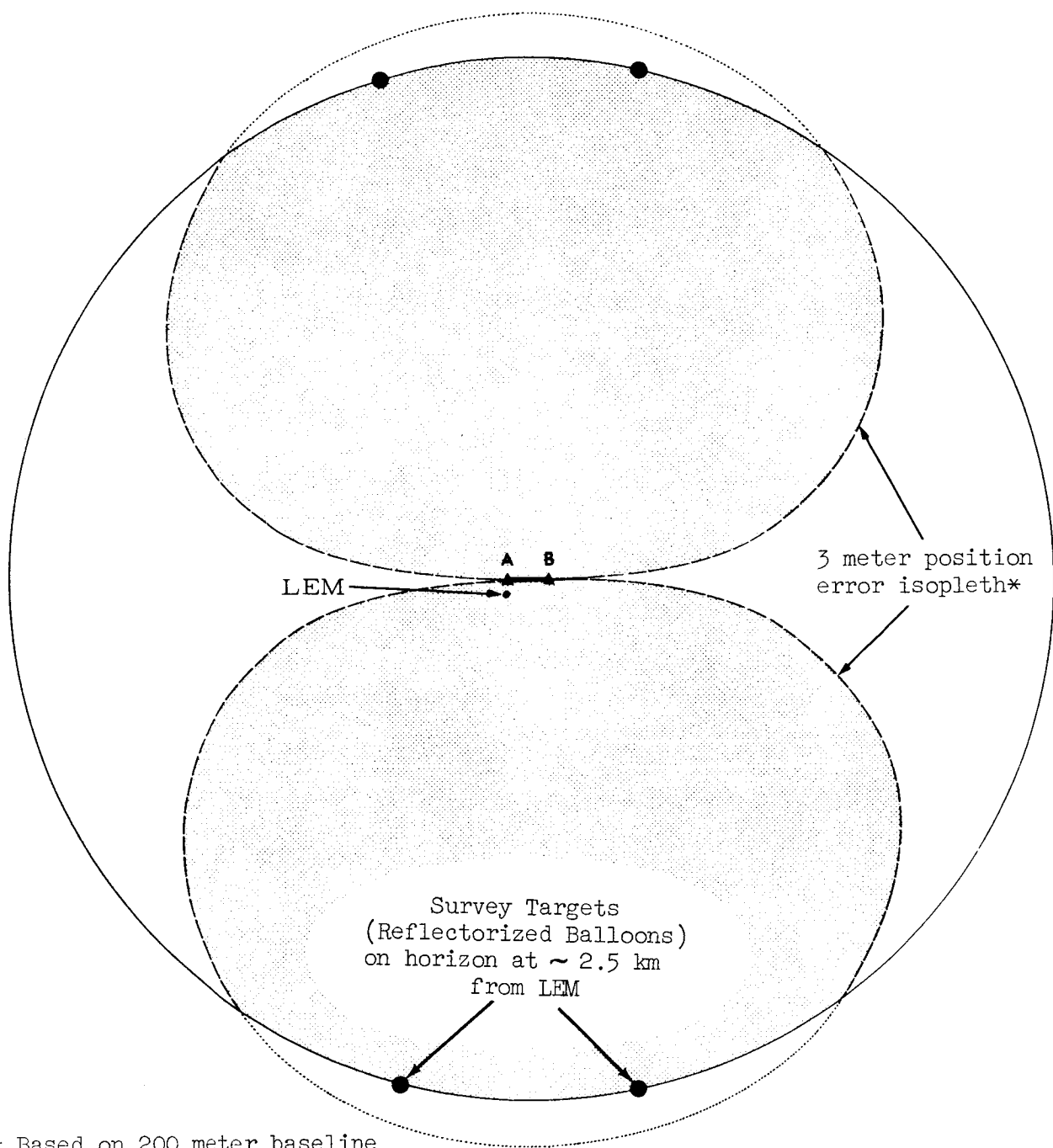
precision frame camera should be on the order of 1:4000-5000, if sufficient target points (5-6) are available in photographs from station A. This base could be expanded to station B within the desired requirement of 1:3000 by utilizing panoramic photographs from stations A and B.

Figure VIII-6 shows the expected capabilities of the short base method for positioning distant targets around the horizon when the expanded base distance (stations A-B) is established with an accuracy of 1:3000, and the angle observations at the ends of the base are within 10 arc-seconds. As indicated, only those targets on the horizon which are located within 45° of the normal to the baseline can be positioned within an accuracy of 3 meters. Therefore, it would be desirable to include an additional camera station for phototriangulation (Scheme 2 of Figure VIII-2) to fix all positions around the horizon.

3. Comparison of Survey Methods

Although the range and angle method seems to be the most promising surveying technique at present for establishing local control points, the short base method was included because the final choice will depend a great deal upon further knowledge of lunar surface conditions, the final configuration of the LEM, and the mobility of the astronauts. Also, each method has inherent advantages over the other which must be considered before final selection of the technique to be used.

The range and angle method can be conducted entirely, and preferably, from the top of the LEM. This has the distinct advantages of eliminating the transporting of equipment on the lunar surface, and of being able to see targets of twice the distance away compared with operations from the lunar surface only. The latter capability is particularly desirable for establishment of photogrammetric control for orbital photography. However, some difficulty may be encountered in the use of ejected balloon targets for ranging operations or in provisions of working room on the top of the LEM. With regard to the latter, the top of the LEM must be reasonably stable and free from vibration, and must also provide room and safety for the operations required; it is probable, however, that the observer may stand in the man-hole at the top of the LEM,



* Based on 200 meter baseline
accurate within 1:3000; angle
observations within 10 arc-
seconds

POSITIONING CAPABILITIES WITH SHORT BASE METHOD

FIGURE VIII - 6

the upper half of his body protruding above the aperture.

Although the short base system would require more time and effort and would be limited to an area of half the radius of that visible from the top of the LEM, it provides some advantages over the range and angle system. The basic advantage is that it provides complete, practically foolproof coverage of the area (i. e. , once the base has been established and panoramic photographs taken from both ends (preferably from the three apexes of a triangle as in Scheme 2 of Figure VIII-2, all discrete points within the photographed area can be located), so that a detailed map of the lunar surface on a local scale can be made, restricted only by the character of the lunar relief. Should the Surveyor and Orbiter series indicate that the landing site would be in an area of considerable relief, the short base method might prove more useful. This method would also provide a means to reference points in any geophysical or geological traverses being carried out.

E. ACCESSORY SURVEY EQUIPMENT

In addition to the surveying instruments discussed above, some accessory components will be required including camera supports, special survey targets, initial leveling devices for cameras, and, possibly, a few other minor items. The most important accessories are discussed in the following

Minor items might include binoculars, 30-meter steel pocket tape and thermometers.

1. Leveling Device

One problem in instrumentation that will be encountered and must be solved is that of leveling the panoramic camera. Various sophisticated systems have been considered in this connection: gravity-operated automatic leveling devices with gimballed camera support, electronically operated automatic leveling devices, gyroscopic devices, etc. The simplest and most feasible at this time, however, seems to be an adaptation of the conventional spirit bubbles used in surveying instruments. It is proposed that, as indicated in 2 below on camera supports, a course level vial or vials be contained in the

support, so that the camera when placed on the support will be leveled theoretically within the range of two orthogonally placed precise level vials inside the camera body. Since these precise levels will be photographed during each exposure, thus providing a permanent record of the level reference and enabling subsequent opposing pairs of photographs to be reduced to the true horizon, no further leveling should be required. However, provision must be made for the astronaut to be able to monitor these internal vials and to adjust the level if necessary; the sensitivity and delicacy of level vials in general indicates the possibility that, because of the rather harsh conditions of the journey to the lunar surface, there is likelihood that the adjustment of these vials will be disrupted to such an extent that when the support is leveled the bubble of one or both of the internal vials will be off the scale, thus necessitating further adjustment of the camera level.

At this point, it would be well to point out some of the limitations of the spirit level. It is an extremely delicate and highly sensitive tool. The bubble is affected by differential heating from external light, so that it must be protected both from radiant heat and from light. A bubble of the sensitivity required in this camera would be termed a "slow" bubble in a conventional surveying instrument, and should be even slower on the lunar surface with its lesser gravitational force. Therefore, considerable care will have to be exercised in allowing enough time for the bubble to settle down for each photograph. Nevertheless, at this time, considering weight limitations, the level vial seems to be the most practical way to provide a gravity based reference for the panoramic camera.

2. Camera Supports

Suitable supports will be required to use the camera systems recommended for the selenodetic operations. If the top of the LEM is used as a camera station, a simple support plate, similar to a conventional tribrach should provide a satisfactory platform. A camera station on the lunar surface will require a mount which may be similar to the conventional tripod, provided it can be supported in a stable condition on the surface.

Supports for the cameras used on the lunar surface should be designed with the following considerations in mind:

1. Stability. Any motion of the camera during an exposure will degrade the precision of the measurements; the rotation of lens of the panoramic camera will require special stability of the support. The low gravity of the moon will increase sensitivity to torques, and jarring disturbances.
2. Portability. Two or three camera supports will be required. They must be designed for the minimum length and bulk which can be extended to the necessary height and stability without undue effort by the user.
3. Convenience. The operations which must be performed include: setting up the support; making it steady; attaching the camera; leveling, pointing and operating the camera; removing the camera; removing the film. For these to be done quickly and easily, the camera height should be limited to about five feet.

With present knowledge of ground conditions, a support resembling the conventional transit tripod may prove most adaptable. Folding or sliding extension legs, perhaps of aluminum tubing, would be required to meet bulk and length limitations.

Design of the supports, of the feet in particular, will be easier following the observations made by the unmanned Surveyor missions. The roughness of the terrain, the texture, rigidity and strength of the surface, the presence of loose particles and their size and depth, may be better known before Apollo.

A hard smooth surface may justify the use of mechanical or chemical binders at or around the feet to insure stability. A vesicular formation may make pointed feet stable; perhaps a flange, or an angle by which the feet may

be hammered into the surface will help. Use of a chemical binder to stabilize a soft surface may also be considered. Another possibility is the use of light-weight plastic bags to be filled on the spot with compacted indigenous surface material. One sack under each tripod leg should furnish much greater density and stability in otherwise loose material.

Two additional factors that must be considered in the design of the camera supports are interchangeability and visibility. Since two cameras are to occupy the same station successively, a leveling head to which each camera can be attached without loss of spatial orientation should be part of the support. This head including a centering rod could also serve as the target at the camera station. A suggested head is the Kern type with centering rod. [13] On this rod is a circular level by which the head can quickly be leveled within two minutes of arc. The centering rod can be marked to define the point in space occupied by the camera. In addition the rod will provide a coarse vertical reference for photography on which it appears.

3. Stadimeter

The short base method will require the astronaut to position his camera some 35 meters from the LEM and again about 200 meters from both this camera station and the LEM. While accuracy in these distances is not critical, it may be difficult even to approximate distances under the unusual conditions expected; thus, some device to aid in estimating these distances within about 10% would be desirable.

If the chosen positions are visible from inside the LEM it would be possible for the inside man to intercept the height of the roving man with a simple stadia viewer. If, however, the astronaut cannot be directed to the proper location from inside the LEM, he may have predetermined markings on his glove, or other suitable item, such that when the arm is fully extended and the markings are held vertical they will intercept the known height of the LEM at the desired distances.

SECTION IX

SUGGESTED SYSTEMS AND PROGRAMS FOR CONDUCTING SELENODETIC OPERATIONS ON THE LUNAR SURFACE

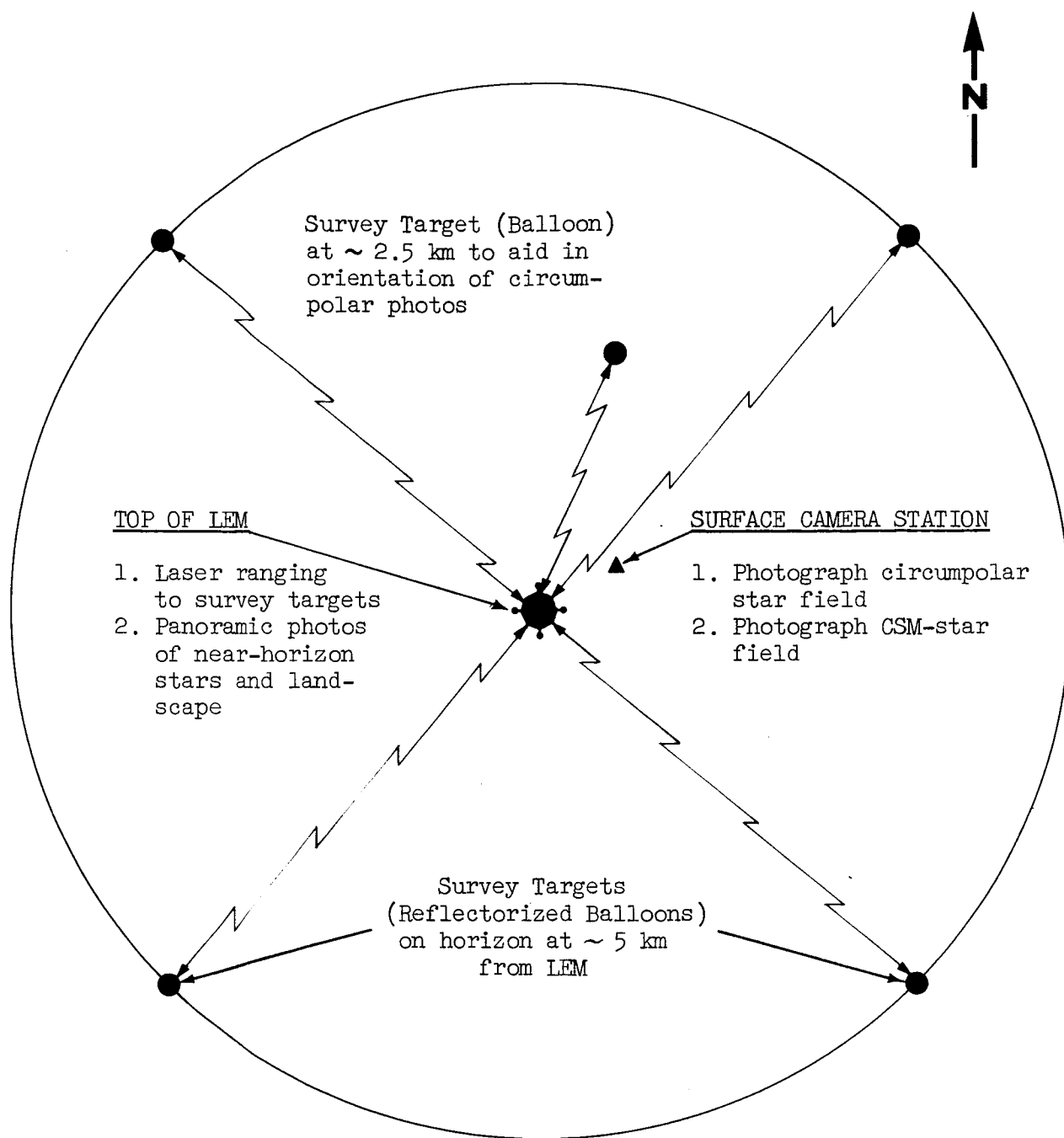
A. INTRODUCTION

It would be unrealistic to propose any one system for selenodetic operations, because of the still limited knowledge of the moon, as well as the many mission constraints; so several systems have been outlined. As lunar knowledge increases (through Ranger, Orbiter, and Surveyor programs) one system or a combination of systems will become apparent as the optimum method. The choice will be affected by whether or not the top of the LEM can be used as an observation station, mobility of the astronaut on the lunar surface, character and degree of relief of the lunar surface, and time available for survey. The following pages describe two possible systems, including procedures devised, instrumentation required, and expected results.

B. SYSTEM I UTILIZING CAMERAS AND LASER RANGER

This system (Figure IX-1) will provide astronomic position of the LEM, its selenocentric position with respect to the CSM, and selenodetic positions of selected targets visible from the top of the LEM (about 5 km). Selenodetic positions will be determined by range and angle measurements from the top of the LEM. Astronomic and selenocentric positions will be determined from either the top of the LEM, or a position on the lunar surface close to the LEM.

The astronauts will begin their selenodetic mission by projecting, to a distance of about 5 km, four reflectorized balloons to serve as mapping control targets or points for orbital photography. The four balloons will be fired at 90° angles, except that no balloon will be fired directly toward the sun, as this would probably render it unphotographable. A fifth balloon will be projected to a distance of about 2.5 km, to serve as a reference point for lunar pole photography. The fifth balloon will be fired to the north (or south in the southern hemisphere), so that it will be visible in photography



Suggested Survey Plan for Selenodetic Measurements - System I

FIGURE IX-1

of the lunar celestial pole. If it appears that topographic relief will provide sufficient orientation to permit matching of photographs, the fifth balloon could be utilized at the longer distance or eliminated from the mission altogether.

A camera support is erected on the lunar surface close to the LEM, in a position from which the lunar celestial pole is visible. (See Figure IX-1.) The precision frame camera is secured to this support and pointed to the pole. The pointing must insure that the lunar horizon and the fifth balloon are visible in the lower part of the picture, which will have a filter screen. After the screen has been put in place, sets of photographs (3-4) of the polar region are taken. During the course of the mission it would be necessary to take at least two sets of celestial pole photographs separated in time as far as possible.

The precision camera will also be used for photographing the CSM against a star background, so can remain on the support throughout the mission, requiring only swinging and pointing of the camera to either the CSM or the polar region. The photograph of the CSM will be taken with the landscape screen removed, and must be related accurately to absolute time (within 1/100th second). At least three photographs should be taken during an orbital pass, preferably in widely separated portions of the sky; and it would be desirable to repeat these observations during another orbital pass if time permits. Times of photographs will be dependent upon the orbit of the CSM. CSM photographs will be taken between the polar photographs, since the operation of pointing the survey camera is of minimal difficulty and time requirement. (Photographing the CSM from the lunar surface would be an optional operation and may not be required if the SXT and dual LOS photographic method (see Section XI) is available in the CSM.)

Distance to the reflectorized balloons will be determined by laser ranging from the top of the LEM. The astronaut will range to each balloon in turn, verbally tape recording the distance from the digital readout, and the approximate direction according to a simple pelorus attached to the

instrument support. In addition, the astronaut will range to any discrete natural features that return a signal, recording range, pelorus angle, and a description of the feature observed to enable correct identification in the photography.

Finally, the astronaut will replace the laser ranger with the panoramic camera, noting the orientation of the camera with the pelorus, so that the ranging may be correctly correlated with the photography. The procedure for the panoramic photography is the most exacting in the entire system. The camera will contain finely adjusted internal level vials (or vertical sensing elements) of a sensitivity of better than 10 seconds of arc, with a total latitude of no more than ± 1 minute of arc. The camera support head will be leveled by means of a level vial or vials attached directly to the head. The camera is then attached to the head, the internal level sensors centered and a photograph taken. The camera will then be rotated 180° about its vertical axis, the internal sensors again centered, and a second photograph taken. These two photographs can be considered as one observation, since the mean of the two photographs will represent a panoramic photograph with its horizon line correctly oriented with respect to the local vertical. This is true even if the vertical sensing devices have not been calibrated properly, since by duplicating the level condition in diametrically opposed photographs the mean of the two will cancel the off-vertical error. As the level vials (or vertical sensors) will be photographed, the centering operation need not be precise; if the value of the level vial divisions is known, the orientation of the photographs can first be corrected to center the vials, subsequently paired to determine true vertical orientation.

As the two photographs diametrically opposed must be treated as one observation, it will be necessary to take at least one more set of paired photographs to provide redundancy in astronomic position determination. Present practice with the zenith camera is to take at least three photographic pairs; experimentation on earth with the panoramic system, including reading and reduction of the films, will indicate the number of panoramic pairs necessary to yield varying degrees of statistical accuracy

of astronomic position. This will be the deciding factor in the determination of the number of panoramic photographs to be taken, since two photographs should suffice for the horizontal and vertical angles to the targets.

In addition to these operations, gravimetric readings will be taken inside the LEM.

The following results would be expected from this program:

1. Lunar Celestial Pole. From the photographs taken by the precision frame camera of the polar region, the lunar celestial pole can be deduced. See Section IV.
2. Selenographic Position. From the panoramic horizon photographs, astronomic position can be computed. From photographs of the CSM, selenocentric position can eventually be determined after appropriate transfers between coordinate systems have been derived. Depending upon accuracy obtainable of these two positions, comparison may give indication of local deflection of the vertical. Gravimetric data may also aid in the overall analysis of these two positions if anomalies are small.
3. Selenodetic Positions. Using the LEM as datum origin, positions of the balloon targets and any other discrete points can be computed. Input for these computations will be range (by laser ranger) and azimuth (from panoramic photographs, oriented with respect to the lunar pole determined by precision frame camera) from the LEM.
4. Elevations. Selenocentric elevation of the LEM will be determined by analysis of both LEM - CSM positional relationship and gravimetric data under the same conditions as in item (2) above. Relative elevation of points ranged to will

be determined by range and vertical angle. Relative elevation to distant points, such as well-defined prominences beyond the near-horizon, can be deduced by range and vertical angle, where the range would be determined from orbital photography.

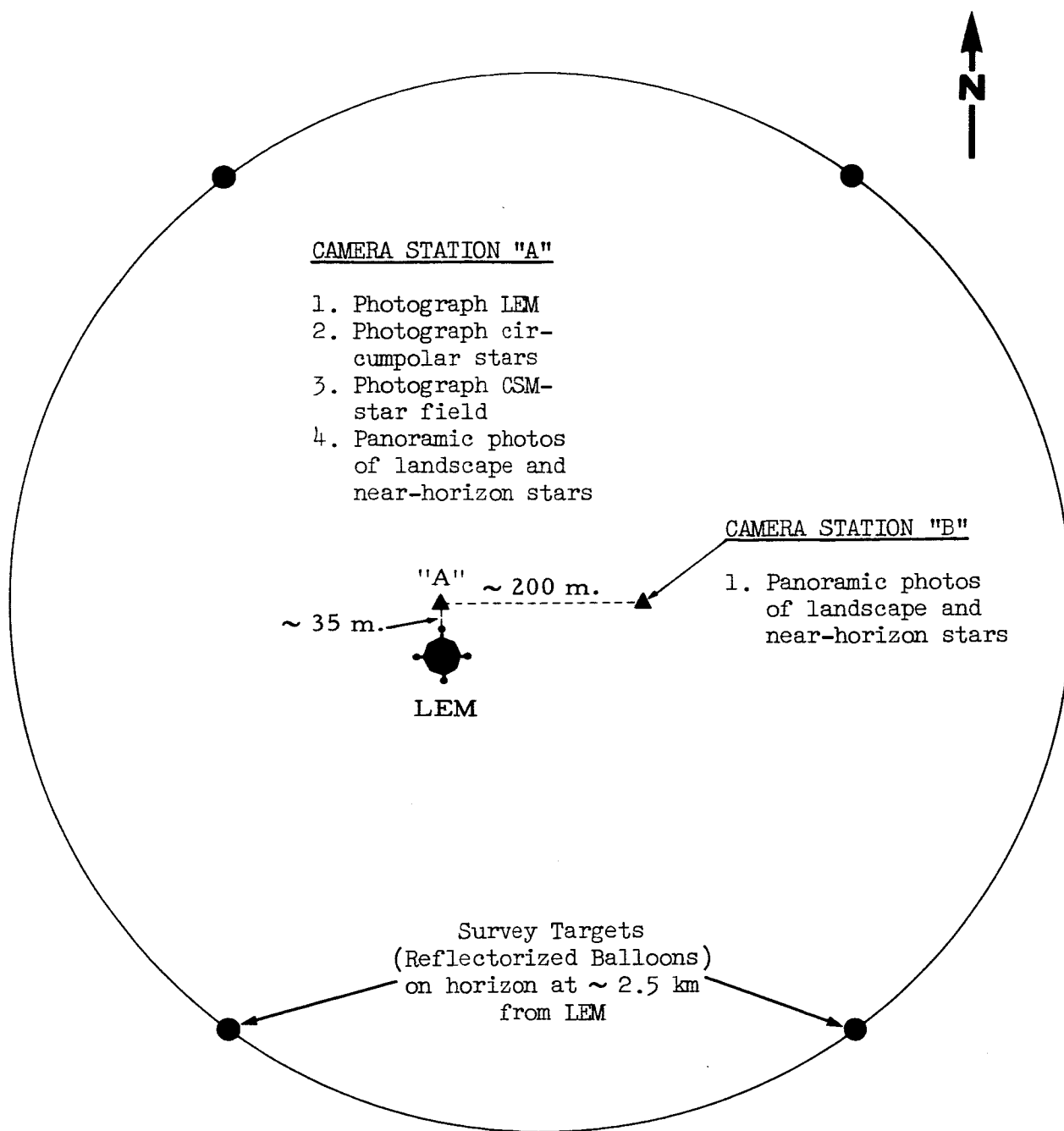
C. SYSTEM II UTILIZING CAMERAS AND STADIA

In this system the laser ranger is not utilized, and all measurements are made photogrammetrically from the lunar surface as indicated in Figure IX-2. Use of the precision frame camera for lunar pole determination and CSM photography is identical, as is use of the gravimeter. The procedure of taking two diametrically opposed panoramic photographs does not change, but use of the photographs does.

Under this system the astronaut will first hang two stadia rods from the top of the LEM or rely on preestablished target points on the LEM for photographic determination of a baseline. (See Section VIII.) He then projects four balloons to a distance of only about 2.5 km, so that they are visible from a height of about 5 feet.

The first camera station A, is established approximately 100 feet distant from the LEM in a northerly direction (or southerly if the landing site is in the southern hemisphere). (See Figure IX-2.) The astronaut will select this position by orienting himself by the stars and determining distance from the LEM by using his stadi-viewer. A camera support will be set up on the lunar surface at this point, the support head leveled, and the precision frame camera attached to the support head. The first photograph will be of the LEM and its associated stadia rods. The camera will remain at this position and be used for the polar and CSM photography, as previously described, until it is replaced by the panoramic camera at the end of the mission.

The second camera station B, will be about 600 feet (200 meters) east or west of the LEM and first station. Its position will be selected by the



Suggested Survey Plan for Selenodetic Measurements - System II

FIGURE IX-2

astronaut using the stars and the stadi-viewer. After setting up and leveling the support, the panoramic camera will be attached to the support head, and a panoramic photo pair will be taken as described under System I.

Just before the end of the final excursion, the astronaut will return to station A, take his last polar photograph, and remove the precision frame camera from the support. He will then replace it with the panoramic camera and take a panoramic pair from this station.

The following results would be expected from this program:

1. Lunar Celestial Pole. Same as under System I.
2. Selenographic Position. Same as under System I, except that redundancy of astronomic position would be provided by comparison of two positions (A and B) selenodetically tied, rather than repeated panoramic pairs at one station.
3. Selenodetic Positions. Using the LEM as datum origin, positions of stations A and B will be determined by photogrammetric base expansion from the two stadia rods hung from the LEM or by relying on preestablished target points on the LEM. Positions of the target balloons and of any discrete lunar features will be determined by intersection from panoramic photographs taken at stations A and B. With stations A and B, however, accurate positioning can only be accomplished in a northerly and southerly direction (see Section VIII).
4. Elevations. Same as under System I, except that range to all near-horizon features will be determined by photogrammetric intersection.

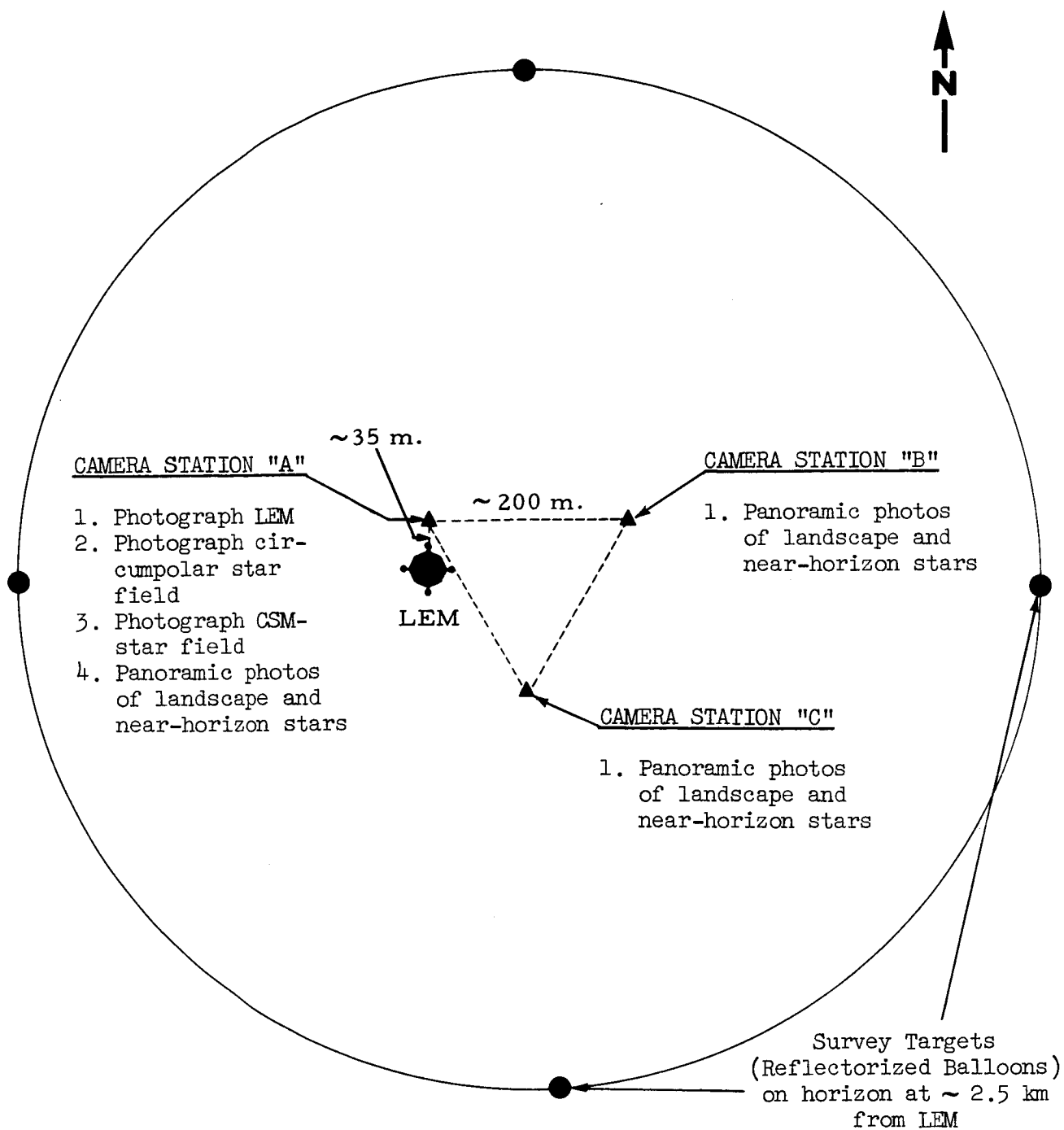
D. SYSTEM II EXTENDED TO ADDITIONAL STATION

Considerable advantage would be gained by establishing and utilizing a third station C (in the same manner as B), as shown in Figure IX-3 which would permit accurate positioning in all directions and would increase certainty of accomplishing a good baseline in any direction. The trade-off, however, is the time required, which is increased by occupying the third station. (See comparison in Table IX-5.)

E. RECOMMENDED PRIORITIES

Requirements for space, weight and time allotments in other disciplines may restrict selenodetic operations to the extent that some of the procedures will have to be curtailed. Therefore the following priorities are assigned, on the assumption that there will be more than one mission:

1. Of primary importance is determination of the lunar celestial pole, which, if it can be repeated on later missions, will aid substantially in refinement of knowledge of the motion of the moon, and will provide the basis for an accurate astronomic position at the LEM landing site (see next item 2).
2. The accurate astronomic position of the LEM and the astronomical azimuth to at least one other identifiable point are important to provide an initial datum for selenodetic operations.
3. Positioning of additional points in relation to the LEM will provide accurate local scale for orbital photography. This operation should receive priority ahead of 1 and 2 above if the Lunar Orbiter is a failure or the CSM SXT operation is not provided. For this the complete System I or System II would be required.



Suggested Survey Plan for Selenodetic Measurement - System II Extended

FIGURE IX-3

4. Finally, accurate determination of the position of the LEM relative to the CSM orbit will provide the selenocentric radius which could be adopted as vertical datum. This operation should receive the first priority, if the CSM SXT is not provided.

Table IX-1 lists recommended priorities showing instrument and time requirement for each operation.

F. TENTATIVE OPERATIONAL PROGRAMS

The following three tables outline tentative programs of lunar surface operations which make use of the alternate systems described above. Table IX-2 presents a program for System I; Table IX-3 presents a program for System II; and Table IX-4 presents the extended program for System II.

These programs assume that three excursions* will be made on the lunar surface by one astronaut at a time, spread over a period of 15 hours and 5 minutes, the excursions to be of 96 minutes, 154 minutes and 132 minutes duration. It is also assumed that the astronaut remaining inside the LEM will be available for gravimetric observations.

The programs contain repetitive operations; these are included for purposes of normal geodetic redundancy, as well as a safety factor of doubling the minimum number of required photographs. This would permit variation of exposure time or aperture to ensure reliable coverage.

Table IX-5 provides a comparison of the three systems, summarizing the estimated time of the survey operations for each lunar excursion and estimated equipment weights and bulk.

* Apollo Mission Planning Task Force, Phase I Progress Report, Vol. III, dtd. 4 May 1964. Grumman Aircraft Engineering Corp.

TABLE IX-1

RECOMMENDED PRIORITIES FOR CONDUCTING
SELENODETTIC MEASUREMENTS ON LUNAR SURFACE

Priority*	Observations For	Procedures	Instrumentation Required			Estimated Time Required (mins.)	
			Equipment	Per Instrument	Estimated Weight (lbs.) Cumulative Total	Per Operation	Cumulative Total (1)
1	Position of Lunar Pole	Circumpolar time-lapse star photography	Precision Frame Camera Camera Support	5 5	10	30	30
2	Astro Position and Azimuth Reference	Horizon-star photography	Panoramic Camera (2) Camera Support	15 -	25	30	60
3	Position of LEM relative to CSM orbit (3)	Photograph CSM against star field	Precision Frame Camera Camera Support	- -	25	30	90
4	Horizontal and vertical control in vicinity of LEM	Laser ranging to survey targets; photography of landscape	Panoramic Camera Laser Ranger Survey Targets with Launcher Camera Support	- 15 20 2	62	40 (4)	130

- (1) Cumulative total is total elapsed time, and includes walking time and time required to allow instrument to settle.
- (2) Precision frame camera could be used for this operation if level indicators and horizontal circle are added.
- (3) These observations are not necessary if LEM can be accurately positioned using CSM equipment (SXT dual LOS photography).
- (4) Part of time required for this operation is covered under Priority No. 2.

TABLE IX-1 (Cont'd)

RECOMMENDED PRIORITIES FOR CONDUCTING
SELENOGRAPHIC MEASUREMENTS ON LUNAR SURFACE

Priority*	Observations For	Procedures	Equipment	Instrumentation Required		Estimated Time Required (mins.)	
				Per Instrument	Cumulative Total	Per Operation	Cumulative Total (1)
4a	Horizontal and vertical control in vicinity of LEM	Establish short base by photogrammetry; photograph LEM; photograph landscape from each end of baseline. (5)	Precision Frame Camera	-			
			Panoramic Camera	-			
			Survey Targets with Launcher	-			
			Camera Support (Lunar Surface)	5			
			Stadia Rods	2	51 (6)	70 (4)	160 (7)

(5) If an additional camera station is added accurate survey control can be established around complete horizon. This would require one additional camera support for a total weight of 56 pounds, and a total time of 215 minutes.

(6) Weights of laser ranger, camera support for top of LEM and one survey target subtracted from total.

(7) Time for priority No. 4 subtracted from total.

Note: Gravity observations are not included in this priority list, since they would be conducted from inside the LEM, and the small weight (~1 lb.) and time (5 mins.) budget suggests that they be made as a matter of course.

*Priorities assigned on the assumption that regions around more than one landing site will be surveyed. A single determination for items 1 and 2 should receive lower priority. Furthermore, items 3 and 4 should receive priority ahead of items 1 and 2 if the Lunar Orbiter and/or CSM SXT operations fail.

TABLE IX-2
TENTATIVE OPERATIONAL PROGRAM
FOR
LUNAR SURFACE MEASUREMENTS
SYSTEM I

System Equipment

Instrument	Bulk (cu. ft.)	Weight (lbs.)	Auxiliary Equipment	Bulk (cu. ft.)	Weight (lbs.)
Laser Ranger	1.2	15	Balloon Launcher	1.2	15
Panoramic Camera	0.9	15	5 Balloons (Survey Targets)	0.05	5
Precision Frame Camera	0.3	5	Camera Support (Top of LEM)	0.1	2
*Gravimeter	<u>0.1</u>	<u>1</u>	Camera Support (Lunar Surface)	<u>0.4</u>	<u>5</u>
Totals (Est.)	2.5	36		1.7	27

System Program

Station	Event No.	Description of Procedure	Time (mins.)
		<u>Excursion 1</u>	
Top of LEM	1	Observe lunar landscape to select balloon sites	5
Surface	2	Select precision frame camera position and carry camera and support to it	3
	3	Erect camera support; secure to lunar surface; level support head	10
	4	Secure camera to support head, point toward pole (frame 4/5 sky, 1/5 landscape); screen landscape	3
	5	Place balloon launcher in launching position	5
	6	Launch five balloons to previously determined locations	10
	7	Return to precision camera; check orientation, take 4 lunar pole photographs; remove screen	3

TABLE IX-2 (Cont'd)

TENTATIVE OPERATIONAL PROGRAM FOR
LUNAR SURFACE MEASUREMENTS - SYSTEM I

Station	Event No.	Description of Procedure	Time (mins.)
	8	**Point camera toward CSM, take CSM-star photograph; repoint, take second photograph; repoint, take third photograph; repoint, take fourth photograph	12
Top of LEM	9	Erect instrument support and level support head	5
	10	Secure laser ranger to support head	2
	11	Range to five balloon targets, recording distance, pelorus direction, and estimated azimuth	10
	12	Range to discrete natural targets, recording description, distance, pelorus direction and estimated azimuth	15
	13	Remove laser ranger, leaving support undisturbed	1
<u>Excursion 2</u>			
Top of LEM	14	Check level of instrument support head	1
	15	Secure panoramic camera to head; center precise vertical sensors	5
	16	(Allow time for camera to stabilize in lunar environment: 10 mins.)	***
	17	Center vertical sensors; verify camera stability; note orientation with respect to pelorus	3
	18	Take two panoramic photographs	1
	19	Center vertical sensors; take two panoramic photographs	2
	20	Center vertical sensors; take two panoramic photographs	2
	21	Rotate camera 180°; center vertical sensors	4
	22	Take two panoramic photographs	1
	23	Center vertical sensors; take two panoramic photographs	2

TABLE IX-2 (Cont'd)

TENTATIVE OPERATIONAL PROGRAM FOR
LUNAR SURFACE MEASUREMENTS - SYSTEM I

Station	Event No.	Description of Procedure	Time (mins.)
	24	Center vertical sensors; take two panoramic photographs	2
	25	Remove cassette; discard camera and instrument support	3
<u>Excursion 3</u>			
Surface	26	Return to precision camera, point camera toward pole (frame 4/5 sky, 1/5 landscape); screen landscape, take 4 lunar pole photographs; remove film pack; return to LEM	8

* Gravity readings will be taken with gravimeter inside LEM: 2 readings, approximately 5 mins. per reading.

** Photographs of CSM will be dependent upon its position; at least three photographs should be taken in widely separated portions of sky. Photographs will not be taken if LEM is positioned by CSM instrumentation (SXT dual IOS photography).

*** Time not charged against this event as the event can be used for other purposes also. Time required is included, however, in total elapsed time of the program.

TABLE IX-3
TENTATIVE OPERATIONAL PROGRAM
FOR
LUNAR SURFACE MEASUREMENTS
SYSTEM II

System Equipment

Instrument	Bulk (cu. ft.)	Weight (lbs.)	Auxiliary Equipment	Bulk (cu. ft.)	Weight (lbs.)
Panoramic Camera	0.9	15	Balloon Launcher	1.2	15
Precision Frame Camera	0.3	5	4 Balloons (Survey Targets)	0.04	4
*Gravimeter	0.1	1	2 Camera Supports	0.9	10
	—	—	2 Stadia Rods	<u>0.3</u>	<u>2</u>
Totals (Est.)	1.3	21		2.4	31

System Program

Station	Event No.	Description of Procedure	Time (mins.)
Top of LEM		<u>Excursion 1</u>	
	1	Observe lunar landscape to select balloon sites	5
	2	Hang 2 stadia rods on LEM	5
Surface	3	Place balloon launcher in position	5
	4	Launch 4 balloons in predetermined pattern	10
LEM to A	5	(Walk to approximate Station A carrying precision frame camera and support: 3 mins.)	***
A	6	Select Station A using stadi-viewer for distance	2
	7	Erect camera support; secure to lunar surface; level support head; secure precision frame camera to head	10
	8	Point precision frame camera to LEM; photograph LEM and stadia rods	4
	9	Point precision frame camera to lunar celestial pole (4/5 sky, 1/5 landscape); screen landscape; take 4 pole photographs; remove screen	6

TABLE IX-3 (Cont'd)

TENTATIVE OPERATIONAL PROGRAM FOR
LUNAR SURFACE MEASUREMENTS - SYSTEM II

Station	Event No.	Description of Procedure	Time (mins.)
	10	**Point precision camera toward CSM; take CSM-star photograph; repoint and take second photograph; repoint and take third photograph; repoint and take fourth photograph	12
A to LEM	11	(Return to LEM: 2 mins.)	***
<u>Excursion 2</u>			
LEM to B	12	(Walk to approximate B carrying panoramic camera and support: 12 mins.)	***
B	13	Select position of B using stadi-viewer for distance	3
	14	Erect camera support; secure to lunar surface, level support head	10
	15	Secure panoramic camera to support head; center precise vertical sensors	5
	16	(Allow time for camera to stabilize in lunar environment: 10 mins.)	***
	17	Center vertical sensors again; verify camera stability	3
	18	Take two panoramic photographs	1
	19	Rotate camera 180°; center vertical sensors	4
	20	Take two panoramic photographs	1
	21	Remove panoramic camera, leaving support	1
B to LEM	22	(Return to LEM: 8 mins.)	***
<u>Excursion 3</u>			
LEM to A	23	(Walk to A: 2 mins.)	***

TABLE IX-3 (Cont'd)

TENTATIVE OPERATIONAL PROGRAM FOR
LUNAR SURFACE MEASUREMENTS - SYSTEM II

Station	Event No.	Description of Procedure	Time (mins.)
A	24	Just prior to end of mission, point precision frame camera to lunar celestial pole (4/5 sky, 1/5 landscape); screen landscape; take 4 pole photographs; remove screen	6
	25	Remove film pack, remove and discard precision frame camera	2
	26	Secure panoramic camera to support head; center precise vertical sensors	5
	27	(Allow time for camera to stabilize in lunar environment: 10 mins.)	***
	28	Center vertical sensors again; verify camera stability	3
	29	Take two panoramic photographs	1
	30	Rotate camera 180°; center vertical sensors	4
	31	Take two panoramic photographs	1
	32	Remove cassette	1
	33	(Return to LEM: 2 mins.)	***
A to LEM			

* Gravity readings will be taken with gravimeter inside LEM: 2 readings, approximately 5 mins. per reading.

** Photographs of CSM will be dependent upon its position; at least three photographs should be taken in widely separated portions of sky. Photographs will not be taken if LEM is positioned by CSM instrumentation (SXT dual LOS photography).

*** Time not charged against this event as the event can be used for other purposes also. Time required is included, however, in total elapsed time of the program.

TABLE IX-4
TENTATIVE OPERATIONAL PROGRAM
FOR
LUNAR SURFACE MEASUREMENTS
SYSTEM II (Extended)

System Equipment

Instrument	Bulk (cu. ft.)	Weight (lbs.)	Auxiliary Equipment	Bulk (cu. ft.)	Weight (lbs.)
Panoramic Camera	0.9	15	Balloon Launcher	1.2	15
Precision Frame Camera	0.3	5	4 Balloons (Survey Targets)	0.04	4
*Gravimeter	0.1	1	3 Camera Supports	1.3	15
			2 Stadia Rods	.3	2
Totals (Est.)	1.3	21		2.8	36

System Program

Station	Event No.	Description of Procedure	Time (mins.)
<u>Excursion 1</u>			
Various	1-11	Same as System II (Table IX-3)	59
<u>Excursion 2</u>			
Various	12-22	Same as System II (Table IX-3)	28
<u>Excursion 3</u>			
LEM to C	23	(Walk to approximate C carrying panoramic camera and support: 12 mins.)	***
C	24	Select position of C using stadi-viewer for distance	3
	25	Erect camera support; secure to lunar surface; level support head	10
	26	Secure panoramic camera to support head; center precise vertical sensors	5
	27	(Allow time for camera to stabilize in lunar environment: 10 mins.)	***

TABLE IX-4 (Cont'd)

TENTATIVE OPERATIONAL PROGRAM FOR
LUNAR SURFACE MEASUREMENTS - SYSTEM II (Extended)

Station	Event No.	Description of Procedure	Time (mins.)
	28	Center vertical sensors again, verify camera stability	3
	29	Take two panoramic photographs	1
	30	Rotate camera 180°; center vertical sensors	4
	31	Take two panoramic photographs	1
	32	Remove panoramic camera, leaving support	1
C to A	33	(Return to A via LEM: 8 mins.)	***
A	34	Just prior to end of mission, point precision frame camera to lunar celestial pole (4/5 sky, 1/5 landscape); screen landscape; take 4 pole photographs; remove screen	6
	35	Remove film pack, remove and discard precision frame camera	2
	36	Secure panoramic camera to support head; center precise vertical sensors	5
	37	(Allow time for camera to stabilize in lunar environment: 10 mins.)	***
	38	Center vertical sensors again; verify camera stability	3
	39	Take two panoramic photographs	1
	40	Rotate camera 180°; center vertical sensors	4
	41	Take two panoramic photographs	1
	42	Remove cassette	1
A to LEM	43	(Return to LEM: 2 mins.)	***

TABLE IX-5

COMPARISON OF TENTATIVE SYSTEMS
FOR SELENODETIC MEASUREMENTS

Item	System I	System II	System II (Extended)
Place of Operation	Entire operation can be conducted from top of LEM if necessary	System requires a surface excursion of up to ~ 200 meters distance from LEM	System requires 2 surface excursions of up to ~ 200 meters distance from LEM
Extent of Lunar Surface Surveyed	Provides position of limited number of selected targets up to 5 km. distant	Provides position of <u>most</u> landscape features and artificial targets up to 2.5 km. distant	Provides position of <u>all</u> landscape features and artificial targets up to 2.5 km. distant
Redundancy	Results dependent upon correct correlation of ranges with targets; possibility of mis-identification of points	Results dependent upon analysis of photographs alone; no chance of mis-identifications	Results dependent upon analysis of photographs alone; no chance of mis-identifications
Time (Mins.)	Event Time Total Elapsed Time	Event Time Total Elapsed Time	Event Time Total Elapsed Time
Excursion 1	84 84	59 64	59 64
Excursion 2	26 36	28 58	28 58
Excursion 3	<u>8</u> <u>8</u>	<u>23</u> <u>37</u>	<u>51</u> <u>93</u>
Total	118 128	110 159	138 215
Weight (lbs.)	63	52	57
Bulk (cu. ft.)	4.2	3.7	4.1

SECTION X

ANALYSIS OF LUNAR ORBITER MAPPING PHOTOGRAPHY

A. INTRODUCTION

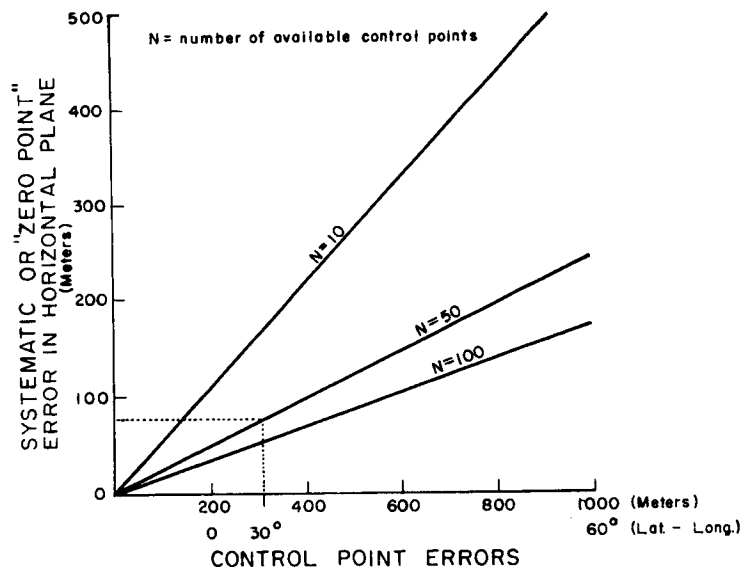
As stated in Section I. B, "Support of Mapping Programs", selenodetic measurements should both take advantage of and serve to improve the accuracy of lunar mapping derived from photography obtained by lunar orbiting vehicles. Therefore, mapping accuracies that could possibly be obtained from currently planned Lunar Orbiters were investigated to make certain that measurements would not be recommended which would be accomplished better by Lunar Orbiters, and to determine what support could be given to Orbiter missions that would further enhance their utility.

As presently planned, the Lunar Orbiter program consists of a series of five photographic reconnaissance missions scheduled to begin late in 1966. Photography will be taken in the lunar region of ± 10 degrees latitude and ± 60 degrees longitude at 50 km heights above the moon's surface with two camera systems; one with a high resolution 24-inch focal length camera in order to obtain the greatest amount of lunar surface detail and texture, and the other a lower resolution 3-inch focal length camera which will be triggered to provide normal 55% overlap stereo coverage for mapping purposes. Ground resolutions of 1-8 meters are expected with these camera systems from the 50 km heights. Although the areas to be photographed have not been finally chosen at this time, the mapping photography will probably provide photographic coverage and, therefore, map coverage of one 200 km x 200 km area per mission within this region of some 2,200,000 square km.

B. RESULTS OF ERROR ANALYSIS

The detailed error analysis made in connection with this study, which is presented in Appendix A, shows that within each 200 km x 200 km area surveyed by the presently planned Lunar Orbiter, precisely identified landmark features could be positioned with a relative accuracy of ± 65 meters in the horizontal plane, and 2-3 times as large as this in the vertical plane.

These features can in turn be tied to the mapping system of the control points with a horizontal error of ± 30 meters to ± 250 meters, depending upon the accuracy and number of control points available. The latter error is defined as the "zero-point" or systematic error in fitting the surveyed area to the map system as a whole. The magnitude of this error as a function of the number and accuracy of control points is illustrated in the graph below.



Expected positional error in fitting Orbiter photography to map control coordinate system.

As shown by the graph, to approach the low end of the range of uncertainties (± 30 meters), it would be necessary to provide 100 control points (landmarks with known coordinates) having an accuracy somewhere around ± 200 meters in a selected coordinate system. Projections of NASA-MSC, however, indicate that there will be at most only one control point available per square degree on the lunar surface, or about 40-50 control points per 200 km x 200 km area. Also these control points will have an accuracy of ± 200 meters at the center of the visible face of the moon, degrading to approximately ± 1000 meters toward the limb. Therefore, a systematic error in horizontal component of the "zero-point" of a surveyed

region would probably be approximately ± 80 meters on the average. The estimated total positional error for any individual lunar feature within a 200 km x 200 km area would then be the combined systematic error and relative positional error or $\sqrt{80^2 + 65^2} \approx 100$ meters. Also, the expected positional relationship or tie between lunar features from one 200 km x 200 km survey area to another would be on the order of 140 meters.

Thus a method which will provide control points that (i) would be of a higher degree of accuracy, (ii) would be of a consistent accuracy over the face of the moon, whether it is near the center or near the limb, or (iii) could be chosen and distributed over the face of the moon in such a way as to tie 200-km squares together would be of value. Investigations of means of establishing such control points by SXT observations from the orbiting CSM while the LEM is on the lunar surface, were made and are presented in the following Section XI.

The analysis of orbital photography in Appendix A also points out that if the configuration of the Lunar Orbiter camera system could be substantially modified so that the photographic instrument would consist of two cameras mounted "back-to-back" and whose optical axes are parallel to each other, considerable improvement in accuracies could be obtained. If both cameras are triggered simultaneously, one would photograph the moon and the other the sky as a reference field. This technique, which is developed in some detail, shows that whereas in the present configuration ± 65 meters seems to be the average relative accuracy in horizontal plane that could be achieved, with the back-to-back camera the corresponding error would be approximately ± 35 meters in horizontal plane. In both instances, the inaccuracy of the altitude is about 2 to 3 times as large.

SECTION XI

USE OF OPTICAL EQUIPMENT ON BOARD THE CSM FOR SELENODETIC OPERATIONS

A. INTRODUCTION

Use of the presently planned Space Sextant (SXT) and Scanning Telescope (SCT) on the CSM for accurately locating the LEM and widely distributed lunar landmarks with respect to the CSM has been considered as a means for extending control over large regions of the lunar surface during the early Apollo missions. If directional sightings of landmarks can be obtained through the SXT, it would be possible (as is well known) to use known positional data from the CSM orbit, together with the measured orientations of the SXT lines of sight to determine or improve the positional interrelationships of lunar features along the orbital path of the CSM, that is, the "ties" between the features and positions of the CSM, and hence of one feature with another, all in the geodetic sense. If the sightings are obtained by photographing landmarks and reference stars through the SXT and simultaneously recording the times and angles of these sightings, the postflight measurement of the photographs and analysis of the resulting data should yield results vastly superior in accuracy to visual settings. As well as improving mapping control, this procedure would make it possible to upgrade the positional accuracy of selected navigational references which may be needed for subsequent lunar missions.

The following paragraphs present an analysis of, first, the conceptual feasibility of such an approach, and, second, the adaptability of the equipment itself. In the first part, the probable magnitude of the errors is discussed, and several seemingly possible operational procedures are outlined.

B. ANALYSIS OF CONCEPT

1. Review of SXT Properties

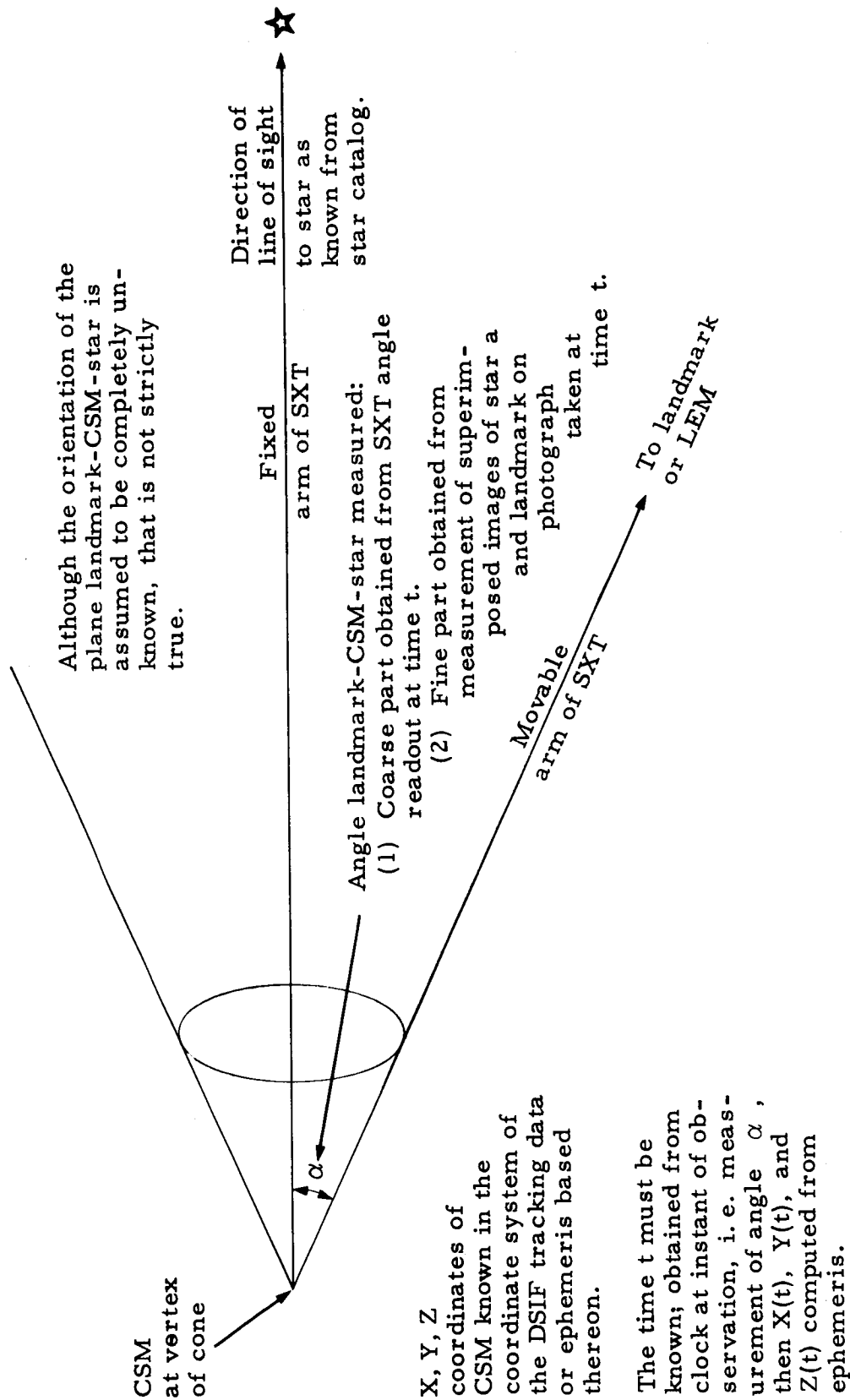
The SXT has the following properties: (1) It can superimpose

the images of two different fields, up to 57° apart in direction. (2) It can measure the angle between the lines of sight of the fixed and movable arms with a precision of $\pm 20''$ ($1:10^4$), without reference to the inertial axes provided by the IMU. (3) It seems feasible to photograph the superimposed fields and to record the angle with a precision of $\pm 20''$ and the time of mid-exposure with a precision of ± 0.01 sec., which corresponds to ± 16 meters at an orbital velocity of 1.6 km./sec. (4) The magnification is large enough so that errors of measuring the photograph would be small compared to $20''$. This judgment is based on the fact that angular errors of photographic measurements due to all optical and photographic causes lumped together are usually about $\pm 100''/(f \text{ in cm})$. (5) The SCT, with 1X magnification and 60° field, is useful chiefly for pointing the movable arm of the SXT, since these two movable telescopes can be ganged together. (All uncertainties given in this sketch are estimates of 1σ).

2. Characteristics of a Single Sighting of a Landmark

A single observation of an angle (landmark-CSM-star) would locate the landmark on a cone in space. The vertex of the cone would be at the position of the CSM (which is determined from terrestrial tracking data and the time of the observation). The axis of the cone would be pointed toward the star, and the vertex half-angle equal to the observed angle (see Figure XI-1). Such a cone is a "surface of position," analogous to a "line of position" in two-dimensional navigation or surveying.

Two such observations determine two cones, which intersect in a curve in space; and a third observation yields a third cone which intersects this curve in at most two points. One of the two points could not be an actual solution for the fix of the landmark, but it will in general be perfectly obvious which of the two intersections is the actual solution. Therefore, three observations of angles, landmark -



CONFIGURATION OF A SINGLE SIGHTING

FIGURE XI - 1

CSM-star, will give a three-dimensional fix on the landmark; that is, the intersection of the three cones will yield the coordinates of the landmark in the same system of selenocentric coordinates that the orbit of the CSM is referred to. The three observations of angle can be made with respect to the same star, or different stars. (If the same star is used, the direction from the CSM to the landmark should be chosen to be quite different, for reasons discussed below.) The "landmark" can be the LEM on the ground; that is, the grounded LEM is only a special case of a landmark.

(a) Sketch of error analysis. Assume that the error of a single measurement of an angle, landmark-CSM-star, is $\pm 20''$, or $1:10^4$. (The actual value is of no great importance for this discussion; if the error turns out to have some other value $\pm \epsilon''$, all results can be scaled up or down by the factor $\epsilon/20$.)

A single such sighting observation (as described above) now defines a conical shell in space, (rather than a cone), with:

Axis in the direction of the star;

Vertex at the position of the CSM;

Half-angle of the vertex = the observed angle (landmark-CSM-star);

Thickness of the shell at any distance or slant range r from the CSM = $2r/10^4$.

The effect of these errors on location fixes will be discussed in detail below.

3. Characteristics of Multiple Sightings on a Landmark

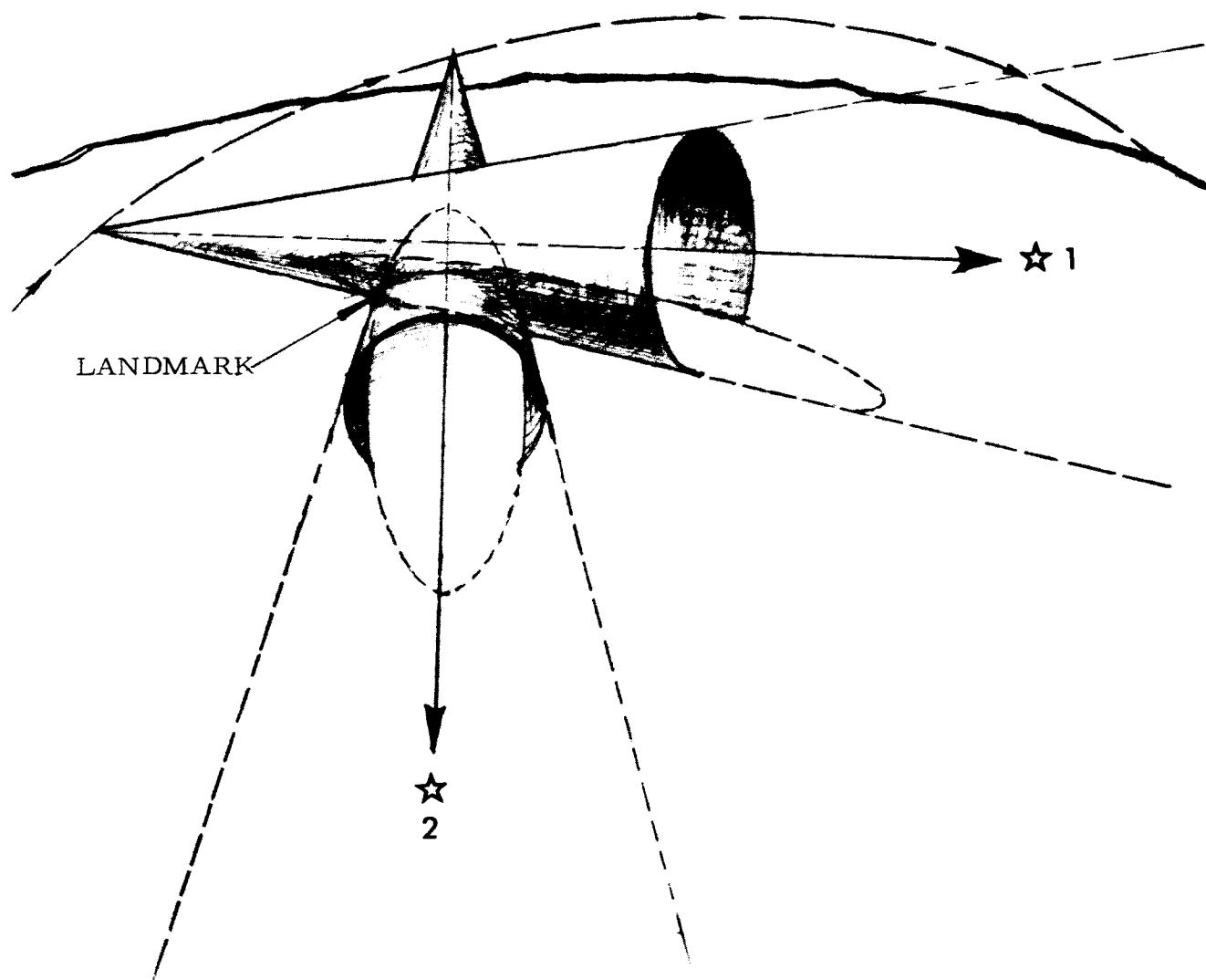
We have already seen that three sightings, leading to three intersecting conical surfaces of position are the minimum number necessary for a three-dimensional fix. The errors of the fix will depend, not only on the errors of each sighting, of the type discussed in paragraph 2 above, but also on the "geometry" of intersecting surfaces.

A prerequisite for a strong geometric solution for a fix is that the normals to surfaces of the intersecting cones, along the curve where the cones intersect, are as nearly perpendicular to each other as can be achieved. (See Figure XI-2.) The uncertainty of the fix in the direction bisecting the acute angle between such pairs of normals varies approximately as the cosecant of the angle between the normals. Thus, other things being equal, if the angle were as small as 30° the precision would be degraded by a factor of 2.

Two sighting observations, each subject to an angular r. m. s. error of $\pm 20''$, define the intersection of two conical shells with an angular thickness of $2\sigma = 40''$, or a thickness of $2r/10^4$, tapering to zero thickness at the vertex. This intersection may be thought of as a curved tube. If the shells intersect nearly orthogonally (as defined above), and if they have the same thickness $2r/10^4$, the cross section of the tube perpendicular to its own axis will be nearly circular, with radius $r/10^4$. (See Figure XI-3a.) If the intersection is at an acute angle

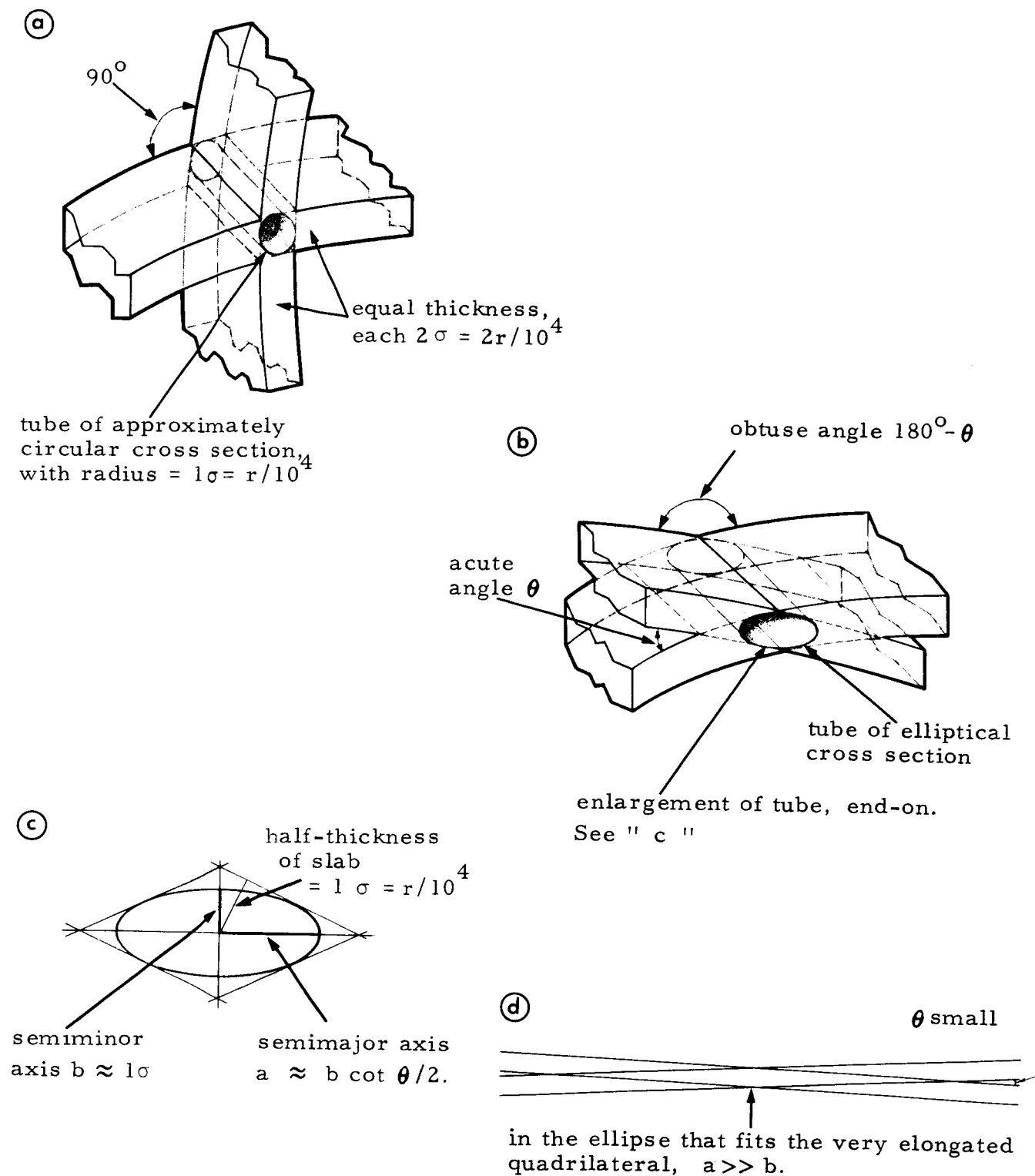
θ , the cross section of the tube will be elliptical, with the semi-minor axis (which is in a direction approximately bisecting the obtuse dihedral angle between the surfaces) equal to about $r/10^4$ and semi-major axis approximately $r/10^4 \times \cot(\theta/2)$. (See Figures XI-3b and 3c.) Obviously, when θ is very small, the major axis of the error ellipse is very large, and as θ approaches 0° , one approaches the case of superimposed shells obtained from repeating a single observation. (See Figure XI-3d.)

The intersection of two cones of unequal thickness $2r_1/10^4$ and $2r_2/10^4$ (corresponding to two different slant ranges, $r_1 > r_2$), defines a tube of more or less elliptical cross section, with semi-major axis $\approx r_1 \cdot \csc \theta / 10^4$ and semi-minor axis $\approx r_2 / 10^4$. (See Figure XI-3e.) Again the smallest dispersion (least cross section of the tube) results when $\theta = 90^\circ$ and the largest when $\theta = 0^\circ$. (The same results would follow if the angular errors, rather than the slant ranges, were different for the two sightings.)



TWO SIGHTING CONES OF POSITION INTERSECTING NEARLY
ORTHOGONALLY AT A LANDMARK

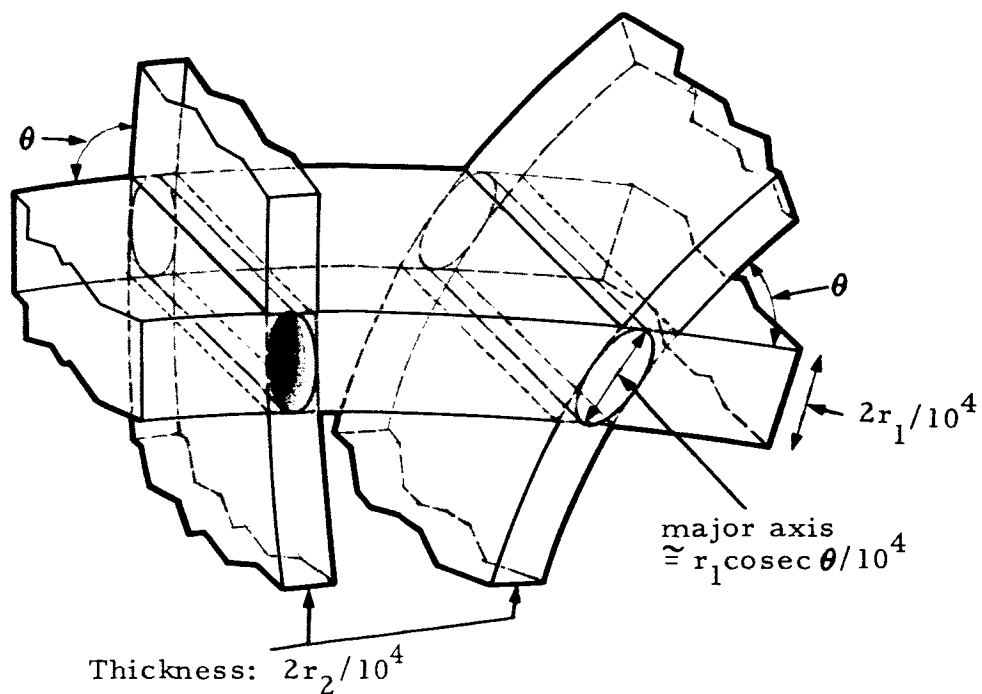
FIGURE XI - 2



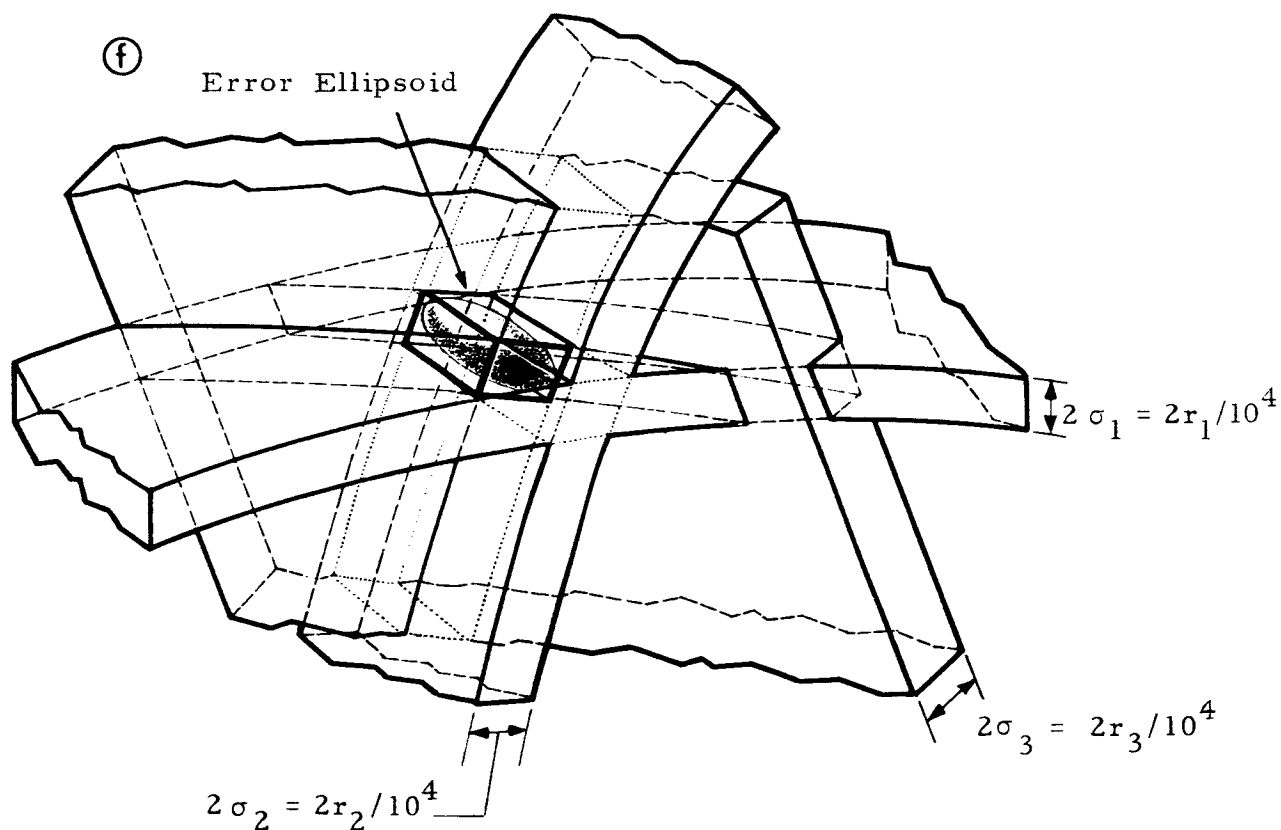
CONES OF INTERSECTIONS - MULTIPLE SIGHTINGS

FIGURE XI - 3

(e)



(f)



CONES OF INTERSECTIONS - MULTIPLE SIGHTINGS

FIGURE IX - 3 (Cont'd)

Intersection of such tubes (either circular or elliptical in cross section) with a third conical shell of thickness $2r_3/10^4$, generated by an observation of a landmark from slant range r_3 , will result in an error ellipsoid. (See Figure XI-3f.) The length of the three semi-axes depends on the thickness of the three shells, and the angles with which they intersect.

Figure XI-3 is an attempt to illustrate all the various foregoing possibilities.

(a) Effect of uncertainties in CSM position. All uncertainties of position discussed in this Section are uncertainties relative to the "position of the CSM", as determined by post-analysis of the DSIF tracking data. The uncertainty of a single instantaneous "ephemeris" position of the CSM (i. e., selenocentric \bar{x}_i, H_i, Z_i , all calculated for a time t_i) is assumed to be ± 100 m in each dimension relative to the tracking station. [1] This degree of precision can be achieved only after accumulation of tracking data over some tens of revolutions and use of these data to obtain a "best fitting" selenocentric orbit obeying Kepler's laws (with perturbations) around the center of mass (or center of attraction) in the Moon. The foregoing statements now require some qualification.

The coordinates of CSM obtained from the tracking data will in the first instance be referred to the coordinate system of the tracking station. If the station coordinates with respect to the Earth's center of mass are known, an immediate transfer to geocentric coordinates can be made. [In principle, the coordinates of the tracking station with respect to the Earth's center of mass can be obtained (or improved, if already known) from the tracking data together with an application of the laws of celestial mechanics; this procedure has in fact been carried out in practice.] Finally, the trajectory of the CSM relative to the center of mass of the Moon

can be accurately obtained if the coordinates of the Moon's center of mass relative to the Earth's center of mass are accurately known. Geocentric coordinates of the center of mass of the Moon are at present uncertain by 1 to 2 km. This uncertainty may well be reduced by the time of the first Apollo manned lunar missions. Even if the geocentric coordinates of the Moon are unknown, however, after a lunar orbiter or the CSM has been tracked in geocentric coordinates for a number of revolutions, a solution of the orbiter or CSM trajectory around the Moon's center of mass can be made which will locate the Moon's center of mass in geocentric coordinates. In either case, another transfer of coordinates can then be made, this time to a new origin at the Moon's center. (See Section III for a more detailed treatment of these problems.)

The terms of reference of the expression, "position of the CSM," used above, also require examination. In all possible schemes of observing angles with the SXT, the observations of a given landmark are made from separate points along the CSM orbit, at separate instants in time. In some of the schemes for observing, the individual observations will be separated by only 1 to 15 minutes (a single pass), which corresponds to a distance of 100 to 1400 km. In other schemes, individual observations are separated by one or more whole orbital revolutions, each about 2 hours long. From these separate times and positions, one would calculate the positions of the cones of position that intersect at the landmark. The vertices of these separate cones of position are at the CSM ephemeris positions at times t_1, t_2, \dots, t_n , so that the locations of the individual vertices are subject to same errors as the CSM position. If times t_1, t_2 , etc. are separated by intervals only minutes long, errors of the CSM positions at those times are certain to be correlated; so that contribution to the uncertainty of the coordinates of a landmark fix based on the intersection of conical surfaces will probably be almost as great as the full ± 100 m of a single instantaneous CSM position. As the separation in time of the observations at t_1, t_2, \dots, t_n becomes longer, it is to be expected that

the degree of correlation among errors of the individual CSM positions will decrease, so that the contribution of this source to the overall uncertainty of position of a landmark may then approach $\pm 100/\sqrt{n}$, where n is the number of individual sightings.

(b) Restrictions on the geometry: Upper and lower limits on slant range. The least slant range at which a landmark can be observed is set by the largest angle that the SXT can measure, which is 57° . If one arm of the SXT is trained on a star close to the visible horizon, then the other arm can reach a landmark 57° below the horizon in vertical angle. At a height of 148 km (80 nm), the dip (vertical angle) of the visible horizon below the horizontal plane (plane orthogonal to the gravity vector) is nearly 23° , so the landmark is $23^\circ + 57^\circ$, or about 80° below the horizontal plane. It is therefore 10° from the nadir of the CSM, as viewed from the CSM. The slant range from the CSM to the ground, 10° from the nadir of the CSM, is 151 km, and this is the smallest possible slant range. There is thus a "blind cone," whose axis is the vertical through the CSM and its subsatellite point, and whose half-angle is 10° from the nadir. The SXT cannot be brought to bear simultaneously on a landmark inside this cone and on a star.

The greatest slant range is the distance to the horizon. From a height of 148 km, this range is about 732 km. Whether a landmark can actually be accurately observed at such an extreme range depends on its visibility. For the time being, we shall assume that it is possible. The LEM could in any case be made visible by equipping it with a bright light-beacon or properly designed reflectors.

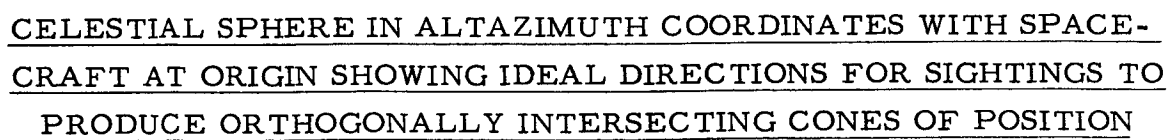
4. General Principles for Ensuring "Good Geometry"

Certain general principles can be laid down for making the three independent sighting observations on a given landmark in such a way

that the three resulting cones of position will intersect each other orthogonally at the landmark. It will not always be possible to put into practice the recipe for orthogonality. The observing schemes suggested below will in most cases constitute compromises between strict adherence to the recipe for orthogonality, and the practical limitations imposed by the relationship between the orbit and the landmarks and by the necessity to avoid unnecessary changes in the attitude of the spacecraft and similar operational constraints.

The general principles for producing three orthogonal cones of position can best be understood by referring to Figure XI-4. This figure shows a celestial sphere in altazimuth coordinates centered on (with origin at) the spacecraft labelled O in the figure. Y is the spacecraft zenith and Y' the nadir. The great circle XZX' represents the horizontal plane through the spacecraft, with OX directed along the orbital velocity vector. (The orbit is assumed to be circular and the velocity therefore horizontal, but this point is not essential for the arguments below.) The axes OX, OY, OZ form a righthanded rectangular coordinate system; and the zenith angle ζ (arc distance from Y) and the relative bearing B measured in the OXZ plane from OX toward OZ correspond to the usual spherical coordinate angles. The slant range r measured along a radius from O constitutes the third spherical coordinate. Instead of the zenith angle ζ , one may also use the (angular) altitude A (= $90^\circ - \zeta$) or the nadir angle N (= $180^\circ - \zeta$).

The small circle $H_1H_2H_3$ represents the visible horizon as seen from the spacecraft, and is parallel to the XZ plane, at a "dip angle" (vertical angle) equal to the arc XH_1 below it. At an orbital height of 148 km (80 nm), the dip angle is nearly 23° ; we shall use this value for illustrative purposes. Three positions of the landmark relative to the spacecraft are indicated at L_1 , L_2 , and L_3 .



148

First, let us concentrate our attention on a sighting L_2 , which may be thought of as the second of a series of three sightings. At this position, the landmark is at the point of closest approach of the spacecraft, that is, at place where the nadir angle of the landmark as viewed from the spacecraft is a minimum. (Also, in this figure, the landmark is in the OYZ plane, at a relative bearing of 90° . Admittedly this is a special case, but this fact is not important to the arguments. In any case, it will always be desirable to obtain at least one sighting of a landmark as close to the spacecraft nadir as possible.) As we have seen, a star (such as S_2), must lie above $H_1H_2H_3$, so the arc ZS_2 cannot exceed 23° ; the SXT will not allow the arc S_2L_2 (or any other similar arc S_iL_i) to exceed 57° , so that the arc L_2Y' must be at least 10° in a real situation. The cone of position for a sighting carried out in a situation like L_2 will intersect the celestial sphere in an arc like ML_2M' . This intersecting arc together with the origin O define a plane OL_2X or the great circle XL_2X' , whose pole P is on the extension of the great circle arc L_2S_2 through the landmark and the reference star. (In this particular case, this great circle happens also to be the vertical circle $Y'ZY$, but that is immaterial.) Alternatively, (1) one can think of an infinitesimal plane element of the conical surface of position in the neighborhood of the landmark L_2 , and use the element to define the plane or great circle XL_2X' and its pole P; or (2) one can think of the plane or great circle XL_2X' as being defined as the great circle tangent to the intersecting arc ML_2M' at the point L_2 . We shall label the cone, plane element, intersecting arc, etc. "No. 2" when necessary to refer to them.

The great circle XL_2X' is the polar great circle to P. The instantaneous drift line of the landmark as viewed from the spacecraft is tangent to this great circle; in fact the whole drift path of the landmark as viewed from the spacecraft (the dashed curve $H_1L_2H_3$) lies in the

general direction of this great circle, falling below it at the end points (near H_1 and H_3). If another conical surface of position were obtained at L_2 with some other (perhaps hypothetical) reference star, lying anywhere on the great circle XL_2X' , such as S^* in Figure XI-4, its infinitesimal plane element would be orthogonal to that of cone No. 2, that is, the dihedral angle between the two surfaces would be 90° at the point on the intersection curve of the two cones where the intersection runs through the landmark. This follows from the polar relations of the two great circles.

Obviously, to qualify as a real sighting, the star S^* must lie within 57° of the landmark, and also lie above the small circle $H_1H_2H_3$. If L_2 were close enough to H_2 , so that the arc L_2H' could be less than 57° , an arc like L_2S^* could represent a real sighting.

But we need, or are looking for, not two, but three mutually orthogonal intersecting conical surfaces, and only two are possible at any one particular situation such as that presented by the spacecraft at O and by the landmark viewed in a particular direction like OL_2 . To obtain three mutually orthogonal surfaces of position, it is necessary to make at least one sighting in another direction, such as OL_1 (when the spacecraft is approaching the landmark) or OL_3 (as the spacecraft is leaving the landmark).

As a practical matter, it would be impossible to obtain two simultaneous SXT sightings on a landmark at a particular position L_2 with two different reference stars, such as S_2 and S^* , because it would certainly take a minute or two to pick up the second star (which requires reorientation of the spacecraft and stabilization in the new attitude) after the first sighting was complete. This means that the observer will have to wait at least one orbital period between the two sightings to be made in the same direction, such as OL_2 . Since

he has to wait anyhow, symmetry (and certain other considerations that will become apparent later) suggests that three separate sightings be made, in three distinct directions OL_1 , OL_2 , and OL_3 , with OL_2 made as near the nadir as possible, and OL_1 and OL_3 symmetrically placed with respect to OL_2 .

Any sighting, such as OL_1 (which for convenience we shall label sighting No. 1) will yield another surface of position orthogonal to sighting No. 2 along OL_2 , so long as the reference star S_1 lies on a great circle L_1S_1 perpendicular to the great circle L_2S_2P . L_1 can be anywhere on the apparent drift path $H''L_2$. Strictly speaking, the great circle L_1S_1 for sighting No. 1 will lie slightly below the great circle XL_2 , and its pole P' will lie slightly below the pole P along the vertical circle $YPZL_2Y'$. The surface of position resulting from sighting No. 1 is, of course, located in space. Although in the context of Figure XI-4, in which the spacecraft is considered to be fixed at O and the landmark to be moving from H'' to L_1 to L_2 to L_3 , etc., one may imagine the act of "carrying forward" surface-of-position No. 1 to superimpose it on surface-of-position No. 2, this procedure is not actually required.

Having picked two directions OL_1 and OL_2 and corresponding directions to reference stars OS_1 and OS_2 , it is now necessary to find a third direction OL_3 and a corresponding direction to a reference star OS_3 that will yield a third surface-of-position orthogonal to the first two. Similarly to the situation regarding L_1 , and for similar reasons, any sighting such as OL_3 with a reference star such as S_3 that lies on a great circle L_3S_3 perpendicular to the great circle L_2S_2P , will yield a surface-of-position No. 3 that is orthogonal to surface-of-position No. 2. We further require that surface-of-position No. 3 be orthogonal to surface-of-position No. 1. This is most easily achieved by requiring that the sightings OL_1 and OL_3 be 90° apart, that is, that the angle L_1OL_3 be 90° .

(a) Symmetry and other considerations. If the direction OL_1 be chosen very close to OL_2 , in order to have two observations near minimum slant range (i. e., in order to minimize the "thickness" $2\sigma = 2r/10^4$ of the surfaces of position due to the angular uncertainty of $20''$), then it will be impossible to find a direction OL_3 that is both perpendicular to OL_1 and also on the drift path. As a bare minimum, it will be necessary to pick the direction OL_1 far enough away from OL_2 to allow OL_3 to lie below the visible horizon $H_1H_2H_3$. In this case, the observation at L_3 will be done at nearly maximum range, and will have rather low weight. (Questions of weight will be discussed in greater detail below.) By moving OL_1 even further from OL_2 , the slant range of L_1 will be increased a little, but the slant range of L_3 can be decreased a great deal, so that the total weight of the three observations will be considerably increased.

(b) Summary. The best compromise for optimizing the geometry of a set of three sightings on a particular landmark, within limitations considered so far, turns out to be as follows:

(1) Choose a "central" sighting observation (central in position only, it need not be central in time between the other two) in a direction OL_2 corresponding to the direction to the landmark near closest approach of the spacecraft, and a reference star in a direction OS_2 which is on the same vertical circle as L_2 .

(2) Choose the other two sightings in directions OL_1 and OL_3 , so that these are perpendicular to each other, and each therefore about 45° from OL_2 . The direction OL_1 is ahead of the spacecraft, at a relative bearing between 0° to perhaps 60° for a landmark on the starboard side, or 300° to 360° for a landmark on the port side. OL_3 is symmetrical to OL_1 with respect to the coordinate plane OYZ , that is, behind the spacecraft, at a relative bearing between about 120° and 180° for a landmark passing to starboard, and between 180° and 240° for a landmark passing to port.

(c) Generalization of optimization procedures. Sighting observations made according to the foregoing plan have somewhat more general properties that may prove useful in selecting any set of three mutually independent sightings, i. e., regardless of whether or not one of the sightings is made near the point of closest approach, etc. Refer again to Figure XI-4. The infinitesimal plane of position from sighting No. 2 defined a great circle XL_2X' whose pole was at P. Now let us label this P_2 . There are corresponding poles for the other two sightings. Let us disregard the fact that the drift path $H''L_2H''$ departs somewhat from the great circle XL_2X' ; this is legitimate in view of (1) the fact that, if L_1 and L_3 are each only 45° from L_2 , the departure is really quite negligible for our purposes, and (2) the fact that departures from orthogonality must actually be quite large before the uncertainties are increased significantly. (Remember that a 10% increase in uncertainty corresponds to cosecant $\theta \approx 1.10$, or $\theta \approx 65^\circ$.)

If we consider that the drift path and the great circle XL_2X' are the same, then the poles P_1 and P_3 , defined respectively by the infinitesimal plane elements of cones-of-position Nos. 1 and 3 in the neighborhood of the landmark, will lie on the great circle XL_2X' extended. As viewed from the CSM, this great circle is the projection against the sky of the angular drift motion of the landmark and passes through the point X on the celestial sphere toward which the CSM is moving. The reference stars S_1 and S_3 also lie on this great circle. Since L_1 is 45° from L_2 , and P_1 is 90° further along the same great circle, P_1 will lie on the polar great circle of P_2 , 135° from L_2 . Similarly, P_3 will lie on the polar of P_2 , 135° along the polar great circle from L_2 , in the opposite direction from P_1 . Thus, P_1 , P_2 and P_3 are at the vertices of a right spherical triangle.

This leads to a rule of general applicability in all situations:

(1) Let the drift path or the instantaneous angular motion of a landmark approximately define a great circle, which we shall call

the drift-path great circle. Choose sighting directions OL_1 , OL_2 , OL_3 along the drift path, with OL_1 and OL_3 approximately perpendicular to each other, and OL_2 (nearly) in the common plane between them.

(2) The drift-path great circle has a pole, P_2 . The two other poles P_1 and P_3 lie on this great circle. Reference star S_2 should lie on or near the great circle L_2P_2 . The direction OS_2 must be within 57° of the direction OL_2 , but above the visible horizon $H_1H_2H_3$.

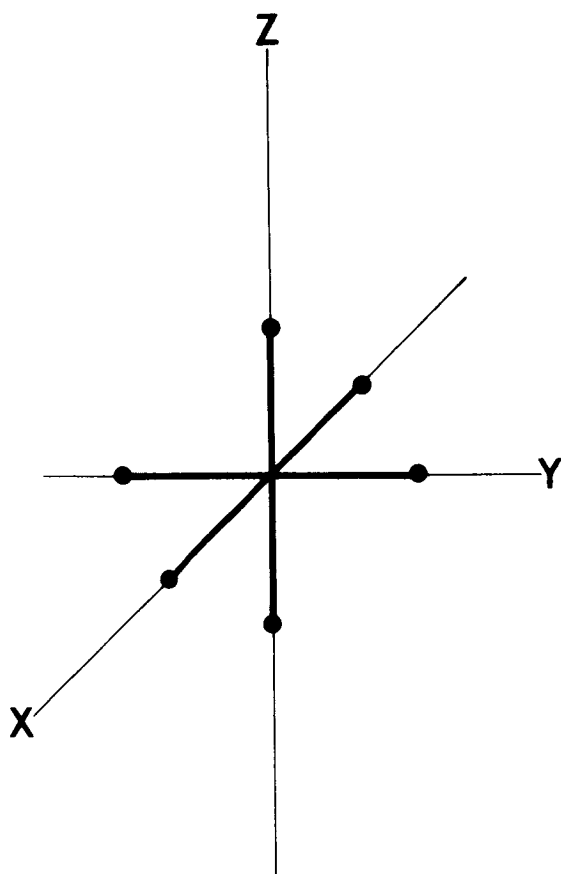
(3) Reference star S_1 for sighting No. 1 should lie on or near the drift-path great circle, between L_1 and the pole P_1 , with the angle S_1OL_1 less than 57° , but with S_1 above the visible horizon. Similarly, the reference star S_3 for sighting No. 3 should lie on or near the same great circle, between L_3 and the pole P_3 , with the angle S_3OL_3 less than 57° , but with S_3 above the visible horizon.

(d) Cautionary comments. A considerable amount of detail has been devoted to the question optimizing the geometry of sightings to result in orthogonally intersecting surfaces. Lest this leave the impression that orthogonality is extremely important, it should be stated once more explicitly that departures from orthogonality up to 25° or so result in only a 10% increase in the uncertainty. In general, if the landmark sightings and their reference stars are kept within 15° to 20° of their ideal direction (with all directions being relative to each other), the increased uncertainties will be altogether insignificant. Considerably more latitude will do no harm, in comparison with the size of the other errors affecting the fix. Finally, it will not always be possible to find three directions OL_i and three reference stars S_i that are located near the ideal places. In practice, if it seems necessary to reduce uncertainties resulting from poor geometry, it will usually be possible to do so by supplying extra sightings to fill in the deficiencies. Some of these questions are taken up below.

5. Concept of "Weight per Unit Solid Angle" as a Means of Planning Sighting Observations

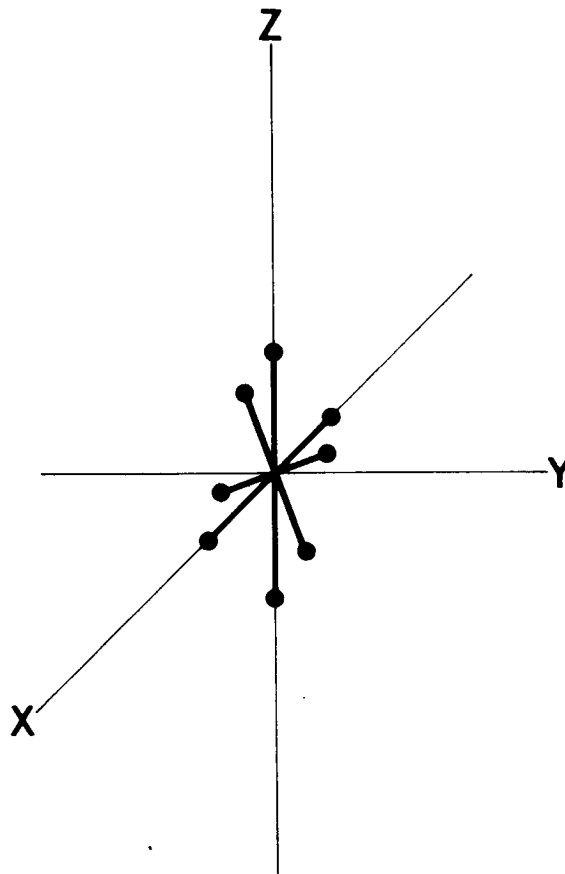
An ideal error ellipsoid (or sphere, if the errors are equal in all directions) can be represented by three numbers, that is, the three dispersions σ_1 , σ_2 , and σ_3 , in three mutually orthogonal directions. One can picture this as three "rods" projecting from a common origin. Let us first replace the σ_i by weights W_i proportional to $1/\sigma_i^2$, and set the length of the rods proportional to these weights. The scale of weighting is of course to a certain degree arbitrary. One might give unit weight to an ideal sighting observation made at minimum slant range. At $h = 148$ km, r_{\min} is about 151 km, and if the angular uncertainty of the sighting is $20''$, the half-thickness of the surface of position (which we might call "slab of position") would be 15 meters. Then $W = 1$ would correspond to $\epsilon_i = \pm 15$ m and the weights of other observations would be given by the usual relation, $W_i = (\epsilon_i / \epsilon_1)^2$.

One observation gives one "slab of position", which locates the landmark in one degree of freedom or one direction -- namely, perpendicular to the slab, or one might say, "inside the slab with a probability of 68% for 1σ ." The location is completely unknown in the other two directions, parallel to the faces of the slab. This fact could be recorded as a rod, drawn from an origin in the appropriate direction, with length equal to the weight. Three slabs intersecting nearly ideally would result in three rods, more or less orthogonal, and of length approaching unity on the weight scale. Non-ideally intersecting slabs, or slabs corresponding to observations of low weight, would result in a figure in which the rods are preferentially in one direction, have lengths short compared to unity, etc. Figure XI-5 is an attempt at representing weight as a function of direction. One could fill in deficiencies in the observing scheme that led to such a figure, by making sightings to produce slabs of position, and therefore rods in Figure XI-5, to fill in those directions that are not well represented in the error distribution (actually, weight distribution), to make the weight distribution more nearly isotropic.



IDEAL

Orthogonal, with all
degrees of freedom
fixed with unit weight



NON-IDEAL

All observations low-weight,
confined to X-Z plane. Re-
quires slabs in the X-Z
plane to fix in Y-direction

WEIGHT DISTRIBUTION OF A FIX AS A FUNCTION OF DIRECTION

FIGURE XI - 5

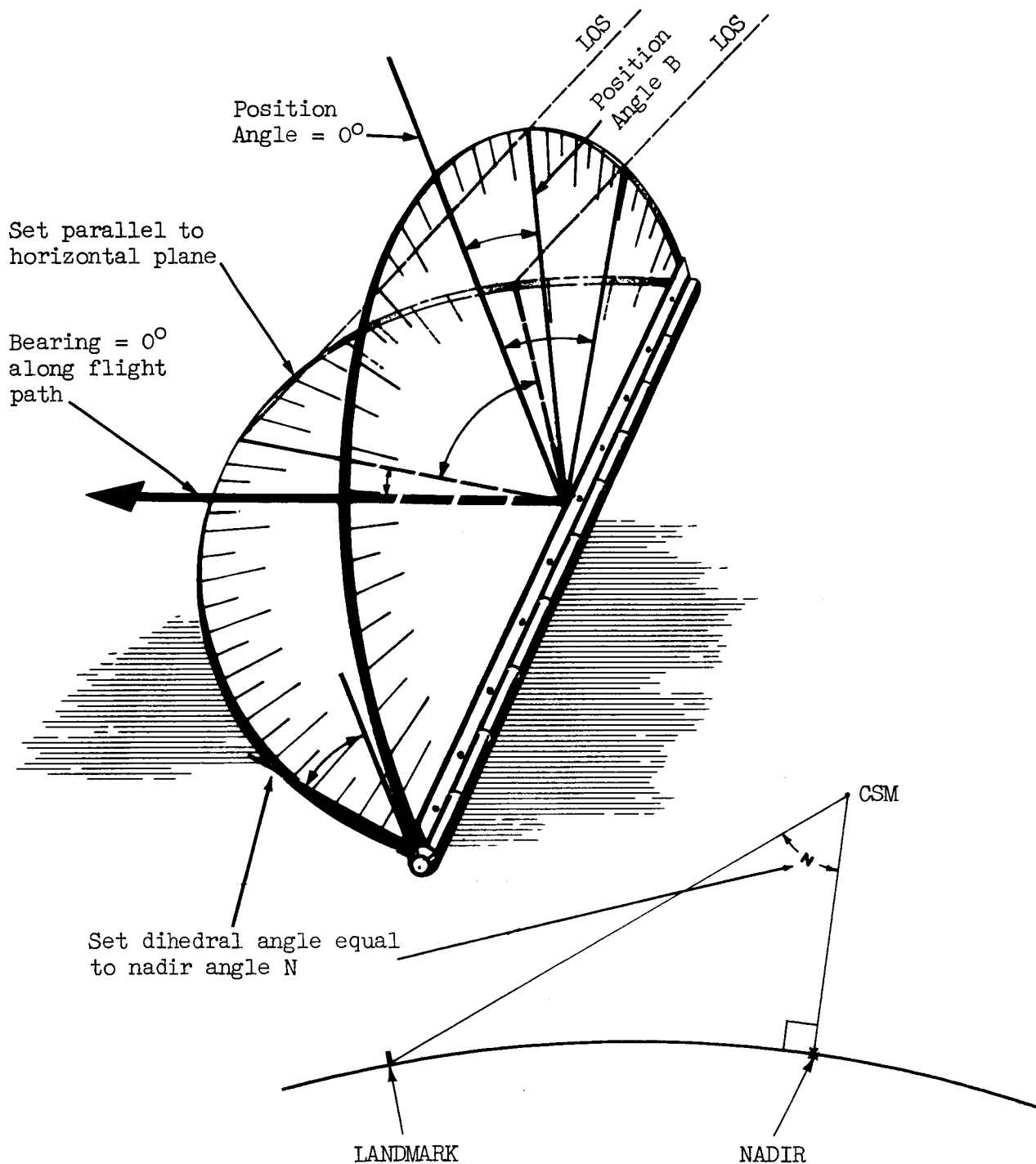
It will ordinarily be unprofitable to go to great lengths in trying to achieve isotropy of weight distribution, for the same reasons given above at the end of Paragraph 4. There may be cases, however, when it is important to get an accurate fix on a landmark some distance off the subsatellite track, that is, one whose minimum slant range is still very large (say, several hundred km), in which case all the single sightings will have low weight.

To fill out the weight distribution in direction, one can use the precepts outlined in Paragraph 4. Figure XI-6 represents a rough-and-ready device, whose use is intended to provide a crude but quick means of determining and recording the bearing of the intersection of a conical surface of position with the ground (the terrain), given the position angle of the observation, and vice versa. Although the location of the terrain level in the vertical direction is not necessarily known, it will always be possible to make a sighting that produces a surface of position that is nearly horizontal at the landmark. For example, the observation can be made at a long slant range. The visible ground surface serves merely as a plane to record directions on, and not as a substitute for a surface of position.

6. Observing Schemes

A wide variety of observing schemes is possible. Three schemes will be outlined below; they are intended as examples, rather than procedures that have been tested and proved to be useful. They are intended further to bring out certain practical considerations that depend on operational constraints: for example, the amount of time required per observation (which has a bearing on the efficiency of the observing scheme), the number of spacecraft attitude changes involved, etc.

The availability of suitably bright reference stars in appropriate directions affects all the schemes alike. The selection of stars for the



DEVICE FOR CONVERTING POSITION ANGLES
TO BEARINGS AND VICE VERSA

FIGURE XI - 6

sightings will be limited to some degree by the faintest stars that can be photographed in a reasonable exposure time, and the number of such stars available in a given region of the sky. We assume that it will be possible to select stars suitable for sightings within a few degrees of any chosen point in the celestial sphere. There are approximately 42,000 square degrees in the sky and about 400 stars brighter than the 5th magnitude; therefore, one star brighter than the 5th magnitude per 100 square degrees on the average. This implies that the bright stars are separated on the average by about 10° , so that it is likely that one or more will be found within 5° of any random point. We also assume that 4th magnitude stars can be photographed with a reasonably short exposure. (Section II discusses the plausibility of these assumptions.)

The three examples of observing schemes are labelled respectively "A", "B", and "C". Observing Scheme "A" is intended for use in those cases where one might wish to concentrate on fixing the location of a relatively small number of landmarks, close to the subsatellite track. Observing Scheme "B" provides a possible procedure for observing a larger number of landmarks, none very intensively, and ranging in position from close to the subsatellite track to perhaps 200-300 km away. Observing Scheme "C" is intended for the observation of remote landmarks, from the slant range where "B" leaves off up to the maximum possible, which coincides with the visible horizon.

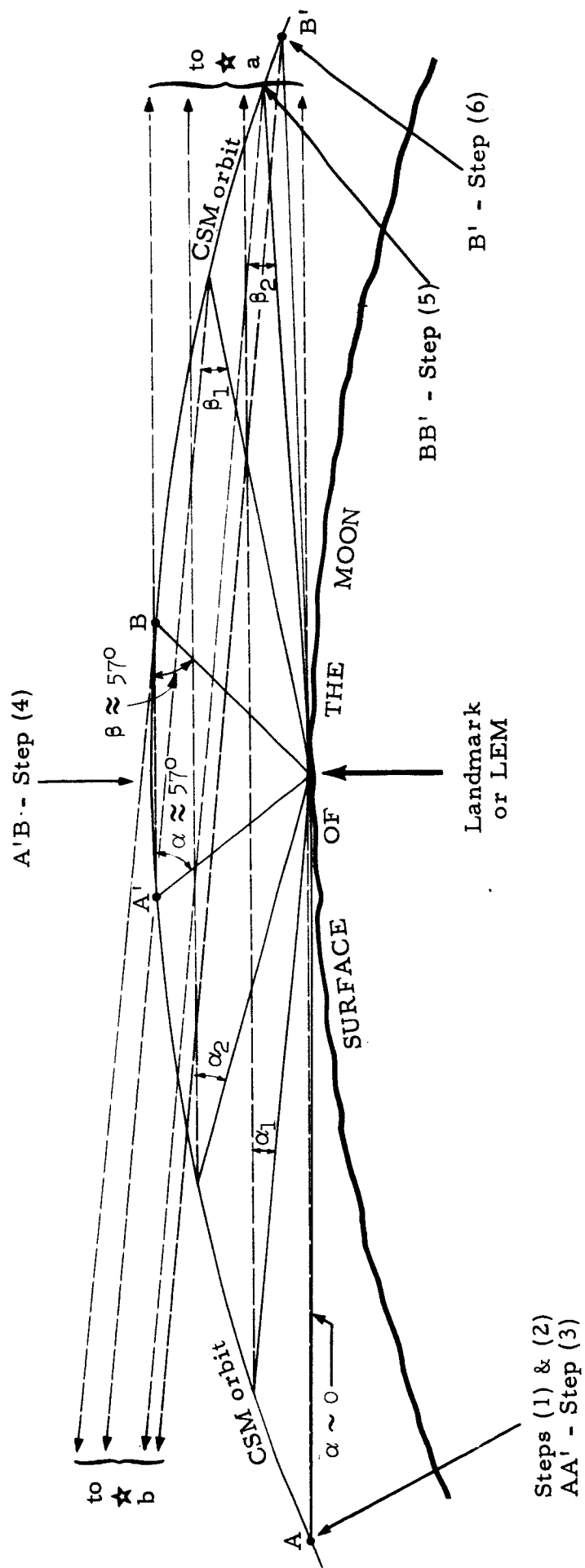
7. Observing Scheme "A" for a Fix on a Single Landmark

There will be situations where it is important to obtain, early in the mission, an accurate fix on a single landmark, not too far from the subsatellite track, devoting as little time as necessary for getting a complete fix. The grounded LEM is a good example of such an important landmark; it is important not only because it will serve as the interim datum to tie the surface survey to the coordinate system of the CSM orbit around the moon's center of mass, but also because it is essential to

know the LEM coordinates with respect to the CSM in order to give the LEM crew instructions for their return. Furthermore, fixes on a landmark in each of the 200 km x 200 km regions photographed by the Lunar Orbiter will be needed to tie these regions together in some single coordinate system, if that has not already been done; three fixes per region are required for this task, since three points define a plane. Scheme "A" is designed to meet this need (although Scheme "B" described below will be more efficient for landmarks at moderate distances off the subsatellite track, if one can afford to wait through three or four full circuits of the CSM around the moon to complete the fix).

(a) A possible procedure for Observing Scheme "A". First we consider a possible procedure for making a single set of observations on a single landmark fairly near the subsatellite track, using one reference star when approaching the landmark, and another star when leaving it astern; this can be visualized by referring to Figure XI-7. The fact that the maximum angle between the two arms of the SXT is 57° , and the fact that one arm is fixed, or movable only to a very limited degree with respect to the body of the CSM, dictates a procedure similar to that outlined below. It is assumed as before that the landmark or the LEM (possibly with beacon or reflector) is visible or photographable through the SXT, from distances of at least 150 km possibly up to 732 km, (i. e., on the visible horizon). If this should turn out to be too extreme an assumption, it will not affect the basic arguments or the scheme.

- (1) As the CSM reaches a point, like A from which the landmark is just visible on or near the skyline ahead, let the fixed member of the SXT be set on a star (a in Figure XI-7), just above the landmark and as close as possible to the skyline. Let the CSM be stabilized as well as possible to keep star a in the field of the fixed member.



SECTION IN ORBITAL PLANE OF CSM

FIGURE XI - 7

- (2) Let the landmark (or LEM) be picked up in the field of the movable member of the SXT, as soon as possible after it is visible, when angle α (landmark-CSM-star a) is small.
- (3) From A to A', when angle α has increased to 57° , make as many observations as possible.

At A' the landmark will go out of reach of the SXT if its fixed arm is still pointed at star a. If star a and landmark are both in the orbital plane the central angle, CSM-moon's center-landmark, will be 2.87° . With a central angle of 2.87° , star a will have risen to $23^\circ - 2.87^\circ$ or about 20° above the skyline, and the landmark will be about $57^\circ - 20^\circ$, or 37° below it. The landmark will be at an angle $N = 90^\circ - 37^\circ - 23^\circ$, or 30° from the nadir, as viewed from the CSM, and the ground arc distance, d , of the landmark from the nadir of the CSM will be 87 km. The slant range, r , from the CSM to the landmark will be 173 km. (If the landmark or star a are not on the orbital plane, all these dimensions will be somewhat different.) The geometry of this situation is to be distinguished from the geometry where the reference star is very close to the skyline, in which case the SXT can reach 57° below the skyline, i. e., to a landmark at nadir angle $N = 10^\circ$, arc distance from subsatellite point $d = 26$ km, and minimum slant range $r_{\min} = 151$ km. There is a "blind cone" for angles $N \leq 10^\circ$, where landmarks simply cannot be reached by the SXT if the other arm is pointed at a star.

- (4) There is a point B on the trajectory of the CSM, symmetrical with A', where the geometry of the landmark relative to the flight path behind the CSM is the same as it is for the forward part of the flight path at A'. During the approximately 2 minutes that it takes the CSM to move from A' to B, the CSM should be pitched about 180° , and a star (b on the diagram) should be picked up in the fixed member of the SXT, and the CSM stabilized as before. Star b can be about 180° from (at the antipode of) star a.

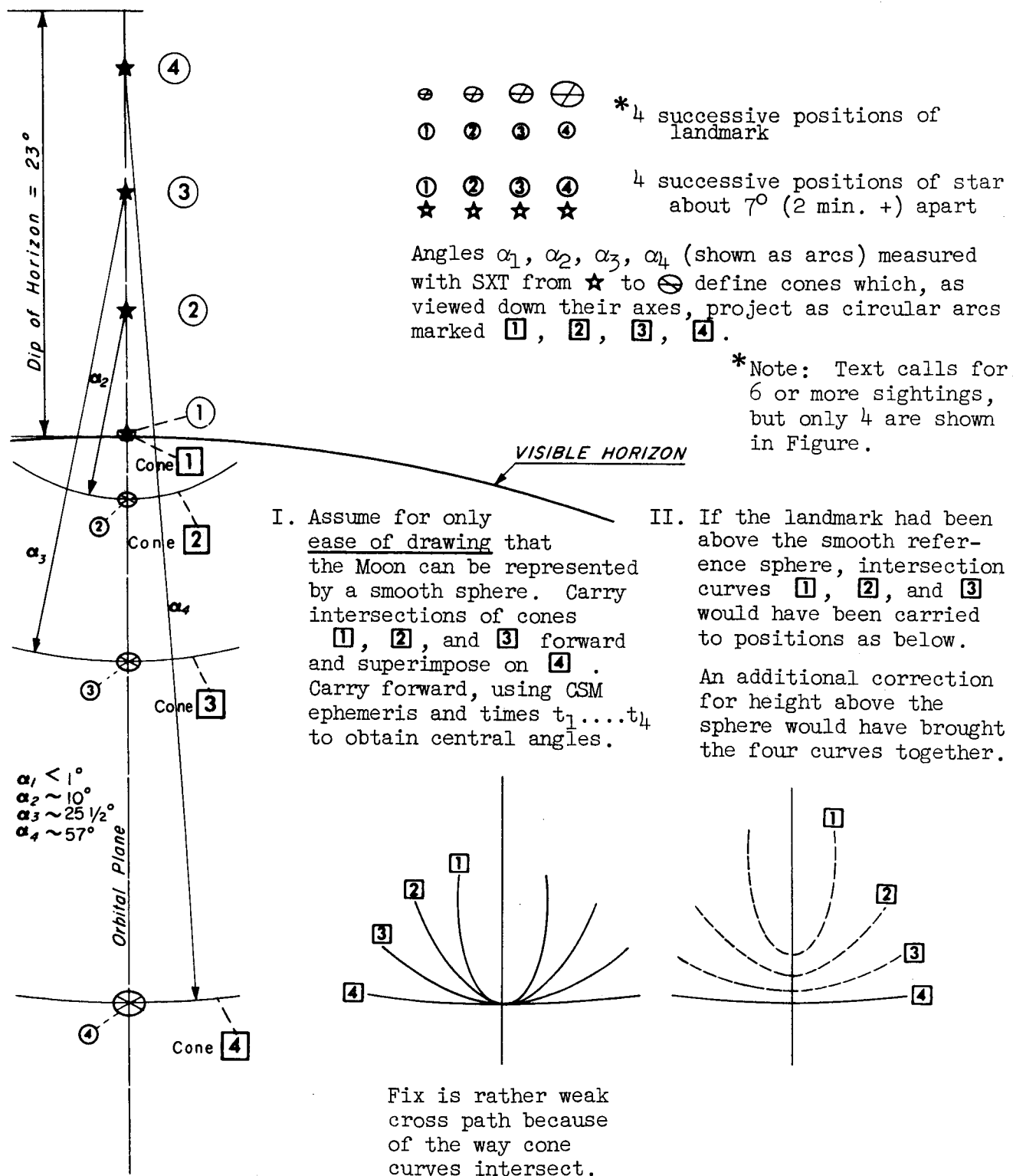
(5) When the CSM reaches the point B, or as soon thereafter as possible, where angle β (landmark-CSM-star b) is 57° and decreasing, so that the movable member of the SXT can be brought to bear on a landmark, a series of measurements of that angle β should begin, with the movable member of the SXT following the landmark. (Repeat of step (3) above, in reverse.)

(6) Continue until the landmark (LEM) is out of sight, or the star b sets as viewed from the CSM, whichever happens first (B' in Figure XI-7).

(b) Geometrical strength of fix as rationale for modifying

Observing Scheme "A". Figures XI-8 and 9 shows that if only the two sets of angles are measured -- angles α_i (landmark-CSM-star a) and angles β_i (landmark-CSM-star b), in which stars a and b are approximately opposite each other in the sky and both approximately in the orbital plane of the CSM -- then the geometry of the three-dimensional fix of the landmark with respect to the orbital positions of the CSM can result in a fix that is good in (1) the X-direction, parallel to the orbit and in (2) the Y-direction or local vertical, but not quite as good in (3) the Z-direction, perpendicular to the orbital plane. (If reference stars are available in exactly the right position to make one set of observations as indicated in Figure XI-8, and the other as in Figure XI-9, this slight defect will be largely taken care of. (See pages 105 - 107 below.)

To rectify this difficulty, it would be possible to pick other stars, say, in directions c and d in Figure XI-10 such that the lines of position CSM-to-landmark will cross the lines of position obtained with stars a and b at an angle as near 90° as possible, and cross each other as near 90° as possible. To pick up all four stars, a, b, c, and d in the same pass of the CSM over the landmark seems rather cumbersome, and would probably waste a good deal of the fuel supply of the attitude jets. It would be more efficient to set on stars a and b during one pass, and on stars c and d the next pass. To strengthen the geometry of the



SUCCESSIVE SIGHTINGS OF LEM (OR LANDMARK)
 AND STAR AS VIEWED FROM CSM AT TIMES $t_1 \dots t_4$

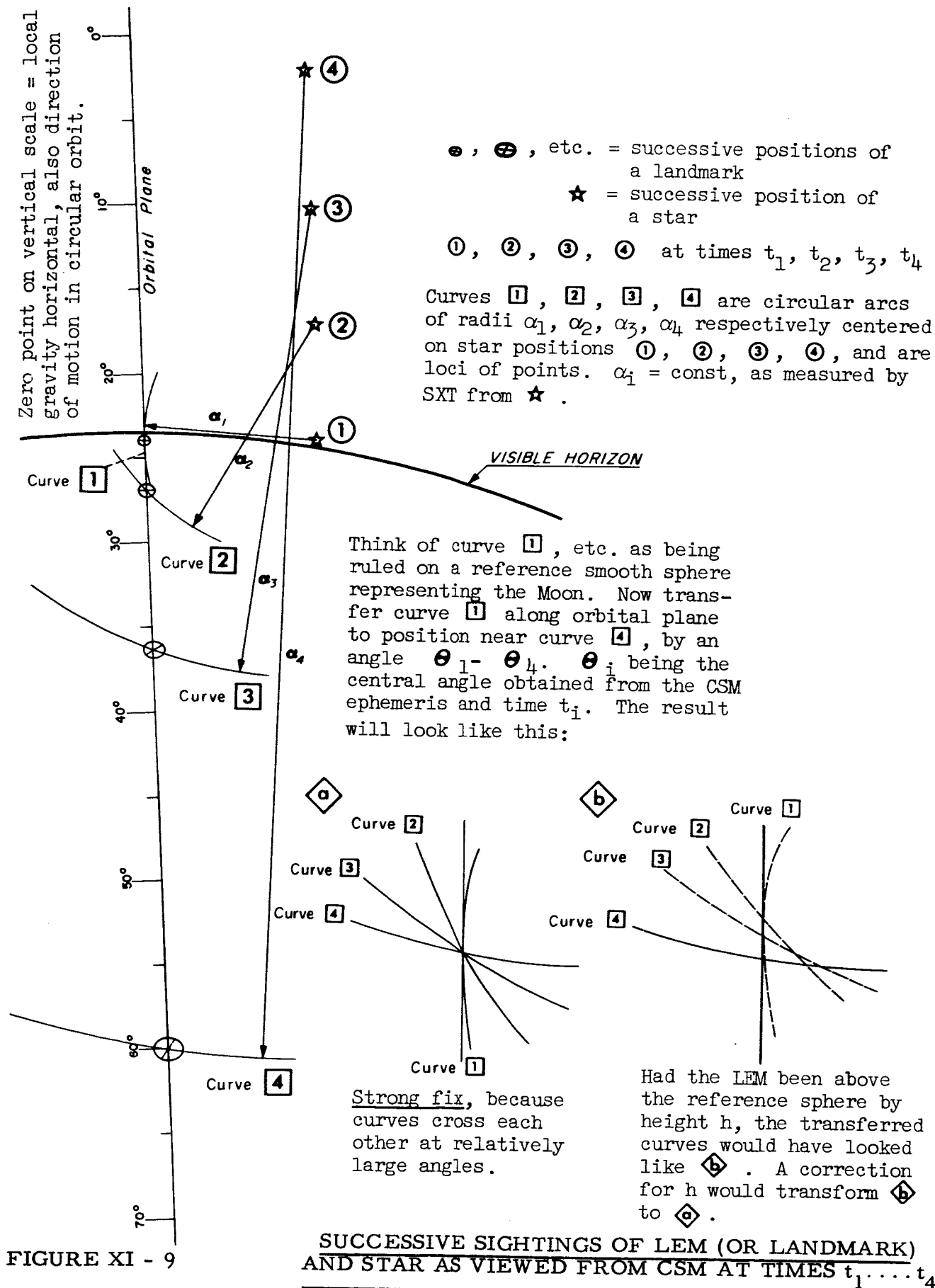


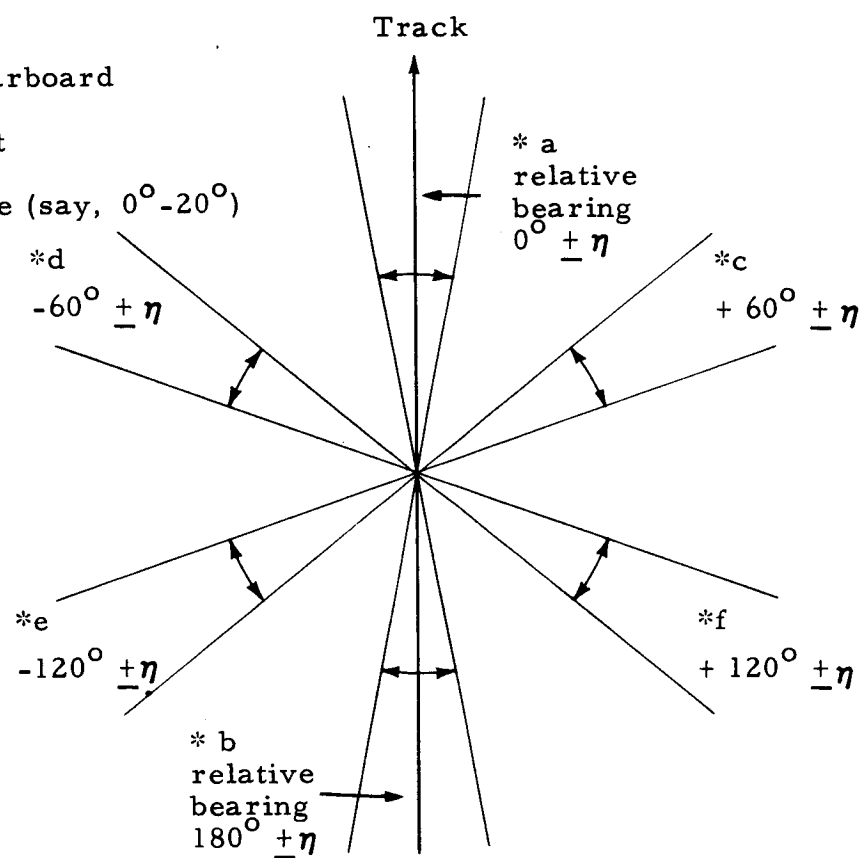
FIGURE XI - 9

Bearings

+ = right or starboard

- = left or port

η = small angle (say, 0° - 20°)



PLAN VIEW - OBSERVING SCHEME "A"

FIGURE XI - 10

fix even further, one could pick stars, as e and f in Figure XI-10. If this were done, then stars c and e could be paired in one pass, and stars d and f in the next, in order to limit most of the spacecraft attitude change to motion around a single axis. (It is assumed here that it is easier and more economical to change the attitude of the spacecraft about 180° in, say, pitch, and only a small angle in roll or yaw, than it is to change all three attitude angles by amounts of the order of 90° .) But only in exceptional cases would one want to devote three entire passes to a single landmark.

A certain amount of flexibility is possible in choice of pairs of stars: e.g., star a on the approach could be paired with star b, or star e, or star f on the retreat; star b on the retreat could be paired with star a, or star c, or star d on the approach.

8. Critique of Observing Scheme "A"

Let us now turn to a more detailed discussion of this observing scheme, in order to analyze the uncertainties associated with it. To begin with, it would be most efficient to distribute the observations in such a way as to use two of the six stars on each of three passes over a landmark or the LEM. In that way, there would be time to obtain several measurements of the angle α between the landmark and a star as the CSM approaches the landmark and the angle α decreases, then several more measurements of the angle β between the landmark and another star as the CSM goes away from the landmark and the angle β decreases.

As noted previously in the outline, the observer would first set the fixed member of the SXT on the reference star by slewing the spacecraft and stabilizing its attitude, then set the movable member of the SXT on the landmark by setting the shaft and trunnion angles of the SXT. Then, as the fixed member is kept on the star and the movable member on the landmark, a series of repeated photographs can be made. (See Part C below of this section for a more detailed discussion of this procedure

and its feasibility.) It is difficult to estimate how long such a series of observations might take, without some simulation to check out the estimate. Let us assume, however, it will take about two minutes to get set on the star and the landmark from some random orientation of the CSM, but only one minute if the spacecraft has been oriented in advance; so that the fixed member points in the direction of a preselected reference star, even before the star has risen over the horizon ahead. Let us assume further that photographs can be obtained at intervals of no change than one minute -- in fact, somewhat less -- the time between exposures being used to follow the passing landmark with the movable member, i. e., to reset the movable arm as necessary.

At an orbital altitude of 148 km (80 n. m.), the slant range to the horizon is about 732 km and the ground-arc distance from the nadir of the spacecraft is 693 km. An observation of a landmark can obviously be made no further away than this. As noted before, landmarks cannot be measured if closer than 10° to the nadir of the spacecraft, i. e., no closer than about 26 km ground-arc distance from the subsatellite point. The slant range to such a point is 151 km. We are thus considering the following ranges of values: (1) slant range, 151-732 km; (2) nadir angle, 10° - 67° ; (3) ground-arc distance, 26-693 km.

At an orbital velocity of 1.62 km/sec the speed of the subsatellite point over the ground is 1.49 km/sec, or 90 km/min. Thus about 6 1/2 mins. elapse between the time a landmark can first be sighted on the horizon near the track and the time it goes out of reach into the cone bounded by $N = 30^{\circ}$. (To chase the landmark into the cone of inaccessibility 10° from the nadir would require setting on another star immediately, but it is the essence of Scheme "A" to stick to one star.) This seems to allow time for (up to) six observations on a landmark or the LEM, using one star while coming up on it, and time for approximately the same number of observations while leaving the landmark astern, now using another star. The two sets, coming up and going away, are symmetrical, so it is not necessary to consider more than one of these sets. The six

successive observations of the angle, landmark-CSM-star, might be carried out typically at slant ranges of, say, 600, 520, 440, 360, 270, and 180 km approximately. If the SXT trunnion angle and the auxiliary photographic offset can be measured with an accuracy of $1:10^4$, as assumed above, then the error in the direction of the normal to the respective conical surfaces of position would be ± 60 , ± 52 , ± 44 , ± 36 , ± 27 , and ± 18 meters, respectively.

Example 1: Assuming a poor geometry as in Figure XI-8, in which the (up to) six cones "nest" and the intersections between the cones (taken two at a time) tend to form a sheaf or bundle of curves running through the landmark in roughly the same direction, then the observations would be rather redundant in locating landmarks in the (two) directions perpendicular to the axis of the bundle, but would do little to locate the landmark accurately in the direction parallel to the axis of the bundle.

To restate the case explored in Paragraph 5 above: (1) if we take $\sigma = 15$ m, corresponding to the minimum slant range of about 151 km above, (2) if we give such an observation a weight $W = 1$ (as if all the observations were a member of a set of observations all made at the same slant range and distributed normally with a dispersion of ± 15 m), and (3) if the individual measurements then be weighted according to the usual rule, $W_i = (\sigma / \epsilon_i)^2$, in which W_i is the weight of the i th observation and ϵ_i is its error, then the uncertainty of the mean position of the landmark perpendicular to the axis of the bundle would be about ± 15 meters $\times (\sum W_i)^{-1/2} \times$ (mean projection factor). The mean projection factor takes care of the "strength of the geometry." Now, with the individual errors assumed at the end of the last paragraph $\sum W_i = 1.44$ so $(\sum W_i)^{-1/2} = 0.83$. If the arithmetic average of the angle ψ between the individual curves (intersections of pairs of cones) and the axis of the bundle is, say 20° , the projection factor is $\sec \psi$, or about 1.03. Thus the cross-axis uncertainty is $\pm 15 \times 0.83 \times 1.03$ m, or about ± 11 m. Along the bundle axis the projection factor is $\operatorname{cosec} \psi$ or about 2.9, so that the uncertainty along the axis is about ± 32 m. The weight can be increased if it proves to be possible to crowd most of the observations into the part of the runs nearest the landmark.

Example 2: As a second example let us assume that the geometry of the intersections is nearly ideal, i. e. , fulfilling one of the following three sets of conditions:

- (1) There are only three intersection curves (three cones taken two at a time), these three have about equal weight, and the three are more or less mutually orthogonal; or
- (2) There are more than three intersection curves, but still of equal weight, and these are distributed more or less randomly in direction (orientation) in space so that they have no preferred axis; or
- (3) There are more than three, and these are of unequal weight, but are distributed in direction (orientation) in such a way that the average weight per unit solid angle is more or less uniform.

Under these circumstances the uncertainty (dispersion) will be the same in all directions. It is not to be expected that three mutually orthogonal cone-intersections, each with unit weight, can be obtained by Observing Scheme A; that is, Case (1) will not occur. In fact, since the observations in the set-of-six are of unequal weight, only Case (3) can be expected ever to occur. In the configuration represented in Figure XI-9, it will tend to occur almost naturally. The first two or three observations at long range, and hence with low weight, will tend to fall together with each other (i. e. , with the relatively small angle between their directions) more closely than they will with the last two or three, and the last two or three will not fall together as closely with each other as the first two or three do with each other. Thus the intersection curves will tend to be distributed so that the weight per unit solid angle approaches uniformity. It would be difficult, however, to attain uniformity of distribution with only one set-of-six; the distribution would be filled out even better with two sets-of-six, one coming up on the landmark, as in Figure XI-8, and the other going away, as in Figure XI-9, or vice versa.

This point may require a little elaboration. Examination of the lie of the cones of position in Figures XI-8 and 9, or for that matter, any possible combination of cones that can be obtained in a single pass over a landmark, shows that to obtain any intersection curves that run horizontally and perpendicular to the subsatellite track (i. e. , in the Z-direction) it is necessary to use at least some cones whose under side, where it intersects the ground, has a rather gentle slope; in other words, the landmark must be observed at quite long range. But these observations have low weight: to build up the weight in this particular direction to achieve a more nearly isotropic error distribution, it would be necessary to repeat a number of these long-range observations. That is exactly what the series of observations in the configuration in Figure XI-8 does, thus supplementing what is lacking in the configuration in Figure XI-9.

With luck, the distribution of the resulting uncertainties may be nearly isotropic, with a one-dimensional dispersion $\sigma = 15$ m (dispersion of the components of the error vectors in the error ellipsoid in a single direction) or a three-dimensional dispersion $\sigma = 22$ m (dispersion of the arithmetic length of the errors in the error ellipsoid, without regard for direction). Even in the "poor geometry" example above, the uncertainty of the fix was estimated to be ± 11 m in two directions and ± 32 m in the third direction. Therefore, except in extreme cases where the utmost possible precision is required, it is doubtful whether there is much point in struggling very hard to achieve either perfect isotropy of the error ellipsoid, or errors small compared to that of the CSM position, assumed to be ± 100 m. The decision as to where the diminishing returns dictate a stop to further efforts need not be made now; it should be deferred until more reliable information is available.

It is to be understood that the numbers cited above are only rough estimates, and that the actual uncertainties would be based, as always, on the deviations of the weighted residuals from a mean, with the vector residuals resolved into components to obtain the dispersion in any particular direction.

The entire foregoing procedure, a set-of-six observations running up on a landmark and another set-of-six going away, takes (as has already been noted) about 15 minutes. The period of a 148-km-high orbit is 7300-odd seconds, or slightly over 2 hours, and only half of this is over the sunlit hemisphere. Therefore, only about 4 landmarks per orbit could be fixed in CSM-referenced coordinates by Observing Scheme "A". This might be stretched to five or six landmarks, if observations of distant sunlit features can either be started while the CSM is still over the dark hemisphere approaching the terminator, or be prolonged after it crosses the terminator into the dark hemisphere. It should also be noted that the tips of some peaks stick up into the sunlight, even some distance from the terminator in the dark hemisphere. There is also the remote possibility of observing by earthshine, although this does not seem at all promising for photography.

9. The Concept of Efficiency: Application to Observing Scheme "A"

Let us now consider two questions:

(1) What is the efficiency of Observing Scheme "A"? To answer this question in any significant way, we must define "efficiency." Let it be measured by the numerical parameter, "weight of the observations carried out per unit time." The overall weighting in this context should naturally include the effect of the geometric projection factors. For instance, Observing Scheme "A" gives the following "efficiencies" in the two earlier examples:

For the case with good geometry: the weight is 2×1.44 or 2.88 in 13 minutes, or 0.22/min. well distributed among three degrees of freedom. The weight can probably be increased to more than 3 easily, giving $\approx 0.25/\text{min.}$

For poor geometry: weight about 2.6 distributed in two degrees of freedom and about 0.06 in the third, for a total of 2.7 in 13 minutes, or 0.21/min., mostly in two of the three degrees of freedom.

This result seems to suggest that, if one could limit oneself to observing only near minimum slant range ($r = 151$ km), and if one could arrange the observations so that the geometry is nearly optimum, three single short-range observations, with a total weight of nearly 3.0, would constitute an observing scheme that would be competitive with Observing Scheme "A", provided it took no longer than 12 minutes to make the three observations. (But see Observing Scheme "B" below.)

(2) Unit weight for a single observation can be achieved, according to the definitions just adopted, for only those landmarks that approach the nadir of the CSM as close as 10° or the subsatellite point as close as 26 km. If observations were literally limited to those of this optimum type, a belt only 54 km wide straddling the subsatellite track as its center line would be covered. This restriction makes impossible another kind of coverage that is obviously desirable, namely, the tying in of remote scattered points, (as far off the track as possible) to a common coordinate system (that of the CSM orbit). Nor can the surface geodetic operation provide geodetic ties or controls over more than a very limited region: at best it can be described as providing horizontal and vertical controls and scale with a precision of about $1:10^4$ over a region bounded by the horizon as seen from the LEM (or nearby high ground), which might be only 5 km in radius. High land around the landing site would of course push back this horizon; the highest peaks may be visible as far as 150 km away, but these will be rare extremes. The point is that the surface operation will not provide control over a very appreciable area compared to the region to be covered by the lunar orbiter mapping mission or, for that matter, present-day maps. Map controls for the invisible hemisphere are entirely lacking, and will probably still be sketchy at the time of first Apollo missions. It seems that the only real opportunity to provide improved controls for the largest possible areas is to try to make SXT sightings of landmarks some distance from the subsatellite track. (See Observing Scheme "C" below.)

Apart from considerations of the desirability of extending geodetic control for maps and lunar orbiter photographs, it is also desirable to fix the location of a number of landmarks for navigation purposes, e. g., for later Apollo missions, especially on the invisible hemisphere of the Moon.

We now examine other possible observing schemes in the light of the foregoing considerations, namely (1) efficiency, as defined above, and (2) coverage.

10. Observing Scheme "B": A Small Number of Fairly High-Weight Observations per Landmark

In Observing Scheme "B" described below, provision is made for observing a relatively large number of landmarks, each with the least possible number of high-weight observations, i. e., made at the closest possible slant ranges compatible with distance of the landmark from the subsatellite track and the possible geometry of the intersections. The intention is to maximize the number of landmark fixes per unit time. The minimum slant range, 151 km, and the corresponding minimum nadir angle, 10° , of course set a lower limit. The scheme should work down to this limit, and also out to landmarks that pass no closer than say, 150-250 km. Also, even landmarks close to the subsatellite track must sometimes be observed at medium slant ranges in order to achieve acceptable intersection geometry.

It will turn out that:

- (1) For landmarks close to the track, but not closer than 26 km, three sightings, disposed much like those described in Section 1.4 above, will give sufficient information.

- (2) For landmarks closer than 26 km from the subsatellite track, the minimum number of sightings may sometimes be four.
- (3) As the distance of the landmarks from the track increases, the minimum number will grow larger, merging with the situation for very distant landmarks covered by Observing Scheme "C" below.

The scheme for items (1) and (3) above will be the basic Observing Scheme "B", and that for item (2) will be "B", Modification 1.

(a) Rationale. A scheme designed to obtain three-dimensional fixes for the largest possible number of landmarks all fairly close to the subsatellite track, should take into account the following factors:

- (1) Other things being equal, each sighting should be made at the closest slant range feasible, to maximize its weight.
- (2) No more than the necessary number of independent sightings should be obtained; this will normally be three, but some poorer geometries will need filling with a fourth observation, or perhaps more.
- (3) Intersections between conical surfaces of positions, or rather the normals to infinitesimal plane elements in the neighborhood of the intersection, should if possible be made to lie in the range $60-90^{\circ}$ (or 60° to 120° , if one also counts the obtuse angle of the intersection), which will keep the geometric degradation factor below 1.16 (16% increase in uncertainty).

- (4) The same reference stars should be used for as many successive sighting observations of (different) landmarks as possible, to avoid having to reset the attitude of the spacecraft and restabilizing it any more than is necessary.
- (5) The observing program of landmarks should be arranged so that the longest possible sequences of landmarks come up on the spacecraft on approximately the same relative bearing at the times when sightings are to be made, again with the purpose of avoiding unnecessary slewing of the spacecraft.
- (6) The general arrangement of the three sightings on any one landmark will approximate the arrangement in Paragraph 4 for the lines of sight OL_1 , OL_2 , and OL_3 for the landmark, OS_1 , OS_2 , and OS_3 for the respective reference stars. (See Figure XI-4.) This provides a ready-made recipe for setting up the basic observing scheme.

Consider now two zones of lunar terrain, each bounded by two small circles, both parallel to the great circle which best fits the subsatellite track, and both on the same side, (i. e., both to starboard, which is north for a westbound orbit; or both to port, which is south); the nearer circle is 26 km from the subsatellite track and the farther circle is perhaps 200 km away. Let us call these two zones the starboard and port "observing zones." For landmarks inside these zones, it will be easy to follow the ready-made recipe with no alterations.

Each landmark in the starboard observing zone should be sighted in the three directions as indicated in Figure XI-4. (1) OL_1 , which is in the starboard forward lower octant; (2) OL_2 which is on the starboard beam, as close to the nadir as the particular landmark is able to get; and (3) OL_3 which is in the starboard aft lower octant. (For landmarks

in the port observing zone, substitute "port" for "starboard" in the foregoing description.)

For a starboard (port) sighting OL_1 , the reference stars will be found in the region of the sky near the drift-path great circle for that landmark, (see Section 1.4 for definition), i. e., either below and to the right (left) of the velocity vector tip X, or around the velocity vector tip X, or above and to the left (right) of X (assuming that the observer is standing vertical and facing forward). The direction OS_1 to the reference star S_1 selected for this sighting must of course be within 57° of OL_1 at the moment of recording the sighting.

For a starboard (port) sighting OL_2 , the reference stars will be found in the region of the sky near the starboard (port) beam and low enough in the sky to allow the angle S_2OL_2 to be less than 57° .

For a starboard (port) sighting OL_3 , the reference stars will be found in the region of the sky near the drift-path great circle for that landmark, i. e., either below and to the left (right) of the point X' (directly astern in the direction of motion) or near the point X', or above and to the right (left) of X' (assuming now that the observer is standing vertical and facing aft). Again, the angle S_3OL_3 cannot exceed 57° .

The bearings and nadir angles for the three sightings can be estimated more precisely, if necessary. The precise values of the directions corresponding to sightings in which the three surfaces of position intersect absolutely orthogonally can easily be calculated by spherical trigonometrical relationships, in which N_{\min} , the minimum nadir angle possible for a given landmark corresponding to the instant of closest approach, would be a parameter. Alternatively, the ground-arc distance of the landmark from the subsatellite track could be used as a parameter. These calculations seem unnecessary here, in view of the following two considerations: (1) drift curves, showing altitude and

relative bearing as a function of the time, with one of the two above-mentioned parameters, have already been calculated by Mercer (MSC, Houston) in connection with Contract No. NAS 9-3006 (Pilotage); (2) the disadvantage of slight departure from orthogonality should be traded off for the advantage of closer slant range.

This second remark needs a little elaboration. In Paragraph 4, it was stipulated that the angle L_1OL_3 should be 90° . It has also been stated that departures of 25° or 30° from orthogonality lead respectively to only a 10% or 16% increase in the uncertainty. On the other hand, if the angle L_1OL_3 were made as small as 65° , that would allow the angles L_1OL_2 and L_3OL_2 to be as small as 33° , and therefore also considerably closer to the nadir; thus the slant range to L_1 and L_3 would be decreased and the uncertainties due to the SXT angle-measurement error decreased in proportion. For N_{\min} small, i. e., for very close landmarks, the tradeoff is in favor of bringing OL_1 and OL_3 in closer to OL_2 by a considerable amount, because of the gain in precision obtained from the shorter slant ranges involved.

The following approximate calculation will bring this out. If L_1OL_2 and L_3OL_2 are both 45° and $N_{\min} = 10^\circ$, then the nadir angles $N(L_1)$ and $N(L_3)$ are both about 45° (actually, $\arccos(\cos N \cos 10^\circ)$, or 45.87°). The slant range r is approximately $h \sec N$, and the rate of change of r with N , dr/dN , is approximately $h \sec N \tan N$, in which h is the height of the CSM above the ground. The relative rate of change of r , dr/rdN , is simply $\tan N$, which is equal to 1. That is, r decreases 100% per radian decrease in N , or 1.74% per degree. On the other hand, the rate of change of geometric degradation factor $\csc \theta$ is $d(\csc \theta)/dN$, or $-\csc \theta \cot \theta d\theta/dN$, or $-2 \cdot \csc \theta \cot \theta$ (since $\theta = 2N$). The relative rate of change of the degradation factor, $d(\csc \theta)/\csc \theta \cdot dN$, is simply $-2 \cot \theta$, which is equal to zero. The cross-over point, at which the rate of relative increase in the geometric degradation factor is matched by the rate of relative decrease in the slant range is given by the equation $\tan N = 2 \cot(2N)$, the solution to which is $N = 30^\circ$.

The implication is that OL_1 and OL_3 should be brought in 45° minus 30° , or 15° , toward OL_2 (a more exact calculation would lead to a slightly different amount). The following should also be noted: (1) for larger values of N_{min} , i.e., for landmarks farther from the subsatellite track, the tradeoff begins to fall off, and eventually becomes negligible. (2) It has been assumed above that the reference stars S_1 and S_3 are near the drift-path great circle, but if it becomes necessary to find stars closer to the vertical circles through L_1 and L_3 , in order to be within 57° of those directions, some degradation will have already been introduced; therefore caution should be exercised in introducing further degradation. In other words, looking again at Figure 4, if one relaxes on the geometry too much, one could wind up with the two poles P_1 and P_3 rather too close to P_2 .

The following table summarizes the altitude angles A , and relative bearings B of landmark sightings L_i and star sightings S_i . These values should be considered representative only, subject to modification according to the foregoing discussion. (Angles are given for a landmark, abbreviated LM in the table, that passes on the starboard side of the CSM. For landmarks passing on the port side, change all B 's to $360-B$.)

Sighting Number	$A(L_i)$	$B(L_i)$	$A(S_i)$	$B(S_i)$
$i = 1$	-45° or somewhat lower	$10-15^\circ$ for IM passing close to nadir; somewhat more for distant IM, or if $A(L)$ is much below -45°	$+10$ to -23° , or whatever is necessary to be within 57° of the IM and still remain near the great circle extension of the apparent drift curve of the IM	Determined by the conditions specified for $A(S)$; in general near 0° .
$i = 2$	As low as possible, i.e. as near -80° as possible	90°	As low as necessary to be within 57° of the IM	90° (i.e., on the same vertical circle as the IM)
$i = 3$	-45° or somewhat lower	$165-170^\circ$ for IM passing close to nadir (conditions as in $B(L_2)$ above)	Same as $A(S_2)$ above	Like $B(S_2)$, in general near 180°

b. General plan of Observing Scheme "B"

(1) Select landmarks in the observing zones, paralleling track on the starboard and port sides. (A suitable total number of landmarks will emerge later.)

(2) Arrange separate lists of landmarks, those in each list being about the same distance from the subsatellite track, and on the same side. The order of landmarks in each list should be from east to west, which is the order in which the CSM will pass the landmarks. The grouping by distance will ensure that all the landmarks on one list will come in succession to approximately the same directions OL_1 , OL_2 , OL_3 , relative to the CSM.

(3) Arrange three lists of reference stars 4th magnitude or brighter. The first list comprises stars in a cap within 23° of the north pole of the CSM orbit (which will be close to the north celestial pole of the Moon, since the CSM orbit will have a very low inclination to the lunar equator); these stars are for sightings of the type S_2OL_2 on the starboard side. The second list comprises stars within 23° of the south pole of the orbit, which are for S_2OL_2 - type sightings on the port side. The third list comprises stars within about 10° of the orbital plane. Some of these will always be near the drift-path great circles of the landmarks. These will be used for sightings of the type S_1OL_1 ahead, and S_3OL_3 behind the spacecraft. The stars on each list should also be arranged from east to west, i. e., in order of decreasing selenocentric right ascension. The reason for these three lists will become apparent later.

c. Basis Scheme "B"

(1) During a single orbital revolution around the Moon, the CSM observer should make sightings of landmarks from only one of the lists

of landmarks, i. e., all those about equally distant from the subsatellite track and all on the same side. These sightings should be of the same type, i. e. OL_1 , OL_2 , or OL_3 , to obviate excessive changes in CSM attitude.

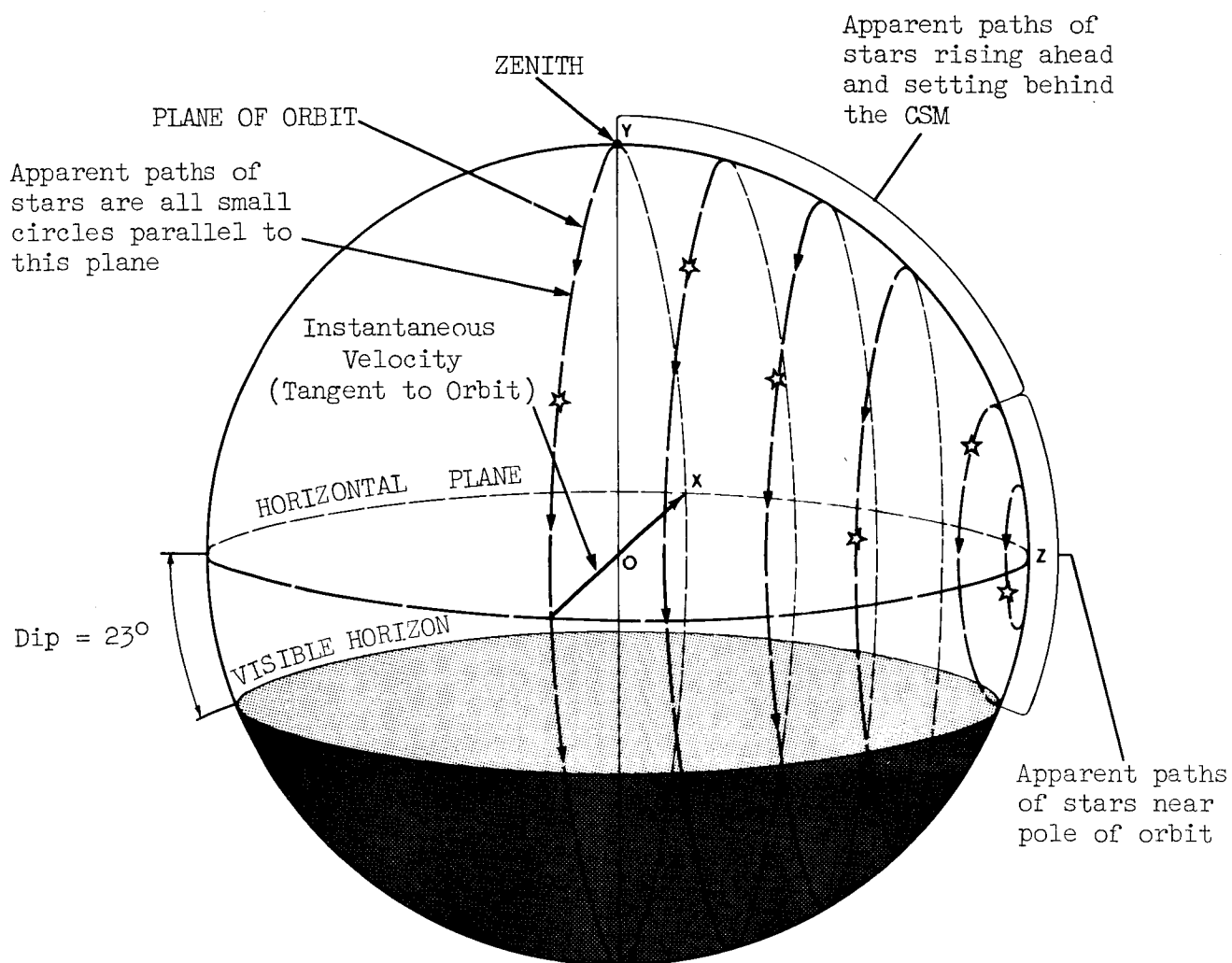
(2) Let the first set be of the type OL_3 . That is, during one revolution, all landmarks should be sighted near the instant of closest approach. The reference stars for these sightings would be chosen from the appropriate "polar cap" list.

(3) During the next circuit of the Moon, these same landmarks should be picked up in sightings of type OL_1 20° to 40° below the visible horizon and bearing 10° to perhaps 30° to one side of the flight path ahead. The reference stars for these sightings will lie near the orbital plane and will successively rise ahead of the spacecraft.

(4) During a third circuit, the same landmarks should be picked up in sightings of the type OL_3 using the same reference stars as in the set OL_1 , except now the stars will be setting behind the spacecraft.

11. Critique of Observing Scheme "B"

(a) Use of a reference star for more than one landmark. It will be recalled that it is desirable to use one reference star for as many successive landmark sightings as possible, in order to avoid unnecessary changes in spacecraft attitude. Figure XI-11 illustrates the "rising" and "setting circles" of stars at different angular distances from the orbital plane, which is essentially equivalent to lunar declination. (The angles are identical if the orbital plane is coincident with the equatorial plane of the Moon.) The "rising" and "setting" of course refer to the apparent motion of the stars from the standpoint of an observer on the CSM who regards himself as stationary. These circles are quite similar to the



RISEING AND SETTING CIRCLES OF STARS ON
CELESTIAL SPHERES CENTERED ON SPACECRAFT

FIGURE XI - 11

diurnal circles of stars as viewed from the Earth's equator. They can be combined with the apparent rate of rotation of the sky, which is the same as the angular orbital motion of the CSM (with opposite sign), so as to give estimates of the length of time that a particular star will remain in approximately the right direction to serve as a reference star for a set of sightings of the same type. For practical purposes, we may take the "diurnal motion" of the stars to be $3^\circ/\text{min}$ eastward.

Polar Cap Stars. Let us first consider reference stars of type S_2 , in one of the "polar caps." Stars within 23° of the poles of the orbit (Z or Z' in Figures XI-4 and XI-11) never set. If this were the only factor that need be considered, the fixed arm of the SXT could be kept pointing at such a star indefinitely. For landmarks in the "closest" list corresponding to the narrow strip with N_{\min} not much greater than 10° , the reference star S_2 must be near $B = 90^\circ$ (or 270°) and $N = 67^\circ$, just above the skyline (visible horizon). As the CSM makes a quarter-revolution around the Moon, that star will move to $B = 67^\circ$ (or 293°), and $N = 90^\circ$; then the star will no longer be within 57° of the innermost strip of landmarks. For landmarks farther out, say with $N_{\min} = 33^\circ$, reference star S_2 can be as much as 23° above the skyline, or very close to a pole of the orbit. Such a star will remain practically stationary in B and N coordinates, and can be used indefinitely from any position in the orbit. For landmarks even farther out, with $N_{\min} > 33^\circ$, the reference star S_2 can be even higher than 23° above the skyline, i. e. clear above the horizontal plane; but it will nevertheless be convenient to choose it as near a pole as possible, to take advantage of a nearly stationary B and N. For landmarks with N_{\min} between 10° and 23° , it will be necessary to change reference stars S_2 occasionally: fairly frequently near the lower limit, but never near the upper limit. For instance, for the intermediate value $N_{\min} = 15^\circ$, star S_2 must be no more than 5° above the skyline ($N(S_2) < 72^\circ$) or else it will be further than 57° from L_2 . If the star be chosen so that it describes a circle 23° in

radius around Z (or Z') i. e., a circle that just misses the skyline at its low point, the star will remain within 5° of the skyline for about 77° of its small-circle arc, which requires about 25 minutes to traverse. During this same 77° arc, $B(S_2)$ will remain within 15° of the beam, i. e. between 75° and 105° on the starboard side, or between 255° and 285° on the port, ranges which conform well enough with the orthogonality constraints.

In sum, it appears that except for landmarks with N_{\min} between 10° and 15° , it will not be necessary to change the reference star S_2 very often.

(c) Stars near the orbital plane. Reference stars for sightings OS_1 and OS_3 will lie fairly close to the orbital plane, and will rise or set nearly along vertical circles. For $N_{\min} = 10^\circ$, the reference stars S_1 or S_3 should lie within 4° of the orbital plane if they are on the same side as the landmark, and within 2° if on the opposite side, if strict orthogonality is to be observed. For $N_{\min} = 45^\circ$, the range increases to 23° on the same side and 12° on the opposite side. Translated into bearings when the stars cross the horizontal plane, these limits become: (1) For the starboard side, $N = 10^\circ$, $B(S_1) = 358^\circ - 4^\circ$, $B(S_3) = 176^\circ - 182^\circ$; $N = 45^\circ$, $B(S_1) = 348^\circ - 23^\circ$, $B(S_3) = 157^\circ - 192^\circ$; (2) for the port side, $N = 10^\circ$, $B(S_1) = 356^\circ - 2^\circ$, $B(S_3) = 178^\circ - 184^\circ$; $N = 45^\circ$, $B(S_1) = 337^\circ - 12^\circ$, $B(S_3) = 168^\circ - 203^\circ$. The stars must also be below $N \cong 102^\circ$ or so, to be accessible.

If OL_1 and OL_3 are brought closer to OL_2 , as suggested above for small values of the parameter N_{\min} , the stars for S_1 and S_3 may have to be moved farther from the orbital plane than the 4° just given -- say, up to 10 or 15° on the same side. The stars must now be below $N \cong 87^\circ$ to be accessible, i. e., within 20° of the skyline.

The rate at which a star rises or sets (altitude or nadir angle increases or decreases) is $3^{\circ}/\text{min}$, times the cosine of its bearing when it crosses the horizontal plane ($N = 90^{\circ}$). Since the minimum numerical value of the cosine for the cases considered in the last paragraph is 0.92, the rate of rising or setting is still 2.7 to $2.8^{\circ}/\text{min}$. The reference stars would thus rise from the skyline ahead (at $N = 67^{\circ}$) to $N = 108^{\circ}$, a vertical angle of 41° , in 14 or 15 minutes, and conversely set through the useful range in the same length of time. When the maximum useful nadir angle is lowered to 87° , as it would be if OL_1 and OL_3 are moved to 30° from OL_2 , the rising or setting time through the useful zone is shortened to 6 or 7 minutes. (See Table XI-1 for a more general treatment of these questions.)

(d) Time consumed and efficiency. We assumed earlier that it will take two minutes to pick up and set the SXT on a star and a landmark, and that photographic records of sightings can be repeated on the same landmark and star at intervals of no greater than one minute. Let us assume that it will take a full minute to reset from one landmark to the next, as long as they follow each other into position on the same line of sight -- same direction -- with respect to the CSM, but two minutes if the switch from one landmark to the next requires a large change in the direction of pointing the movable arm of the SXT. (None of the assumptions about the time required to make settings, either in this paragraph or earlier, are necessarily very realistic; but it is difficult to obtain a better basis for making estimates until at least some simulation studies can be carried out.)

These assumptions, together with the considerations explored in the previous subsection above, lead to the following estimates:

(1) Innermost strip of landmarks with N_{min} close to 10° , and with OL_1 and OL_3 brought up to 30° from OL_2 . In these directions,

TABLE XI-1

Time in Minutes Taken by a Star

To Rise from Altitude $-A^{\circ}$ to Altitude $+A^{\circ}$ To Set from Altitude $+A^{\circ}$ to Altitude $-A^{\circ}$

As a Function of A and the Relative Bearing $\pm B$ or $180^{\circ} \pm B$ of the
 Star When It Crosses the Horizontal Plane
 Due to an Orbital Motion of the Spacecraft of $3^{\circ}/\text{min}$.

A	Sin A	B: 0°	10°	20°	30°	40°	50°	60°	70°	80°
5.8°	0.1	1.9	2.0	2.1	2.2	2.5	3.0	3.9	5.7	11.9
11.5°	0.2	3.8	3.9	4.1	4.4	5.0	6.0	7.8	11.9	--
17.5°	0.3	5.8	5.9	6.2	6.8	7.7	9.3	12.3	20.5	--
23.5°	0.4	7.8	8.0	8.4	9.1	10.5	12.8	17.6	--	--

$N(L_1) = N(L_3) = 31.5^\circ$, and $r(L_1) = r(L_3) = 176$ km, so that the uncertainties in the surfaces of position are 17.7 m. The total weight is: 1.00 for the sighting S_2OL_2 , and $2 \times (15/17.6)^2 \times 0.866^2$ for geometric degradation, or 0.55 for the other two, or 2.1 altogether. If OL_1 and OL_3 had been left in their normal positions 45° away from OL_2 , N would have been 45.9° , r would have been 223 km, and ϵ 22.3 meters. The total weight would have been $1.00 + 2 \times (15/22.3)^2$, or 1.90, somewhat less than the first case.

In the first case ($L_1OL_3 = 60^\circ$), the reference stars S_1 and S_3 would have to be changed every 6-7 minutes, and would require 2 minutes to pick up, thus allowing, say 4 sightings per 7 minutes. In the second case ($L_1OL_3 = 90^\circ$), the reference stars S_1 and S_3 would have to be changed every 14-15 minutes and would require 2 minutes to pick up, thus allowing, say 12 sightings per 15 minutes. In both cases, the reference star S_2 would have to be changed certainly every 15 minutes or so, thus allowing, say, 12 sightings per 15 minutes also. These amount to about 48 sightings on 48 different landmarks per revolution (remembering that only 60 minutes are spent over the sunlit side). Since three revolutions will be required to complete the job of three sightings on each landmark, we arrive at the figure, 48 landmark fixes in 180 daylight minutes, with each fix having a weight of 1.9 to 2.1. The efficiency, in the sense defined before, is therefore 0.38 to 0.42/minute, a good deal higher than for Observing Scheme "A".

(2) More remote strip of landmarks, $N_{\min} = 45^\circ$. Without going into so much detail as for the last case, it is possible to say that the general effect of moving out to a strip of landmarks farther from the subsatellite path is: (i) to increase the length of time that the SXT fixed arm can remain pointing at a reference star without having to shift to another, at least for sightings of the type S_2OL_2 ; (ii) to decrease the weight of the observations because of the increased slant range. Item (i) may look like an advantage, but it is not a very

great one, because sightings of the type S_1OL_1 and S_3OL_3 cannot be speeded up much and so constitute a bottleneck. The rising or setting rate of $2.7^\circ/\text{minute}$ is still fast enough to move a reference star out of the useful zone in 15 minutes or so. This time can be lengthened only by using stars farther from the orbital plane, with some degradation in the geometry.* As for Item (ii), the slant ranges will now be about 219 km for r_2 and 349 km for r_1 and r_3 , so that the total weight will be 0.85. The efficiency will be about 0.23/minute, comparable with that of Observing Scheme "A". There still remains the advantage that many more landmarks can be covered than in "A", although each fix will of course have a lower weight.

(e) Observing Scheme "B", Modification 1. For landmarks in a strip of terrain closer than $N_{\min} = 10^\circ$, i. e., closer than 26 km to the subsatellite track, a sighting of the type S_2OL_2 , with S_2 and L_2 on or near the vertical circle perpendicular to the orbital plane, is no longer possible. The direction OL_2 , at which L is closest but still observable, breaks up into a pair of directions OL_{21} where the drift path of L enters, and OL_{22} , where it leaves the blind cone. These two directions will be symmetrical with respect to the OYZ-plane. Similarly the pole P_2 of infinitesimal plane element of position (or "slab of position" of paragraph 5) will divide into two symmetrically placed points, one, P_{21} , between the original P_2 and X , and the other, P_{22} , between P_2 and X' . (Refer to Figure XI-4.) We now see a situation where four sightings begin to become necessary. As long as N_{\min} is not much less than 10° , P_{21} and P_{22} will remain fairly close to P_2 , and the number of sightings can be limited to three without loss of geometrical fix strength. If the forward pole P_{21} and sighting $S_{21}OL_{21}$ be chosen, and the forward tilt of OP_{21} is great enough to begin to degrade the geometry of the intersection with the surface of position of S_1OL_1 , this can be counteracted by moving OL_1 away from OL_{21} , bearing in mind the

*But note Observing Scheme "B", Modification 2, for remote landmarks discussed in Section 12 below.

same kind of trade-offs between intersection geometry and slant range that have already been discussed in detail. (Alternatively, if the aft sighting $S_{23}OL_{23}$ be chosen, the direction OL_3 can be moved away from OL_{23} .)

Eventually, as N_{min} gets very small, P_{21} and P_{23} will have moved rather close to P_1 and P_3 respectively, even if these have been "backed off", as suggested in the last paragraph, so that they will take the place of P_1 and P_3 in the geometry. Before this stage is reached, the best geometry is conserved if all four poles and corresponding sightings are used. When this stage is finally reached, however, it is necessary to find replacements for the poles P_1 and P_3 which will indicate the proper direction for sightings. The poles for the new sighting direction will be in the general vicinity of the region vacated by P_2 . To obtain symmetry with a forward sighting, like $S_{21}OL_{21}$, it will be necessary to locate a pair of new poles, one to starboard and the other to port, each at a nadir angle of about 135° (altitude 45°), and somewhat ahead of the OYZ-plane. Sightings based on these poles should be made on the landmark when it is in the middle foreground, at a moderate slant range. We have now arrived at a geometry that resembles the forward half of the layout for Observing Scheme "A" with reference stars low in the sky, one more or less straight ahead, and the other two at relative bearings in the neighborhood of 60° and 300° respectively. The whole foregoing scheme could be reversed, i. e., be set up for the aft hemisphere.

Pressed to its logical conclusion, Observing Scheme "B", Mod. 1, would be rather clumsy. The pole P_{21} or P_{23} corresponds to the sighting at smallest slant range, on the edge of the blind cone. This means that the reference star S_{21} or S_{23} is barely above the skyline, and rising or setting vertically. Stars in this position would be usable for probably no more than a single minimum slant-range sighting on a single landmark in a single pass, thus requiring the acquisition of a new reference star after each sighting. If the minimum slant range at which one attempts to observe is relaxed, in order to avoid frequent reacquisition of reference stars -- e. g., if it relaxed so that $N = 23^\circ$ -- then the situation is even more nearly like the forward (or aft) hemisphere of Observing Scheme "A", and the weights of the observations are similar.

12. Distant Landmarks; Observing Scheme "C"

Observing Scheme "B" can be extended to landmarks at somewhat greater distances from the subsatellite track than the 151 km, or minimum slant range $r_{\min} = 219$ km, corresponding to a minimum nadir angle $N_{\min} = 45^\circ$. The errors in this region become larger, reaching a maximum at the visible horizon or skyline, and the weight correspondingly decreases; therefore, a large number of sightings per landmark is required to attain the same accuracy. Furthermore, as one tries to obtain fixes on landmarks from 200 km on toward the visible horizon, it becomes increasingly difficult to obtain a conical surface of position that dips steeply away from the observer in the CSM; i. e., one forming a small dihedral angle with the orbital plane, or one whose normal is in or near the vertical plane containing the CSM and the landmark, and directed away from the observer at a low angular altitude. The CSM does not get into a position, the geometry of which relative to the landmark allows such a sighting to be made. This implies that the error ellipsoid around the most distant landmarks will unavoidably be elongated in the direction perpendicular to the orbital plane of the CSM, or more exactly, along the mean line of sight to the landmark (line of sight at closest approach). In other intermediate cases, the ellipsoid can be oblate, with horizontal uncertainty in each degree of freedom about equal and both larger than the vertical uncertainty.

In the extreme case -- that of a landmark whose minimum slant range is nearly equal the range to the visible horizon (about 732 km), so that it appears briefly over the horizon on the beam of the CSM -- only two kinds of sightings (or their equivalents) are essentially possible: (i) with the reference star in the same vertical plane as the landmark, so that the conical surface of position is horizontal at the landmark, and (ii) with the reference star just above the visible horizon, but some distance right or left of the landmark in bearing, so that the conical surface of position is vertical at the landmark and also approximately orthogonal to the orbital plane. Assuming as before a linear error of $r \cdot 10^{-4}$, where r is the slant range, we would obtain a cigar-shaped error ellipsoid with

axes $73n^{-1/2}$ (where n is the number of independent sightings) transverse to the line of sight, but very long in the direction of the line of sight. (Since the position along the line of sight is completely indeterminate if one is dependent on the sightings alone, the uncertainty along the line of sight is in principle infinite, but it is actually limited by the preexisting error of location of the landmark, whatever that may be. In any case it cannot be larger than 732 km, the slant range to the landmark.)

Let us examine a somewhat less extreme case, namely, a landmark at such a distance that it rises at relative bearing 45° (or 315°) and sets at relative bearing 135° (or 225°), thus passing through 90° of relative bearing while above the horizon. At this distance from the CSM, it is still possible to obtain three mutually nearly orthogonal intersecting surfaces of position: (i) the vertical plane on relative bearing 45° (or 315°), (ii) the vertical plane on relative bearing 135° (or 225°), and (iii) a nearly horizontal plane. The first of these can be obtained just after the landmark rises, using a reference star just above the horizon but left or right of the landmark in bearing; the second can be obtained just before the landmark sets (with similar conditions for the reference star); and the third can be obtained any time, with a reference star vertically above the landmark.

Solving the spherical triangles for a landmark that passes through a range of 90° in relative bearing between rising and setting, one obtains the following results: the CSM traverses 33.4° of its orbit, taking about 11 minutes. The minimum slant range is 526 km, and the minimum ground arc distance is 486 km. The error ellipsoid will be $49n^{-1/2}$ meters in the vertical direction, and about $70n^{-1/2}$ meters in each of the horizontal directions, under the same assumptions as before. The minimum nadir angle (corresponding to the point of closest approach) is 65.8° , so that the maximum angular distance below the visible horizon or skyline is less than 2° . This result implies that the part of the moon's surface visible from the CSM will still be workable for fixing landmarks out to a distance that would look very close to the

skyline. Although it might be possible to push the limit of workability a few kilometers past the slant range of 526 km just quoted -- say, 600 -- it seems likely that, within a degree or so of the skyline, with line of sight that is so close to grazing incidence where it intersects the ground, terrain features will become so badly superimposed that only conspicuously high landmarks which project above the general terrain irregularities can be sighted on.

(a) Procedures for Observing Scheme "C". For the nearer end of the slant ranges contemplated (220 km to the horizon), the procedures would be identical to those for the farther end of the range for "B" (up to 220 km slant range), and need not be described in detail. That is, there is no sharp line of demarcation where Scheme "B" ceases to be effective, and at first the only extension of "B" would be a provision for obtaining more observations per landmark to keep the uncertainties smaller than some arbitrary standard of acceptability. For landmarks at greater distances, the region of the sky in which one would look for suitable reference stars would shrink to that part of the sky in two sectors of relative bearing centered on the relative bearings 90° (to starboard) and 270° (to port), and generally low in the sky (although they can be as high as 55° above the skyline for some of the sightings described above). Since stars in these regions of the sky are not too far from the two poles of the orbital plane, they will be displaced relatively slowly by the orbital motion of the CSM, and it will be necessary to pick up fresh reference stars only infrequently.

The main feature of Scheme "C" will be based on the desirability of making repeated observations of the same landmark. We might consider the numerical example above as being representative of conditions (i. e., coverage) beyond which it will be undesirable to go, except perhaps in the case of a very small number of important landmarks that happen to be at extreme distances from the subsatellite track. In the numerical example, the error of a single observation, 49 to 70 m, 3 or 4 times the adopted unit weight error of 15 m, so that it would be necessary to observe each landmark 10 to 20 times for each degree

of freedom, or 30 to 90 times altogether, in order to achieve a fix of weight equivalent to that of a close landmark with three optimum observations.

It is perhaps worth noting two possible observing procedures:

(i) An extension of Scheme "B", already mentioned, which we might call "B", Modification 2, for landmarks in the range of minimum slant ranges 220 km to perhaps 350 km; this would be identical to Scheme "B", except that to keep the uncertainty low, perhaps twice as many observations or more would be obtained -- say, six to fifteen altogether.

The efficiency of this procedure can be estimated by taking a typical numerical example (see Section 11 above, under sub-head Time Consumed and Efficiency). Let us take a landmark whose minimum slant range is 300 km: on the starboard side it would rise at relative bearing 20° and set at 160° (70° ahead and behind the beam, respectively); on the port side these relative bearings would be 340° and 200° respectively. It would be visible for 14 or 15 minutes; its minimum nadir angle N_{\min} is 50.3° , about 17° below the visible horizon. For an unmodified extension of Scheme "B", with $r_1 = r_3 = 500$ km, and $r_2 = 300$ km, the weight of a set of three observations would be about 0.38, which would lead to an efficiency, in the sense previously defined, of not much more than 0.1 per minute. The efficiency would be improved somewhat by making a set of several repeated observations of the same landmark and same reference star, of course at the expense of observing fewer landmarks altogether.

This result implies that for landmarks somewhere between 220 km and 300 km minimum slant range, it would pay to switch over to Scheme "C", described next below.

(ii) Scheme "C". This scheme would be brought into play for landmarks at slant ranges far enough away that the efficiency of Scheme "B", Modification 2, falls below that possible with "C". As we have just noted, this cross-over point will occur at a minimum slant range generally somewhere between 220 km and 300 km. The cross-over point will be influenced by the accuracy that is desired for a particular landmark fix. The main point is that Scheme "B", Modification 2, does not lend itself so readily to the quick repetition of sightings on the same landmark, using the same reference star to obtain all the necessary intersecting surfaces of position; at the point where it becomes desirable to obtain, say, twenty sightings of a landmark to ensure the required accuracy, Scheme "C" will probably be found to be more efficient.

In the situation under discussion, the landmark will never be more than a few degrees below the skyline: remember that we found a maximum angular distance of 17° below the skyline for $r_{\min} = 300$ km. The length of the visible arc it describes as it drifts across the beam of the CSM will be 140° in relative bearing for $r_{\min} = 300$ km; at somewhat greater distances it will fall below 114° (i. e., $2 \times 57^{\circ}$), and so will always be within "SXT reach" of a reference star situated close to the skyline and on the beam of the CSM, i. e., at relative bearing 90° on the starboard side, or 270° on the port side. It now becomes possible to pick up a landmark as it rises, together with a reference star in the location just noted, make repeated sightings as the landmark and the same star as the landmark drifts astern, stopping only when the landmark sets. It might be possible to make, say, two sightings per minute, or even more, since all that is now involved is the resetting of the movable arm of the SXT on the landmark after each sighting (assuming that the reference star remains in the field of the fixed arm). One could thus squeeze in a series of twenty observations for a ten-minute pass.

Such a series of observations would automatically be fairly well distributed from the standpoint of the geometry and the isotropy of the error ellipsoid. The surfaces of position from sightings made shortly after rising (somewhere in the middle of a forward quadrant), using a reference star very low in the sky and near the YZ-plane, will intersect those obtained shortly before setting at quite a large angle, at least up to well over 500 km. Both these planes will be approximately vertical, and so will both intersect the surfaces obtained near the middle of the run approximately orthogonally. The surfaces -- "slabs" -- of position near the beginning and end of the run will have a thickness corresponding to $\sigma \cong 70$ m, since they will be obtained at extreme ranges corresponding to about 700 km; in the middle of the run, the thickness of the (more or less horizontal) slab of position will correspond to $\sigma = 40$ m at $r_{\min} = 400$ km; 50 m at $r_{\min} = 500$ km, etc. If only three observations are obtained, one each at the beginning, middle, and end of the run, the resulting error ellipsoid will be somewhat anisotropic. In the first place, this hardly makes any difference. In the second place, even if it made a difference, some isotropy would be restored by repeated observations made at approximately equal time intervals, because the geometry of such a pass automatically causes the landmark to spend more time nearer the middle of the forward or aft quadrants than near straight abeam.

Assuming (1) that the rate of making sightings on the same landmark, using the same reference star, is 2/min, (2) that it takes 2 minutes to pick up a fresh landmark and possibly also a fresh reference star after the previous landmark has gone out of reach, and (3) taking $\sigma = 60$ m as a typical uncertainty, and 10 minutes as the duration of the landmark pass, we obtain for a typical efficiency the result: $20 \times (15/60)^2$ per 12 minutes, or

about 0.1/min. This is not very high, but higher than can be obtained by an extension of Scheme "B" to such distances.

As noted before, the whole effort to obtain location fixes on landmarks slowly breaks down as one goes to landmarks at greater and greater distances from the subsatellite track. Progressively the following things happen: (1) the relative bearing B at which a landmark rises gets closer and closer to 90° or 270° (starboard or port respectively), and the bearing at which it sets correspondingly approaches $180^\circ - B$ (i. e., approaches 90° or 270° as B approaches 90° or 270° respectively); (2) it becomes increasingly difficult, and finally impossible, to obtain surfaces of position whose intersections will yield information about the position of a landmark along the line of sight; information is obtained only about the two degrees of freedom transverse to the line of sight; (3) the duration of the pass during which the landmark is in sight becomes shorter and shorter, thus setting smaller and smaller limits to the number of observations it will be possible to make.

One final note is in order concerning relative efficiencies of Schemes "B" and "C". It will have been noticed that the improvement in efficiency of "C" over "B" at distances at which they are competitive arose from the fact that in "C" the use of a single reference star near the pole of the orbit, and hence in position for a comparatively long time, made it possible to save the time consumed in "B" in picking up fresh reference stars at frequent intervals for observations of the type S_1OL_1 and S_1OL_3 (see Figure XI-4). It will be recalled that the necessity to replace stars for sightings in these positions at frequent intervals was the determining factor in limiting the rate at which landmarks could be fixed. This situation can be alleviated somewhat, at distances near the upper limit for which "B" can be used (i. e., $r_{\min} = 200$ to 300 km), by selecting reference stars for sightings Nos. 1 and 3 toward the pole of the orbit, as far as the SXT will reach. This will generally put them inside the orbital "polar cap" -- hence in

a useful position for a relatively long time, and not requiring immediate replacement. If reference stars are chosen in this region, however, some of the strength of the intersection geometry is lost -- less so if the stars for sightings Nos. 1 and 3 are close to the skyline, more so if they are higher. Reference to Figure XI-4 will show, incidentally, that the general rule that the poles of the three intersecting planes of position should be within 20° or so of the vertices of an octant on the sphere is still valid.

13. Summary of Observing Schemes

Table XI-2 summarizes the various observing schemes which have been discussed in paragraphs 6-12 above showing their coverage, number of observations per landmark, accuracy of resulting fixes and efficiency.

TABLE XI - 2
OBSERVING SCHEMES⁽¹⁾
SUMMARY OF CHARACTERISTICS

Label and Purpose	Coverage r_{\min} : minimum slant range N_{\min} : minimum nadir angle d : ground-arc dist.	Number of Obs'ns/Landmark & Accuracy of Resulting Fix ⁽²⁾ (Relative to CSM position) in Meters	Rate of Obtaining Landmark Fixes: Efficiency ⁽³⁾	Number of ⁽⁴⁾ Landmarks per 12 Orbits
Scheme A: for a relatively small number of landmarks, close to subsatellite track (1 complete run = 2 1/2 runs, one approaching the landmark, the other going away.)	$r_{\min} \leq 173 \text{ km}$ ⁽⁵⁾ $N_{\min} \leq 300$ $0 \leq d \leq 87 \text{ km}$	1 run: 6 x 2*, ⁽⁶⁾ Some anisotropy, ⁽⁷⁾ 15 m in each degree of freedom 2 runs: 6 x 4 * ± 11 m, isotropic 6 runs: 6 x 6 * ± 8 m, isotropic	4 landmarks/hr. 0.21 to 0.25/min. 2 landmarks/hr. 0.21 to 0.25/min. 1 landmark/hr. 0.21 to 0.25/min.	50 25 12
Scheme B: for a relatively large number of landmarks, using the least number of highest-weight observations	$151 \text{ km} \leq r_{\min} \leq 220 \text{ km}$ $100 \leq N_{\min} \leq 450$ $26 \text{ km} \leq d \leq 155 \text{ km}$	Inner edge of zone: 1 x 3 * slightly ellipsoidal ⁽⁸⁾ ± 15 m A=10° B=±90° ± 18 m in plane ± 18 m to first. Outer edge of zone: 1 x 3 * ellipsoidal ± 22 m toward A=50° B=±90° ± 35 m in plane ± 35 m to first.	16 landmarks/hr. 0.38 to 0.42/min. 16 landmarks/hr. 0.23/min.	190 190

Scheme B Modification 1: for closer-in landmarks(9)	$r_{\min} \leq 151 \text{ km}$ $N_{\min} \leq 100$ $0 \leq d \leq 26 \text{ km}$	1 x 4 * slightly ellipsoidal ± 12 to 20 m	10-4 → landmarks/hr. 0.3 → 0.12/min.	120 50
Scheme B Modification 2: for more distant landmarks (consists of repetition)(9)	$220 \text{ km} < r_{\min} < 300 \text{ km}$ $450 < N_{\min} < 500$ $155 \text{ km} < d < 255 \text{ km}$	1 run: 1 x 3 * (10) ellipsoidal ± 30 m toward A=550 B=±900 ± 50 m } in plane ⊥ ± 50 m } to first 4 runs: 4 x 3 * ellipsoidal ± 15 m, ± 25 m, ± 25 m 9 runs: 9 x 3 * ellipsoidal ± 10 m, ± 13 m, ± 13 m	16-20 landmarks/hr. 0.10-0.12/min. 4-5 landmarks/hr. 0.12/min. 2-3 landmarks/hr. 0.12-0.15/min.	190-240 50-60 20-40
Scheme C: for distant land- marks (out to ex- treme slant range)	$220 \text{ km} < r_{\min} < 730 \text{ km}$ (11) $N > 450$ $d > 155 \text{ km}$	$r_{\min} = 300 \text{ km}$ 20 x 1 * ellipsoidal ± 15 m toward A=500 B=±900 ± 22 m } in plane ⊥ ± 22 m } to first 400 km: 20 x 1 * ellipsoidal ± 16 m toward A=700 B=±900 ± 35 m toward A=00 B=00 ± 35 m toward A=200 B=±900 525 km: 16 x 1 * (13) highly prolate ellipsoid 100 m along line of sight A=20 B=±900 25 m } vertical } across 25 m } horizontal } line of sight	6 landmarks/hr. (12) 0.20 to 0.30/min. 6 landmarks/hr. 0.16 to 0.21/min. 6 landmarks/hr. 0.12/min.	70 70 70

NOTES FOR SUMMARY TABLE XI-2 ON OBSERVING SCHEMES

- (1) This table is based on observing schemes described in this report, which are intended only to supply examples of possible schemes that cover all circumstances reasonably well. There is no intention of claiming that this set exhausts all possibilities; experience gained from simulation or on an actual flight will probably make it possible to improve on this set. One of the principal purposes of this table is to exhibit trade-offs between the different schemes -- in accuracy, number of landmarks that might be observed in the time allowed, etc.
- (2) Accuracies are based on an assumed accuracy of 20 arc-sec ($1:10^4$) for the measurement of the angle between a landmark and a reference star. If the actual r.m.s. turns out to be θ'' , all estimates in this column must be multiplied by the factor $\theta/20$. Estimated errors refer to landmark position relative to CSM position.
- (3) Efficiency is defined as the total weight of the observations accumulated per minute of operations, allowing 2 minutes to pick up a fresh reference star, 2 minutes to pick up a fresh landmark in a different direction from the previous one, 1 minute to pick up a landmark in the same direction as the previous one, and 0.5 minute to repeat an observation on the same landmark (with the same reference star) as the previous observation. Unit weight corresponds to a single optimum sighting with assumed uncertainty of 15 m.
- (4) These numbers correspond to the maximum assumption, that the total time that the CSM is over sunlit regions is devoted entirely to SXT sightings. This is, of course, unrealistic; so these numbers should be multiplied by a factor (< 1) corresponding to the fraction of this time that the astronaut's other duties will allow him to devote to making sightings. On the other hand, the numbers can be increased somewhat, on the assumption that it will be possible to make some sightings of the sunlit region when the CSM is a little way into the shadow.
- (5) Numbers indicating the limits of the range of applicability of each scheme are not to be taken as inflexible boundaries. (See Note 9.)
- (6) Notation $6 \times 1^*$ means "6 sightings on a landmark, using a single reference star," $6 \times 2^*$ means "6 sightings on a landmark using one star, and 6 more using another," etc.

- (7) The degree of anisotropy noted is influenced by the choice of geometry, etc. The numbers noted correspond in general to the most nearly isotropic case, considering the number of observations and reference stars.
- (8) Coordinates A and B are respectively the altitude and bearing of the error axis in question, as seen from the landmark. $B = 0^\circ$ is the direction along a parallel to the subsatellite track, $B = +90^\circ$ is perpendicular away from the track on the starboard side, etc.
- (9) Modifications 1 and 2 of Scheme "B" are included to show that this scheme can be extended into the domain of "A" (nearer the track) and "C" (farther from the track). The errors for some of the entries under Mod. 1 are intended to indicate a trend toward deteriorated results as one tries to apply "B" further and further outside its intended range.
- (10) The example for Scheme "B", Modification 2, was calculated with $r_{\min} = 300$ km, to make it directly comparable with the first entry under Scheme "C".
- (11) It is highly doubtful whether sightings can be made clear to the horizon, except possibly on conspicuously high landmarks standing out on the skyline.
- (12) At $r_{\min} = 300$ km, a landmark will drift a total of 140° in relative bearing while it is in view, which is too great a reach for the SXT from a single reference star. To stay within 57° of a star, the range in bearing must be reduced. The estimate of $0.30/\text{min}$ for the maximum efficiency is derived from the perhaps somewhat optimistic assumption that it will still be possible to get in 20 sightings (with now somewhat higher weight, since they are confined to the inner 115° of the drift arc) in a time which may be reduced to as little as 9 minutes.
- (13) For $r_{\min} = 525$ km, the number of observations has been reduced to 16, on the assumption that it will not be possible to pick up most landmarks farther away than 600 km, which has the effect of reducing the time available for making sightings.

C. ANALYSIS OF EQUIPMENT AND OBSERVING TECHNIQUES

In view of the conceptual feasibility of landmark positioning by means of SXT observations, methods for making observations for selenodetic purposes have been studied. Photographing through the SXT, as outlined below, appears to be the best means of observing and recording observations for later reduction.

1. Photographic Methods for the SXT Observations

Two methods for obtaining photographic recordings through the SXT were investigated: (1) single line-of-sight photography and (2) dual line-of-sight photography. These methods are outlined in Table XI-3 showing the operations with the SXT and Scanning Telescope (SCT) required to make a single observation.

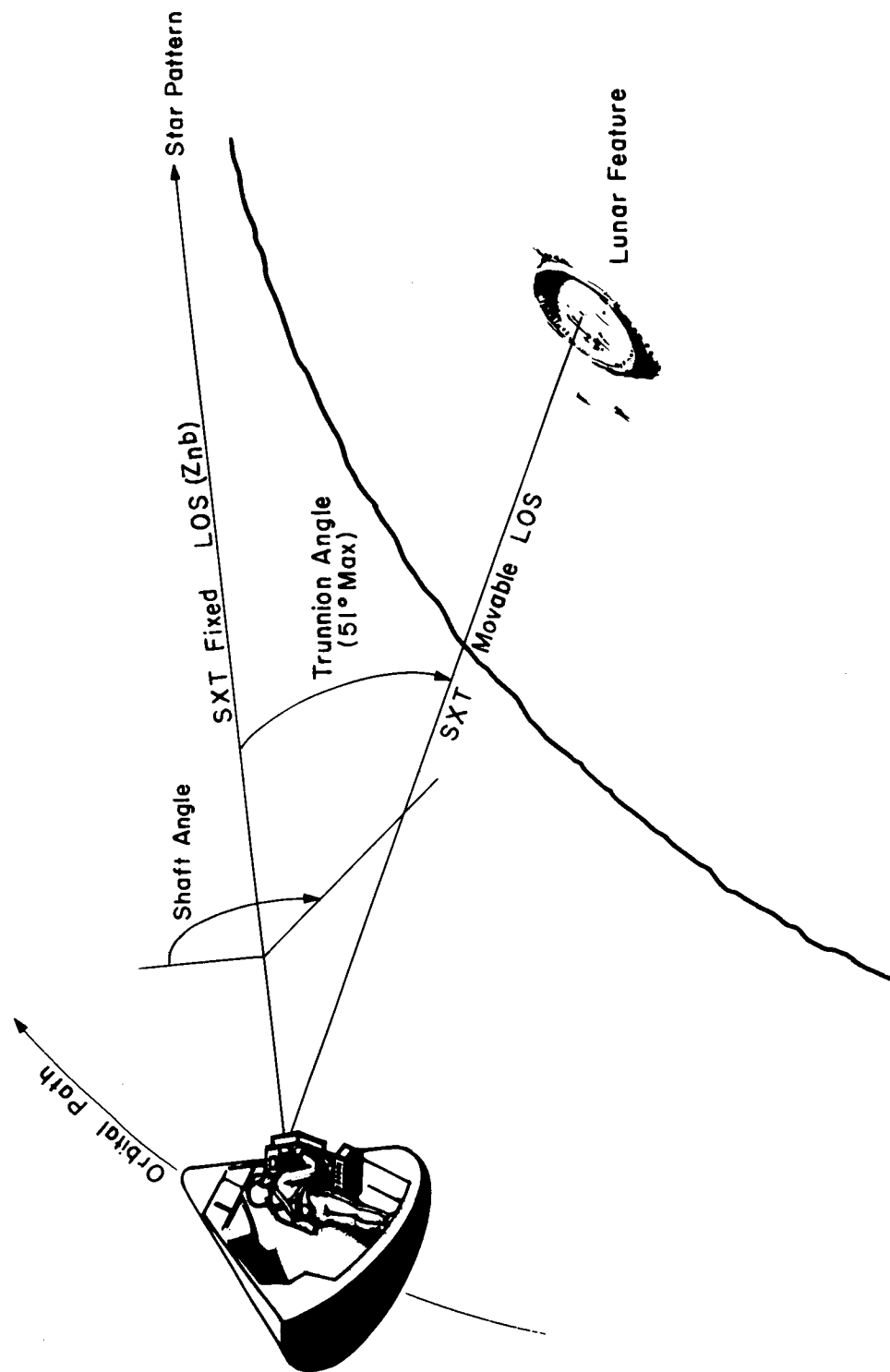
For single line-of-sight (LOS) photography it would be necessary to use the Inertial Measurement Unit (IMU) to define the orientation of the SXT lines-of-sight (trunnion and shaft angles). SXT angles can be recorded within about 10 arc-seconds; the IMU alignment, however, is limited to a precision of about 1 mr (3.44 arc-minutes) which would in turn severely limit the accuracy that can be obtained with SXT sightings. Because of this restriction, single LOS photographs are not recommended for selenodetic purposes.

With the dual LOS photographic method, orientation of the fixed SXT LOS would be established from the recorded star field and the angle between the two LOS would be obtained from the SXT readout, plus a small correction from measurement of the offset star-to-landmark on the photograph. Thus the IMU would not be required for orientation reference, although it would be useful for setting the fixed LOS on a selected star. Application of the dual LOS method would require that the SXT lines-of-sight be reversed from their normal use in midcourse navigation, as shown in Figure XI-12, as the movable LOS (star LOS) is used for landmark photography and the fixed LOS is used

TABLE XI-3

TECHNIQUES CONSIDERED FOR OBTAINING PHOTOGRAPHIC RECORDINGS OF SXT SIGHTINGS

<u>METHOD</u>	<u>PROCEDURES FOR USING SXT & SCT</u>	<u>COMMENTS</u>
SXT dual line-of-sight photography of lunar landmark and star field.	<p>Mode 1 - Attitude of CSM is changed by astronaut to bring <u>SXT fixed LOS</u> to desired star field. SCT in 0° mode is used as aid for selection of star field. SCT in slave mode drives SXT movable LOS to target. IMU not required. Obtain photo of landmark and <u>superimposed star field</u>. Record SXT angles and time of photo observations.</p> <p>Mode 2 - IMU is fine-aligned. CSM attitude controlled by G&N system to drive SXT fixed LOS to desired star field. SCT is used in slave mode to drive SXT movable LOS to lunar landmark. Obtain photo of landmark and superimposed star field and record SXT angles and time of photo recording.</p> <p>Mode 3 - SXT fixed LOS is on random star field, and <u>SXT movable LOS</u> on lunar landmark. SCT in slave mode drives SXT movable LOS to target. IMU not required. Obtain photo of landmark and <u>superimposed star field</u>. Record SXT angles and time of photo observations.</p>	<p>Preferred - requires <u>minimum CSM electrical power</u> and attitude control fuel.</p> <p>Preferred - minimizes <u>astronaut workload</u>.</p> <p>Random star field inadequate for photography, because there will generally not be enough bright stars in a random field.</p>
SXT single line-of-sight photography of lunar landmark.	<p>IMU is fine-aligned. SCT in slave mode drives SXT movable LOS to lunar landmark. Record time and SXT angles with respect to IMU axes when photo recording is made.</p>	<p>Low precision - depends on IMU alignment 1 mr. (Not recommended)</p>



SXT DUAL LOS PHOTO OPERATIONS

FIGURE XI - 12

for photographing the star field. (This aspect will be considered in a later discussion.)

As described in Table XI-3, two preferred modes of SXT dual-LOS photography are envisioned. These modes differ only in the workload imposed on the astronaut and in the demands for CSM electrical power and attitude control propellant.

Mode 1: Attitude control action is similar to that employed in the midcourse navigation measurement. IMU is off. The astronaut uses the minimum impulse controller to position a desirable star field within the SXT fixed LOS field of view. When the drift rate is sufficiently reduced, the astronaut points the SXT movable LOS, so that the lunar feature is within the field of view. A photograph is taken, and a mark command is simultaneously made to record time of exposure, SXT trunnion angle, and SXT shaft angle. This record provides the largest component of angle landmark-CSM-star; the photograph provides the small (fine) component.

Mode 2: The attitude control action is similar to that employed in an orbital navigation measurement. IMU is operating and aligned, but is used only for attitude control. A desirable star pattern is centered in the SXT fixed LOS field of view and is automatically maintained within the field of view by the stabilization and control system. The astronaut directs the SXT movable LOS so that the lunar feature is within the field of view. A photograph is taken, and a mark command is simultaneously made to record time of exposure, SXT trunnion angle, and SXT shaft angle. (Details as before.)

If it is found through appropriate simulation tests that the CSM astronaut is able to employ Mode 1 successfully, there will be no special demands on the CSM electrical power and attitude control propellant for dual-LOS photographing operations. If, however, it develops that

the astronaut must employ Mode 2, the mission requirements will dictate how many SXT dual-LOS photographs can be taken as limited by the power and fuel budget. It is noted that in both modes the astronaut employs the SCT as an aid to center the SXT fixed LOS on the star field; this is similar to midcourse navigation where the SXT fixed LOS is centered on a landmark. The Slave Telescope Switch in the 0° position will align the SCT along the SXT fixed LOS enabling the astronaut to select the star pattern.

It would be advantageous if the astronaut could neglect the exact positioning of the SXT fixed LOS on the star field, as considered in Mode 3 (see Table XI-3). In this case, he would only be required to ensure that the SXT fixed LOS clears the lunar horizon. However, the SXT 1.8° field of view covers only 2.54 square degrees, so chances are that a random positioning of the SXT would provide only one star greater than 7th magnitude within its field of view. It is not possible to photograph stars of this high a magnitude through the SXT and have them superimposed on a photograph of a lunar feature, because it is necessary to use a fast exposure of the order of 0.01 second for the landmark to limit its image smear in the photograph. With this exposure time, it would be necessary to acquire at least a 4th magnitude star in the SXT field of view to obtain a successful star exposure (see Part B.2 below). Therefore, a random star field would not be useful and the astronaut would have to select a desirable star pattern, as described in the preferred modes of operation, Modes 1 and 2.

While in lunar orbit, the high angular rate of a lunar feature with respect to the CSM makes it necessary for the astronaut to use the SCT to position the feature within the field of the SXT movable LOS. With the Slave Telescope Switch in the star line position, the astronaut centers the lunar feature in the SCT field of view. This action will bring the lunar feature within the SXT field of view. The astronaut can center the feature in the SCT to within 1 milliradian. At 120 nm

slant range, this SCT centering error amounts to 0.12 nm on the lunar surface, while the SXT 1.8° field of view encompasses 3.8 miles.

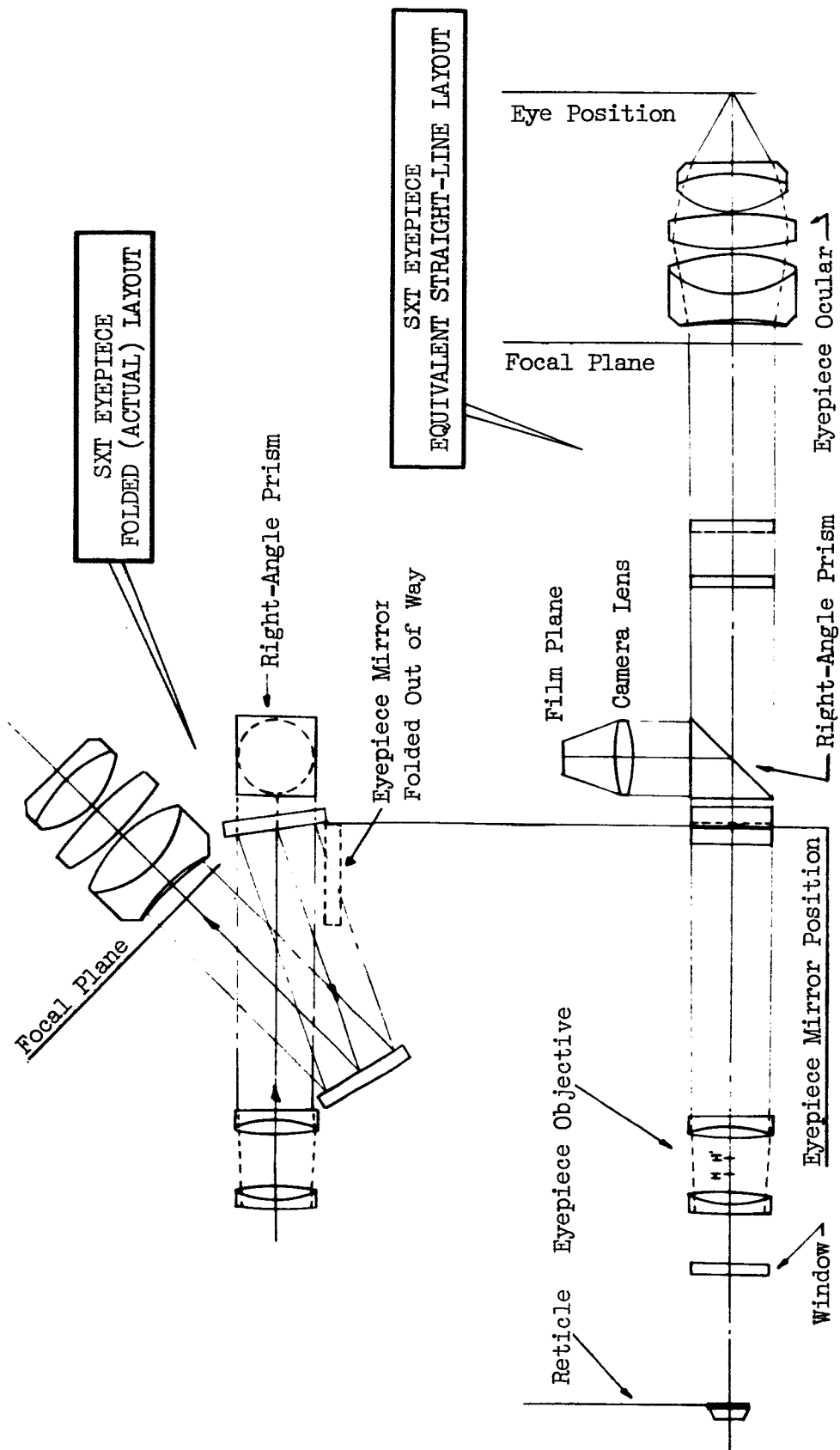
2. Photographic Requirements for SXT Dual LOS Method

At present, the SXT "star" LOS (articulated) has a transmittance of about 20% and the SXT "landmark" LOS (spacecraft fixed) has a transmittance of about 6%. It is assumed that the light paths can be reversed for dual LOS photography, either temporarily or permanently, so that the transmittance of the fixed LOS will be 20%. With this transmittance and an exposure time of 0.01 second, it should be possible to photograph 4th magnitude stars if fast-speed, non radiation-resistant film can be used within the CSM. For example, the estimated integrated exposure energy required to record a 4th magnitude star through the SXT is .00224 meter-candle-second. This exposure should produce a satisfactory density on Kodak Royal-X Pan or Kodak Spectroscopic Type ID₂ films. It is recognized that the actual value of the optimum exposure, with the complete SXT-camera-film combination will have to be determined by experiment. However, at this time, it appears that there should be no difficulty in obtaining a suitable superimposed exposure of a selected star (4th magnitude or higher) and a lunar landmark with existing extreme contrast films, such as the multilayer film developed by Edgerton, Germeshausen and Gries.

As noted earlier, in order to obtain photographs through the SXT it will be necessary to reverse the roles of the lines-of-sight of the SXT. This could be accomplished by changing the light transmission of the existing beam splitter in the SXT fixed LOS, and interposing snap-in, snap-out attenuating filters in both LOS light paths. In this manner the rays of the lines-of-sight as used in the G&N operation could be temporarily reversed for dual LOS photography.

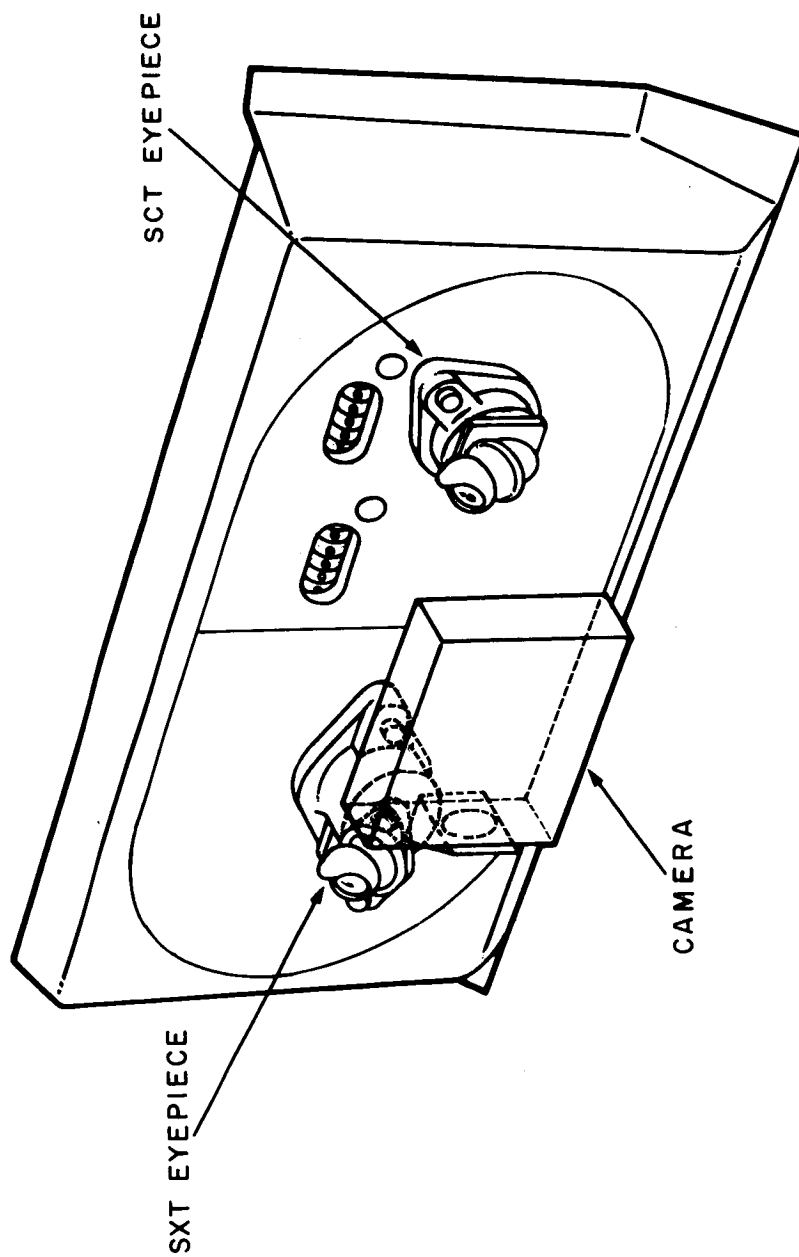
If the SXT had originally been designed so that its fixed LOS were used for star sighting and its movable LOS used for landmark observations, there would be no need to make any modifications for the proposed dual LOS photographic operations, other than installation of a simple recording camera.

A possible location for the SXT camera that will not require major changes in optics-nav-base design is at the SXT Eyepiece and Relay Assembly (Figures XI-13 and XI-14). The mirror closest to the eyepiece ocular can be made to move into or out of the optical path, much as in a typical single lens reflex camera. With the mirror at the "in" position, the SXT can be used normally. At the time of exposure, the mirror snaps out of the optical path, and the image is transmitted to the camera. It is estimated that a 16 mm. film cassette camera would be suitable for photographing through the SXT. A control switch added to the optics panel would be used to actuate the camera and the mark command to record the time of exposure.



POSSIBLE SEXTANT LAYOUT FOR DUAL LOS PHOTOGRAPHIC OPERATIONS

FIGURE XI - 13



SUGGESTED MODIFICATION TO CSM OPTICAL PANEL

FIGURE XI - 14

REFERENCES

1. Brobrovnikoff, N. T., "Natural Environment of the Moon," Ohio State Research Foundation, June 1959. Contract No. AF 33(616)-5914. DDC Doc. No. AD 242 177.
2. The Rand Corporation, "Studies of the Physical Properties of the Moon and Planets" JPL Contract N-33561 (NAS 7-100).
3. Levy, R. J., "Lunar Photometry for Navigation," Geophysical Corporation of America. Technical Report 62-10-A, February 1962. DDC Doc. No. 273 310.
4. Parker, H. M., et al, "Evaluation of the Lunar Photometric Function", Res. Lab. for Eng. Sciences, Univ. of Virginia Report No. AST-4015-101-64U, January 1964.
5. Eimer, M., "Photography of the Moon from Space Probes," JPL Tech. Report No. 32-347, January 15, 1963.
6. Kopal, Z. and Finlay, E. B. "Proceedings of a Conference on Problems of Lunar Topography," held at Bagneres-de-Bigorre in April 1960. Dept. of Astronomy, Univ. of Manchester Tech. Scientific Note No. 1, March 1961, DDC Doc. No. 277 724.
7. Markowitz, W. "The Photographic Zenith Tube and the Dual-Rate Moon-Position Camera," Kuiper and Middlehurst: Telescopes, "Stars and Stellar Systems," Vol. I, Univ. of Chicago Press, 1960.
8. Taback, I., "Lunar Orbiter: Its Mission and Capabilities," paper presented at 10th Annual Meeting of AAS, May 1964.
9. Schmid, H., "Precision Photogrammetry a Tool of Geodesy," Photogrammetric Engineering, Vol. XXVII, No. 5, Dec. 1961.
10. Hallert, B.K., "Investigation of the Geometrical Quality of the Relative and Absolute Orientation Procedures and the Final Results of the Photogrammetric Procedure." U.S. Army Engineer Geodesy, Intelligence and Mapping Research and Development Agency, Research Note No. 6, 24 August 1962.
11. Karara, H. M., "Reduction of the Effect of the Deflection of the Vertical on Photogrammetric Work in Geodetically Unexplored Regions," Photogrammetric Engineering, Vol. XXVI, No. 1, March 1960.
12. Texas Instruments Incorporated, "Survey of Lunar Surface Measurements, Experiments and Geologic Studies," Final Report Contract No. NAS 9-2115, 30 August 1964.
13. Matthias, H., "Autocentering," Surveying and Mapping, Vol. XX, No. 2, June 1960.

APPENDIX A

ANALYSIS OF THE ACCURACY OF LUNAR ORBITAL PHOTOGRAPHY
FOR DETERMINATION OF SELENODETIC POSITIONS

It is assumed that a satellite is traveling around the moon (the theory would be identical for a satellite traveling around any body), and that there is mounted on the satellite a camera whose optical axis is directed fairly accurately toward the center of the moon. At regular intervals, the camera takes photographs of the lunar surface to be used to establish the coordinates of points on the lunar surface ("target points") with respect to a coordinate system that is anchored in the body of the moon.

To aid in this task, the following additional information is assumed to be available:

(1) Estimates of the position of the camera (as a function of time) within a certain accuracy; i. e., the positions and their variances from earth-based observations (radar tracking) and subsequent accurate determination of the orbit. The camera positions thus obtained will be originally in topocentric (tracking station) or geocentric coordinates, which can be converted to coordinates with the moon's center of mass as origin when a definitive circumlunar orbit is desired. The scale of these coordinates will be in meters, based on an assumed value for the velocity of light. One would expect this coordinate system which we might call "barycentric coordinates", to differ systematically from the "map coordinates" of item (2) below.

(2) Estimates of the coordinates of at least a sample of the "target points" (lunar features) and their variances will be known from earth-based selenodetic investigations; these coordinates are based on the apparent figure of the moon, and will be referred to as "map coordinates" where necessary for clarity. The scale of this system is provided by the radius of the moon. In the treatment discussed below, it will be seen that the coordinates of unknown points will have this same scale.

In addition, the following auxiliary information would be helpful, but is assumed not to be available:

(3) Linear distance of the camera from one certain point on the lunar surface, observed by radar within the satellite itself.

(4) Estimates for orientation parameters of the camera (i. e., direction of the optical axis and orientation angle of the camera on the optical axis), (with the associated covariance matrix) for every exposure, obtained for instance from stellar photographs taken with a camera that is rigidly mounted back-to-back with the camera taking the moon photographs, such that the optical axes of both cameras lie in the same line.

It is the purpose of this analysis to estimate as closely as possible the accuracy, expressed in terms of standard deviation, with which coordinates of the lunar "target points" can be determined, specifically in "map coordinates". This accuracy depends, of course, on the entirety of the circumstances of the experiment. Relationships between the parameters of the experiment and the resulting standard deviations will be kept as general as possible, so that results derived can be used either to create experimental conditions such that some predetermined accuracy requirement can be satisfied, or that the accuracy of results for a variety of experiment conditions can be predicted.

A completely rigorous prediction would require the analysis of observations gathered in the actual situation, which is clearly impossible. However, it is essential only that a fair estimation of the expected accuracy will be available, and this can be obtained by investigating an idealized model situation. The problem consists of establishing the normal equations which one could obtain if the unknowns were solved for by the method of least squares, and finding the covariance matrix of the unknowns, by inverting the matrix of the normal equations.

The elements of the matrix of the normal equations consist of product sums, mostly arrived at in such a way that every condition equation

contributes one term to the sum. In the case that the sums contain a sufficient number of terms, originating from condition equations pertaining to a fairly uniform variation of the observing conditions, the sums of products can be replaced by definite integrals over the same products. (If these integrals are difficult to evaluate, their values may be approximated by the procedure employed in a recent paper by Eichhorn and Williams (1963).)

The general treatment of the problem by means of approximation of the sums by integrals produces general formulas, instead of numbers that are valid only in one instance.

Alternate Approaches. It should be emphasized that this investigation cannot point out the best (or most accurate) way to establish coordinates of lunar target points by circumlunar satellite photography in general. It is, however, intuitively clear that coordinates of points will be most accurately determined by sighting (and photography is essentially equivalent to sighting) if the lines of sight intersect at the target in an angle of 90° . This will occur in the presently discussed situation only if the field of view of the camera is at least 90° . It is quite possible to manufacture a camera which will provide the equivalent of a gnomonic projection (or a projection which can be transformed into a gnomonic projection by a known relationship) over a field greater than 90° diameter. However; the standard deviation of a position measured on a photographic plate (glass or other) is for short focal lengths (i. e., under 7000 mm), roughly proportional to the camera's focal length. This means that the weight of a position is proportional to the square of the focal length, and thus that the focal length of the camera should be as long as feasible. If one considers that doubling the focal length will - ceteris paribus - multiply the "value" of the results by a factor of four, and that the relative increase in the cost of the experiment caused by doubling the focal length is probably of much smaller magnitude, at least up to a certain point, it is evident that the economy of the situation demands that the focal length be made as long as other technological circumstances of the experiment will permit.

The linear size of the camera field is one of the limitations imposed on the focal length, as the accuracy of photographic portions becomes very sensitive to deviations of the film from a plane when the size of the field exceeds, say $5^{\circ} \times 5^{\circ}$. Plates used for wide-angle astrometry (fields of $5^{\circ} \times 5^{\circ}$ and above) are usually carefully tested for planeness before use.

A combination of long focal length and wide-angle field necessitates large plates which cannot always be made with the required flatness, and would present formidable handling problems in space. It seems that the maximum practicable plate size, in relation to the smallest acceptable field of view, determines the upper limit of the focal length.

It should be pointed out that much more favorable geometric conditions can be achieved by mounting not just one, but a battery, at least two, of cameras on a single vehicle. If the satellite carries two cameras, whose optical axes make an angle of 90° with each other, and an angle of 45° with the direction to the center of the moon, the same objects on the lunar surface will, in different positions of the camera-carrying satellite, be viewed from directions which differ by 90° and thus be most accurately determined by the intersection of the rays.

The foregoing possibility was not considered in this analysis because only one camera was stipulated. It seems, however, that this stipulation may be standing in the way of the optimum instrumentation which would make a circumlunar satellite selenodetically most effective.

Consider, for instance, the situation in which the photographic instrument consists of two cameras, which are mounted "back to back" and whose optical axes are parallel to each other. In what follows, we shall call such an assembly a "double camera." If both cameras are triggered simultaneously, one will photograph the moon and the other the sky. The photography of the sky will be the same which one would have obtained with another camera situated on the moon at the point where the optical axis of the satellite camera directed towards the moon penetrates the moon's surface, the optical axis of the hypothetical ground-based camera coinciding with the axis of the satellite camera but pointing in the opposite direction. The image of the camera-carrying satellite would then appear on the star photograph at the penetration point of the optical axis of the hypothetical ground-based

camera. Thus a double camera mounted on a satellite will give the same type of information as a surface based camera which photographs a satellite. It follows that those techniques of terrestrial satellite geodesy involving observations of the satellite against the star field could be followed for "satellite selenodesy" without the necessity of a lunar landing, if double cameras (or one of their equivalents) are employed.

If more than one double camera is mounted on the satellite in a rigid assembly, which can be triggered at the same time, one may employ the same reduction techniques which are employed in terrestrial satellite flash triangulation. In such an assembly, only one "sky camera" would be necessary, as the directions of the optical axes of the several moon cameras and the sky camera may be accurately calibrated before the instrument assembly is used on a circumlunar satellite for selenodetic experiments. Accuracy predictions for experiments with more than one moon camera can (cautiously) be made from accuracy predictions for only one lunar camera as treated in this paper, because one may regard the two halves of the field of one camera as two fields produced by separate cameras and one may make certain extrapolations, provided appropriate precautions are observed. In any case, one should consider whether the presently planned arrangement provides an optimum balance of cost and accuracy.

Geometrical Conditions. (See Figure pg. A-33) We arbitrarily anchor within the body of the moon a right handed rectangular Cartesian coordinate system, the "selenocentric system", and orient the axes of this system in such a way that it best fits the coordinates of landmarks derived in one of the various selenodetic investigations that have been carried out by means of earth-based astronomy, i. e., one of the "map coordinates" systems. In such a system, let the coordinates of a point on the lunar surface (a "target point") be represented by the position vector $\underline{X}^T = (X, Y, Z)$, with X toward the mean center of the visible hemisphere (near Mosting A) and Z toward the lunar north pole.

The position vector of the camera (lens center) in the selenocentric system is $\underline{\Xi}^T = (\Xi, H, Z)$. The orientation of the camera is given by (1) the normal unit vector \underline{n} , which is parallel to the optical axis of the camera, which originates at the point where the optical axis penetrates the plate, and which points away from the moon's surface; and (2) an orientation parameter which measures the angle that a certain (arbitrary)

camera-anchored direction in the plane of the plate makes with a zero direction (in other words the position angle of the camera on its own optical axis). If we denote the vector from the center of the lens to the target point by $\underline{x}^T = (x, y, z)$ we have the relationship

$$\underline{x} = \underline{X} - \underline{\Xi}, \quad (1)$$

which is one of the fundamental equations of our problem. In (1), it is, of course, convenient if all vector components are referred to the same system of axes. (We are ignoring for the time being the fact that, although (1) is geometrically exact, in a practical situation the numerical values substituted for a particular \underline{X} may be obtained from a "map system" while those for $\underline{\Xi}$ may come from a "barycentric system" derived from tracking data.)

We now define a camera-anchored coordinate system as follows. The origin is at the point where the optical axis penetrates the plate. The xy-plane is (parallel to) the plane of the plate. The positive z-axis is in the same direction as the normal vector \underline{n} , defined above and the positive x-axis is in the direction of an arbitrarily fixed fiducial mark (which will appear on all plates in exactly the same position with regard to the camera). In what follows, it will sometimes be convenient to assume the origin of this "camera system" at the center of the lens, but with axes parallel to those just described. This can be done without committing a serious error because the distance between the center of the lens and the penetration point of the optical axis is short.

Disregarding for the moment the fact that the origins of the selenodetic and the camera systems are different, we may describe the orientation of the two systems with respect to each other by a set of Eulerian angles ρ , σ , τ , which are defined in such a way that the relationship between the components of any vector \underline{x} in the two systems is given by the equation

$$\underline{x}_c = \mathcal{R} \underline{x}_s, \quad (2)$$

in which \underline{x}_c and \underline{x}_s represent the components of the vector in the camera system and the selenodetic system respectively, and \mathcal{R} is a transformation matrix defined by

$$\mathcal{R} = \mathcal{R}_3(\tau) \mathcal{R}_1(\sigma) \mathcal{R}_3(\rho) \quad (3)$$

in which $\mathcal{R}_1(\sigma)$ indicates the matrix that performs a rotation by the angle σ about the x-axis, and $\mathcal{R}_3(\tau)$ the matrix which performs a rotation by τ about the z-axis, etc. It can be seen that ρ , σ , τ would be the longitude of the node, the inclination, and longitude of the perihelion, if the xy-plane of the camera system were to define a planetary orbit plane (with the x-axis pointing toward perihelion) with respect to, say, an equatorial or ecliptic system (or in our analogous case, the selenocentric system), in which the XY-plane is the fundamental plane.

In what follows, we shall occasionally need the elements of the matrix \mathcal{R} . We thus write

$$\mathcal{R} = \begin{pmatrix} \alpha^T \\ \beta^T \\ \gamma^T \end{pmatrix} = \begin{pmatrix} \cos \tau \cos \rho - \sin \tau \cos \sigma \sin \rho & -\cos \tau \sin \rho - \sin \tau \cos \sigma \cos \rho & \sin \tau \sin \sigma \\ \sin \tau \cos \rho + \cos \tau \cos \sigma \sin \rho & -\sin \tau \sin \rho + \cos \tau \cos \sigma \cos \rho & -\cos \tau \sin \sigma \\ \sin \sigma \sin \rho & \sin \sigma \cos \rho & \cos \sigma \end{pmatrix}$$

where α , β , and γ are a triple of orthonormal vectors whose meaning is clear from the above. From (1) and (2) the following relation exists between the coordinates of a target point in the camera system and the other quantities involved:

$$\underline{x}_c = \mathcal{R}(\underline{X} - \underline{\Xi})_s \quad (5)$$

In order to establish a relationship between the coordinates measured on the plate and the unknown parameters, we establish the relationship between the camera centered coordinates \underline{x}_c of a point and the coordinates

ξ and η , with which the image of the point will be measured on the photographic plates.

For this purpose we make the assumption that the axes of the system in which the coordinates of the images are measured are parallel to the x and y axes of the camera centered system, but that the coordinates of the penetration point of the optical axis in this system are -u and -v respectively. If now ξ and η are measured x and y coordinates respectively of the image of a point whose camera-centered space coordinates are x, y and z, then we have

$$\xi + u = f \frac{x}{z} ; \quad \eta + v = f \frac{y}{z} \quad (6)$$

where f is the focal length of the camera, expressed in the same units as ξ and η . Then with the help of (4), (5) and (6), we set up:

$$\begin{aligned} U \equiv \xi + u - f \frac{\alpha_1(X-\Xi) + \alpha_2(Y-H) + \alpha_3(Z-Z)}{\gamma_1(X-\Xi) + \gamma_2(Y-H) + \gamma_3(Z-Z)} &= 0 \\ V \equiv \eta + v - f \frac{\beta_1(X-\Xi) + \beta_2(Y-H) + \beta_3(Z-Z)}{\gamma_1(X-\Xi) + \gamma_2(Y-H) + \gamma_3(Z-Z)} &= 0 \end{aligned} \quad (7)$$

which are the fundamental equations of condition connecting the measurements ξ and η to the unknowns, namely $u, v, f, \Xi, H, Z, X, Y, Z, \rho, \sigma, \tau$, the latter three occurring implicitly in the α , β , and γ . (The height h is also unknown, but is a function of (Ξ , H, Z) and the radius of the moon, which implicitly sets the scale.)

The "unknowns" or parameters may be classified in three groups:

a. u, v and f will occur in every exposure, and retain their same values for all different plates.

b. Only a selection of X, Y, Z will occur on every plate, but whenever they occur on different plates, they have the same values.

c. The values for Ξ , H, Z, ρ , σ , τ , will be constant for all equations of condition that are derived from the same plate (exposure), but will vary from one plate to the next.

Linearization of the Equations of Condition. If we want to use equations (7) as condition equations in a least squares solution, we must bring them into a form where observations and unknowns are connected with linear relations. This is done by assuming that approximate values for the unknowns and the observations are available from some source, so that the functions may be developed as Taylor series in the corrections to the unknowns, and broken off after the first-order terms. We thus need the derivatives of U and V with respect to the observations and the unknowns.

Carrying out the differentiations, we obtain the following expressions:

$$\frac{\partial(U,V)}{\partial(\xi,\eta)} = \mathcal{J}; \quad \frac{\partial(U,V)}{\partial(u,v)} = \mathcal{J} \quad (8)$$

where \mathcal{J} is the unit matrix, $\begin{pmatrix} 1 & 0 \\ 0 & 1 \end{pmatrix}$

We also see that

$$\frac{\partial U}{\partial f} = -\frac{x}{z}; \quad \frac{\partial V}{\partial f} = -\frac{y}{z} \quad (9)$$

where, of course, x, y, and z must be expressed in terms of the components of \underline{X} , Ξ , and of ρ , σ , τ by equation (5).

Using the vectors $\underline{\alpha}$, $\underline{\beta}$, $\underline{\gamma}$ defined by (4), we may rewrite the system (7):

$$U = \xi + u - f \frac{\underline{\alpha} \cdot (\underline{X} - \underline{\Xi})}{\underline{\gamma} \cdot (\underline{X} - \underline{\Xi})} ; \quad V = \eta + v - f \frac{\underline{\beta} \cdot (\underline{X} - \underline{\Xi})}{\underline{\gamma} \cdot (\underline{X} - \underline{\Xi})} \quad (7a)$$

Differentiating U as expressed in (7a) with respect to $\underline{X} - \underline{\Xi}$, we get

$$\frac{\partial U}{\partial (\underline{X} - \underline{\Xi})} = \frac{f}{z^2} \left\{ \underline{\alpha} [\underline{\gamma} \cdot (\underline{X} - \underline{\Xi})] - \underline{\gamma} [\underline{\alpha} \cdot (\underline{X} - \underline{\Xi})] \right\}$$

from which one sees that

$$\frac{\partial U}{\partial (\underline{X} - \underline{\Xi})} = \frac{f}{z^2} \left\{ (\underline{X} - \underline{\Xi}) \times (\underline{\alpha} \times \underline{\gamma}) \right\}$$

As $\underline{\alpha}$, $\underline{\beta}$, $\underline{\gamma}$ are a triple of orthonormal vectors, so that $\underline{\beta} = \underline{\gamma} \times \underline{\alpha}$, we get in more conventional notation:

$$\begin{pmatrix} \frac{\partial U}{\partial \Xi} \\ \frac{\partial U}{\partial H} \\ \frac{\partial U}{\partial Z} \end{pmatrix} = \frac{f}{z^2} [\underline{\beta} \cdot (\underline{X} - \underline{\Xi})] = - \begin{pmatrix} \frac{\partial U}{\partial X} \\ \frac{\partial U}{\partial Y} \\ \frac{\partial U}{\partial Z} \end{pmatrix} \quad (10)$$

and analogously

$$\begin{pmatrix} \frac{\partial V}{\partial \Xi} \\ \frac{\partial V}{\partial H} \\ \frac{\partial V}{\partial Z} \end{pmatrix} = - \frac{f}{z^2} [\underline{\alpha} \cdot (\underline{X} - \underline{\Xi})] = - \begin{pmatrix} \frac{\partial V}{\partial X} \\ \frac{\partial V}{\partial Y} \\ \frac{\partial V}{\partial Z} \end{pmatrix} \quad (11)$$

In order to obtain the other derivatives we need, we take the derivatives of \mathcal{R} with respect to the orientation variables ρ , σ , τ . It turns out that

$$\frac{\partial \mathcal{R}}{\partial \rho} = \begin{pmatrix} (e_3 \cdot \underline{\alpha})^T \\ (e_3 \cdot \underline{\beta})^T \\ (e_3 \cdot \underline{\gamma})^T \end{pmatrix} \quad (12)$$

where $e_3^T = (0, 0, 1)$,

$$\frac{\partial \mathcal{R}}{\partial \sigma} = \begin{pmatrix} \underline{\gamma}^T \sin \tau \\ \underline{\gamma}^T \cos \tau \\ -(\underline{\alpha}^T \sin \tau + \underline{\beta}^T \cos \tau) \end{pmatrix} \quad (13)$$

and

$$\frac{\partial \mathcal{R}}{\partial \tau} = \begin{pmatrix} \underline{\beta}^T \\ -\underline{\alpha}^T \\ 0 \end{pmatrix} \quad (14)$$

From (7a) we get immediately, using (12)

$$-\frac{z^2}{f} \frac{\partial U}{\partial \rho} = \left[(e_3 \cdot \underline{\alpha}) \cdot (\underline{X} - \underline{\Xi}) \right] \left[\underline{\gamma} \cdot (\underline{X} - \underline{\Xi}) \right] - \left[(e_3 \cdot \underline{\gamma}) (\underline{X} - \underline{\Xi}) \right] \left[\underline{\alpha} \cdot (\underline{X} - \underline{\Xi}) \right]$$

and from this, considering the well known formulas

$$\underline{a} \cdot (\underline{b} \times \underline{c}) = \underline{b} \cdot (\underline{c} \times \underline{a}) = \underline{c} \cdot (\underline{a} \times \underline{b})$$

$$\text{and } (\underline{a} \times \underline{b}) \cdot (\underline{c} \times \underline{d}) = (\underline{a} \cdot \underline{c})(\underline{b} \cdot \underline{d}) - (\underline{a} \cdot \underline{d})(\underline{b} \cdot \underline{c}),$$

we obtain

$$\frac{\partial U}{\partial \rho} = -\frac{f}{z^2} \left[(Z - Z) \gamma - \beta_3 r^2 \right] \quad (15)$$

and quite analogously

$$\frac{\partial V}{\partial \rho} = + \frac{f}{z^2} \left[(Z-Z)X - \alpha_3 r^2 \right] \quad (16)$$

where $r^2 = (X-\Xi)^2 + (Y-H)^2 + (Z-Z)^2$ (17)

Similarly, we get by differentiating (7a) with respect to σ and using (13)

$$- \frac{z^2}{f} \frac{\partial U}{\partial \sigma} = \left\{ \left[\gamma \cdot (X-\Xi) \right]^2 \sin \tau + \left[(\alpha \sin \tau + \beta \cos \tau) \cdot (X-\Xi) \right] \left[\alpha \cdot (X-\Xi) \right] \right\}$$

from which we obtain (considering that $\alpha^T \cos \tau - \beta^T \sin \tau = (\cos \rho, \sin \rho, 0)$)

$$\frac{\partial U}{\partial \sigma} = - \frac{f}{z^2} \left\{ r^2 \sin \tau + \gamma \left[(X-\Xi) \cos \rho + (Y-H) \sin \rho \right] \right\} \quad (18)$$

and analogously

$$\frac{\partial V}{\partial \sigma} = - \frac{f}{z^2} \left\{ r^2 \cos \tau - \chi \left[(X-\Xi) \cos \rho + (Y-H) \sin \rho \right] \right\} \quad (19)$$

Finally we get from (7a), considering (14) and (6)

$$\frac{\partial U}{\partial \tau} = -(\eta + v), \quad \frac{\partial V}{\partial \tau} = +(\xi + u) \quad (20)$$

Specialization of the Derivatives. We now have all the derivatives necessary to set up the equations of condition from which the normal equations can be established. To make general accuracy predictions from the equations as they now stand is extremely difficult due to the unwieldiness of the expressions. In order to obtain expressions that are easier to

handle and still provide a realistic model for the actual situation, the following assumptions are made:

If the satellite revolves around the moon strictly in the equatorial or XY plane, we may write

$$\begin{aligned}\Xi &= (R + h) \cos \phi \\ H &= (R + h) \sin \phi \\ Z &= 0\end{aligned}\tag{21}$$

where R is the radius of the moon, h the height of the vehicle above the moon's surface, and ϕ is an angle describing the position of the satellite (selenocentric longitude, measured eastward from the x axis toward the y axis). We also assume that the attitude of the vehicle can be controlled well enough so that the xz -plane always coincides with the XY -plane, and that the negative z -axis (i. e., the optical axis of the vehicle) always points towards the center of the moon. This means that

$$\rho = 90^\circ + \phi, \quad \sigma = 90^\circ, \quad \tau = 0\tag{22}$$

Furthermore, let us assume that the photographic plate is sufficiently well aligned that we may put $u = o = v$. If we evaluate the derivatives given by (8)-(20) under these assumptions, we obtain, after some calculation:

$$\frac{\partial U}{\partial f} = -\frac{\xi}{f}, \quad \frac{\partial V}{\partial f} = -\frac{\eta}{f}\tag{23}$$

$$\begin{pmatrix} \frac{\partial U}{\partial \Xi} \\ \frac{\partial U}{\partial H} \\ \frac{\partial U}{\partial Z} \end{pmatrix} = - \begin{pmatrix} \frac{\partial U}{\partial X} \\ \frac{\partial U}{\partial Y} \\ \frac{\partial U}{\partial Z} \end{pmatrix} = -\frac{1}{Z} \begin{pmatrix} \xi \cos \phi + f \sin \phi \\ \xi \sin \phi - f \cos \phi \\ 0 \end{pmatrix}\tag{24}$$

$$\begin{pmatrix} \frac{\partial V}{\partial \Xi} \\ \frac{\partial V}{\partial H} \\ \frac{\partial V}{\partial Z} \end{pmatrix} = - \begin{pmatrix} \frac{\partial V}{\partial X} \\ \frac{\partial V}{\partial Y} \\ \frac{\partial V}{\partial Z} \end{pmatrix} = - \frac{1}{Z} \begin{pmatrix} \eta \cos \phi \\ \eta \sin \phi \\ f \end{pmatrix} \quad (25)$$

$$\begin{aligned} \frac{\partial U}{\partial \rho} &= \frac{1}{f} (\xi^2 + f^2) & \frac{\partial V}{\partial \rho} &= \frac{1}{f} \xi \eta \\ \frac{\partial U}{\partial \sigma} &= -\frac{1}{f} \xi \eta & \frac{\partial V}{\partial \sigma} &= -\frac{1}{f} (\eta^2 + f^2) \\ \frac{\partial U}{\partial \tau} &= -\eta & \frac{\partial V}{\partial \tau} &= \xi \end{aligned} \quad (26)$$

while (8) remains unchanged.

In order properly to simulate the actual situation, we must now express the factor $-1/z$ by the measured coordinates ξ and η and the parameters R and h (which are constant for a particular frame), and f , which is constant for the whole survey.

From the geometry of the situation we have

$$\left[z + (h + R) \right]^2 + x^2 + y^2 = R^2$$

from which we obtain, considering equation (6) and our assumptions concerning u and v ,

$$z = - \frac{1}{1 + \frac{\xi^2 + \eta^2}{f^2}} \left(h + R - \sqrt{R^2 - h(h + 2R) \frac{\xi^2 + \eta^2}{f^2}} \right) \quad (27)$$

Although (27) is rigorous, it is not very useful because it contains ξ and η irrationally, thus immensely complicating the investigation. There are, however, two fairly small quantities that can be used to develop expression (27) as a power series, one is h/R and the other $\frac{\xi^2 + \eta^2}{f^2}$. The former will be small if the height of the orbiting vehicle is small compared to the moon's radius, and the latter will be smaller than one for all cameras where the diagonal of the field spans less than 90° . For the planned experiment, where h and the field of view are stipulated to be in the order of 50 km and less than 60° respectively, h/R is about $1/35$ and $\frac{\xi^2 + \eta^2}{f^2}$ cannot exceed $4/25$, so they are certainly small enough. The expansion of (27) yields, up to the fourth order, for $1/z$

$$\frac{1}{z} = -\frac{1}{h} \left[1 - \frac{1}{2} \frac{h}{R} \frac{\xi^2 + \eta^2}{f^2} - \frac{1}{4} \left(\frac{h}{R} \right)^2 \left(\frac{\xi^2 + \eta^2}{f^2} \right)^2 - \dots \right]. \quad (27a)$$

In what follows, we shall carry the development only to the second order and thus write

$$\frac{1}{z} = -\frac{1}{h} (1 + \Delta) \quad \text{with} \quad \Delta = -\frac{1}{2} \frac{h}{R} \frac{\xi^2 + \eta^2}{f^2} \quad (27b)$$

(i. e., $|\Delta| \leq \frac{1}{4} \delta$ in (29) below),

so that we now have

$$\begin{pmatrix} \frac{\partial U}{\partial \bar{x}} \\ \frac{\partial U}{\partial H} \\ \frac{\partial U}{\partial \bar{z}} \end{pmatrix} = - \begin{pmatrix} \frac{\partial U}{\partial X} \\ \frac{\partial U}{\partial Y} \\ \frac{\partial U}{\partial \bar{z}} \end{pmatrix} = \frac{1}{h} (1 + \Delta) \begin{pmatrix} \xi \cos \phi + f \sin \phi \\ \xi \sin \phi - f \cos \phi \\ 0 \end{pmatrix} \quad (24a)$$

and

$$\begin{pmatrix} \frac{\partial V}{\partial \Xi} \\ \frac{\partial V}{\partial H} \\ \frac{\partial V}{\partial Z} \end{pmatrix} = - \begin{pmatrix} \frac{\partial V}{\partial X} \\ \frac{\partial V}{\partial Y} \\ \frac{\partial V}{\partial Z} \end{pmatrix} = \frac{1}{h}(1+\Delta) \begin{pmatrix} \eta \cos \phi \\ \eta \sin \phi \\ f \end{pmatrix} \quad (25a)$$

The Normal Equations. The coefficients of the normal equations are the sums of the products of the derivatives. For that part of the normal equations that originates from considering the various points on the lunar surface whose images will appear and be measured on a plate, these sums can be approximated by integrals, as pointed out by Eichhorn and Williams (1963). There it was shown that

$$\sum x^i y^k = \begin{cases} \frac{n \cdot a^{i+k}}{(i+1)(k+1)2^{i+k}} & \text{if } i \text{ and } k \text{ are both even} \\ 0 & \text{if either } i \text{ or } k \text{ is odd (or both odd)} \end{cases}$$

on a plate of the format $a \times a$, where n is the number of points on a plate. For any plate with n stars on it, the product sums will be given approximately by the following expressions (in which we introduce the abbreviation

$$\delta = \frac{a^2}{f^2} \frac{h}{R} \approx 1.9 \times 10^{-3} \quad (29)$$

and neglect δ^2):

$$\begin{aligned} \sum \left(\frac{\partial U}{\partial \Xi} \right)^2 &= \frac{n}{h^2} \left[\cos^2 \phi \frac{a^2}{12} \left(1 - \frac{7}{30} \delta \right) + \sin^2 \phi f^2 \left(1 - \frac{1}{6} \delta \right) \right] \\ \sum \frac{\partial U}{\partial \Xi} \frac{\partial U}{\partial H} &= \frac{n}{h^2} \sin \phi \cos \phi \left[\frac{a^2}{12} \left(1 - \frac{7}{30} \delta \right) - f^2 \left(1 - \frac{1}{6} \delta \right) \right] \\ \sum \frac{\partial U}{\partial \Xi} \frac{\partial U}{\partial \rho} &= \frac{n}{h} \sin \phi \left[\frac{a^2}{12} \left(1 - \frac{7}{30} \delta \right) + f^2 \left(1 - \frac{1}{12} \delta \right) \right] \end{aligned} \quad (30)$$

$$\sum \frac{\partial U}{\partial \Xi} \frac{\partial U}{\partial u} = \frac{n f}{h} \sin \phi \left(1 - \frac{1}{12} \delta\right)$$

$$\sum \frac{\partial U}{\partial \Xi} \frac{\partial U}{\partial f} = -\frac{n}{f h} \cos \phi \frac{a^2}{12} \left(1 - \frac{7}{60} \delta\right)$$

$$\sum \left(\frac{\partial V}{\partial \Xi} \right)^2 = \frac{n}{h^2} \cos^2 \phi \frac{a^2}{12} \left(1 - \frac{7}{30} \delta\right)$$

$$\sum \frac{\partial V}{\partial \Xi} \frac{\partial V}{\partial H} = \frac{n}{h^2} \sin \phi \cos \phi \frac{a^2}{12} \left(1 - \frac{7}{30} \delta\right)$$

$$\sum \frac{\partial V}{\partial \Xi} \frac{\partial V}{\partial f} = -\frac{n}{f h} \cos \phi \frac{a^2}{12} \left(1 - \frac{7}{60} \delta\right)$$

$$\sum \left(\frac{\partial U}{\partial H} \right)^2 = \frac{n}{h^2} \left[\sin^2 \phi \frac{a^2}{12} \left(1 - \frac{7}{30} \delta\right) + \cos^2 \phi \cdot f^2 \left(1 - \frac{1}{6} \delta\right) \right]$$

$$\sum \frac{\partial U}{\partial H} \frac{\partial U}{\partial \rho} = -\frac{n}{h} \cos \phi \left[\frac{a^2}{12} \left(1 - \frac{7}{60} \delta\right) + f^2 \left(1 - \frac{1}{12} \delta\right) \right]$$

$$\sum \frac{\partial U}{\partial H} \frac{\partial U}{\partial u} = -\frac{n f}{h} \cos \phi \left(1 - \frac{1}{12} \delta\right)$$

$$\sum \frac{\partial U}{\partial H} \frac{\partial U}{\partial f} = -\frac{n}{h f} \sin \phi \frac{a^2}{12} \left(1 - \frac{7}{60} \delta\right)$$

(30)

$$\sum \left(\frac{\partial V}{\partial H} \right)^2 = \frac{n}{h^2} \sin^2 \phi \frac{a^2}{12} \left(1 - \frac{7}{30} \delta\right)$$

$$\sum \frac{\partial V}{\partial H} \frac{\partial V}{\partial f} = -\frac{n}{h f} \sin \phi \frac{a^2}{12} \left(1 - \frac{7}{30} \delta\right)$$

$$\sum \left(\frac{\partial V}{\partial Z} \right)^2 = \frac{n f^2}{h^2} \left(1 - \frac{1}{6} \delta\right)$$

$$\sum \frac{\partial V}{\partial Z} \frac{\partial V}{\partial \sigma} = -\frac{n}{h} \left[\frac{a^2}{12} \left(1 - \frac{7}{60} \delta\right) + f^2 \left(1 - \frac{1}{12} \delta\right) \right]$$

$$\sum \frac{\partial V}{\partial Z} \frac{\partial V}{\partial u} = \frac{n f}{h} \left(1 - \frac{1}{12} \delta\right)$$

$$\sum \left(\frac{\partial U}{\partial \rho} \right)^2 = n \left(\frac{a^4}{80 f^2} + \frac{a^2}{6} + f^2 \right)$$

$$\sum \frac{\partial U}{\partial \rho} \frac{\partial U}{\partial u} = \frac{n}{f} \left(\frac{a^2}{12} + f^2 \right)$$

$$\sum \left(\frac{\partial V}{\partial \rho} \right)^2 = \frac{n}{f^2} \frac{a^4}{144}$$

$$\begin{aligned}
\sum \left(\frac{\partial U}{\partial \sigma} \right)^2 &= \frac{n}{f^2} \frac{a^4}{144} \\
\sum \left(\frac{\partial V}{\partial \sigma} \right)^2 &= n \left(\frac{a^4}{80} + \frac{a^2}{6} + f^2 \right) \\
\sum \frac{\partial V}{\partial \sigma} \frac{\partial V}{\partial v} &= -\frac{n}{f} \left(\frac{a^2}{12} + f^2 \right) \\
\sum \left(\frac{\partial U}{\partial \tau} \right)^2 &= n \frac{a^2}{12} \\
\sum \left(\frac{\partial V}{\partial \tau} \right)^2 &= n \frac{a^2}{12} \\
\sum \left(\frac{\partial U}{\partial u} \right)^2 &= n = \sum \left(\frac{\partial V}{\partial v} \right)^2 \\
\sum \left(\frac{\partial U}{\partial f} \right)^2 &= \frac{n a^2}{12 f^2} = \sum \left(\frac{\partial V}{\partial f} \right)^2
\end{aligned} \tag{30}$$

Except for the product sums involving derivatives with respect to the X, Y, Z, which require special treatment, those product sums not listed are zero.

$$\text{If we denote } \frac{1}{h} \sum \frac{\partial U}{\partial \lambda} \frac{\partial U}{\partial \mu} + \frac{\partial V}{\partial \lambda} \frac{\partial V}{\partial \mu} \equiv [\lambda, \mu] \quad \text{for short}$$

we get from (30) the following expressions for these approximated product sums which are different from zero:

$$\begin{aligned}
[\Xi, \Xi] &= \frac{1}{h^2} \left[\frac{h^2}{6} \cos^2 \phi \left(1 - \frac{7}{30} \delta \right) + f^2 \sin^2 \phi \left(1 - \frac{1}{6} \delta \right) \right] \\
[\Xi, H] &= \frac{1}{h} \sin \phi \cos \phi \left[\frac{h^2}{6} \left(1 - \frac{7}{30} \delta \right) - f^2 \left(1 - \frac{1}{6} \delta \right) \right] \\
[\Xi, \rho] &= \frac{1}{h} \sin \phi \left[\frac{a^2}{12} \left(1 - \frac{7}{60} \delta \right) + f^2 \left(1 - \frac{1}{12} \delta \right) \right] \\
[\Xi, u] &= \frac{f}{h} \sin \phi \left(1 - \frac{1}{12} \delta \right) \\
[\Xi, f] &= -\frac{\cos \phi}{h f} \frac{a^2}{6} \left(1 - \frac{7}{30} \delta \right)
\end{aligned} \tag{31}$$

$$\begin{aligned}
[H, H] &= \frac{1}{h^2} \left[\frac{a^2}{6} \sin^2 \phi \left(1 - \frac{7}{30} \delta \right) + f^2 \cos^2 \phi \left(1 - \frac{1}{6} \delta \right) \right] \\
[H, \rho] &= -\frac{1}{h} \sin \phi \left[\frac{a^2}{12} \left(1 - \frac{7}{60} \delta \right) + f^2 \left(1 - \frac{1}{12} \delta \right) \right] \\
[H, u] &= -\frac{f}{h} \cos \phi \left(1 - \frac{1}{12} \delta \right) \\
[H, f] &= -\frac{\sin \phi}{hf} \frac{a^2}{6} \left(1 - \frac{7}{60} \delta \right) \\
[Z, Z] &= \frac{f^2}{h^2} \left(1 - \frac{1}{6} \delta \right) \\
[Z, \sigma] &= -\frac{1}{h} \left[\frac{a^2}{12} \left(1 - \frac{7}{60} \delta \right) + f^2 \left(1 - \frac{1}{12} \delta \right) \right] \\
[Z, v] &= \frac{f}{h} \left(1 - \frac{1}{12} \delta \right) \\
[\rho, \rho] &= \frac{7a^4}{360f^2} + \frac{a^2}{6} + f^2 = [\sigma, \sigma] \\
[\rho, u] &= \frac{1}{f} \left(\frac{a^2}{12} + f^2 \right) = -[\sigma, v] \\
[\tau, \tau] &= \frac{a^2}{6} \\
[u, u] &= 1 = [v, v] \\
[f, f] &= \frac{a^2}{6f^2}
\end{aligned} \tag{31}$$

The Covariance Matrix of the Parameters. In order to predict the expected accuracy (expressed, say, by the variance or the standard deviation) of the lunar map coordinates of the "target points" derived from the Orbiter images, the covariance matrix of the quantities of which the coordinates are a function must be known. These quantities are primarily the measurements ξ and η , while the parameters are, of course, Ξ , H , Z , ρ , σ , τ , u , v , f . The relationship between the coordinates X , Y , Z and the measurements and parameters is given by (5) and (6). As was pointed out in the above quoted paper by Eichhorn and Williams (1963), the variance

of a quantity which is derived from measurements in the way these seleno-detic coordinates are obtained may be regarded as composed of the "random" variance, due to the random errors in the measurements ξ and η , and the variance of the systematic error, due to the unavoidable inaccuracies of the parameters. (The analogous expression in the paper referred to is the "plate constant variance"). It will be shown in what follows that the most important part of the "systematic variance" (i. e., the variance of the systematic errors) can be kept below the accidental variance. (Note that the expressions "accidental error", "accidental variance", etc. retain the rather specialized meaning of "being associated with the accidental error of measurement" throughout this discussion.)

We will from now on assume that the parameters u , v and f are identical for all frames, and that only the camera position \bar{x} , H , Z , and the camera orientation ρ , σ , τ are the "frame constants" (corresponding to the plate constants in conventional photographic astrometry). It is quite plausible that the parameters u , v , and f should be "problem constants" and not frame constants, if one considers that the relative position of frame and camera can very accurately be kept in check by (say) employing fiducial marks. As the camera in space operates as if it were not subjected to gravity, and as there is no "handling" in contrast to terrestrial applications, there is little reason to assume that u and v will change from one frame to the next.

The same reasoning cannot quite be applied to the focal length, because it changes with the temperature. But then, frames will be taken only of parts of the moon's surface which are exposed to sunlight; while taking frames, the camera will thus always be exposed to the sun and under these circumstances, the apparatus will have the same temperature (and therefore the same focal length) for all frames. And even if the focal length varies from one frame to the next, a two-parametric formula (containing a temperature term) should satisfactorily represent the focal length in all frames.

The covariance matrix of the parameters \bar{x} , H , Z , ρ , σ , τ , u , v , f can now in principle be established in the following way:

From the observations available for every target point, set up the normal equations for these parameters for every frame, and combine them (simply by adding corresponding terms) with the inverse covariance matrix of estimates for the parameters that may be available from outside sources, for instance, vehicle coordinates \bar{x} , H , Z from earth-based observations, and orientation parameters ρ , σ , τ from, say, a double-camera arrangement as previously described.* Thus, every frame would yield a system of normal equations. If the frame constants \bar{x} , H , Z and ρ , σ , τ are eliminated from each of these systems, we obtain from the complete equation system for every frame a reduced system which contains u , v , and f only. The matrix, which is the sum of the matrices whose elements are the coefficients of the reduced systems, is now, except for a constant factor which is the inverse variance of unit weight, the covariance matrix of u , v and f . Thus summation will, of course, in the general case have to be replaced by an integration, the same process that was, in principle, applied to obtain the estimates for the product sums. This information may now be used to get the covariance matrix of a typical set of frame constants and the u , v , f , by going back to the triangularized matrices that were established during the process of eliminating the frame constants from the normal equations.

In principle, this process is easy and clear cut, and involves only direct algebraic operations so that their results, namely the terms of the covariance matrix, can be obtained. In practice, however, the situation

* We are tacitly assuming that \bar{x} , H , Z and X , Y , Z can be rigorously observed in the same system. This assumption is, of course, only approximately true and was made only in order not to let the investigation become unmanageably complicated. For the purpose of actual reductions, the systems in which the camera coordinates and the lunar coordinates are reckoned would have to be connected by a six-parametric transformation, i. e., a zero point shift and a general rotation.

is much less simple. While the terms of the inverse covariance matrix (which are given by and composed of expressions by (31), zeros, and the inverted covariance matrices of the available estimates of the parameters) are relatively simple, the process of elimination and the inversion of the matrix in general involves a formidable number of algebraic operations and leads to expressions of such complexity that they become virtually unmanageable.

The problem is, therefore, to obtain a reliable estimate of the accuracy of the positions without a complete and rigorous inversion of the matrix of the normal equations of the parameters. We shall see in what follows that this is very well possible, provided that the general conditions are such that the expected systematic variance of the positions does not exceed the expected accidental variance, so that the final accuracy of the coordinates is still primarily determined by the accuracy with which the positions of the target points, as recorded on the frames can be measured.

If we assume temporarily that previously obtained estimates for neither the vehicle coordinates Ξ , H , Z , nor the attitude parameters ρ , σ , τ are available, we can try to eliminate the frame constants from the normal equations for every frame. The coefficients of a system of this type are, of course, given by (31), and zeros wherever required.

The elimination can be performed by following the very useful scheme of S. Vasilevskis. In line with the notation used in his paper (which is fairly standard in the classical literature on least squares), we denote by $[\lambda, \mu, 1]$ the appropriate coefficients of the normal equation system from which Ξ has been eliminated, (λ and μ are any two of the remaining parameters); we denote by $[\lambda, \mu, 2]$ the appropriate coefficient of the system from which Ξ and H have been eliminated, and so forth. $[\lambda, \mu, 6]$ would then, of course, be the coefficients of the system from which all the frame constants have been eliminated and in which only the "problem constants" u , v and f remain.

One obtains after a somewhat tedious calculation:

$$[H, H, 1] = \frac{a^2 f^2}{6h^2} \frac{1}{\frac{a^2}{6} \cos^2 \phi (1 + \frac{1}{6} \delta) + f^2 \sin^2 \phi (1 + \frac{7}{30} \delta)}$$

$$[H, \rho, 1] = -\frac{a^2 \cos \phi}{6h} \frac{\frac{a^2}{12} (1 - \frac{7}{30} \delta) + f^2 (1 - \frac{19}{60} \delta)}{\frac{a^2}{6} \cos^2 \phi (1 - \frac{7}{30} \delta) + f^2 \sin^2 \phi (1 - \frac{1}{6} \delta)}$$

$$[H, u, 1] = -\frac{a^2 f \cos \phi}{6h} \frac{1 - \frac{19}{60} \delta}{\frac{a^2}{6} \cos^2 \phi (1 - \frac{7}{30} \delta) + f^2 \sin^2 \phi (1 - \frac{1}{6} \delta)}$$

$$[H, f, 1] = -\frac{\sin \phi}{6h} \frac{a^2 f (1 - \frac{17}{60} \delta)}{\frac{a^2}{6} \cos^2 \phi (1 - \frac{7}{30} \delta) + f^2 \sin^2 \phi (1 - \frac{1}{6} \delta)}$$

$$[Z, Z, 2] = \frac{f^2}{h^2} (1 - \frac{1}{6} \delta) \quad (32)$$

$$[Z, \sigma, 2] = -\frac{1}{h} \left[\frac{a^2}{12} (1 - \frac{7}{60} \delta) + f^2 (1 - \frac{1}{12} \delta) \right]$$

$$[Z, v, 2] = \frac{f}{h} (1 - \frac{1}{12} \delta)$$

$$[\rho, \rho, 3] = \frac{a^2}{20f^2} \left[\frac{a^2}{4} (1 + \frac{1}{27} \delta) + \frac{f^2}{9} \delta \right] = [\sigma, \sigma, 4]$$

$$[\rho, u, 3] = \frac{a^2 \delta}{360f} = -[\sigma, v, 4]$$

$$[\tau, \tau, 5] = \frac{a^2}{6}$$

Those not listed are identically zero, at least up to terms of the order δ . We further find that all coefficients of the system from which the frame constants have been eliminated (i. e., $[\lambda, \mu, b]$) are zero.

The way the calculations were made shows that the problem constants and the vehicle coordinates are linearly dependent, at least up to quantities of the second order (δ is a small quantity of the second order), and that it is therefore impossible to solve the problem, unless a different approach is used or unless estimates for the vehicle coordinates are available. As we are actually assuming the availability of estimates for the vehicle coordinates (affected, of course, by the unknown difference between orbital barycentric coordinates and map coordinates), this result poses no real threat for the feasibility of the project.

For the sake of completeness, we list below some elements of the covariance matrix (divided by n , the number of contributing observations and the variance of unit weight) of the frame constants. λ, μ denotes the element thus described. Those not listed are zero.

$$\begin{aligned} \langle \tau, \tau \rangle &= \frac{6}{a^2} ; \langle \sigma, \sigma \rangle = \langle \rho, \rho \rangle = \frac{20f^2}{a^2} \frac{1}{\frac{a^2}{4}(1 + \frac{1}{27}\delta) + \frac{f^2}{9}\delta} \\ \langle Z, \sigma \rangle &= \langle H, \rho \rangle = \frac{20h}{a^2} \frac{\frac{a^2}{12}(1 + \frac{1}{20}\delta) + f^2(1 + \frac{1}{12}\delta)}{\frac{a^2}{4}(1 + \frac{1}{27}\delta) + \frac{f^2}{9}\delta} \\ \langle Z, Z \rangle &= \frac{h^2}{a^2 f^2} \frac{1}{18} (1 + \frac{1}{8}\delta) \frac{7a^4 + 60a^2 f^2 + 20f^4}{\frac{a^2}{4}(1 + \frac{1}{27}\delta) + \frac{f^2}{9}\delta} \end{aligned} \quad (33)$$

$\langle \Xi, \Xi \rangle$, $\langle H, H \rangle$, $\langle \Xi, H \rangle$ and $\langle \Xi, \rho \rangle$ are also different from zero; these are rather lengthy expressions. Finally, the covariance matrix of the vehicle coordinates was also computed under the assumption that they were calculated from a system which contained no other unknowns beside themselves, especially not the attitude parameters ρ, σ, τ .

We denote the terms thus obtained by a bar. The results are:
 $\{\overline{Z}, \overline{Z}\}$ as before. Non-zero off-diagonal terms exist only for
 $\{\overline{\Xi}, \overline{H}\}$.

$$\begin{aligned}\{\overline{H}, \overline{H}\} &= \frac{6h^2}{a^2 f^2} \left[\frac{a^2}{6} \cos^2 \phi \left(1 - \frac{7}{30} \delta\right) + f^2 \sin^2 \phi \left(1 - \frac{1}{6} \delta\right) \right] \left(1 + \frac{2}{5} \delta\right) \\ \{\overline{\Xi}, \overline{H}\} &= -\frac{6h^2}{a^2 f^2} \sin \phi \cos \phi \left[\frac{a^2}{6} \left(1 - \frac{7}{30} \delta\right) - f^2 \left(1 - \frac{1}{6} \delta\right) \right] \left(1 + \frac{2}{5} \delta\right) \\ \{\overline{\Xi}, \overline{\Xi}\} &= \frac{6h^2}{a^2 f^2} \left[\frac{a^2}{6} \sin^2 \phi \left(1 - \frac{7}{30} \delta\right) + f^2 \cos^2 \phi \left(1 - \frac{1}{6} \delta\right) \right] \left(1 + \frac{2}{5} \delta\right)\end{aligned}\quad (34)$$

From equations (21) it was to be expected that the expressions for $\overline{\Xi}$ and \overline{H} would result from each other; this agreement may be taken as an indication of the correctness of the calculations involved in the setup of the formulas.

The Accuracy of Final Coordinates: Numerical Example. All the difficulties encountered in the general analytic treatment of the problem could, of course, be avoided, if numerical models for various conditions were set up, and the appropriate matrices were inverted on a computer. It may appear at first glance that thereby more reliable values for the expected accuracy of selenodetic coordinates would be obtained. But if this advantage were actually gained, it would be gained only at the not inconsiderable cost of many hours of computer time and at the expense of the generality of the treatment.

In the rest of this paper we shall show, in part by heuristic considerations and in part by using the formulas derived above, how the generality of the investigation may be maintained even if some of the complete rigor has to be sacrificed. But then, this is really no great loss, as the setup of a model covariance matrix is not a rigorous procedure anyway.

It is clear from the outset that the circumlunar satellite technique will bring forth reasonable results only if a region, considerably larger than

what can be covered on a single frame, is covered by overlapping frames that are reduced simultaneously as a block. Exactly this is planned; see for instance Taback (1964) who proposes to cover a target area of $40,000 \text{ km}^2$, i. e., a square field with sides of 200 km, from a satellite flying at an altitude of 50 km so that every target point appears on at least two (but preferably more) frames.

Let us now assume that the camera has a focal length of f , that the size of the frame is $a \times a$ and that the vehicle passes over the terrain at an altitude of h . Assume further that there is generous (at least twofold) overlap, and let n be the number of target points on a frame (here assumed to be the same for every frame), N the number of available control points,

E_c the dispersion of their map coordinates in the plane of the moon, M the number of frames covering the area, and ϵ_r the standard deviation with which the plate coordinates of a target point may be measured on a frame.

From Table II in the paper by Eichhorn and Williams (1963) we gather that the average plate-constant variance for the corresponding model type (called III in that paper) is 3.00.

If we denote by E_r the error in a target point coordinate (in the tangential plane) corresponding to ϵ_r , then we obviously have

$$\frac{\epsilon_r}{f} = \frac{E_r}{h} \quad (35)$$

If we assume that the systematic error of the tie of a single frame to the system for the whole 200 km x 200 km block is $(3/n)^{1/2}$, where n is the number of usable sharp target points in the overlap of the frame and its neighbors (regarded as a unit), we see that for something like 30 target points this systematic error is less than 1/3 the accidental error of measurement; we may thus regard the whole complex of plates as one big plate, tightly tied together by the overlaps, and treated as such. One can reflect further that the error ϵ_v of u or v (essentially for a square field) will be given by

$$\epsilon_v = \sqrt{3/N} \epsilon_T \quad (36)$$

where N is the number of control points, and where ϵ_T is computed from (35) using E_c for E_T .

Let us now consider the range of possible values of the errors, making the most plausible assumptions concerning the range of values for ϵ_T , the standard error of unit weight; for N , the number of control points in the surveyed region for which map coordinates are known; for E_T , the expected standard error of a map coordinate for one of these control points (E_T); and for n , the number of usable landmarks per frame ("pass points" in photogrammetric terminology). Let us list the range of plausible values, one by one.

For ϵ_T : 2μ is the best that can possibly be done with photographic plates and sharply defined images; 10μ is probably optimistic for the kind of optics and image readout contemplated; it is said that the distortions of the image scan may produce errors as large as 50μ . For N : The predicted average spacing of lunar landmarks whose map coordinates will have been obtained by earth-based astrometric methods is one per square degree of the lunar surface, or one per 920 km^2 . For a $200 \text{ km} \times 200 \text{ km}$ surveyed area, the expected number would thus be 40 to 45. For E_T : For points near the center of the moon's visible hemisphere (within 30°), the expected r.m.s. value of E_T is about 300 m corresponding to a single degree of freedom in the horizontal plane, and about 800 m in the vertical direction. For points about 60° from the center, the expected value of E_T (horizontal) is about 900 m and E_T (vertical) about 500 m. We may take 200 m to be the smallest reasonable value, and 1000 m to be the greatest. For n : From the Ranger photographs (allowing for some further improvement), one would guess that the number of sharp features suitable for making overlap ties will vary with the roughness of the terrain -- that in rough terrain, sharp features will be plentiful and n will be limited only by the number needed to make an adequate tie; but that in smooth terrain it may be difficult to ensure that n will be greater than 20 or 30.

Optimistic case. If we take a camera focal length $f = 7.5$ cm (3") and orbit it at an altitude $h = 50$ km, we get

$$\varepsilon_v = \sqrt{3/N} \cdot 1.5 \times 10^{-6} E_T$$

Assuming (optimistically) that E_T , the standard error of a lunar map coordinate of a control landmark as established from terrestrial observations, is 200 m we get

$$\varepsilon_v = \sqrt{3/N} \cdot 0.3 \text{ mm}$$

or

$$\varepsilon_v \approx 0.5 \sqrt{1/N} \text{ mm}$$

To keep ε_v below 10μ we would need more than 2500 control points, while 100 control points of this accuracy will keep ε_v below 50μ . From (35) we see that the zero point accuracy E_{x_0} , with which the complex of the target points can represent the control points, is given by

$$E_{x_0} = \frac{h}{f} \varepsilon_v \quad (37)$$

With $h/f = 10^6/1.5$ and $\varepsilon_v = 50 \mu$, for 100 control points with a standard deviation of 200 m, we get for E_{x_0} about 35 m. From (35), with $h = 50$ km, $f = 7.5$ cm, the error corresponding to $\varepsilon_T = 10 \mu$ would be $E_T = 6.6$ m and that corresponding to $\varepsilon_T = 50 \mu$ would be $E_T = 33$ m. Since there will not be even 100 control points available (we have just estimated 40 or 50), and their errors will be on the average higher than 200 m, it will be appreciated that, to get the most of a circumlunar survey for geodetic purposes, a high priority should be accorded to trying to increase both the number of control points and the accuracy of their lunar map coordinates, whether this is done by terrestrial observations or by preliminary circumlunar photographic surveys made at a height greater than 50 km above the moon's surface.

As that error imposed on the lunar coordinates of points derived from the Orbiter photographs by the errors in u and v is common to all target points, the estimate of E_c just given (33 m) and also those given in the

next two examples must be regarded as a measure of the accuracy of relative coordinates -- i. e., relative to the coordinate system of the 200 km x 200 km block.

Pessimistic case. Assume now that E_T , the standard error of a lunar map coordinate of a control landmark as established from terrestrial observations, is 1000 m. Using the same value of the scale factor $f/h = 1.5 \times 10^{-6}$ as before, we obtain

$$\epsilon_v = \sqrt{3/N} \times 1.5 \text{ mm} = 2.6/\sqrt{N} \text{ mm}$$

Nearly 70,000 control points would be needed to keep ϵ_v below 10μ , and 2700 to keep it below 50μ . This number of control points will not be available for some time, if ever.

Compromise. For the region within 30° of the center of the moon's visible hemisphere, we assumed E_T (horizontal) ≈ 300 m and E_T (vertical) ≈ 800 m to be good compromise values. With $E_T = 300$ m, $N = 43$, $f/h = 1.5 \times 10^{-6}$, one obtains the estimate $\epsilon_v = 120\mu = 0.12$ mm. From (37), we obtain E_{x_0} , the zero-point error of the coordinate system on the ground (expected mismatch between the lunar mapping coordinate system for the whole visible hemisphere and the piece of the coordinate system represented by the 40-odd control points in the surveyed area):

$$E_{x_0} = (10^6/1.5) \times (0.12 \times 10^{-3} \text{ m}) = 80 \text{ m.}$$

Other errors. As the effect of ϵ_f , the error in u , v (or U , V , or ξ , η , which are all practically the same) due to the error of the focal length is essentially $\sqrt{\frac{\epsilon_f}{hM}}$, we can see that the focal length may be regarded as so accurately known that its error has no effect on the errors of the final positions.

The largest errors that can be introduced into u or v (or ϵ and η respectively) due to the errors in the orientation elements ρ , σ , τ , are

$$\left(\frac{\partial v}{\partial \rho} \sqrt{\{\rho, \rho\}}\right), \text{ etc.}$$

We have the required formulas in (26). The error caused by the error in τ cannot exceed $\frac{1}{2} \frac{\sqrt{6}}{\sqrt{n}} \varepsilon_\tau$, which is about $\frac{1.23}{\sqrt{n}} \varepsilon_\tau$. With $n = 30$ (which is reasonable) the error caused by τ is less than 1/4 the standard error of unit weight, i. e., insignificant.

From (26) and (33), and neglecting $\frac{1}{2} a^2$ in comparison to f^2 , we see that the errors in ξ and η caused by the uncertainties in ρ and σ cannot exceed

$$\varepsilon_\rho = \varepsilon_\sigma = 4 \sqrt{\frac{f}{n}} \left(\frac{f}{a}\right)^2 \varepsilon_\tau \quad (38)$$

For $f/a = 75 \text{ mm}/60 \text{ mm} = 1.25$, $(f/a)^2 \approx 1.5$, we get from (38)

$$\varepsilon_\rho = \varepsilon_\sigma \approx \frac{15}{\sqrt{n}} \varepsilon_\tau$$

which would, for 36 target points per frame, produce $\varepsilon_\rho \approx 125 \mu$, a maximum error 2 1/2 times that of the standard error of unit weight. However, the effect in a final position will be from 1/2 to 2/3 of this amount, as the final positions are obtained from taking the mean of the results from at least two individual frames.

Remarks about double camera. The formula (38) is derived from (33), which takes into account the relation of the vehicle positions to the other variables. We shall now compare this to the case in which the orientation parameters are known independently, e. g., obtained by a double-camera arrangement. In this case, $\{\sigma, \sigma\}$ (as well as $\{\rho, \rho\}$) would be given by $\frac{1}{[\rho, \rho]}$ from (31), which is basically $\frac{1}{f^2}$, so that in this case we would approximately have

$$\varepsilon_\rho = \varepsilon_\sigma = \frac{1}{\sqrt{n}} \varepsilon_\tau. \quad (38a)$$

An associated attitude check, involving only a few (say, 15) stars with a camera identical to that used for the moon surface photography would be sufficient to keep the ε_ρ and ε_σ to only a quarter or so of ε_τ . This makes it apparent that the installing of a double camera would, conservatively, quadruple the weight of the final positions. If this factor is compared to the extra cost which a double camera would add to the total project cost, it will probably be found well worth the outlay.

Finally, we come to the influence of an error in Ξ and H on ξ . By doing this for $\phi = 0$, i. e., $\cos \phi = 1$ and $\sin \phi = 0$, we find from (24a) that $(\partial U / \partial \Xi)_{\max} = a/2h$, and from this and (34)

$$\epsilon_{\Xi} = \frac{1}{\sqrt{n}} \frac{\sqrt{6}}{2} \epsilon = \frac{1.23}{\sqrt{n}} \epsilon \quad (39)$$

However, we now have to redefine exactly what ϵ and what n are. As we have used formula (34), we have treated the covariance of Ξ , H, Z; ρ , σ , τ , as insignificant, so that ϵ should be taken to be ϵ_{σ} , and n therefore as the number of independent σ and ρ that occur on one plate. With four-fold overlap (2 plates = 1 overlap, etc.), there would be five σ and five ρ , so that $n \approx 10$. Taking $n = 9$, we get $\epsilon_{\Xi} = 0.4 \epsilon_{\sigma}$, or generally, $\epsilon_{\Xi} \approx \epsilon_{\tau}$ if no independent estimates for ρ , σ , τ are obtained from a double camera, then $\epsilon = \epsilon_{\tau}$ and n is the number of target points. We would thus get, for $n = 36$, for instance, $\epsilon_{\Xi} \approx \frac{1}{3} \epsilon_{\tau}$, so that ϵ_{Ξ} would have practically no influence on the final accuracy compared to ϵ_{τ} .

We may thus summarize our results as follows: The systematic error of the zero point (i. e., ϵ_{x_0}) depends critically on the number and accuracy of the available control points in the area covered. Under the present circumstances an inaccuracy in the zero point coordinates producing an inaccuracy of about 80 m in the lunar coordinates with respect to the system of the reference points (the "map" system) seems unavoidable.

By way of summary, we have

For N = 100,	$E_{\tau} = 200$ m:	$E_{x_0} = 30$ m (optimistic)
For N = 40-50,	$E_{\tau} = 300$ m:	$E_{x_0} = 80$ m (expected average)
For N = 40-50,	$E_{\tau} = 1000$ m:	$E_{x_0} = 250$ m (pessimistic)

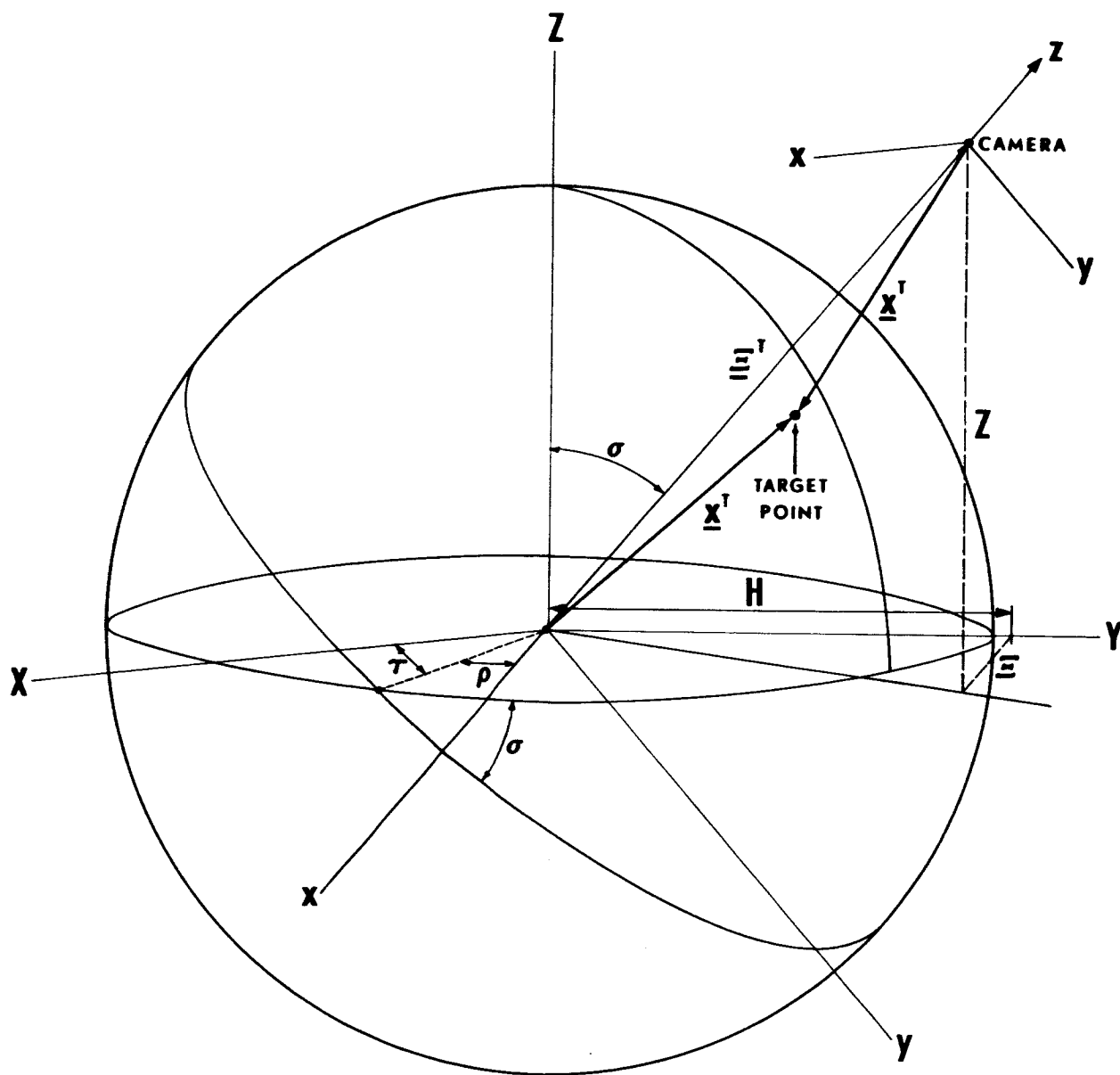
The relative accuracy of a target point's coordinates in the tangential plane to the moon (i. e., in the system determined by their entirety) is

mainly limited by the accuracy of the ρ and σ , while Ξ , H , Z , and τ contribute only a fraction of the standard deviation of unit weight. If we assume the average target point to occur and be measured on three frames, we get $\epsilon_\rho \approx 75 \mu$. Assuming that 100μ is a more realistic figure, we see that this corresponds on the ground for the Taback (1964) figures ($h = 50$ km, $f = 7.5$ cm) to an inaccuracy of about 65 m (equation 35) for coordinates in the plane of the horizon, while the inaccuracy of the altitude, determined by a 45° intersection, is about two to three times as large (2.4 to 2.6 with certain assumptions).

If, however, a double camera is employed for the independent determination of the attitude parameters (ρ , σ , τ), the accuracy is only slightly worse than that corresponding to ϵ_τ so that ± 35 m for coordinates in the horizontal plane and ± 90 m for altitude would be the standard deviation.

Literature:

- Eichhorn H. & Williams, (A. 1963, Astron-Journ. 68, 221)
 Taback, I., 1964, 10th Meet. Am. Astronaut. Soc, Repr. 64-7
 Vasilevskis, S. 1940, Publ. Obs. Univ. Riga No. 4.



GEOMETRY OF LUNAR ORBITAL PHOTOGRAPHS

APPENDIX B
DETERMINATION OF THE INSTANTANEOUS POLE
AND ASTRONOMICAL LATITUDE ON THE MOON BY
MOON-BASED FIXED CAMERA

A. INTRODUCTION

The exact determination of the terrestrial equatorial coordinates (i. e., right ascension and declination proper) of the direction of the instantaneous axis of rotation of the moon would establish data useful for the orientation of earth-based lunar photographs, and would also lay the foundation for astronomical selenodesy in terrestrial fashion. Nearly all astronomic geodetic work (with transits, theodolites, sextants, or other instruments) presumes the knowledge of sufficiently accurate right ascensions and declinations of a sufficient number of stars, implying the knowledge of the location of the pole of rotation.

When we speak of right ascensions and declinations in this context, we have in mind selenocentric right ascensions and declinations, which would be defined using the kinematic parameters (direction of axis of rotation, node between lunar equator and ecliptic, or something equivalent thereto) of the moon as we use those of the earth for defining earth-based right ascension and declination. If we were able to convert earth-based right ascension and declination to moon-referred selenocentric right ascension and declination, we could use them on the moon in the same way for astronomical selenodesy as we use their terrestrial equivalents for terrestrial navigation. Below is outlined the theory of a method, together with suggestions for its practical application, which will permit one to determine (earth centered) right ascension and declination of the axis of a rotating body in space (as, for instance, the moon) with any desired accuracy by relatively simple means.

B. THEORY AND METHODS

1. Fixed Camera Star Trails

Suppose we have a camera rigidly connected to a body that rotates in space

on an axis which always remains parallel to itself, i. e., without anything like precession or nutation. Suppose, also, that the positions of the stars in the sky are described by a selenocentric right ascension A and a selenocentric declination D which are defined with respect to the body's equator and a suitably chosen substitute for the vernal equinox, i. e., zero point of the right ascension system.

If the celestial coordinates corresponding to the tangential point of the camera are A_0 and D_0 , and if Ξ and H are standard coordinates on the plate oriented with respect to the AD system, the relationship between A , D on the one hand and Ξ , H on the other hand is given by the well known formulas

$$\begin{aligned}\cot D \sin(A-A_0) &= \frac{\Xi}{\sin D_0 + H \cos D_0} \\ \cot D \cos(A-A_0) &= \frac{\cos D_0 - H \sin D_0}{\sin D_0 + H \cos D_0}\end{aligned}\tag{1}$$

We now assume that the shutter of the camera is opened at periodic intervals for a short time, so that images of the stars will be recorded as such short trails that they cannot be distinguished from points. If the camera is not moved between successive exposures, all images of the same star will lie on an ellipse. This would be the same ellipse as the one on which all stars with the same declination (but different right ascensions) lie. Its equation is obtained by eliminating $A-A_0$ from the system (1), for instance by squaring and adding. Thus, one obtains after some manipulation.

$$\Xi^2 + H^2 + \frac{\cos^2 D_0}{\sin^2 D} \left[(1 - H^2) \cos D_0 - 2H \sin D_0 \right] - \cot^2 D = 0\tag{2}$$

or, in somewhat different form

$$\Xi^2 + H^2 \left(1 - \frac{\cos^2 D_0}{\sin^2 D} \right) - H \frac{\sin^2 D_0}{\sin^2 D} + \left(1 - \frac{\sin^2 D_0}{\sin^2 D} \right) = 0\tag{2a}$$

From both (2) and (2a) one can see that, if $D_0 = \frac{\pi}{2}$, i. e., if the tangential point is at the pole, the equation becomes

$$\Xi^2 + H^2 - \cot^2 D = 0 \quad (2b)$$

i. e., the images lie on circles with the radius $\cot D$.

If one assumes the usual relationship between measured coordinates, x, y and standard coordinates Ξ, H , namely

$$\begin{aligned} \Xi &= ax + by + c \\ H &= -bx + ay + d \end{aligned} \quad (3)$$

and inserts this into (2) or (2a) one obtains the equation of the curve on which all the images lie in terms of certain parameters and the measured coordinates.

We have chosen (3) to be the simplest form possible for the relationship between the measured and the standard coordinates. Generally, one would have to consider a much more complicated relationship in order to take care of the various aberrations of the lens system. In the particular application under consideration, one may regard the lens aberrations as non-existent, because they can be carefully calibrated before they are used in the field, i. e., on the moon. Corrections for the lens aberrations will then be applied to the measured coordinates.

2. Least Squares Adjustment for Hierarchy of Unknowns

The equations (3) inserted into (2) (or 2a)) will have the following unknowns: D_0, a, b, c, d , which are common to all "traces" on the plate (i. e., all those series of pictures produced by one and the same star), and D , which is of course different for every star. This will result in a system of normal equations that must be solved in steps. Generally, the situation is as follows:

Suppose we have a system of the type as occurs above, that is, we may split the unknowns into sets X_i so that every equation will contain only elements of one set of unknowns, and a set X , elements of which occur in every equation.

The normal equations are formed from the observation equations in the conventional manner. Under the circumstances, we are going to have n sets of normal equations, which may be written in matrix notation in the following way

$$\begin{pmatrix} A_i & B_i \\ B_i^T & C_i \end{pmatrix} \begin{pmatrix} X_i \\ X \end{pmatrix} = \begin{pmatrix} L_i \\ \Lambda_i \end{pmatrix} \quad i = 1, \dots, n \quad (4)$$

where the meaning of the symbols (all of which represent matrices (including column matrices, i. e., vectors)) is clear. Considering that the systems (4) are normal equations, some simple calculations show that the vector of unknowns denoted by \underline{X} , i. e., whose elements occur all throughout the entire system, is given by

$$X = \left[\sum_{i=1}^n (C_i - B_i^T A_i^{-1} B_i) \right]^{-1} \left[\sum_{i=1}^n (\Lambda_i - B_i^T A_i^{-1} L_i) \right] \quad (5)$$

and the individual X_i are simply

$$X_i = A_i^{-1} (L_i - B_i X) \quad (5a)$$

where the X must first have been computed from (5). It is easy to extend this algorithm to the case where there are more classes of sets of unknowns which form a hierarchy, such that unknowns of a higher class occur in a smaller number of equations.

3. Feasibility of Absolute Declination Determinations

From equation (2b) it is apparent that the scale of the photographs, namely $a^2 + b^2$, and the declination D cannot be separated if the pole of rotation is the tangential point on the plate. In order to determine the scale when the tangential point coincides with the pole of the selenocentric declinations, at least one declination must be known, and vice versa. It will be difficult to separate scale and declination even in the case when pole and tangential point do not coincide but are close. On the other hand, the independent determination of scale and absolute selenocentric declinations is not impossible in the general case. If we consider, for instance a camera with a field of view of over 90° and direct it so that the selenocentric declination of the tangential point is 45° , it will have images of both the equator and the pole on the plate. The images of equatorial stars and of the pole can immediately be identified. The pole is projected as a point (or as a circle with infinitely small radius) and the image of the equator (and of the equator only) is a straight line. The photograph identifies the distance which corresponds to 90° ; thus the scale is established. The images of all the parallels will, of course, be ellipses. By analogy one can thus see that the determination of absolute selenocentric declinations from photographs is possible in the fashion indicated. This may be of importance if it is possible to define the zenith point on a plate very accurately, which is mainly a problem of adjustment and setup of this instrument, and may not be possible (or desirable) in the circumstances of a short visit to the moon. It will probably be more profitable to determine the geocentric right ascension and declination of the pole of the moon's rotation, and its zenith distance at the place of observation.

4. General Conditions of the Problem

If a system of normal equations, set up from condition equations of the type (2a) in connection with 3 were solved for the unknowns occurring therein, we would only get information about the various D and $A - A_0$, i. e., we would only establish selenocentric right ascension and declination of various

stars. In order to find, however, the right ascension and declination of the body's (moon's) axis of rotation, we would have to establish a relationship between the attitude parameters of the moon's axis, and terrestrial and selenocentric right ascension and declination.

A relationship between selenocentric right ascension and declination A and D , right ascension and declination proper α and δ , and selenocentric right ascension and declination of the moon's axis of rotation \mathcal{A} and \mathcal{D} is established as follows:

Suppose x, y, z is the coordinate system associated with right ascension and declination, so that

$$\begin{aligned}x &= \cos \delta \cos \alpha \\y &= \cos \delta \sin \alpha \\z &= \sin \delta\end{aligned}$$

and X, Y, Z the coordinate system associated with the selenocentric right ascension and declination, so that

$$\begin{aligned}X &= \cos D \cos A \\Y &= \cos D \sin A \\Z &= \sin D\end{aligned}$$

and Z is parallel to the moon's instantaneous axis of rotation. The (XYZ) system is obtained from the (xyz) system by first rotating by the angle Ω around the z -axis, and then by the angle I around the new X -axis, where Ω is the angle between the direction to the vernal equinox γ (i. e. the x -axis) and the line of intersection between the equatorial planes of moon and earth (i. e., the X -axis); and I is the angle (inclination) between the two equatorial

planes. Thus,

$$\begin{pmatrix} X \\ Y \\ Z \end{pmatrix} = R_1(I)R_3(\Omega) \begin{pmatrix} x \\ y \\ z \end{pmatrix} \quad (6)$$

(R_1 (R_3) signifying a rotation matrix on the x (z) axis). Equating the coordinates of the Z-axis in the (xyz system in terms of \mathcal{A} , \mathcal{D} and Ω , I, we obtain

$$\begin{aligned} \cos \mathcal{D} \cos \mathcal{A} &= \sin I \sin \Omega \\ \cos \mathcal{D} \sin \mathcal{A} &= -\sin I \cos \Omega \\ \sin \mathcal{D} &= \cos I \end{aligned} \quad (7)$$

from which

$$I = 90^\circ - \mathcal{D}, \text{ and } \mathcal{A} = \Omega - 90^\circ$$

Inserting this in (6) and developing, we obtain

$$\begin{aligned} \cos D \cos A &= \cos \delta \sin(\alpha - \mathcal{A}) \\ \cos D \sin A &= \sin \delta \cos \mathcal{D} - \cos \delta \sin \mathcal{D} \cos(\alpha - \mathcal{A}) \\ \sin D &= \sin \delta \sin \mathcal{D} + \cos \delta \cos \mathcal{D} \cos(\alpha - \mathcal{A}) \end{aligned} \quad (8)$$

In a rigorous adjustment of the measurements, \mathcal{A} and \mathcal{D} would be regarded as unknowns and computed from the system.

We now go back to the original problem. We assume we are making a number of exposures within a certain interval of time and keep the camera rigidly connected to the moon. The exposures must be short enough so that

the images of the stars do not appear elongated. Due to the slow angular speed of the moon, about 1/30 of that of the earth, the "trace" of a star 10 cm from the center of rotation reaches a length of only about 15 μ during an exposure lasting for one minute. A one-inch aperture lens would produce measurable images of sixth magnitude stars on fairly sensitive film during this interval, a three-inch aperture lens at least eighth magnitude stars.

The time interval between the successive exposure (between the (i-1)st and the i-th exposure) is φ_i , measured in the same units as selenocentric right ascension, which means that we would have to express φ_i in time units based on the rotation period of the moon rather than that of the earth.

If the subscripts k refer to the star, and i to the exposure numbers respectively (starting with 1, so that $\varphi \equiv 0$), we obtain from combining equations (1) and (5):

$$\frac{\cos \sigma_k \left[\sin(\alpha_k - \mathcal{A}) \cos(A_o + \varphi_i) - \sin \mathcal{D} \cos(\alpha_k - \mathcal{A}) \sin(A_o + \varphi_i) \right] + \sin \sigma_k \cos \mathcal{D} \sin(A_o + \varphi_i)}{\sin \sigma_k \sin \mathcal{D} + \cos \sigma_k \cos \mathcal{D} \cos(\alpha_k - \mathcal{A})} = \frac{\overline{\Xi}_{ik}}{\sin D_o + H_{ik} \cos D_o}; \quad (9)$$

$$\frac{\cos \sigma_k \left[\sin(\alpha_k - \mathcal{A}) \sin(A_o + \varphi_i) + \sin \mathcal{D} \cos(\alpha_k - \mathcal{A}) \sin(A_o + \varphi_i) \right] - \sin \sigma_k \cos \mathcal{D} \cos(A_o + \varphi_i)}{\sin \sigma_k \sin \mathcal{D} + \cos \sigma_k \cos \mathcal{D} \cos(\alpha_k - \mathcal{A})} = \frac{\cos D_o - H_{ik} \sin D_o}{\sin D_o + H_{ik} \cos D_o}$$

where we express $\overline{\Xi}_{ik}$ and H_{ik} by (3), namely

$$\overline{\Xi}_{ik} = ax_{ik} + by_{ik} + c$$

$$H_{ik} = -bx_{ik} + ay_{ik} + d$$

Assume that we have made n exposures and that they have produced groups of images of m different stars. We then will have $2mn$ equations, in the following unknowns: the $n-1$ $\varphi_i, \mathcal{A}, \mathcal{B}, A_0$ and D_0 , a, b, c, d depending on the status of knowledge regarding the α_k and σ_k , and the α_k and σ_k themselves. It is seen, however, that all the α occur only in the combination $\alpha_k - \mathcal{A}$, so that the system (9) is not capable of determining \mathcal{A} unless at least some of the α_k are known. This is understandable if one considers that, as far as the kinematics of the earth go, the zero point of the right ascension system (the vernal equinox) is completely arbitrary; its definition is rather given dynamically and involves the earth's orbit. If no right ascensions are known, one can put arbitrarily $\mathcal{A} = 0$ and count the right ascensions from \mathcal{A} .

5. Approaches to Solutions of the Equations

The reduction could proceed in several ways, depending on the amount of knowledge one has concerning the α_k and σ_k . (We must have approximate values for all unknowns since the system is non-linear, and we shall discuss later how these may be obtained.)

α_k and σ_k occur only in those equations that are generated from the measurements of the star with number k ; there will normally be $2n$ of these. All these equations will also contain one φ_i and those unknowns that are common to the whole plate. According to the procedure described around the formulas (4), (5) and (5a) we can eliminate the α_k and σ_k and end up with a system in which occur only the φ_i , and the unknowns common to the entire plate. Using the same procedure, we can eliminate the φ_i from this system (as all of the resulting equations will contain only one φ_i but all the other unknowns) and arrive at a system which contains only those unknowns that occur in every equation. We solve for these unknowns, and by substituting their values back can solve for the φ_i and get the α_k and σ_k as the last step.

The situation is more complicated if previous estimates for the α_k and

σ_k and their variances are available. This is the case in practice, as the right ascensions and declinations of all stars whose images will appear on the photograph can be taken from one or more catalogues; in the case of a lunar application, where mainly bright stars are involved, very accurate positions will be available for them, some even from the FK4. As a matter of fact, a photograph of the prospective dimensions could yield positions of such low accuracy (i. e. , with standard deviation of well over 2") that one could introduce the positions into the calculations simply as known parameters, to whose improvement the observations at hand cannot contribute. This will simplify the reductions of observations made on the moon.

In 1955, D. Brown developed an algorithm for making least squares solutions in the case where the observations are correlated and when any number of observations may occur in an equation of condition. (Ballistic Research Laboratory at Aberdeen, Report #934). If one regards the available catalogue positions α_{kc} and δ_{kc} and their standard deviations (which are, of course, fairly accurately known) as a set of observations with a given covariance matrix, and if the final values of these coordinates α_k and δ_k are also carried as unknowns, we can add the equations of condition.

$$\alpha_{kc} - \alpha_k = 0, \quad \delta_{kc} - \delta_k = 0 \quad k = 1, \dots, m \quad (10)$$

to the set of equations of conditions provided by (9) and regard the set of (9) and (10) as the equations of condition of the system; Brown's algorithm can then be applied straightforwardly.

The necessary initial values for the unknowns can be obtained as follows:

Regarding only the images produced by the i th exposure at a time, we can, in the manner which is standard in photographic astrometry, determine coordinates of the tangential point and establish a relationship between \overline{H}_{ik} on the one hand and x_{ik} and y_{ik} on the other hand, getting independent sets of a_i, b_i, c_i, d_i . (As a check, one should verify that to a very high degree of approximation $a_i^2 + b_i^2 = a_j^2 + b_j^2$.)

Close to the pole (which should be close to the center of the plate for practical applications), the coordinates of the images of the same star lie on circles, the center of which is a point with the coordinates x_0, y_0 . Taking two exposures (1 and 2) of two stars (1 and 2), we have thus

$$\begin{aligned} x_{2k} &= (x_{1k} - x_0) \cos \varphi + (y_{1k} - y_0) \sin \varphi \\ y_{2k} &= -(x_{1k} - x_0) \sin \varphi + (y_{1k} - y_0) \cos \varphi \end{aligned} \quad k = 1, 2$$

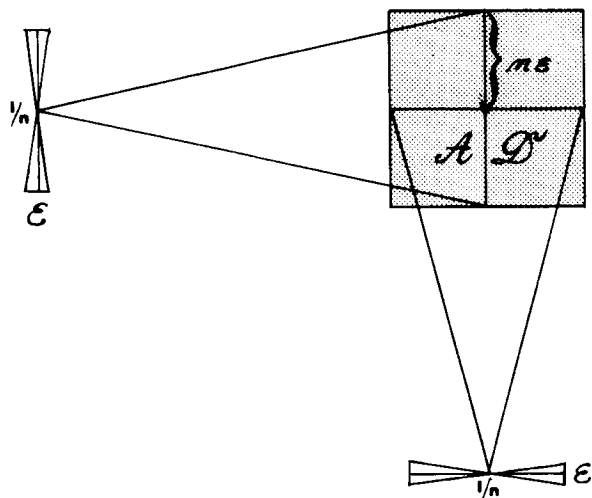
From these (four) equations, x_0, y_0 and φ can be computed.

From x_0 and y_0 one gets Ξ_0 and H_0 , and from these \mathcal{A} and \mathcal{D} , while φ results from the calculation above. A_0 and D_0 are now also known, because their Ξ and H are byproducts of the first (single exposure) adjustments, so that their α_0 and σ_0 is known, and from these and the just obtained \mathcal{A} and \mathcal{D} , system (8) will permit one to obtain D_0 and A_0 . In this (or an equivalent) way, one can obtain fairly good first approximations to the unknowns which are necessary for a least squares calculation with non-linear equations.

6. Estimation of Accuracy of the Pole's Coordinates Determination

A rigorous approach would be to start from equations (9) and (10) and to set up the normal equations for a model star distribution and a model exposure pattern, and invert these equations under conditions that are as general as possible, so that the variances of \mathcal{A} and \mathcal{D} become known as functions of the circumstances of the exposure. This would be analogous to the way in which Eichhorn and Williams (Astr. Journ. May 1963) treated the question of the accuracy of astrometric positions. If a solution in this way is attempted, one eventually comes to tremendously complicated formulas which are difficult to keep track of. However, we can show that one can heuristically arrive at the minimum accuracy without going through the tremendously complicated model calculations in the general case.

Determination of the accuracy is analogous (in a vastly simplified but basically equivalent case) to the determination of the accuracy of the center of a circle, determined from short arcs (all of which have the same center) by drawing radii which are perpendicular to the end points of the arc. (Points in between contribute less to the total weight.) If the arc is $1/n$ radians long as shown below, and the position of the end points has a standard deviation of \mathcal{E} , the width of the "standard deviation pencil" at the center will be $n\mathcal{E}$. If the radius through the ends is combined with another one belonging to a star with an A (right ascension) about 90° different, the point \mathcal{A}, \mathcal{D} will be determined and its coordinates will have standard deviations of $\sqrt{2n} \mathcal{E}$. A combination of $2^{3/2} n^2$ pairs of images will therefore be needed to determine



the coordinates of the pole of the selenocentric coordinates with standard coordinates with a standard deviation of \mathcal{E} . If N stars are available, the standard coordinates will be determined with standard deviations \mathcal{E}_p given by

$$\mathcal{E}_p = n \sqrt{\frac{2^{3/2}}{N}} \mathcal{E}$$

In a lunar experiment, the two extreme exposures would be 12^h apart, having then described the arc of ~ 0.1 radians so that $n \sim 10$. Therefore, 300 star pairs, which are easily obtainable on a camera with a field radius of 15° , 1^m exposure with a 2 or 3-inch aperture lens, will determine the pole of the moon's rotation as accurately as the star positions can be measured. Assuming that a focal length of 1000 mm yields star positions of $1''$ accuracy, a camera with a focal length of r millimeters (a field 15° wide and a 2 to 3-inch aperture lens) will enable one to determine the geographic latitude of the station on the moon with an accuracy of at least $\frac{1000}{r}$ seconds of arc. A 150 mm focal length camera (with the other postulated characteristics) would, therefore, from only two exposures 12^h apart yield a latitude accuracy of at the worst $7''$, which is probably much better than what one could do with

a theodolite. The other advantage is that the only equipment needed is a firmly established calibrated camera; accuracy of the timing of the exposures is quite immaterial.

From the discussion above, it is shown how the accuracy of λ and ϕ (and thus the selenographic latitude) is obtained from cameras with other characteristics. Note that the minimum accuracy from a very simplified model has been discussed which, however, is essentially the same (for our purposes) as the exact one.

7. Setup of the Camera

The foregoing analysis is valid only if the relative position of the camera with respect to the moon is the same for all exposures. This can most easily be accomplished by not allowing the camera to be moved or touched throughout the whole experiment. However, it may not be possible to adhere to this requirement. If the camera has to be moved between exposures, one must make sure that there are provisions to rectify the various exposures with respect to each other. A portion of the lunar landscape, that appears on the lower edge of the plates, could be used as an extended series of fiducial marks and serve this purpose adequately, as long as it is clear which image of the horizon goes with what star exposure.

The camera must point in the direction of the lunar celestial pole, which is sufficiently well known for this purpose. If the experiment is to yield not only the exact location of the lunar pole, but also the selenographic latitude of the observing station, the camera must be carefully leveled and its scale well known, so that the actual latitude, i. e., the angular distance of the pole from the horizon, can be computed from the measurements on the plate. An artificial mark (balloon) close to the horizon would serve this purpose very adequately.

APPENDIX C

OBSERVATIONS FROM THE MOON OF THE EARTH'S POSITION AGAINST THE BACKGROUND OF STARS FOR SELENODETIC PURPOSES

A. INTRODUCTION

There are two possibilities, neither of which look very promising, of making observations of the Earth from the Moon to obtain selenodetic data. These are:

(1) Occultations of stars by the Earth.

(2) Position of Earth referred to the surrounding star field, with a technique analogous to the Markowitz Dual-Rate Moon Camera (Ref. 1), or straight photographs (or other recorded image) with an instrument of sufficiently long focus.

B. OCCULTATIONS OF STARS BY THE EARTH

It appears that the Earth's atmosphere will prevent occultation observations from being accurate enough to be useful for selenodetic purposes. Analysis follows.

The limb of the earth that covers or uncovers a particular star will be either cloudy or clear. If the limb is cloudy, it will be difficult to determine the effective radius of the earth $R_\phi + h$, where R_ϕ is the radius of the Earth for the latitude of the point on the limb where the star is covered (or uncovered), and h is the height of the top of cloud layer. R_ϕ can be calculated with an accuracy of ± 30 meters (= uncertainty of the radius and of the geoid height); but the uncertainty of h could be 15 km in an extreme case.

It is possible that a large number of occultations could be observed and their positions and times fitted to a moving ellipse representing the outline of the solid Earth. Occultations occurring in cloudy regions

would show large residuals, all in the sense of $R_{\phi} + h > R_{\phi}$. The large residuals in cloudy regions would tend to be grouped in a non-random way, and such non-random large positive residuals could be rejected according to some rule. This procedure would lead to a selection of occultation observations made at points where the limb is clear, which, however, would not get around a different set of difficulties presented by a clear limb.

Occultations by a clear limb would be subject to large uncertainties arising from refraction and extinction. The horizontal refraction at sea level is approximately 30'-37', but is subject to large variations (up to another 30' under unusual atmospheric conditions producing mirages, looming, etc.). Even under normal conditions the uncertainty is $\sim 2'$. The amount of both the refraction itself and its uncertainty are sensitive functions of temperature and pressure along the path, (which for practical reasons cannot be measured with sufficient accuracy. These quantities would be doubled for a ray from a star grazing the Earth's surface. (Ref. 2.)

Extinction in visible wavelengths in clear air is ~ 0.3 magnitude/atmosphere, or a little greater; but this quantity is quite variable, and depends on the haze and aerosol content of the atmosphere along the path. If one takes the density scale height of the atmosphere to be approximately 10 km, then a horizontal line of sight passes through about 3.8 atmospheres for a terrestrial observer, and a grazing ray passes through about 7.2 atmospheres for an extraterrestrial observer. The total extinction would thus be at least 2.2 magnitudes, which represents a reduction by a factor of about 8 in brightness.

A star sinking through the atmosphere and getting fainter (or one emerging and getting brighter) could thus present the observer with a problem as to when exactly it disappears (or appears), quite apart from the erratic effect caused by clouds.

Corrections for refraction and extinction are affected by the height of the geographical horizon that constitutes the occulting limb, e. g., by a mountain range or a plateau. Refraction in an air path over a range and a plateau, even when they are the same height, tends to behave differently in the two cases. (These refraction uncertainties are, of course over and above the uncertainties of the skyline itself, which could probably be handled, since the contour of any given cross section of the Earth is quite well known.)

Conclusion: Occultation observations would be subject to uncertainties of about $\pm 4'$ or $\pm 200''$ under the very best conditions, and at least half the time would be a great deal worse. This error corresponds to nearly 400 km on the surface of the Moon. To be better than already exists (say, ± 800 m), the Earth's position against the stars would have to be measured with an angular error not exceeding $\pm 800 \text{ m} / 4 \times 10^5 \text{ km}$ or 0.2×10^{-5} radian, or about $0.''4$. If the occultation errors ($\pm 200''$ per observation) were randomly distributed, 250,000 observations would be required to reduce the overall uncertainty to $\pm 0.''4$. This is not practicable.

C. MOON CAMERA TECHNIQUE APPLIED TO THE EARTH FROM THE MOON

Direct imaging of the Earth against a star field in a telescope, without a Moon Camera attachment, will not be discussed separately, because anything that can be achieved in this way can be achieved better with a Moon Camera. Conclusions about the use of Moon Camera apply a fortiori to the use of telescopes without the camera.

The Dual-Rate Moon Camera (Ref. 1) was developed by Wm. Markowitz, Chief of the Time Service, U. S. Naval Observatory, to obtain precise observations of the position of the Moon against the stars for time determinations (using the orbital motion of the Moon as a clock), and for determination of the geocentric position of the

observer. It is attached to a telescope of focal length long enough to give an image of adequate scale. The telescope is driven at the sidereal rate. The camera is essentially a plateholder with light yellow filter, which holds a plate on which images of stars formed by the telescope objective are photographed with exposures of some seconds or minutes, if need be. (Actual exposures are 10-25 seconds on 103 G emulsion with a refractor of 12 inches aperture and 180 inches focal length.) It also contains a plane-parallel neutral filter rotating in such a way as to hold the image of the Moon stationary against the starfield. The filter cuts the light by a factor of 1000, so that the Moon will be correctly exposed in the 10-25 seconds required for the starfield. The time is recorded at that instant when the plane of the rotating neutral filter is parallel to the plane of the stationary yellow filter. The errors from all sources from a single night's run (several exposures) are of the order of $\pm 0.''15$ in right ascension and somewhat less in declination. This corresponds to an uncertainty in geocentric position of ± 280 m. If the same kind of observations could be made of the Earth from the Moon, the same error in selenocentric coordinates would presumably result.

On the face of it, an uncertainty of ± 280 m. represents a considerable reduction of the present uncertainty, and would be worth trying to attain. There are, however, difficulties, such as the following:

(1) These results are obtained with a telescope with aperture of 30 cm and focal length of nearly 5 m, with an equatorially aligned sidereal drive. This is a rather large and complicated instrument to take to the Moon and set up there.

(2) One could substitute a smaller instrument, with corresponding decrease in focal length f and increase in error, $= 0.''15 \times 5/f$ (meters) $= 0.''75/f$ (meters).

(3) One could dispense with the equatorial mount and sidereal drive, on the grounds that the slow rotation of the Moon would not require it. The rotation rate of the Moon is about $0.^\circ54/\text{sec}$. With exposures of 10 or more seconds, and with the Earth at low (selenocentric) declination, stars would trail $5''$ or more, which is 0.12 mm (if $f = 5\text{ m}$), which is rather large. Furthermore, the number of usable reference stars would be diminished, because stars within a magnitude or so of the useful limit with normal photography (in which a sidereal drive is used) would not leave a usable trail.

(4) To save weight, one could conceivably dispense with the telescope tube, but the plateholder would of course have to be shaded from sunlight, both direct and reflected from the surrounding terrain. Without a tube, there would be difficulty in maintaining alignment to the requisite precision with an open-work mount for the objective lens.

(5) Unlike the Moon, the Earth's limb (as noted above) is fuzzy and subject to uncertainties due to irregularities of cloud cover height, and would be impossible to measure against the background of reference stars with the same precision possible in the case of lunar photographs.

Terrestrial landmarks visible (or, rather, photographable) from the Moon might provide sharp enough points to measure, but this is quite dubious. If n such points on the Earth could be identified, the geocentric coordinates of the object actually being set on with the hairline of the measuring engine would have to be known with an error of about $\pm \mathcal{E} n^{1/2}$, where \mathcal{E} is the error being aimed at for the coordinates of the observing station on the Moon. If we take $\mathcal{E} = 200\text{ m}$ as being worth while, and if $n = 100$, then the quality of the image of the Earth, and its resolution, must be good enough that the exact terrestrial landmark can be identified with sufficient certainty to locate it within $\pm 2\text{ km}$. This sounds fairly easy, but it is not. It should be remembered that: (1) a 30-cm aperture has a resolving power of about $\pm 0.^\circ4$ (0.8 km at the distance of the Moon); (2) there are not many

landmarks that offer sufficient contrast with their surroundings to locate within 2 km on photographs taken through the Earth's atmosphere, if the TIROS-NIMBUS photographs are any indication. Very small islands, or the tips of sharp promontories or fjords, are perhaps the most promising type of landmark.

Conclusion: It appears that any one of the above-mentioned difficulties makes this method marginal, and that the combination of them all is sufficient grounds for eliminating further consideration of the method at this time. This is not to say that it will never be useful: it may become useful at such a time as one can afford to devote several hundred pounds of precious payload to such highly specialized equipment.

References

1. Markowitz, W. "The Photographic Zenith Tube and the Dual-Rate Moon-Position Camera" Kuiper and Middlehurst, Telescopes, "Stars and Stellar Systems," Vol. I, University of Chicago Press, 1960.
2. Chauvenet, W. "A Manual of Spherical and Practical Astronomy", Vol. I "Spherical Astronomy" Dover, 1960

APPENDIX D

FORMULAS FOR REDUCTION OF PANORAMIC PHOTOGRAPHY TO DETERMINE ASTRONOMICAL POSITION AND AZIMUTH, AND SELENOCENTRIC COORDINATES OF SURVEY TARGETS

A. INTRODUCTION

The panoramic camera recommended in this report provides a means of obtaining astronomical position and orientation, and angular relationships for surveying, with the minimum demands upon astronaut for time and specialized training.

The following paragraphs provide a brief error analysis of the expected capabilities of this photography and a derivation of formulas that may be used in reducing the photo observations.

B. PRELIMINARY ANALYSIS

Assume that a panoramic camera with characteristics as proposed in Appendix E with angular accuracy of 10" for each component of plate measurement is leveled and N photographs obtained of about 50 stars symmetrically distributed around the horizon. For the following discussion, assume plate coordinates can be converted to azimuths and zenith distance angles. Then the following equations may be used to make differential corrections to an assumed astronomical position of the camera.

$$d\beta = -\cos \alpha d\phi - \cos \phi \sin \alpha d\omega \quad (a)$$

$$d\alpha = -\sin \alpha \cot \beta d\phi + \frac{\sin \phi \sin \beta - \cos \phi \cos \alpha \cos \beta}{\sin \beta} d\omega \quad (b)$$

These expressions are developed by differentiating the law of cosines and the relationship between three sides and two angles of the astronomical triangle APS, and simplifying. As shown in Figure 1, A is the assumed position of the camera, P is the pole of the moon, S is the substellar projection of a star on the celestial sphere, α and β are the computed values of azimuth

and zenith distance for the assumed position A , ϕ is the assumed latitude, ω is the difference of longitudes of the camera and star, and D is the declination of the star, with reference to the moon's equator.

We observe that for the panoramic camera, the zenith distance is near 90° , and the $\sin \beta$ in the denominator will cause no difficulty. Equation (a) shows that the East-West stars most effectively determine longitude, and North-South stars most effectively determine latitude, as is intuitively evident. The azimuth equation (b) shows that azimuth measurements will be valueless for position determination for landing sites near the equator except for stars near the upper edge of the photographed star field. However, plate scale is effectively measured by azimuth, as will be subsequently discussed.

1. Astronomical Position.

The estimated error for astronomical latitude and longitude is given by $\frac{\sqrt{2 \cdot 10''}}{\sqrt{nN}}$ where n is the number of stars (images on the plate), since each star contributes one degree of freedom to the system of equations. The error in the vertical scaling of the plate is assumed to be $10''$. With 4 photographs and 50 stars per photograph, the error is $1''$.

A realistic position uncertainty, however, must take into account the standard error associated with the lunar pole. By taking 12 hour time lapse photographs of the polar star field on a single mission with a 150 mm lens of 2 or 3-inch aperture, this error will amount to $(1000/150) \approx 7''$ (See Appendix B). This is the controlling error. The total error of astronomical position will initially be $7''$ or about 60 m as measured on the lunar surface. As additional pole determinations are made on subsequent missions the position of the pole will become refined and the error will be reduced. Eventually, it should be possible to determine the physical librations of the moon as well, and calculate the position of the lunar pole at any time with the same sort of accuracy as is possible for the earth's pole now. At any stage of this improvement in knowledge of the instantaneous position of the moon's pole, the astronomical position of the camera can be revised.

2. Astronomical Azimuths and Zenith Distances.

If astronomical azimuth and zenith distances can be scaled to $10''$ in a single photograph, the azimuths and zenith distances to the same object in N photographs would be in error due to plate scaling errors by $10'' / \sqrt{N}$. To this must be added the transverse error of the pole or $7''$, so the total errors in azimuth and in zenith distance will be $\sqrt{\frac{100}{N} + 50} \approx 10''$. For laying out a local triangulation network, estimates of angular measurement uncertainty between two objects is $\frac{\sqrt{2} \cdot 10''}{\sqrt{N}} \approx 10''$, since the pole error will cause a systematic error in the orientation of the whole network and will not affect angular relationships between stations of the net.

C. DERIVATION OF EQUATIONS

1. Astronomical Position.

We start with the notion of two coordinate systems fixed with relation to the stars. \underline{A} , \underline{B} , \underline{C} , are fixed in the moon with \underline{C} parallel to the instantaneous rotation axis of the moon. \underline{A} is parallel to the line from the center of the reference surface to the point on the lunar surface where the ecliptic crosses the equator of date. \underline{B} completes the right handed triad. An auxiliary coordinate system (\underline{l} , \underline{m} , \underline{n}) is the other fixed coordinate system, with \underline{l} in the direction of the star at the instant of exposure. Related to these two fixed coordinate systems are the topographic (gravity) axes ($\underline{\lambda}$, $\underline{\mu}$, $\underline{\nu}$) at the camera station, the camera axes ($\underline{\zeta}$, $\underline{\xi}$, $\underline{\eta}$) fixed in the camera and moon-centered axes (\underline{U} , \underline{V} , \underline{W}) rotating with the moon. Diagrams of the angular relationships connecting the various coordinate systems, a glossary of symbols and definitions of these symbols will be found in Attachment 1.

As the optical axis of the panoramic camera rotates, it intersects the cylindrical film in a line which may be called the principal line of the plate. The principal point on the film may be defined as the point on the principal

line where the camera has completed half of its rotation, and the epoch of the plate may be defined as the time at which the optical axis passes through the principal point. (See Figure 2.)

The relations between plate variables, the direction of the star and the camera axes are given by:

$$v = fa \equiv f \tan^{-1} \left[-\frac{\bar{\eta} \cdot \underline{\xi}}{\bar{\eta} \cdot \underline{\eta}} \right] \quad (1)$$

$$u = f \cot b \equiv f \left[\frac{\eta \cdot \bar{\eta}}{\eta \cdot \bar{\xi}} \right]$$

In the determination of astronomical position by means of differential corrections, the following relations are useful and are derived in Attachment 2.

$$\begin{bmatrix} d\bar{l} \\ d\bar{m} \\ d\bar{n} \end{bmatrix} = \begin{bmatrix} 0 & K_1 & K_2 \\ -K_1 & 0 & K_3 \\ -K_2 & -K_3 & 0 \end{bmatrix} \begin{bmatrix} \bar{l} \\ \bar{m} \\ \bar{n} \end{bmatrix} \equiv \begin{bmatrix} 0 \\ 0 \\ 0 \end{bmatrix} \quad \begin{bmatrix} d\underline{\xi} \\ d\underline{\eta} \end{bmatrix} = \begin{bmatrix} 0 & L_1 & L_2 \\ -L_1 & 0 & L_3 \\ -L_2 & -L_3 & 0 \end{bmatrix} \begin{bmatrix} \underline{\xi} \\ \underline{\eta} \end{bmatrix} \quad (2)$$

Differentiating (1) and utilizing (2), the following observation equations result

$$dv = adf + fda \equiv adf + f \left\{ \sin b K_2 - \cos b K_3 + L_1 \right\} \quad (3)$$

$$du = \cot b df - \csc^2 b f db \equiv \cot b df - \csc^2 b f \left\{ \sin a L_2 + \cos a L_3 + K_1 \right\}$$

From which the following results are useful later as a check. The K's and L's are scalars the form of which is to be determined.

$$da \equiv -\sin b K_2 - \cos b K_3 + L_1 \quad (4)$$

$$db \equiv \sin a L_2 + \cos a L_3 + K_1$$

Writing $E_1 = \begin{bmatrix} 0 & 1 & 0 \\ -1 & 0 & 0 \\ 0 & 0 & 0 \end{bmatrix}$, $E_2 = \begin{bmatrix} 0 & 0 & 1 \\ 0 & 0 & 0 \\ -1 & 0 & 0 \end{bmatrix}$, and $E_3 = \begin{bmatrix} 0 & 0 & 0 \\ 0 & 0 & 1 \\ 0 & -1 & 0 \end{bmatrix}$

the following relations will be applied to determine the L's and the K's. An example of the derivation of one of them is included in Attachment 2.

$$\begin{aligned}
 \left[\frac{\partial \bar{l}}{\partial a}, \frac{\partial \bar{m}}{\partial a}, \frac{\partial \bar{n}}{\partial a} \right]^T &= \left[-\sin b E_2 - \cos b E_3 \right] \left[\underline{l}, \underline{m}, \underline{n} \right]^T \\
 \left[\frac{\partial \bar{l}}{\partial b}, \frac{\partial \bar{m}}{\partial b}, \frac{\partial \bar{n}}{\partial b} \right]^T &= +E_1 \left[\underline{l}, \underline{m}, \underline{n} \right]^T \\
 \left[\frac{\partial \underline{\xi}}{\partial g_2}, \frac{\partial \underline{\xi}}{\partial g_2}, \frac{\partial \underline{\eta}}{\partial g_2} \right]^T &= \left[-\sin g_1 E_1 + \cos g_1 E_2 \right] \left[\underline{\xi}, \underline{\xi}, \underline{\eta} \right]^T \\
 \left[\frac{\partial \underline{\xi}}{\partial \gamma}, \frac{\partial \underline{\xi}}{\partial \gamma}, \frac{\partial \underline{\eta}}{\partial \gamma} \right]^T &= \left[-\cos g_1, \cos g_2 E_1, -\sin g_1, \cos g_2 E_2 - \sin g_2 E_3 \right] \left[\underline{\xi}, \underline{\xi}, \underline{\eta} \right]^T \\
 \left[\frac{\partial \underline{\lambda}}{\partial \phi}, \frac{\partial \underline{\mu}}{\partial \phi}, \frac{\partial \underline{\nu}}{\partial \phi} \right]^T &= -E_3 \left[\underline{\lambda}, \underline{\mu}, \underline{\nu} \right]^T \quad \left[\frac{\partial \underline{\xi}}{\partial g_1}, \frac{\partial \underline{\xi}}{\partial g_1}, \frac{\partial \underline{\eta}}{\partial g_1} \right]^T = -E_3 \left[\underline{\xi}, \underline{\xi}, \underline{\eta} \right]^T \\
 \left[\frac{\partial \underline{\lambda}}{\partial \omega}, \frac{\partial \underline{\mu}}{\partial \omega}, \frac{\partial \underline{\nu}}{\partial \omega} \right]^T &= \left[+\sin \phi E_1, -\cos \phi E_2 \right] \left[\underline{\lambda}, \underline{\mu}, \underline{\nu} \right]^T \\
 \left[\frac{\partial \underline{U}}{\partial \theta}, \frac{\partial \underline{V}}{\partial \theta}, \frac{\partial \underline{W}}{\partial \theta} \right]^T &= E_1 \left[\underline{U}, \underline{V}, \underline{W} \right]^T
 \end{aligned} \tag{5}$$

From the definitions of the relations between coordinate systems the following equations apply:

$$\left[\underline{\bar{l}}, \underline{\bar{m}}, \underline{\bar{n}} \right]^T = R_3^T(3\pi/4+b) R_1^T(3\pi/4) R_3^T(\pi/2-a) R_1^T(2\pi-g_1) R_2^T(2\pi-g_2) R_3^T(2\pi-\gamma) R_1^T(\pi/2-\phi) R_3^T(\pi/2+\omega) R_3^T(\theta) \left[\underline{A}, \underline{B}, \underline{C} \right]^T \tag{6a}$$

$$\left[\underline{\xi}, \underline{\xi}, \underline{\eta} \right]^T = R_1^T(2\pi-g_1) R_2^T(2\pi-g_2) R_3^T(2\pi-\gamma) R_1^T(\pi/2-\phi) R_3^T(\pi/2+\omega) R_3^T(\theta) \left[\underline{A}, \underline{B}, \underline{C} \right]^T \tag{6b}$$

It is convenient to define:

$$P^T = \begin{bmatrix} P_{11} & P_{21} & P_{31} \\ P_{12} & P_{22} & P_{32} \\ P_{13} & P_{23} & P_{33} \end{bmatrix} = R_3^T(3\pi/4+b) R_1^T(3\pi/4) R_3^T(\pi/2-a)$$

$$\begin{aligned}
Q^T &= R_3^T(3\pi/4+b) R_1^T(3\pi/4) R_3^T(\pi/2-a) R_1^T(2\pi-g_1) R_2^T(2\pi-g_2) R_3^T(2\pi-\gamma) \\
U^T &= R_3^T(3\pi/4+b) R_1^T(3\pi/4) R_3^T(\pi/2-a) R_1^T(2\pi-g_1) R_2^T(2\pi-g_2) R_3^T(2\pi-\gamma) R_1^T(\pi/2-\phi) R_3^T(\pi/2+\omega) \\
S^T &= R_1^T(2\pi-g_1) R_2^T(2\pi-g_2) R_3^T(2\pi-\gamma) \\
T^T &= R_1^T(2\pi-g_1) R_2^T(2\pi-g_2) R_3^T(2\pi-\gamma) R_1^T(\pi/2-\phi) R_3^T(\pi/2+\omega)
\end{aligned} \tag{7}$$

Differentiating 6(a) and using 5 and 7.

$$\begin{aligned}
\left[d\bar{L}, d\bar{M}, d\bar{N} \right]^T &= \left[(-\sin b E_2 - \cos b E_3) da + E_1 db - P^T E_3 P dg_1 + (-\sin g_1 P^T E_1 P \right. \\
&+ \cos g_1 P^T E_2 P) dg_2 + (-\cos g_1 \cos g_2 P^T E_1 P - \sin g_1 \cos g_2 P^T E_2 P - \sin g_2 P^T E_3 P) d\gamma - Q^T E_3 Q d\phi \\
&\left. + (\sin \phi Q^T E_1 Q - \cos \phi Q^T E_2 Q) d\omega + U^T E_1 U \frac{\partial \theta}{\partial t} dt \right] \left[\bar{L}, \bar{M}, \bar{N} \right]^T
\end{aligned} \tag{8}$$

and differentiating 6 (b) and using 5 and 7

$$\begin{aligned}
\left[d\xi, d\zeta, d\eta \right]^T &= \left[-E_3 dg_1 + (-\sin g_1 E_1 + \cos g_1 E_2) dg_2 + (-\cos g_1 \cos g_2 E_1 - \sin g_1 \cos g_2 E_2 \right. \\
&\left. - \sin g_2 E_3) d\gamma - S^T E_3 S d\phi + (\sin \phi S^T E_1 S - \cos \phi S^T E_2 S) d\omega + T^T E_1 T \frac{\partial \theta}{\partial t} dt \right] \left[\xi, \zeta, \eta \right]^T
\end{aligned} \tag{9}$$

Also if R is any unitary rotation matrix whatever, then we observe that:

$$R^T E_1 R = \begin{bmatrix} 0 & R_{33} & -R_{32} \\ -R_{33} & 0 & R_{31} \\ R_{32} & -R_{31} & 0 \end{bmatrix} \quad R^T E_2 R = \begin{bmatrix} 0 & -R_{23} & R_{22} \\ R_{23} & 0 & -R_{21} \\ -R_{22} & R_{21} & 0 \end{bmatrix} \quad R^T E_3 R = \begin{bmatrix} 0 & R_{13} & -R_{12} \\ -R_{13} & 0 & R_{11} \\ R_{12} & -R_{11} & 0 \end{bmatrix}$$

Equating corresponding elements of 2 and 9 and noting that $P_{33} = 0$

$$\begin{aligned}
K_1 &= db - P_{33} dg_1 - \cos g_1 P_{23} dg_2 + (\sin g_1 \cos g_2 P_{23} - \sin g_2 P_{13}) d\gamma - Q_{13} d\phi + \\
&\quad (\sin \phi Q_{33} + \cos \phi Q_{23}) d\omega + U_{33} \frac{\partial \theta}{\partial t} dt = 0 \\
K_2 &= -\sin b da + P_{12} dg_1 + (\sin g_1 P_{32} + \cos g_1 P_{22}) dg_2 + (\cos g_1 \cos g_2 P_{32} - \sin g_1 \cos g_2 P_{22} \\
&\quad + \sin g_2 P_{12}) d\gamma + Q_{12} d\phi + (-\sin \phi Q_{32} - \cos \phi Q_{22}) d\omega - U_{32} \frac{\partial \theta}{\partial t} dt = 0
\end{aligned} \tag{10}$$

$$K_3 = -\cos b da - P_{11} dg_1 + (-\sin g_1 P_{31} - \cos g_1 P_{21}) dg_2 + (-\cos g_1 \cos g_2 P_{31} + \sin g_1 \cos g_2 P_{21} - \sin g_2 P_{11}) d\gamma - Q_{11} d\phi + (\sin \phi Q_{31} + \cos \phi Q_{21}) d\omega + U_{31} \frac{\partial \theta}{\partial t} dt = 0$$

$$L_1 = -\sin g_1 dg_2 - \cos g_1 \cos g_2 d\gamma - S_{13} d\phi + (\sin \phi S_{33} + \cos \phi S_{23}) d\omega + T_{33} \frac{\partial \theta}{\partial t} dt \quad (10)$$

$$L_2 = \cos g_1 dg_2 - \sin g_1 \cos g_2 d\gamma + S_{12} d\phi + (-\sin \phi S_{32} - \cos \phi S_{22}) d\omega - T_{32} \frac{\partial \theta}{\partial t} dt$$

$$L_3 = -dg_1 - \sin g_2 d\gamma - S_{11} d\phi + (\sin \phi S_{31} + \cos \phi S_{21}) d\omega + T_{31} \frac{\partial \theta}{\partial t} dt$$

The above equations satisfy (4). By setting $g_1 = g_2 = \gamma$ $dg_1 = dg_2 = d\gamma = dt = 0$ then $a = \alpha$, $b = \beta$ and K_1 and K_2 are (a) and (b) which is another check of these equations.

One further simplification is possible. It is well known that matrix multiplication is not commutative. Specifically, except in special cases,

$$R_3(2\pi - \gamma) R_2(2\pi - g_2) R_1(2\pi - g_1) \neq R_3(2\pi - \gamma) R_1(2\pi - g_1) R_2(2\pi - g_2) \quad (A)$$

The order in taking the misleveling angles g_1 and g_2 is purely one of definition. The angles g_1 and g_2 are expected to be small $\leq 30''$. Approximating $\cos g = 1$, $\sin g = \delta g$ rads and assuming $\delta g_1 \delta g_2 = 0$ (actually $\delta g_1 \delta g_2 \leq 0''.01$), then the equality sign in (A) holds. Making this approximation and solving K_2 for da , K_1 for db , simplifying, and substituting in 3, then the observation equations are:

$$(c-o) = a df + \left\{ \sin a \cot b dg_1 + (-\sin g_1 + \cos g_1 \cos a \cot b) dg_2 + [-1 - \cot b (\cos a \delta g_1 - \sin a \delta g_2)] d\gamma + [\cot b \sin(a+\gamma) - (\sin \gamma \delta g_1 - \cos \gamma \delta g_2)] d\phi - \{ (-\sin \phi + \cos \phi \cot b \cos(a+\gamma)) - (\cos \phi \cos \gamma + \sin \phi \cot b \cos a) \delta g_1 + (-\cos \phi \sin \gamma + \sin \phi \cot b \sin a) \delta g_2 \} d\omega - \{ (-\sin \phi + \cos \phi \cot b \cos(a+\gamma)) - (\cos \phi \cos \gamma + \sin \phi \cos a \cot b) \delta g_1 + (-\cos \phi \sin \gamma + \sin \phi \cot b \sin a) \delta g_2 \} \frac{\partial \theta}{\partial t} dt \right\} \quad (11)$$

$$(c-o) = \cot b df + f \csc^2 b \left\{ -\cos a dg_1 + \sin a dg_2 + (\sin a \delta g_1 + \cos a \delta g_2) d\gamma - \cos(a+\gamma) d\phi - [\cos \phi \sin(a+\gamma) - \sin \phi (\sin a \delta g_1 + \cos a \delta g_2)] d\omega - [\cos \phi \sin(a+\gamma) - \sin \phi (\sin a \delta g_1 + \cos a \delta g_2)] \frac{\partial \theta}{\partial t} dt \right\}$$

where (c-o) stands for computed minus observed.

Of the nine differentials:

$d\bar{\phi}$ and $d\bar{\omega}$ are corrections to the assumed astronomical latitude and longitude of the camera.

$d\gamma$ is similar to the familiar rotation term (Z) in the classical variation of coordinates solution of geodesy.

dg_1 and dg_2 are corrections to the misleveling angles g_1 and g_2 . If these terms in dg_1 and dg_2 are included in the solution, then two additional equations

$$dg_1 = k_1, \text{ and } dg_2 = k_2$$

should be adjoined to system. The values of the k's correspond to the observed values of g_1 and g_2 on the level vials. The terms in dg_1 and dg_2 should be removed, if it is not desired to adjust the bubble angles.

$\frac{\partial \theta}{\partial t}$ is the angular rate of rotation of the moon. dt is the correction to the observed epoch of the plate. If dt is included in the solution an additional equation, $dt = c$, with c corresponding to the observed epoch of the plate, is added to the system of equations. The terms in dt should be removed from the solution if it is not desired to adjust the epoch of the plate. The terms in dt can be used in a different way. Suppose the positions of the stars in the lunar equatorial system of coordinates have been determined for the epoch of the plate but not for the instant of exposure of the individual star, then the terms in dt may be considered a correction to the star position due to the finite time of rotation of the camera. Therefore, dt will be the time difference between the plate epoch and the exposure of the star. In this case, the terms in dt should be evaluated and used to reduce the residuals.

da and db are corrections to the camera angles. They are the values of the terms in brackets in the corresponding equations.

The coefficients of $d\phi$ and dt in the (15a) equation are small. Therefore, this equation serves to determine df and $d\gamma$.

df corresponds to either a uniform change in the focal distance or to a uniform shrinkage of the film.

2. Astronomical Azimuths and Zenith Distances

Plate angles a and b from equations are given as

$$\begin{aligned} a &= v/f \\ b &= \cot^{-1} [u/f] \end{aligned}$$

The vector $\underline{\bar{\ell}} = \sin \bar{a} \sin \bar{b} \underline{\bar{\lambda}} + \cos \bar{a} \sin \bar{b} \underline{\bar{\mu}} + \cos \bar{b} \underline{\bar{\nu}}$ in the topocentric coordinate system, but

$$[\underline{\bar{\ell}}, \underline{\bar{m}}, \underline{\bar{n}}]^T = Q^T [\underline{\lambda}, \underline{\mu}, \underline{\nu}]^T$$

Therefore equating components of $\underline{\bar{\ell}}$

$$\sin \bar{\alpha} \sin \bar{\beta} = Q_{11}$$

$$\cos \bar{\alpha} \sin \bar{\beta} = Q_{21}$$

$$\cos \bar{\beta} = Q_{31}$$

and

$$\begin{aligned} \bar{\alpha} &= \tan^{-1} \frac{Q_{11}}{Q_{21}} \\ \bar{\beta} &= \tan^{-1} \left[\frac{(Q_{11}^2 + Q_{21}^2)^{1/2}}{Q_{31}} \right] \end{aligned}$$

The above equations may be used to compute the preliminary and final astronomical azimuths and zenith distances. For simulation purposes, the panoramic camera and the methods of data reduction outlined here may be used with earth-based photography to test its effectiveness. Results of high precision should not be expected due to the high variability of vertical refraction. One of the standard methods of computing vertical refraction must be employed and the residuals reduced accordingly. On the assumption that the computed vertical refraction is in error by about the same amount for all lines radiating from the camera to the stars, a term $-f \Delta b$ with Δb being the correction to the computed refraction could be added to the right hand side of the (11b) equations.

3. Selenocentric Coordinates

A short summary of the methods by means of which selenocentric and selenodetic coordinates of survey points may be determined given the coordinates of an origin on the surface of the moon and enough other observed quantities will be outlined without writing the equations out in full.

Another set of coordinate axes is necessary which will be near but not usually coincident with the astronomically oriented topographic coordinate system $(\bar{\lambda}, \bar{\mu}, \bar{\nu})$. Designate the local selenodetic system by $(\underline{\lambda}, \underline{\mu}, \underline{\nu})$. The differences in coordinate systems are due to the deflections of the vertical. Corresponding angles in the two systems are distinguished by bars over the astronomical angles. The base vectors $\underline{l}, \underline{m}, \underline{n}$ defined in the glossary are not fixed with regard to the stars.

$$U^T = R_3^T(3\pi/4 + b) R_1^T(3\pi/4) R_3^T(\pi/2 - \alpha) R_1^T(2\pi - \gamma_1) R_2^T(2\pi - \gamma_2) R_3^T(\pi/2 - \gamma) R_1^T(\pi/2 - \phi) R_3^T(\pi/2 + \omega)$$

Since

$$[\underline{l}, \underline{m}, \underline{n}]^T = U^T [\underline{U}, \underline{V}, \underline{W}]$$

(12)

$$\begin{bmatrix} \underline{l} \\ \underline{m} \\ \underline{n} \end{bmatrix} = U^T R_3 \left[\begin{pmatrix} \pi/2 + \omega \end{pmatrix} \right] R_1 \left[\begin{pmatrix} \pi/2 - \phi \end{pmatrix} \right] \begin{bmatrix} \underline{\lambda} \\ \underline{\mu} \\ \underline{\nu} \end{bmatrix}^T$$

$$\text{Since } \underline{l} = \sin \alpha \sin \beta \underline{\lambda} + \cos \alpha \sin \beta \underline{\mu} + \cos \beta \underline{\nu}$$

Equating components of \underline{l} and solving for α and β we have

$$\alpha = \tan^{-1} \left[\frac{-\sin \omega U_{11} + \cos \omega U_{21}}{-\sin \phi \cos \omega U_{12} - \sin \phi \sin \omega U_{22} + \cos \phi U_{32}} \right]$$

$$\beta = \tan^{-1} \left[\left[\frac{(-\sin \omega U_{11} + \cos \omega U_{21})^2 + (-\sin \phi \cos \omega U_{12} - \sin \phi \sin \omega U_{22} + \cos \phi U_{32})^2}{\cos \phi \cos \omega U_{13} + \cos \phi \sin \omega U_{23} + \sin \phi U_{33}} \right]^{1/2} \right]$$

Rectangular space coordinates. The following equations have been taken from (1) with obvious modifications due to the difference in base surfaces, e. g., a sphere instead of a spheroid.

The transformation and inverse transformation between rectangular space coordinates and selenodetic coordinates are:

$$\begin{aligned} U &= (R+h) \cos \phi \cos \omega & \omega &= \tan^{-1} \left[\frac{V}{W} \right] \\ V &= (R+h) \cos \phi \sin \omega & \phi &= \tan^{-1} \left[\frac{W}{(U^2 + V^2)^{1/2}} \right] \\ W &= (R+h) \sin \phi & h &= (U^2 + V^2 + W^2)^{1/2} - R \end{aligned} \quad (13)$$

If (a, b, c) are the components of the unit vector $\underline{\ell}$ in the direction of the line from the camera at point (U_1, V_1, W_1) to point (U_2, V_2, W_2) and s is the length of the line where the subscripts refer to quantities associated with points 1 and 2 respectively. (See Figure 3.)

$$\begin{aligned} (U_2 - U_1) &= sa \\ (V_2 - V_1) &= sb \\ (W_2 - W_1) &= sc \end{aligned} \quad (14)$$

The angles α, β and the length s follow from

$$\begin{aligned} s \sin \alpha, \sin \beta &= -(U_2 - U_1) \sin \omega_1 + (V_2 - V_1) \cos \omega_1 \\ &= (R+h_2) \cos \phi_2 \sin(\omega_2 - \omega_1) \end{aligned} \quad (15)$$

$$\begin{aligned}
s \cos \alpha, \sin \beta_1 &= -(U_2 - U_1) \sin \phi, \cos \omega_1 - (V_2 - V_1) \sin \phi, \sin \omega_1 + (W_2 - W_1) \cos \phi, \\
&= (R + h_2) \left[\sin \phi_2 \cos \phi_1 - \cos \phi_2 \sin \phi_1 \cos(\omega_2 - \omega_1) \right] \\
s \cos \beta_1 &= (U_2 - U_1) \cos \phi, \cos \omega_1 + (V_2 - V_1) \cos \phi, \sin \omega_1 + (W_2 - W_1) \sin \phi, \\
&= (R + h_2) \left[\sin \phi_2 \sin \phi_1 + \cos \phi_2 \cos \phi_1 \cos(\omega_2 - \omega_1) \right] - (R + h_1)
\end{aligned} \tag{15}$$

The azimuth and zenith distance of the prolongation of the same line at P_2 are obtained by interchanging the subscripted quantities $\begin{smallmatrix} 1 \rightarrow 2 \\ 2 \rightarrow 1 \end{smallmatrix}$ and changing the sign of s since the length will now be measured in the direction opposite to $\underline{\ell}$. The back azimuth is now $(\alpha_2 + 180^\circ)$ and the back zenith distance is $(180^\circ - \beta_2)$. Hence, given the selenodetic coordinates of two points, we may directly determine the selenodetic length, azimuth, and zenith distance and back azimuth and back zenith distance of the straight line joining them. (See Figure 3.)

The inverse problem of finding the coordinates of point 2 given the coordinates of point 1 and the azimuth, zenith distance and length of the line between them may be determined from the following equations:

$$\begin{aligned}
(R + h_2) \cos \phi_2 \cos(\omega_2 - \omega_1) &= (R + h_1) \cos \phi_1 - s \sin \phi_1 \cos \alpha, \sin \beta_1 + s \cos \phi_1 \cos \beta_1, \\
(R + h_2) \cos \phi_2 \sin(\omega_2 - \omega_1) &= s \sin \alpha, \sin \beta_1, \\
(R + h_2) \sin \phi_2 &= (R + h_1) \sin \phi_1 + s \cos \phi_1 \cos \alpha, \sin \beta_1 + s \sin \phi_1 \cos \beta_1,
\end{aligned} \tag{16}$$

and from (13).

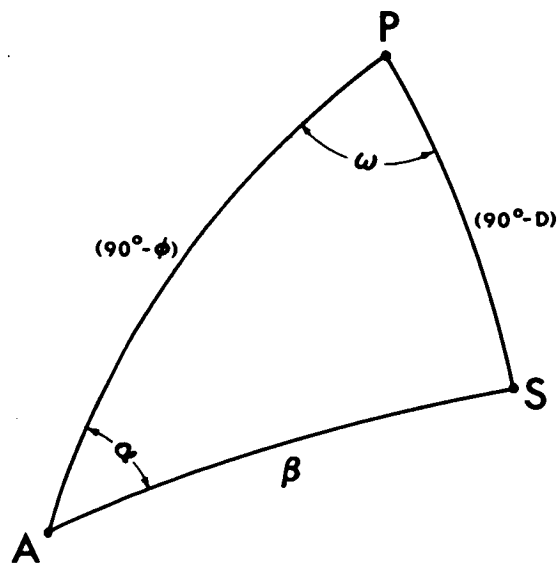
The side lengths of triangulation proceeding from a known base line may be computed from the law of sines, the known base line length and the following. Note that the triangulation is composed of plane triangles in space, and does not refer to triangles on the surface of a sphere.

If a , b and \bar{a} , \bar{b} are plate angles for two images on the plate and if I is the angle included between them, then

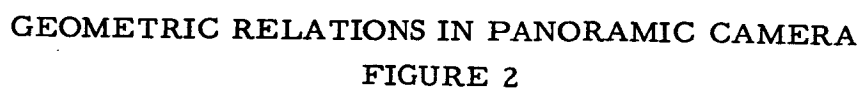
$$\cos I = \cos b \cos \bar{b} + \sin b \sin \bar{b} \cos (\bar{a} - a).$$

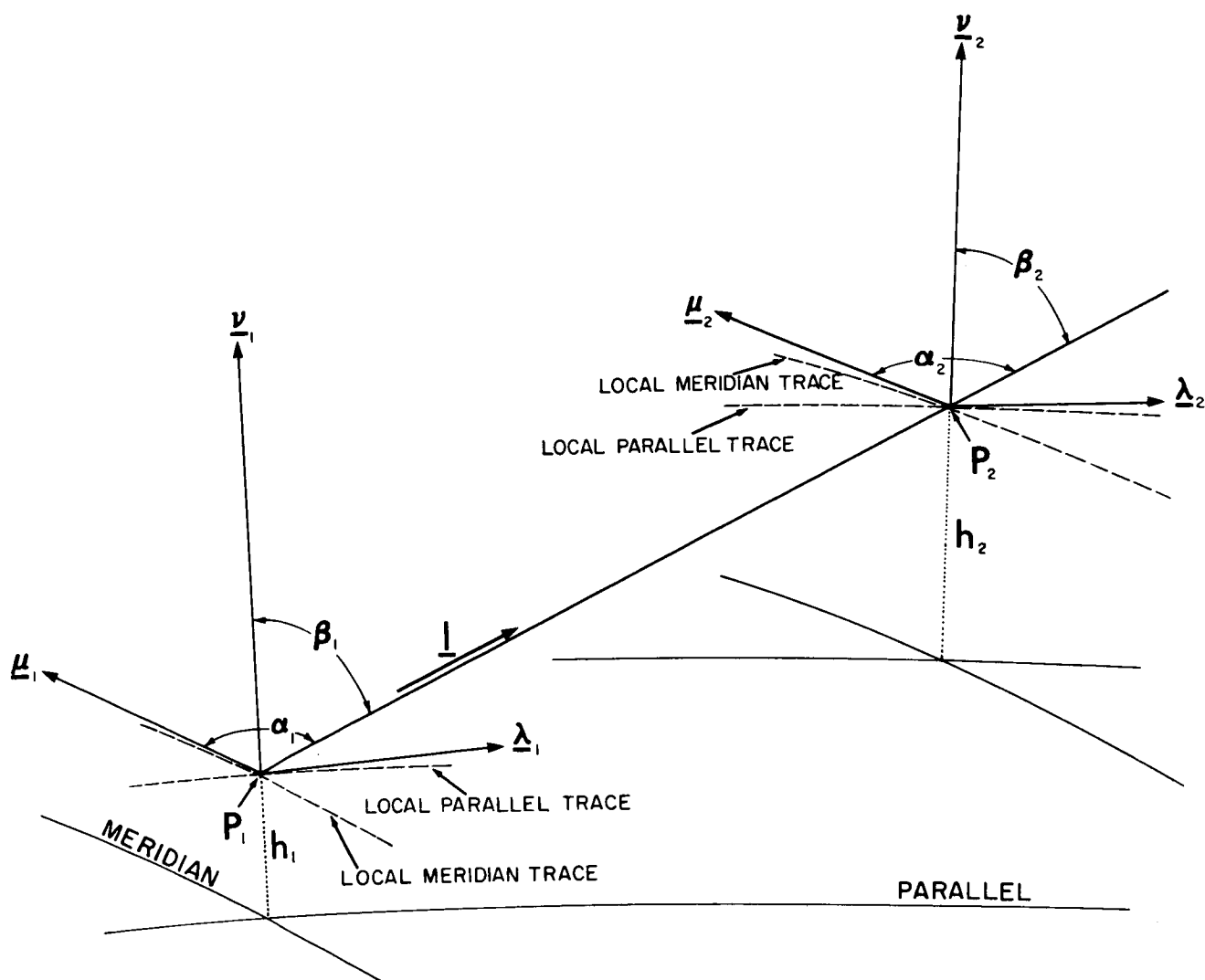
Variation of coordinates. The equations relating changes in plate coordinates with changes in the end coordinates of two ends of the observed line may be easily obtained, but are not included here because of their lengthy derivations. Reference is made to [1][3] which solves the problem for ordinary geodetic triangulation on earth. The object is to develop expressions for da and db for substitution in (3). This can be done by developing two different expressions for $(d\bar{l}, d\bar{m}, d\bar{n})$ and equating the two, one from (12) and the other starting from (14). Note that $(d\bar{l}, d\bar{m}, d\bar{n})^T \neq (O, O, O)^T$ in general. The $(d\bar{l}, d\bar{m}, d\bar{n})$ from (14) can either be in terms of differential corrections to rectangular coordinates $\left[(dU_1, dV_1, dW_1) (dU_2, dV_2, dW_2) \right]$ or to selenodetic coordinates $\left[(d\phi_1, d\omega_1, dh_1) (d\phi_2, d\omega_2, dh_2) \right]$ provided allowance is made for the non-parallelism of $(\lambda_1, \lambda_2) (\mu_1, \mu_2)$ and (ν_1, ν_2) .

Change of the Selenodetic Coordinate System. It can be expected that the initial selenodetic coordinate system employed will undergo changes. These changes may be composed of (1) a translation in space of the origin of the coordinate system to better coincide with the center of mass of the moon; (2) rotations about the \underline{U} , \underline{V} , \underline{W} axes to make the \underline{W} axis parallel to the instantaneous rotation axis of the moon; and (3) changes in the size and shape of the base surface (sphere) into a spheroid say. Should these problems arise reference is made to [3], page 13.



ASTRONOMICAL TRIANGLE
FIGURE 1





LOCAL SELENODETIC COORDINATE SYSTEMS

FIGURE 3

REFERENCES

1. Hotine, Martin, "A Primer of Non Classical Geodesy" presented to International Geodetic Association at Toronto in 1957.
2. Eichhorn, Heinrich, "On the Use of Panoramic Cylindrical Projection in Photographic Astrometry," Astro. Journal 68, No. 3, April 1963.
3. Molodenskii, M. S. et al, "Methods for Study of the External Gravitational Field and Figure of the Earth" translated from Russian by Israel Program for Scientific Translations for National Science Foundation and Department of Commerce, 1962.

APPENDIX - Attachment 1

GLOSSARY

A, B, C, *
are an orthonormal set of unit vectors in order (1, 2, 3) fixed with respect to the stars. C is parallel to the instantaneous rotation axis of the moon. A is in the direction of the intersection of the ecliptic with the equator of date of the moon. B completes the triad.

l, m, n
are an auxiliary orthonormal set of unit vectors in order (1, 2, 3) fixed with respect to the stars. l points in the direction of a particular star, and is by definition in the direction given by plate angles a and b with respect to the camera axes ξ, ξ, η. m is in the direction given by plate angles a and (90° + b). n is in the direction (a - 90°) and b = 90° with respect to the camera axes ξ, ξ, η.

ξ, ξ, η
are an orthonormal set of base vectors in order (1, 2, 3) fixed in the camera. η is parallel to the rotation axis of the camera. ξ is in the direction of the optical axis of the camera when it has completed half of its rotation. ξ completes the triad.

a
is the horizontal camera angle, the dihedral angle between the planes defined by (ξ, η) and (l, η) and is positive from ξ towards ξ.

b
is the vertical camera angle between the vectors η and l positive from η toward the plane of ξ and ξ.

*Note vectors are denoted by underlining.

g_1 is the misleveling angle obtained from the leveling vial in the plane of $\underline{\xi}$ and $\underline{\eta}$, positive in the sense of rotation of $\underline{\xi}$ into $\underline{\eta}$.

g_2 is the misleveling angle obtained from the second leveling vial which is assumed to be in the plane of $\underline{\eta}$ and $\underline{\zeta}$. It is positive in the sense of rotation of $\underline{\eta}$ into $\underline{\zeta}$.

γ is the rotation angle in the plane of $\overline{\lambda}$ and $\overline{\mu}$ corresponding to the azimuth of the axis $\underline{\xi}'$ which has been reoriented by the misleveling angles g_1 and g_2 .

$\overline{\lambda}$, $\overline{\mu}$, $\overline{\nu}$ are an orthonormal set of unit vectors at a point on the surface of the moon. $\overline{\nu}$ is in the direction of the local gravity vector. $\overline{\mu}$ is in the plane of (\underline{W} , and $\overline{\nu}$) and points toward astronomical north. $\overline{\lambda}$ completes the triad and points in the direction of local astronomical east. (These definitions may not be in harmony with the usual astronomical convention regarding the moon.)

ϕ is astronomical latitude, the angle between the plane of (\underline{U} and \underline{V}) and $\overline{\nu}$ measured from the plane of (\underline{U} and \underline{V}) toward $\overline{\nu}$. It is positive in the northern hemisphere and negative in the southern hemisphere.

ω is the astronomical longitude of the camera, the dihedral angle between the planes of (\underline{U} , \underline{V}) ($\overline{\nu}$, \underline{W}). It is positive in the sense of rotation of the moon about its axis.

\underline{U} , \underline{V} , \underline{W} are an orthonormal set of unit vectors in order (1, 2, 3). \underline{W} is parallel to the instantaneous rotation axis of the moon. \underline{U} is parallel to the line joining the center of the reference surface and the (0, 0) point on the moon's surface. \underline{W} completes the triad. \underline{U} , \underline{V} , \underline{W} rotate with the moon.

θ

is the dihedral angle between the planes of (A, C) and (U, W) at the epoch of the plate.

l, m, n

are an orthonormal set of unit vectors in order (1, 2, 3) defined similarly to \bar{l} , \bar{m} , \bar{n} with respect to $\underline{\zeta}$, $\underline{\xi}$, $\underline{\eta}$, except that l, m, n are not fixed relative to the stars, and that l points towards a landmark or survey signal.

λ , μ , ν

are an orthonormal set of unit vectors at point P which is at a height h above the reference surface (sphere). ν , λ , μ are respectively parallel to the normal to the base surface, the tangent vector to the parallels, and the tangent vector to the meridians at the point P' on the base sphere directly under the point P.

h

is the height above or below the base sphere.

ϕ

is the selenodetic latitude, the angle between the plane of the moon's equator and the position vector of a point. It is measured from the plane of the moon's equator towards the pole. It is positive in the northern hemisphere and negative in the southern hemisphere.

ω

is the selenodetic longitude, the dihedral angle between the planes defined by (U, V) and (ν , W). It is positive towards the east. (This may be different from the standard astronomical convention.)

$\overline{\alpha}$

is the astronomical azimuth, the dihedral angle between the planes defined by ($\bar{\nu}$, W) and ($\bar{\nu}$, \bar{l}), and is measured clockwise from astronomical north.

$\overline{\beta}$

is the astronomical zenith distance, the angle between the vectors $\bar{\nu}$ and \bar{l} . It is positive from $\bar{\nu}$ towards \bar{l} .

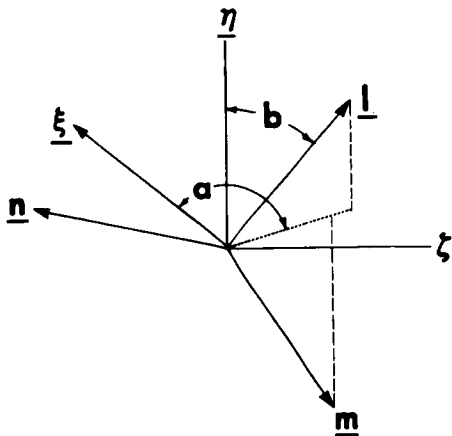
α

is the selenodetic azimuth, the dihedral angle between the planes defined by (\mathcal{V} , W) and (\mathcal{V} , 1). It is measured clockwise from selenodetic north.

β

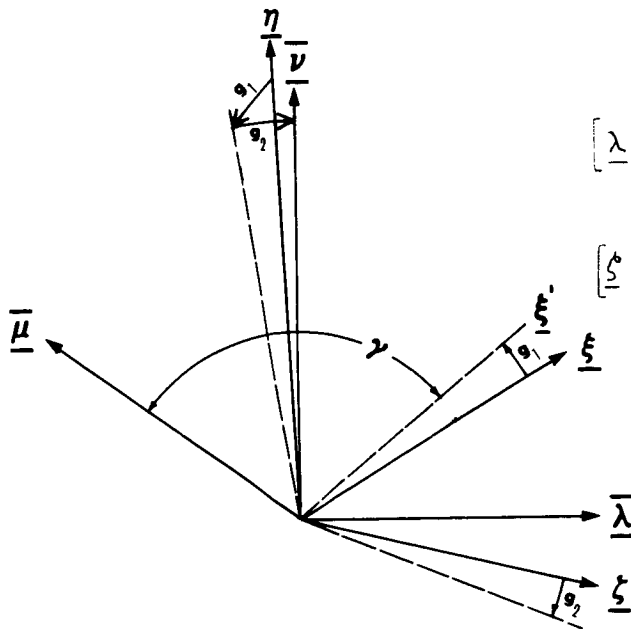
is the selenodetic zenith distance, the angle between the vectors \mathcal{V} and 1 . It is positive from \mathcal{V} towards 1 .

RELATIONS OF COORDINATE SYSTEMS



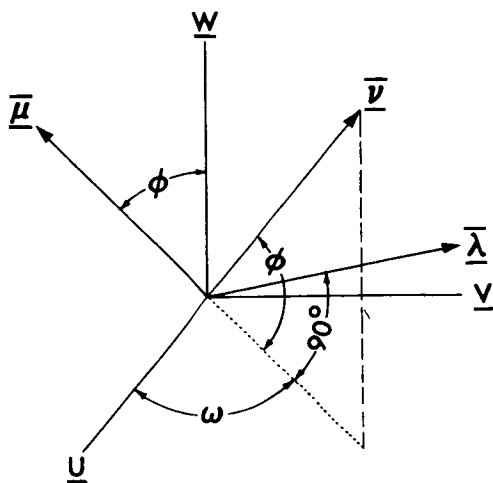
$$\begin{bmatrix} \underline{\xi} & \underline{\xi} & \underline{\eta} \end{bmatrix}^T = R_3(\pi/2 - \alpha) R_1(3\pi/4) R_3(3\pi/4 + b) \begin{bmatrix} \underline{l} & \underline{m} & \underline{n} \end{bmatrix}^T$$

$$\begin{bmatrix} \underline{l} & \underline{m} & \underline{n} \end{bmatrix}^T = R_3^T(3\pi/4 + b) R_1^T(3\pi/4) R_3^T(\pi/2 - \alpha) \begin{bmatrix} \underline{\xi} & \underline{\xi} & \underline{\eta} \end{bmatrix}^T$$



$$\begin{bmatrix} \underline{\lambda} & \underline{\mu} & \underline{\nu} \end{bmatrix}^T = R_3(2\pi - \gamma) R_2(2\pi - g_2) R_1(2\pi - g_1) \begin{bmatrix} \underline{\xi} & \underline{\xi} & \underline{\eta} \end{bmatrix}^T$$

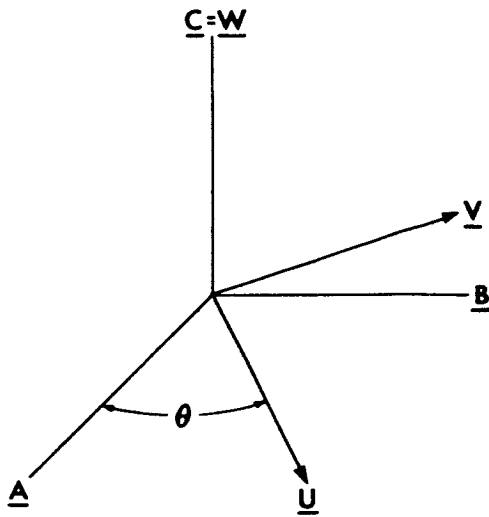
$$\begin{bmatrix} \underline{\xi} & \underline{\xi} & \underline{\eta} \end{bmatrix}^T = R_1^T(2\pi - g_1) R_2^T(2\pi - g_2) R_3^T(2\pi - \gamma) \begin{bmatrix} \underline{\lambda} & \underline{\mu} & \underline{\nu} \end{bmatrix}^T$$



$$\begin{bmatrix} \underline{u} & \underline{v} & \underline{w} \end{bmatrix}^T = R_3(\pi/2 + \omega) R_1(\pi/2 - \phi) \begin{bmatrix} \underline{\lambda} & \underline{\mu} & \underline{\nu} \end{bmatrix}^T$$

$$\begin{bmatrix} \underline{\lambda} & \underline{\mu} & \underline{\nu} \end{bmatrix}^T = R_1^T(\pi/2 - \phi) R_3^T(\pi/2 + \omega) \begin{bmatrix} \underline{u} & \underline{v} & \underline{w} \end{bmatrix}^T$$

RELATIONS OF COORDINATE SYSTEMS (Cont.)



$$[\underline{A}, \underline{B}, \underline{C}]^T = R_3(\theta) [\underline{U}, \underline{V}, \underline{W}]^T$$

$$[\underline{U}, \underline{V}, \underline{W}]^T = R_3^T(\theta) [\underline{A}, \underline{B}, \underline{C}]^T$$

APPENDIX D - Attachment 2

1. The Skew Symmetry of the Coefficient Matrices

Assume

$$1. \begin{bmatrix} d\bar{l} \\ d\bar{m} \\ d\bar{n} \end{bmatrix} = \begin{bmatrix} k_{11} & k_{12} & k_{13} \\ k_{21} & k_{22} & k_{23} \\ k_{31} & k_{32} & k_{33} \end{bmatrix} \begin{bmatrix} \bar{l} \\ \bar{m} \\ \bar{n} \end{bmatrix} \quad \begin{bmatrix} d\xi \\ d\zeta \\ d\eta \end{bmatrix} = \begin{bmatrix} l_{11} & l_{21} & l_{31} \\ l_{12} & l_{22} & l_{32} \\ l_{13} & l_{23} & l_{33} \end{bmatrix} \begin{bmatrix} \xi \\ \zeta \\ \eta \end{bmatrix}$$

It will be sufficient to prove that the matrix of k_{ij} 's is skew symmetric since the proof for the matrix of l_{ij} 's is exactly similar.

To determine the k 's and l 's we have the following relationships

$$2. \quad \begin{aligned} \bar{l} \cdot \bar{l} &= 1 & \bar{l} &= \bar{m} \times \bar{n} \\ \bar{m} \cdot \bar{m} &= 1 & \bar{m} &= \bar{n} \times \bar{l} \\ \bar{n} \cdot \bar{n} &= 1 & \bar{n} &= \bar{l} \times \bar{m} \end{aligned}$$

Differentiating the above

$$3. \quad \begin{aligned} \bar{l} \cdot d\bar{l} &= 0 & d\bar{l} &= d\bar{m} \times \bar{n} + \bar{m} \times d\bar{n} \\ \bar{m} \cdot d\bar{m} &= 0 & d\bar{m} &= d\bar{n} \times \bar{l} + \bar{n} \times d\bar{l} \\ \bar{n} \cdot d\bar{n} &= 0 & d\bar{n} &= d\bar{l} \times \bar{m} + \bar{l} \times d\bar{m} \end{aligned}$$

From (1) and (3)

$$\begin{aligned} \bar{l} \cdot d\bar{l} &= k_{11} = 0 \\ \bar{m} \cdot d\bar{m} &= k_{22} = 0 \\ \bar{n} \cdot d\bar{n} &= k_{33} = 0 \end{aligned}$$

$$d\bar{l} \cdot \bar{m} = k_{12}$$

$$d\bar{m} \cdot \bar{l} = k_{21} = (d\bar{n} \times \bar{l} + \bar{n} \times d\bar{l}) \cdot \bar{l} = \bar{n} \times d\bar{l} \cdot \bar{l} = \bar{l} \times \bar{n} \cdot d\bar{l} = -\bar{m} \cdot d\bar{l} = -k_{12}$$

$$\therefore k_{21} = -k_{12}$$

$$d\bar{l} \cdot \bar{n} = k_{13}$$

$$d\bar{n} \cdot \bar{l} = k_{31} = d\bar{l} \times \bar{m} \cdot \bar{l} + \bar{l} \times d\bar{m} \cdot \bar{l} = \bar{m} \times \bar{l} \cdot d\bar{l} = -\bar{n} \cdot d\bar{l} = -k_{13}$$

$$\therefore k_{31} = -k_{13}$$

$$d\bar{m} \cdot \bar{n} = k_{23}$$

$$d\bar{n} \cdot \bar{m} = k_{32} = d\bar{l} \times \bar{m} \cdot \bar{m} + \bar{l} \times d\bar{m} \cdot \bar{m} = \bar{m} \times \bar{l} \cdot d\bar{m} = -\bar{n} \cdot d\bar{m} = -k_{23}$$

$$\therefore k_{32} = -k_{23}$$

2. Example of Differentiation of base vectors

$$\begin{bmatrix} \bar{\lambda} \\ \bar{\mu} \\ \bar{\nu} \end{bmatrix} = \begin{bmatrix} -\sin \omega & \cos \omega \\ -\sin \phi \cos \omega & -\sin \phi \sin \omega \cos \phi \\ \cos \phi \cos \omega & \cos \phi \sin \omega \sin \phi \end{bmatrix} \begin{bmatrix} \underline{U} \\ \underline{V} \\ \underline{W} \end{bmatrix}$$

$$\begin{bmatrix} \frac{\partial \bar{\lambda}}{\partial \phi} \\ \frac{\partial \bar{\mu}}{\partial \phi} \\ \frac{\partial \bar{\nu}}{\partial \phi} \end{bmatrix} = \begin{bmatrix} 0 & 0 & 0 \\ -\cos \phi \cos \omega & -\cos \phi \sin \omega & -\sin \phi \\ -\sin \phi \cos \omega & -\sin \phi \sin \omega & \cos \phi \end{bmatrix} \begin{bmatrix} \underline{U} \\ \underline{V} \\ \underline{W} \end{bmatrix}$$

$$= \begin{bmatrix} 0 & 0 & 0 \\ -\cos \phi \cos \omega & -\cos \phi \sin \omega & -\sin \phi \\ -\sin \phi \cos \omega & -\sin \phi \sin \omega & \cos \phi \end{bmatrix} \begin{bmatrix} -\sin \omega & -\sin \phi \cos \omega & \cos \phi \cos \omega \\ \cos \omega & -\sin \phi \sin \omega & \cos \phi \sin \omega \\ 0 & \cos \phi & \sin \phi \end{bmatrix} \begin{bmatrix} \bar{\lambda} \\ \bar{\mu} \\ \bar{\nu} \end{bmatrix}$$

$$= \begin{bmatrix} 0 & 0 & 0 \\ 0 & 0 & -1 \\ 0 & 1 & 0 \end{bmatrix} \begin{bmatrix} \bar{\lambda} \\ \bar{\mu} \\ \bar{\nu} \end{bmatrix} = -E_3 \begin{bmatrix} \bar{\lambda} \\ \bar{\mu} \\ \bar{\nu} \end{bmatrix}^T$$

APPENDIX E
PROPOSED CAMERA CHARACTERISTICS FOR SURFACE
SELENODETIC OPERATIONS

A. INTRODUCTION

Selenodetic measurements proposed under this study are based largely on the use of photographic observing techniques to:

1. Photograph the circumpolar stars to determine the instantaneous pole.
2. Photograph the CSM against the star field to determine the position of the LEM landing site with relation to the CSM orbit.
3. Photograph near-horizon stars to determine the astronomic latitude and longitude of the landing site.
4. Determine astronomic azimuths and zenith distance angles to visible objects for establishing local, horizontal and vertical control in vicinity of the LEM landing area.

Two types of metric camera systems are recommended to accomplish these observations: a panoramic camera to photograph survey targets and lunar surface features against the star background; and a precision frame camera capable of photographing the circumpolar star field, the orbiting CSM against a star background, and the LEM from a nearby station (for base line determination). These cameras are discussed in the following paragraphs and their general characteristics are listed in Table I.

B. PANORAMIC CAMERA

The selection of the panoramic horizon camera as a basic instrument follows from the decision to rely on photographic techniques for

angle measurements because of the capability of recording a great deal of information in one operation. The utmost simplicity of operation and the inclusion of stars, terrain, and survey targets, substantially all around the horizon in a single exposure, as promised by the panoramic camera, seem to afford maximum results with least effort.

There are two general types of panoramic cameras: direct scanning cameras which employ rotating lenses, and those that scan by means of rotating mirrors or prisms. There are also various mechanical configurations, including some that require moving films which are difficult to keep in perfect synchronization with the optical scanning system.

Obviously an acceptable camera for surveying purposes must be of high metric quality. An example of the optical design on which the proposed camera is based may be found in an existing panoramic camera developed by Photogrammetry, Inc. [1, 2] This particular camera was designed for terrestrial surveys and has a rather high metric accuracy ($\sim \pm 40$ arc-seconds). It could be redesigned to include the design features recommended in the following paragraphs.

The panoramic camera recommended for lunar use employs an optical system designed around a horizontal fixed-focus lens with mirrors above and below it which together fold the optical axis back toward the field, permitting placement of both nodal points in a vertical axis about which the entire optical system rotates. (See Figure 1.) The film is stationary, held against a cylindrical film guide, and is exposed through a scanning slit which moves past the focal plane as the optical system rotates about the vertical axis of the camera. (See Figure 2.)

A metric accuracy of 10 arc-seconds is desirable for the selenodetic measurements and should be attainable with the proposed

camera system. To satisfy this need, a quality lens of ~ 100 mm focal length is recommended, together with the use of Kodak SO 243 film which has high resolution and radiation resistance. These components, operating without atmospheric effects, should deliver a lens-film image spread of 5 microns or less [3], comparable with a resolution of 200 lines per mm. and a potential scalar accuracy better than 10 arc-seconds. (One commonly used panoramic photogrammetric camera consistently produces a resolution of 100 lines per mm. working through the atmosphere and exposing on SO 1213 film, which has lower resolution than SO 243 [4].

The camera would be capable of providing 350° coverage of the horizon, as indicated in Figure 2. Inability to photograph the complete horizon is due to the requirement for entry and exit of film into the focal plane. The field of view of the camera in the vertical direction provides 25° coverage of the star field above the horizon and 5° coverage below to contain the terrain.

The camera would use 70 mm. roll film and provide an exposure format of 60 mm. $\times \sim 610$ mm. as shown in Figure 3. A 50-foot roll of film would provide over 20 exposures, which would be sufficient for the proposed photographic operations on the lunar surface.

Exposure time of the camera is governed by the width and speed of the scanning slit, which must not be excessively wide since near its edges exposed film areas are slightly out of the true focal plane because of the cylindrical configuration. A 5° slit, having its edges $2\frac{1}{2}^\circ$ from the optical axis could probably be used without degrading the image resolution perceptibly. Such a slit scanning at a rate to provide 0.25 second exposures would require 17.5 seconds for the full 350° scan of the camera.

A means of timing both beginning and end of the full scan is required to permit correction for fractional time intervals in the reduction

of the stellar photographs. For this purpose a small time-piece such as an Accutron watch should be installed in the camera for edge-photographing at the beginning and end of the scan to constitute a check not only on the real time of the exposure, but also its correctness of scan time. (This device, however, would require referencing to LEM real time.)

The cylindrical film guide must be dimensionally precise to hold the film accurately in the cylindrical surface at the focal distance from the axis of rotation of the optical system. To obtain the desired metric accuracy, it is proposed that a reseau be placed in the focal plane of the camera so that possible effects of film shrinkage and distortion can be controlled and eliminated when the photography is reduced. The reseau would register photographically but would not obscure image detail. The reseau graduations should be etched tick marks about 2 mm. long, on the order of 5 microns wide, showing the intersection points of an orthogonal grid (~ 10 mm. spacing). The spacing of the reseau intersection needs further consideration, and should be determined on the basis of the dimensional stability of the film, and the optical-mechanical limitations in design and construction of the camera. The reseau would be accurately calibrated before installation in the camera; after installation the combined lens-reseau-film system would be precisely calibrated.

Simultaneous photography of the stars and terrain would be facilitated, despite the great range of exposure differences, by providing different slit widths for the star field and terrain portions of the picture. (See Figure 3) It should be possible to provide an adjustable terrain-exposure slit width, to be set by the operator in accordance with an exposure meter reading. It is probable, however, that the slit can be preset in fixed width of opening in accordance with photographic experience which could be gained prior to the mission.

Partial atmospheric pressure must be maintained in the camera to prevent loss of lubricants in moving parts and possible damage to the film by outgassing or ablation, so the camera body must be completely sealed, with control levers entering through leakproof fittings. Photographic viewing must be done through a window; in this case, an optical system of high quality to prevent distortion. It will necessarily have a slight lens effect, however, which will be compensated by an auxiliary dome corrector lens installed near the principal lens. Since an internal pressure of 0.5 atmosphere will suffice for the prevention of damage, it is suggested that possibly the camera could leave earth at atmospheric pressure, and the case be provided with a relief valve permitting loss of pressurization gas down to the half-atmosphere level when the camera enters vacuum environment. This may reduce strength requirements and danger of possible distortions of the case and the optical dome.

Design features of the proposed panoramic camera should also include:

1. A barrel-shaped, epoxy-impregnated cast aluminum housing, surmounted by the optical dome.
2. External levers for motor winding and film advance, shutter operation, scanning slit setting (if any).
3. Large, easily manipulated foot screws for leveling, to be placed on a platform or tripod as necessary.
4. Edge photographic recording of exposure counter, clock and level bubbles.
5. External round bubble for approximate leveling and two 5" per division level vials inside, arranged for edge photography, and visible externally through periscope.

6. Scan motor, spring-driven and governor-controlled wound by lever in single operation with film transport.
7. Low-reflectance hard coating on all optical air-glass interfaces.
8. Magazine containing 50 feet of 70 mm. film, to provide over 20 exposures, one to a winding; preferably pressure-sealed to permit return of film without camera, with partial gas pressure and without damage.
9. Design and construction to resist damage and calibration errors due to the anticipated shocks and accelerations of flight and landing.
10. Total estimated weight of 15 lbs.

The camera would be calibrated, loaded, and sealed on earth prior to the start of a lunar mission. It is suggested that the loaded camera, with its partially exposed film be returned to earth for extraction and measurement of the film; however, the film, fully wound into the receiving spool, may be extracted for return without the camera, provided it is stored for return in a sealed container at some degree of gas pressure to prevent damage.

To operate the panoramic camera on the moon, the spring motor is wound (and the film transported between exposures) by a single operation of an external lever. The lower scanning slit is adjusted to suit the indications of an exposure meter (if provided); the camera is set on a firm support, preferably on a platform on top of the LEM, although a tripod on the ground may be used, if necessary; the instrument is leveled as accurately as possible, using the external round bubble and

subsequently the internal bubbles in conjunction with the leveling foot screws; the astronaut moves to clear of the line-of-sight; and the exposure lever is operated. The timing of star observations will not be critical owing to the slow lunar rotation, and it is proposed that the beginning (and possibly the end) of the scan be announced by the astronaut for voice recording on the LEM time-referenced tape record.

C. PRECISION FRAME CAMERA

A precision frame camera is proposed for the remaining operations of the selenodetic survey, i. e., circumpolar photography, photography of the CSM against the star field, and photography of the LEM to establish a short base line. While a high degree of metrical accuracy is required for these operations, particularly for the circumpolar star photos, no reference to the vertical or horizontal vectors are necessary; hence, the camera will need no level vials, graduated circles or spindle mountings.

The camera should be capable of providing a metrical accuracy of 5 arc-seconds. To achieve this degree of accuracy a 6 inch (~ 150 mm) focal length, $f/3$, lens is required. The camera must be mechanically rigid and contain an extremely flat focal plane.

The field of view should be about 40° , which will require an image format of ~ 110 mm square. Roll film in widths of 125 mm will satisfy the format dimensions and 10 feet of film would permit about 25 exposures, which would be sufficient for selenodetic observations.

The camera will carry a bright frame view finder usable by the astronaut for approximate pointing of the camera, and it will be mounted on a light trunnion over a base suitable for setting on the LEM top platform or a field tripod, so that the camera can be clamped in any desired orientation.

The precautions specified for the panoramic camera in respect to pressurizing of the camera and film magazine, to shock resistance, to heat precautions, and to low-reflectance coating of all air-glass surfaces in the optical system, apply equally to the frame camera.

An essential output of the camera will be a shutter-actuated signal to the LEM time-referenced magnetic tape record, whereby the instant of beginning of any CSM photograph can be recorded. In view of the high velocity of the CSM, about 1600 meters per second, the resolution of the timing should be to .01 second in order to reduce the uncertainty in LEM position.

Since this camera will be used in an operation where terrain and circumpolar stars will be photographed simultaneously, a dense focal plane filter will be provided, movable by an external control into the 5° edge of the frame which will contain the terrain. This will prevent gross over-exposure of the terrain portion of the picture. The density of this filter should be predetermined, since adjustment on the lunar surface would probably be difficult.

A focal plane reseau, similar to that proposed for the panoramic camera, will be required to counter the effects of film shrinkage and distortions that will result where the film is not properly held in the true focal plane. Use of a reseau would not be required, however, if photographic glass plates --optically flat to a few fringes of light-- could be used in place of film. If the number of exposures required for the proposed selenodetic measurement is reduced to ~ 5 , it should be possible to use glass plates of about 4" x 5" size without adding appreciably to the weight of the camera, which would also improve accuracy of data reduction. Requirements for photographing the CSM against the star background will utilize most of the exposures obtainable with a roll film camera; however, these observations could be eliminated if the SXT dual LOS photographic method in the CSM is adapted. In that event, the minimum number of exposures needed

with the frame camera reduces to 5-7, and use of glass plates should seriously be considered. It would also eliminate the timing readout and recording requirement previously mentioned.

General Comments. Although two different type cameras are proposed for maximum capability and flexibility in performance of the measurements, it would be possible to perform all the survey operations with the precision frame camera. The horizontal photography of near-horizon stars, terrain, and survey targets, would then consist of a series of overlapping photographs encompassing the horizon, as in conventional phototheodolite work. This approach would require addition of the usual phototheodolite components to the camera, including leveling screws, level vials to be edge photographed, a precision horizontal circle to be read and recorded to relate the several photographs, and substantially more exacting work on the part of the astronaut.

The significant trade-off consideration is weight. If weight and volume of the two cameras can be carried, they would provide the most capability with less work; if the weight cannot be carried, the precision frame camera with phototheodolite components would suffice.

D. STELLAR PHOTOGRAPHY REQUIREMENTS

Since the intended use of the two cameras will include stellar photography, it is necessary to compute the estimated exposure requirements for the photographic situations, which are:

- 1 - Circumpolar stars, using precision frame camera
- 2 - CSM against star field, using precision frame camera
- 3 - Lunar features and near-horizon stars, using panoramic camera

A reasonable assumption is that 500 stars should be photographed for situation 1, 50 for situation 2, and 50 for situation 3. Assuming random distribution of stars, and that in situations 1 and 3, 5° of the camera field is occupied by terrain, the magnitude of the faintest stars in the field of view can be estimated. The following table lists the illuminance and total numbers of stars [5].

<u>Star magnitude</u>	<u>Illuminance meter-candles</u>	<u>Number of stars in whole sky</u>
(No atmospheric attenuation)		
0	2.65×10^{-6}	3
1	1.65×10^{-6}	11
2	4.21×10^{-7}	35
3	1.67×10^{-7}	101
4	6.66×10^{-8}	289
5	2.65×10^{-8}	1059
6	1.06×10^{-8}	3056
7	4.21×10^{-9}	8416
8	1.67×10^{-9}	23216

Using this table, the magnitude of the faintest stars to be photographed in each case is determined as follows:

	Situation		
	1	2	3
Star field in camera view	40° x 35°	40° x 40°	25° x 350°
Star field as percentage of whole sky	3.4	3.9	21.2
Number of stars required	500	50	50
Then the whole sky number of stars must be	15,000	1,300	240
Faintest magnitude stars to be photographed	8	6	4

Exposure time for photographing the faintest stars is determined using the exposure equation [6];

$$E = \frac{D^2}{d^2} \times (I \cdot T \cdot t)$$

where

- E = exposure, meter-candle-seconds
- D = effective aperture, mm
- d = image spread, mm
- I = stellar illuminance, meter-candles
- T = lens transmittance
- t = shutter exposure time, seconds

The exposure value E, is computed for the three photographic situations assuming exposure times of 5 sec. for circumpolar star photos, 0.5 sec. for CSM-star field photos, and 0.25 sec. for photos of near-horizon stars:

	Situation			
	1 (8th mag.)	2 (6th mag.)	(0 mag.)*	3 (4th mag.)
D	50	50	50	29
d	.005	.005	.005	.005
I	$1.67 \cdot 10^{-9}$	$1.06 \cdot 10^{-8}$	$2.65 \cdot 10^{-6}$	$6.66 \cdot 10^{-8}$
T	0.9	0.9	0.9	0.9
t	5.0	0.5	.003**	0.25
E	0.75	0.48	0.72	0.50
Log E	T.88	T.68	T.86	T.70

* The CSM is assumed to be as bright as a 0 magnitude star.

** Since the CSM will exhibit rapid image motion on the film, the effective exposure time for the CSM will be less than the camera shutter exposure time (0.5) in case B. Based on an orbital height of 130 km and a velocity of 1.6 km/sec, the CSM effective exposure time will be:

$$t_{\text{csm}} = \frac{\text{Image Size}}{\text{Velocity}} \times \text{Photo Scale Factor}$$

Substituting the orbit and camera data, t_{csm} is found to be:

$$t_{\text{csm}} = \frac{(5 \times 10^{-6})}{1.6 \times 10^3} \times \frac{130 \times 10^3}{0.15} \approx 0.003 \text{ seconds}$$

The above exposures should produce satisfactory density on Kodak SO 243 film, which has a usable range from $\log E = T.50$

upward [7] . This film has the radiation-resistance necessary for lunar work, as well as fine resolution in the order of 200 + lines/mm.

In situations 1 and 3 the terrain will appear on the lower portion of the photograph. To prevent extreme over-expose of the bright area, a neutral density filter must be used to reduce the effective time of this exposure to make it consistent with the exposure time for the stars and CSM.

TABLE I
Proposed Camera Characteristics For Surface
Selenodetic Measurements

	Panoramic Camera	Precision Frame Camera
Application	To photograph: low altitude stars; terrain; local survey targets	To photograph: circumpolar stars; CSM against star field; LEM for baseline determination
Lens Focal Length Aperture Diaphragm	To be selected 100 mm - fixed focus f/3.5 Variable to f/22	To be selected 150 mm - fixed focus f/3 Variable to f/22
Field of View	30° vertical, set 25° above and 5° below horizontal. 350° horizontal field of view	40° x 40°
Shutter Speed	Single moving slit, in two widths to provide 0.25 second exposure above horizon; 0.05 second (or selected speed) for the lunar terrain	Variable, 0.1 to 1.0 second plus time exposure
Image Format Filter	60 mm x ~ 610 mm Exposure control accomplished with focal plane slit width (possibly photochromic filter)	110 mm x 110 mm Neutral density, 0.5% transmission, movable into 5° strip of focal plane to decrease terrain exposure
Focal Plane	Cylindrical	Flat
Reseau	Orthogonal grid, 10 mm. format	Orthogonal grid, 10 mm. format
Levels	Round bubble for rough leveling. Two 5"/division internal vials at 90°	None

TABLE I (Cont'd)

Proposed Camera Characteristics For SurfaceSelenodetic Measurements

	Panoramic Camera	Precision Frame Camera
Edge Data	Exposure number, clock and two level vials	Exposure number and clock (optional)
Exposure Timing	1.0 sec.	0.01 second time signal recorded on LEM time-referenced tape. (1.0 sec. by self-contained clock optional)
Overall Metric Accuracy	10 seconds	5 seconds
View Finder	None	Bright frame finder
Heat Shield	Reflectorized exterior, insulation in housing	Same
Pressurization	0.1 to 1.0 atmosphere	Same
Weight (est.)	15 pounds	5 pounds
Volume (est.)	1500 cubic inches	500 cubic inches
Exposure Meter	(optional)	(optional)

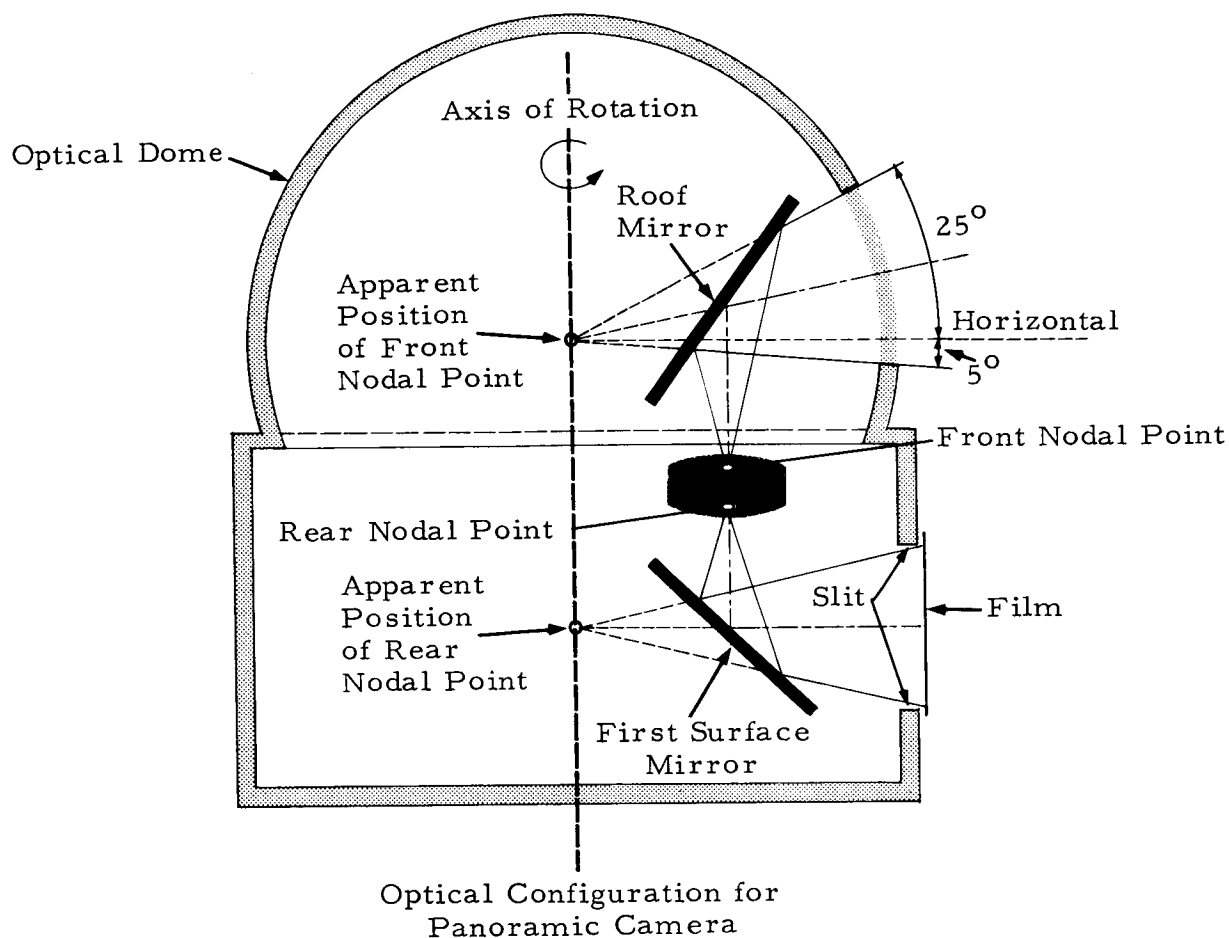


FIGURE 1.

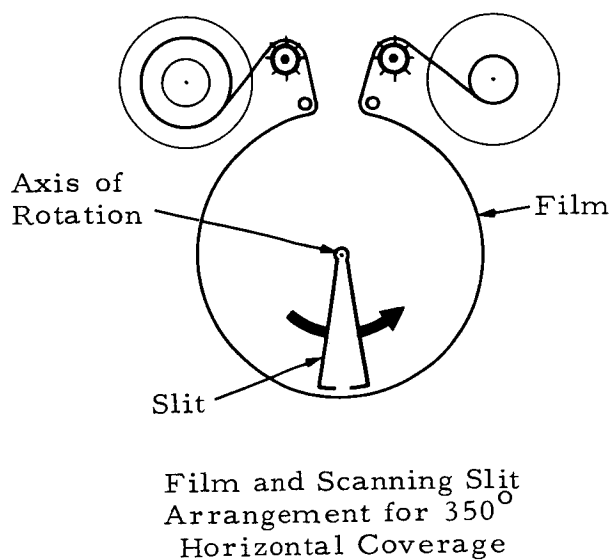


FIGURE 2.

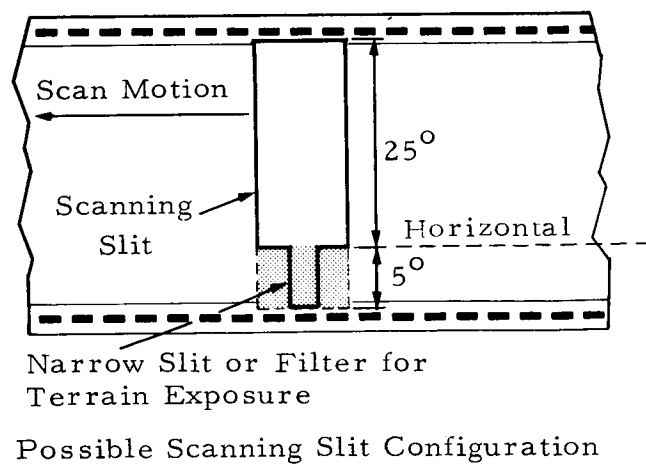


FIGURE 3.

References

1. G. T. McNeil, NavScan: A Dual Purpose Panoramic Camera, Photogrammetric Engineering, Vol. XXVII, No. 3, 1961.
2. NavScan Lo Instrumentation Manual, Nov., 1963, Photogrammetry, Inc., Rockville, Md.
3. Instrumentation for Aerial Photographic Experiments, Cornell Aeronautical Lab., Inc., Report VF-1478-P-1, 1961 (Appendix C: Analysis of Passive Point Source Targets).
4. Itek Laboratories, Panoramic Progress, Part 1, Photogrammetric Engineering, Vol. XXVII, No. 5, Dec. 1961.
5. Smithsonian Physical Tables.
6. F. A. Jenkins and E. H. White, Fundamentals of Optics, 2nd Ed., McGraw Hill, N. Y. 1950, p. 297.
7. R. G. Tarkington, Kodak Panchromatic Negative Films for Aerial Photography, Photogrammetric Engineering, Vol. XXV, No. 5, Dec. 1959.

APPENDIX F

SURVEY TARGETS FOR USE ON THE LUNAR SURFACE

A. INTRODUCTION

Proposed surface selenodetic operations outlined in this study require use of ground survey targets within a local control scheme about the LEM landing area. Precise relative location of the targets involves distance ranging and photographic direction finding from the LEM site, and they must therefore be detectable from the LEM as well as from orbiting photographic vehicles. Since for best utility in mapping control they should be as far from the LEM as possible, it is preferable to photograph them from the LEM top, where range of visibility will be about 5 km, rather than from the ground, where range may be only 2.5 km.

B. TYPES OF TARGETS

Two types of photographic targets are considered, diffusely reflecting and point source. The former must be of sufficient size, and must present sufficient contrast against the lunar surface, to be detectable as shapes in Orbiter photographs. With point source targets, the reflected light energy must produce a detectable point image in the photographs. We consider both types:

1. Diffusely Reflecting Targets

The size necessary can be computed. Assuming a lens-film resolution of 200 lines/mm. (which is exceptional but within the capability of a good lens and Kodak SO 243 film [1]), a high contrast target must be approximately 12 feet in least dimension to be resolved with a 3-inch focal length lens from a height of 50 km. This is at the threshold of resolution for the planned Orbiter mapping camera, [2] hence a considerably larger size, perhaps 25 feet, would be prudent.

Diffusely reflecting targets of such size have been found impracticable, as noted below:

- a) Rigid panels would be prohibitively heavy and bulky.
- b) Powders or paint sprays applied to the lunar surface seem impracticable because of the difficulty of covering the irregular, jagged, and porous surface material hypothesized from photometric studies.
- c) Coated cloth or plastic materials for use as self-spreading flat targets might be suitable, but it is unlikely that they could be reliably installed at remote locations.

Moreover, any of the foregoing would require supplementary structures in order to be observable from the LEM position.

2. Point Source Targets

Self-luminous light sources, such as searchlights and flares, require power sources which impose weight burdens. Fortunately, self-luminous sources are not needed since reflected sunlight during the lunar day can be utilized for point source targets.

Foil streamers of aluminum or other bright materials when draped over a surface of any roughness could provide numerous glints of sunlight (constituting not a single point source, but many such sources scattered over an area). The problem of emplacing these materials at a remote distance from the LEM would involve extremely difficult prediction of the probable pattern spread and total effective reflectance. The streamers, like the diffusely reflecting targets, would probably not be seen from the LEM.

Specular reflection of sunlight from plane mirrors would provide sufficient light but could be used only in static pre-fixed configuration. This suggests the use of spherical mirrors, which reflect in nearly all directions

with little difference in luminance, as the most suitable means of providing ground targets detectable in both surface and orbital photography.

In confirmation of the usefulness of such targets in aerial photography, it is reported that the U. S. Coast and Geodetic Survey has successfully photographed reflected sunlight from small garden-type crystal balls, and from Volkswagen hub caps, at heights of several miles. Such targets were small, whereas we propose larger reflectors (mylar balloons) for the greater heights involved. Appropriate balloon size can be computed.

The image of the sun in a convex spherical mirror is small -- in effect a point source, though of finite size. The image in a 5-foot radius sphere, for example, has a diameter of about 0.28 inch ($60'' \times \sin 1/2$ the angle subtended by the sun, or $16'$). The luminance of this small image is that of the sun reduced by the reflectance factor of the mirror surface, and it can be seen and photographed at great distances against a low contrast background.

To determine the necessary size of a reflectorized spherical balloon that would produce an adequate exposure on the film of an Orbiter camera, we consider first the D-log E curve for Kodak SO 243 film, finding that a satisfactory exposure density is achieved for values of log E greater than 1.5 ($E = 0.317$ meter-candle-seconds). Applying the exposure equation from [3],

$$MCS = 4.4 B y \left(\frac{R \times D}{H \times K_{lf}} \right)^2 \cdot t$$

where we assume:

MCS	(lowest usable E in m-c-s) = 0.317
B	(solar disc luminance in c/m^2) = 2.1×10^8 (no atmosphere loss)
y	(reflectance of mirror in percent) = 70
D	(diameter of camera lens in inches) = 0.67

R	(radius of mirror) (to be found)
H	(altitude of camera in feet) = 1.61×10^5 (50 km)
K_{lf}	(lens-film image spread in microns) = 5
t	(exposure time in seconds) = 0.02

Solving, R is found to be 58.3 inches; so a 10-foot diameter balloon appears adequate. It should be noted that the MCS value can be increased by increasing the radius of the balloon (a square function); moreover, the film response can be raised several orders of magnitude by selection of faster emulsions (though at greater risk of radiation fogging [4]).

C. EMPLACEMENT OF SELF-INFLATING BALLOONS

It is apparent that some type of ejection system will be required to emplace the proposed target balloons at their desired locations. Launching devices such as a compressed-gas gun or a spring-driven catapult could possibly be designed for this purpose. The gas gun could be conveniently charged from a compressed gas bottle whereas the spring launcher could be cocked by a jack mechanism. The use of either type of launcher would require some care and effort on the part of the astronaut in aiming the launcher in the desired direction and in achieving the correct launch elevation angle. A firm support for the launcher would be necessary to obtain full effectiveness.

As a guide to the launcher design problem, we calculate the launch energy required. For injecting the targets we use the equation for maximum range, corresponding to a launch elevation angle of 45° :

$$V = \sqrt{g_m R}$$

where:

V = launch velocity required at 45° elevation in feet/second
 g_m = acceleration of gravity at moon's surface, in feet/second²
 R = emplacement range, in feet (neglecting curvature)

The launch energy in foot-pounds, is therefore:

$$\text{Energy} = 1/2 M v^2 = 1/2 M g_m R$$

where M = mass of the projectile, in slugs.

The weight of the packaged balloon is taken to be one pound, in which case the package has a mass of 1/32 slug. Using the above equation the launch energy required for emplacement ranges of 2.5 km and 5 km is found to be:

	<u>2.5 km</u>	<u>5 km</u>
Launch Velocity	209 ft/sec.	295 ft/sec.
Energy	688 ft-lbs.	1375 ft-lbs.

It seems possible to design a launcher within reasonable size and weight to deliver these energies for boosting the targets.

D. CONCLUSION

Considering the importance of placing targets beyond the range of astronaut travel, as well as weight and size limitations, ballistically emplaced self-inflating mylar balloons are recommended. A 10-foot diameter reflectorized balloon will give reasonable assurance of visibility at 5 km distance from the LEM despite minor surface irregularities. Moreover, such a balloon will produce reflected sunlight bright enough to provide images in Orbiter photographs. It is estimated that such a target can be packaged within a pound in weight, and that a self-opening package and self-inflating device can be developed. Launching by a compressed gas gun or a spring-driven catapult is suggested.

References

1. Kodak Panchromatic Negative Films for Aerial Photography,
Raife G. Tarkington, Photogrammetric Engineering, Dec. 1959.
2. Langley Research Center, Lunar Orbiter: Its Mission and Capability,
Taback, Paper, 10th Ann'l Meeting American Astronautical Soc.
3. Cornell Aeronautical Lab. Inc., Report VF-1478-P-1 Instrumentation
for Aerial Photographic Experiments, 1961 (Appendix C: Analysis
of Passive Point-Source Targets).
4. Eastman Kodak Co., Effective Characteristic Curves of Certain Gamma-
Ray-Fogged Aerial and Color Photographic Films, G. M. Corney,
1961.

APPENDIX G
COMPARATIVE EVALUATION OF LASER AND RADAR
FOR RANGING ON THE MOON

A. INTRODUCTION

The requirement is for an equipment to measure from a point on the surface of the moon the distance to a semi-cooperative target, that is, one having good reflectance and spherical shape, and also to a non-cooperative object such as a mountain peak. The maximum distance to the semi-cooperative object will be ≈ 5 km and to the non-cooperative one ≈ 30 km. Accuracy desired is about 1 part in 5,000 or 1 m at 5 km and 6 m at 30 km. (In practical operation, the accuracy will be a fixed distance, not proportional to the distance.)

Two techniques are available for this purpose -- radar and laser. The requirements for the two conditions of semi-cooperative and cooperative targets are very different, but, for the reasons outlined in the paragraphs which follow, the laser appears superior to the radar for both types of targets.

B. PRINCIPAL EQUIPMENT CHARACTERISTICS REQUIRED:

1. Low data rate. High data rate capability is not useful since there will be substantial time intervals between measurements.
2. Area illuminated must be small so that the distance measured is associated with a specific and clearly definable area. This is particularly important for the non-cooperative target.
3. Frequency band width must be large to provide the required range accuracy. Generally this is obtained with a sharp rise-time of the transmitted pulse, or by a measurement of phase. The latter can provide extremely high accuracy, but is applicable only for point targets or targets of accurately known

shape. The most reliable information will depend similarly on the shortness of the pulse and, secondarily, on the sharpness of the wave front for the non-cooperative targets.

4. Size must be small.
5. Weight must be small.
6. Prime power requirement must be small.
7. Installation and operation of the equipment must be very simple.

C. CHARACTERISTICS OF SEMI- AND NON-COOPERATIVE TARGETS

There is considerable difference in performance requirements of the ranging equipment when ranging on the non-cooperative targets versus the semi-cooperative targets not only because of the increased distance, but also due to the reflecting area. The useful reflecting area for a non-cooperative target is all the reflecting area contained within a range resolution element. At 30 km with an illumination beam area of 225 sq. m, the useful reflecting area of a rocky mountain top is likely to be only a small percentage of the beam area, probably not more than 10%. With a semi-cooperative target, however, consisting of a sphere 3 m in diameter, for example, at a distance of 5 km almost exactly the full beam (6.5 milliradian beam width) will be incident symmetrically on the sphere to a maximum range depth of 1 m; so if the desired range resolution is 1 m, the useful reflecting area will be equal to the full beam area. In this case, even if a smaller range resolution is required, the full beam area can be used by using a matched filter, matched to the known returning waveform.

The physical basis of the system limitation will also depend on the range. In the absence of absorbing atmosphere, the limitation of the laser ranging operation will be the noise of the system itself for the semi-cooperative target for which the range is short. For the non-cooperative target at

longer ranges, the limitation will probably be the ambient illumination of the sun. A non-cooperative target at 30 km will probably require more than 1,000 times as much power as that needed for a semi-cooperative target at 5 km; however, this is not prohibitive (see paragraph D.2 below).

D. COMPARISON OF LASER AND RADAR

Comparisons of each of the above principal system characteristics for a radar and a laser are outlined below:

1. The illuminated area will depend on the beam width. A ruby laser has a beam width of about 0.5 milliradians; a semiconductor laser with appropriate collimating optics would have about the same beam width. A Ku-band radar, which would undoubtedly be used if a radar were selected, and utilizing an inflated antenna, would have a beam width no smaller than 5 milliradians. At 5 km, the laser would illuminate an area of some 6 m^2 and the radar 600 m^2 respectively. This difference alone would make the selection of the laser over the radar mandatory.
2. Low data rate directs attention to low average power with high concentration of energy. The laser technique of Q switching fits this requirement. A ruby laser can provide very short pulses with peaks of power in the megawatts, the relatively large interval between pulses being used for building up the energy for the next pulse. Such high peak powers are obtainable with relatively small batteries. Semiconductor lasers are able to provide peak powers approaching 100 watts. These may prove satisfactory because of their small size and high efficiency for semi-cooperative targets, but not for the non-cooperative ones. Radar, on the other hand, has as one of its valuable characteristics a high data rate capability which is of little or no value for the present application.

3. Power requirement depends on the efficiency and duty factor. Item 2 above shows that the duty factor can be very low, such as 20 nanoseconds in 10 or 15 seconds, or 2×10^{-7} . The efficiency of a ruby laser is low, yet the short duty cycle means that it would require little average power, say a few watts for the distant target. A few watts to feed the laser and all associated circuits should be ample, even for the non-cooperative target. The semi-conductor laser also requires extremely low average power. A low power Ku radar using a 50 milliwatt klystron has an efficiency of about 5%. The total power for this equipment would therefore be only a few watts.
4. The frequency band of both the laser and the radar is large. Laser pulses can be made as short as 20 nanoseconds, corresponding to a ranging distance of 3 m, with a rise time of a few nanoseconds. With a Ku radar, band widths of 1 gc can be obtained. In this respect the laser and the radars are of similar capability. Resolution capability, however, is not entirely dependent on the frequency band, since the targets are not point-sources. The received pulse will be the result of reflections at various distances and will appear smeared. With a suitable target, the front edge of the return pulse, corresponding to reflection at the nearest surface of the target, can be measured with an accuracy possibly as good as 0.1 to 0.2 of the pulse length. If, however, the nearest reflecting area (one range resolution deep) is small, there may be appreciable loss of accuracy. With the semi-cooperative target it should be possible to obtain reliably an accuracy of the order of 30 cm if necessary. With non-cooperative targets some experience and training may be desirable to select the target or the portion of a target which will provide the greatest accuracy.
5. The size and weight of the laser will involve a trade-off between the size of the receiving aperture and the power. The

laser design will depend on whether its operation is limited to the semi-cooperative targets or extended to non-cooperative targets.

In a radar the antenna would be by far the largest component, possibly an inflated paraboloid 3 m in diameter. A larger antenna would provide little gain because of the decreasing accuracy of the surface as the size increases. The weight of a Ku band radar, not including antenna and power supply, is about 10 lbs. The total weight would probably be between 20 lbs. and 30 lbs. including 5 lbs. for the antenna and its supporting stand and 15 lbs. for the rest of the equipment.

6. The operation of the ranging equipment can be made very simple. In this respect there would be little difference between the laser and the radar. In either case a telescope would be used to line up the equipment with the target and the range measurement made as with a regular radar. In the case of the laser, the source optical system can be used for the laser and the telescope.

In summary, the principal and dominant advantage of the laser is its narrow beam width. It also has a slight advantage in weight, possibly also in power. It has considerable advantage in size, because the radar requires a large antenna, although this unit is small until it is inflated. In resolution, and ease of operation the laser and the radar are about the same. An accuracy of about 30 cm can be expected with semi-cooperative target and probably about 1 m with non-cooperative target with both laser and radar.

The design of the equipment for the semi-cooperative target can be based on the work now in progress at the Lincoln Laboratories. At this stage it is understood that a range of 2 km has been obtained with equipment, not including batteries, contained in one-eighth of a cubic foot using a semi-conductor laser. It can reasonably be expected that a

range of 5 km will be reached with a semi-cooperative target. Total weight may be as low as 10 or 15 lbs.

For the non-cooperative target, a solid state laser such as a ruby laser will probably be necessary. This unit will be considerably larger. Estimates of probable weight and size are not considered sufficiently reliable to refer to. Actual equipment approaching the requirements have been relatively heavy, well over 40 lbs. Projection would lead to an expectation realistically of 30 or 35 lbs. and optimistically of 20 lbs.